

AD-A121 132

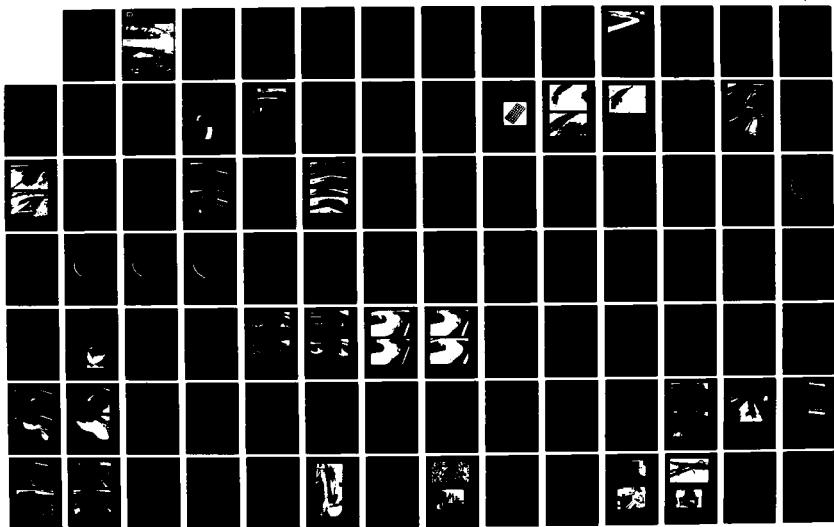
THE STREAMBANK EROSION CONTROL EVALUATION AND
DEMONSTRATION ACT OF 1974 S. (U) ARMY ENGINEER
WATERWAYS EXPERIMENT STATION VICKSBURG MS HYDRA.

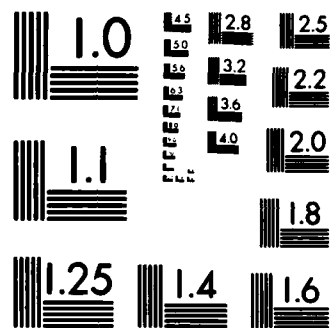
174

UNCLASSIFIED

M P KEOWN ET AL. DEC 81 WES/TR/H-77-9-APP-B F/G 13/2

NL





MICROCOPY RESOLUTION TEST CHART
NATIONAL BUREAU OF STANDARDS-1963-A

DA 121132



12

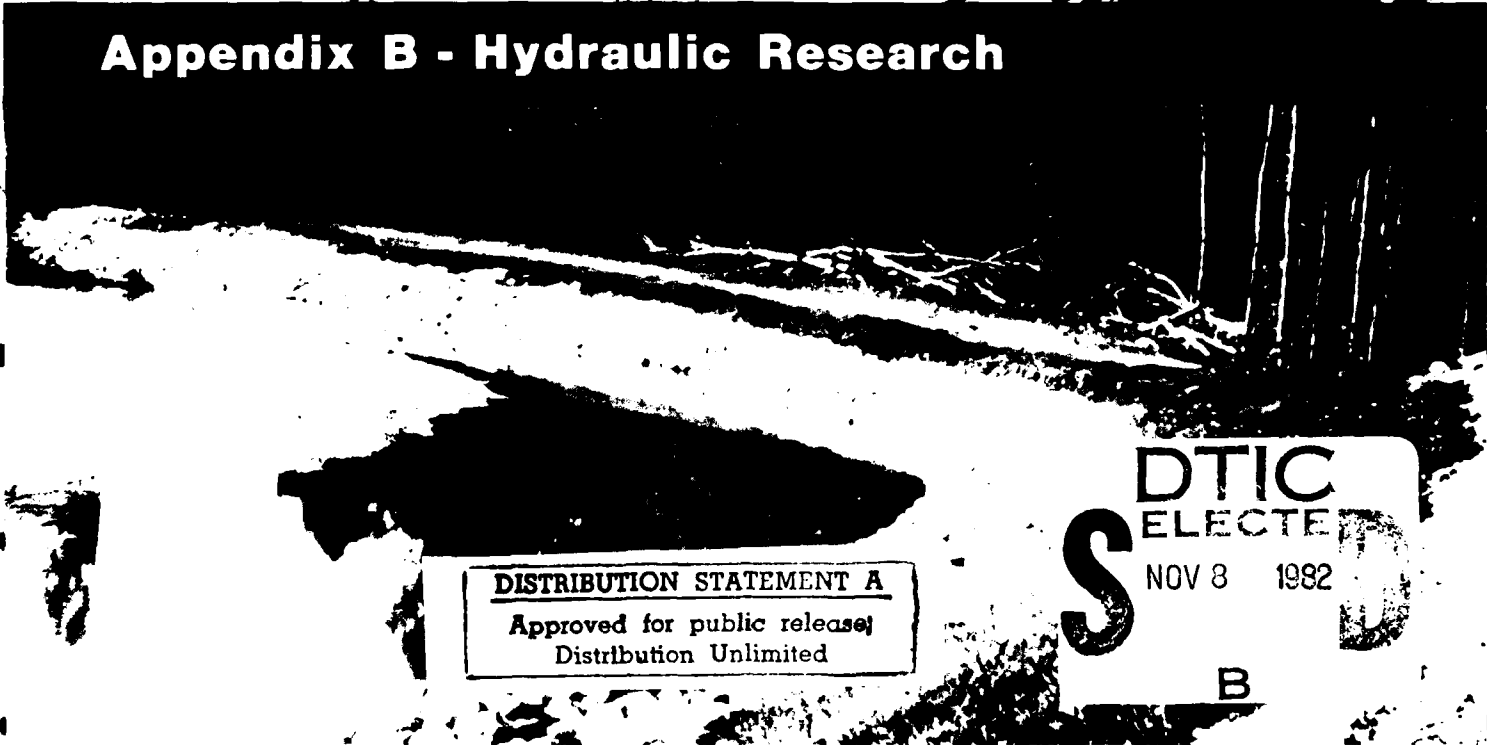
**US Army Corps
of Engineers**

December 1981

**THE STREAMBANK EROSION CONTROL
EVALUATION AND DEMONSTRATION ACT OF 1974
SECTION 32, PUBLIC LAW 93-251**



Appendix B - Hydraulic Research



DISTRIBUTION STATEMENT A

Approved for public release;
Distribution Unlimited

DTIC
ELECTE

NOV 8 1982

B



Rock Toe With Tie-Backs



Precast Block Paving



Board Fence Dikes

Unclassified

SECURITY CLASSIFICATION OF THIS PAGE (When Data Entered)

REPORT DOCUMENTATION PAGE		READ INSTRUCTIONS BEFORE COMPLETING FORM
1. REPORT NUMBER	2. GOVT ACCESSION NO.	3. RECIPIENT'S CATALOG NUMBER
Technical Report H-77-9	AD A12132	
4. TITLE (and Subtitle)		5. TYPE OF REPORT & PERIOD COVERED
LITERATURE SURVEY AND PRELIMINARY EVALUATION OF STREAMBANK PROTECTION METHODS		Final report
		6. PERFORMING ORG. REPORT NUMBER
7. AUTHOR(s)		8. CONTRACT OR GRANT NUMBER(s)
Malcolm P. Keown Elba A. Dardeau, Jr. Noel R. Oswalt Edward B. Perry		
9. PERFORMING ORGANIZATION NAME AND ADDRESS		10. PROGRAM ELEMENT, PROJECT, TASK AREA & WORK UNIT NUMBERS
U. S. Army Engineer Waterways Experiment Station Hydraulics Laboratory, Mobility and Environmental Systems Laboratory, Soils and Pavements Laboratory P. O. Box 631, Vicksburg, Miss. 39180		Work Unit 02
11. CONTROLLING OFFICE NAME AND ADDRESS		12. REPORT DATE
Office, Chief of Engineers, U. S. Army Washington, D. C. 20315		May 1977
14. MONITORING AGENCY NAME & ADDRESS (if different from Controlling Office)		13. NUMBER OF PAGES
		262
		15. SECURITY CLASS. (of this report)
		Unclassified
		15a. DECLASSIFICATION/DOWNGRADING SCHEDULE
16. DISTRIBUTION STATEMENT (of this Report)		
Authorized for public release; distribution unlimited.		
17. DISTRIBUTION STATEMENT (of the abstract entered in Block 20, if different from Report)		
18. SUPPLEMENTARY NOTES		
19. KEY WORDS (Continue on reverse side if necessary and identify by block number)		
Bank erosion Bank protection		
20. ABSTRACT (Continue on reverse side if necessary and identify by block number)		
<p>A preliminary study of streambank erosion control was conducted with the major emphasis on an extensive literature survey of known streambank protection methods. In conjunction with the survey, preliminary investigations were conducted to identify the mechanisms that contribute to streambank erosion and to evaluate the effectiveness of the most widely used streambank protection methods. The results of the literature survey and the two preliminary investigations are presented herein.</p>		

(Continued)

DD FORM 1473 EDITION OF 1 NOV 65 IS OBSOLETE

Unclassified

SECURITY CLASSIFICATION OF THIS PAGE (When Data Entered)

Unclassified

SECURITY CLASSIFICATION OF THIS PAGE(When Data Entered)

20. ABSTRACT (Continued).

The text of the "Streambank Erosion Control Evaluation and Demonstration Act of 1974" is presented in Appendix A. A list of commercial concerns that market streambank protection products is provided in Appendix B. Appendix C contains a glossary of streambank protection terminology. A detailed bibliography resulting from the literature survey is provided in Appendix D, and a listing of selected bibliographies related to streambank protection are provided in Appendix E. ←

Unclassified

SECURITY CLASSIFICATION OF THIS PAGE(When Data Entered)

FINAL REPORT TO CONGRESS

**THE STREAMBANK EROSION CONTROL
EVALUATION AND DEMONSTRATION ACT OF 1974
SECTION 32 PROGRAM**

APPENDIX B HYDRAULIC RESEARCH

**Consisting of
A BRIEF SUMMARY REPORT AND EIGHT INDIVIDUAL REPORTS
ON HYDRAULIC LABORATORY INVESTIGATIONS**

**U.S. ARMY CORPS OF ENGINEERS
December 1981**

APPENDIX B

HYDRAULIC RESEARCH

CONTENTS

	Page
Channel Flow Protection	B-1-1 to 38
Bank Protection Techniques Using Spur Dikes	B-2-1 to 29
Bank Protection Techniques Using Gabions	B-3-1 to 9
Movable Bed Model Studies	B-4-1 to 86
Effects of Navigation on Bank Stability in Confined Waterways	B-5-1 to 35
Effects of Propeller Wash from Inland Navigation on Channel Bottom Stability	B-6-1 to 13
Wave and Seepage-Flow Effects on Sand Streambanks and Their Protective Cover Layers	B-7-1 to 95
Wave Stability Study of Riprap-Filled Cells	B-8-1 to 56



Accession For	
NTIS GRA&I	<input checked="" type="checkbox"/>
DTIC TAB	<input type="checkbox"/>
Unannounced	<input type="checkbox"/>
Justification	
<i>PER APPENDIX A</i>	
By	
Distribution/	
Availability Codes	
Dist	Avail and/or Special
<i>A</i>	

CHANNEL FLOW PROTECTION

SECTION 32 PROGRAM
STREAMBANK EROSION CONTROL EVALUATION AND DEMONSTRATION
CHANNEL FLOW PROTECTION
Hydraulic Laboratory Investigation

PART I: INTRODUCTION

1. Under the Section 32 Program, hydraulic research was conducted to demonstrate and evaluate several new and existing streambank protection methods. These methods were tested to determine their ability to withstand the hydraulic forces imposed by channel flow and to qualitatively compare the scour and depositional characteristics of the methods. The goal of this research was to study flow characteristics in alluvial river bends and identify any new protection techniques that can be recommended for field use and to provide additional improved design information for several existing protection techniques.

PART II: MODEL APPURTENANCES AND TEST PROCEDURES

2. The model tests were conducted in a curved channel facility (Figure 1) having both sand bed and banks. Channel side slopes were initially molded to 1V on 2H and point bars were placed on the inside of the channel bends. No attempts were made to reproduce soil conditions in the model but sand was recirculated through the channel to simulate bed-load movement. A discharge hydrograph (Figure 2) was developed to represent long periods of low flow followed by a short duration bank-full discharge and each type of protection was exposed to four repetitions of the hydrograph.

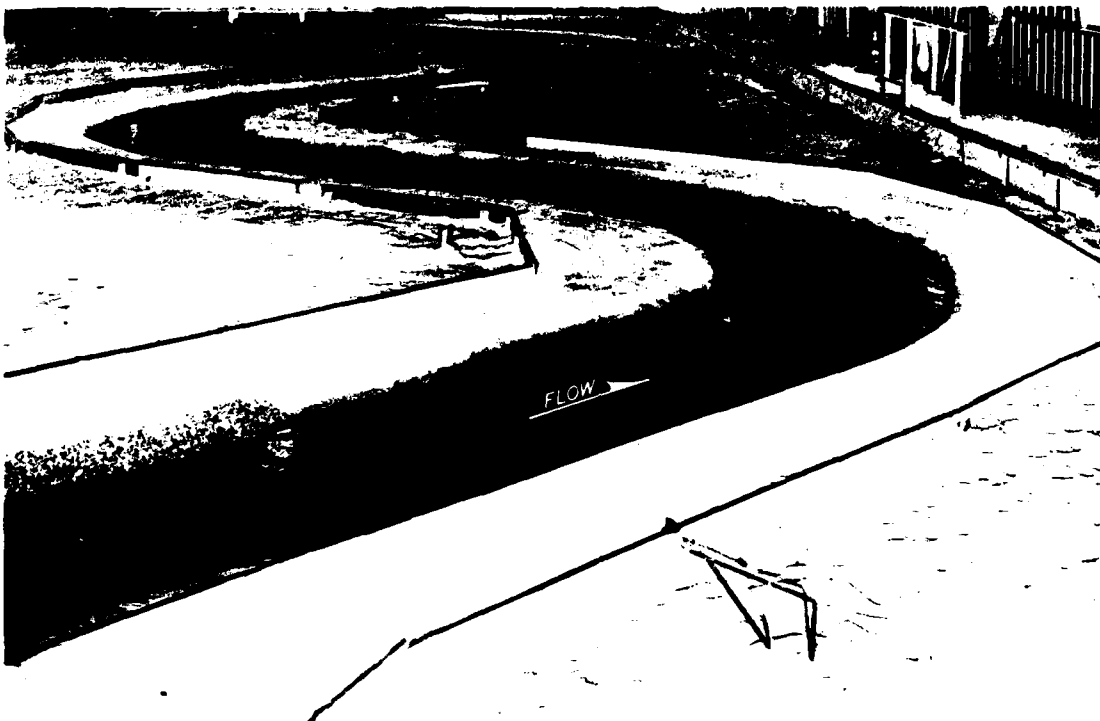


Figure 1. Curved channel facility

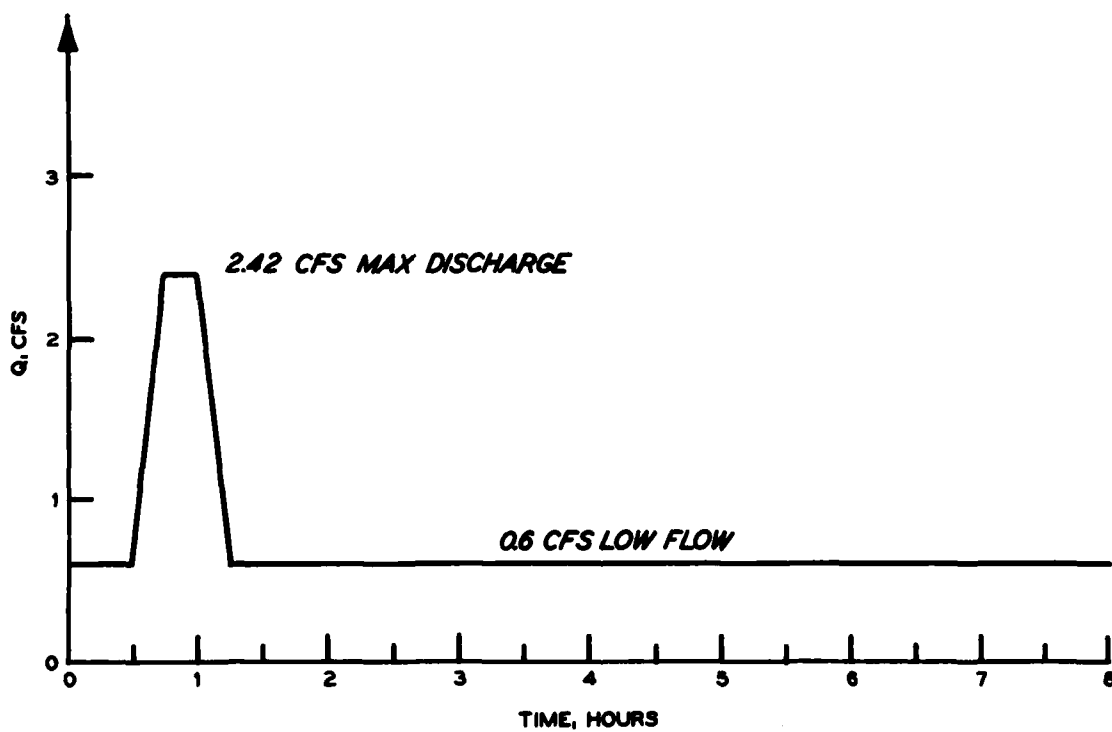


Figure 2. Model discharge hydrograph

PART III: PERTINENT LITERATURE AND TEST RESULTS

Flow Characteristics in Alluvial River Bends

3. Design of bank protection for an alluvial channel bend requires knowledge of the mechanics of flow in curved channels. Distributions of velocities and forces in a channel bend are important in designing the size or strength of a protection technique as well as the extent required for protection. Prediction of distribution of those parameters for relatively large projects can be undertaken in physical and mathematical models. For smaller projects, simpler methods must be employed because of economics, time, etc. The purpose of this section is to investigate the design guidance that is available for the relatively small project.

4. The prediction of maximum velocity that occurs in a channel bend is required for design of various bank protection techniques. The California Highway Department (1970) estimates impinging velocities on concave banks of channel bends to be 1-1/3 times the average stream velocity. Rozovski (1957) has done work on flow in channel bends and concludes that the nonerosive velocity in a bend will be less than in a straight run by about 20 percent. This conclusion was based on comparing velocities measured in a model channel bend and straight reach and by using movable-bed models to compare beginning of sediment motion in a channel bend and straight reach. Rozovski states regarding a movable-bed model:

The results of the experiments disprove the assertion made by various authors that the cause of channel erosion in bends is the "impact" of the stream on the concave bank and that at the entry into a bend considerable erosion must take place. In actual fact, at the entry part of the bend...a certain rise of the bottom near the concave bank is observed. The most intensive erosion of the channel takes place near the exit of the bend, which...is explained by the shifting of the maximum velocity toward the concave bank and its continuation.

5. Castle (1956) reported on measurements of several rivers in California relating the maximum attack velocities in channel bends to the mean channel velocity. The mean channel velocities were relatively low (≤ 4.5 fps) and results are shown in Plate 1. At the maximum observed

average channel velocity of 4.3 fps, the maximum velocity observed in the channel bend was 7.9 fps or 1.85 times the average channel velocity. Castle also reported that short-term velocities ranged up to 50 percent greater than the long-term mean velocity. Al-Shaik (1964) conducted extensive velocity measurements in curved concrete channels with mild slopes and low ratios of width/depth. The maximum velocity observed at the downstream end of the bend was approximately 20 percent greater than the mean channel velocity.

6. Flow in channel bends has been described by the concepts of free and forced vortices (Einstein and Harder 1954), but techniques for applying these concepts to the longitudinal velocity distribution in natural channel bends could not be found in the literature.

7. Velocities in the model alluvial channel were measured to define the distribution throughout the channel bend. The model bend turned an angle of approximately 100 deg with a channel width/center-line radius ratio of 0.55. Cross sections shown in Plates 2 and 3 were formed by allowing the sand channel with riprap on the concave bank to reach equilibrium for the hydrograph shown in Figure 2. Riprap was then placed on the bottom and convex banks and velocities were taken with a pitot tube. The values shown in Plates 2 and 3 are the surface velocities/average channel velocities for discharges of 2.8 and 9.0 cfs, respectively. These velocities range up to 1.8 times the average channel velocity in the downstream tangent of the curve. The maximum surface velocities are higher than the maximum impingement velocities discussed in paragraph 4 but close to the reported velocities by Castle in paragraph 5. Both the model channel and the bends studied by Castle were relatively sharp (large channel width/radius ratio) which partially explains the high values of maximum velocity.

8. Study of the shear distribution that occurs in a channel bend was conducted by Ippen et al. (1960) and Yen (1965). These results are valuable in the design of bank protection measures. Apmann (1972) presents available data relating the maximum shear/mean shear as a function of the channel width/center-line radius ratio in Figure 3. The following conclusions are drawn by Apmann:

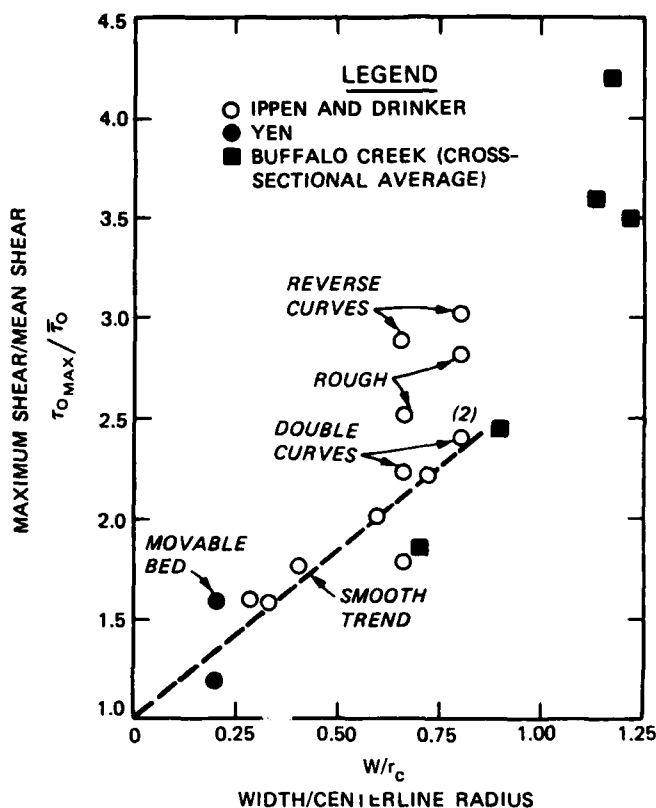
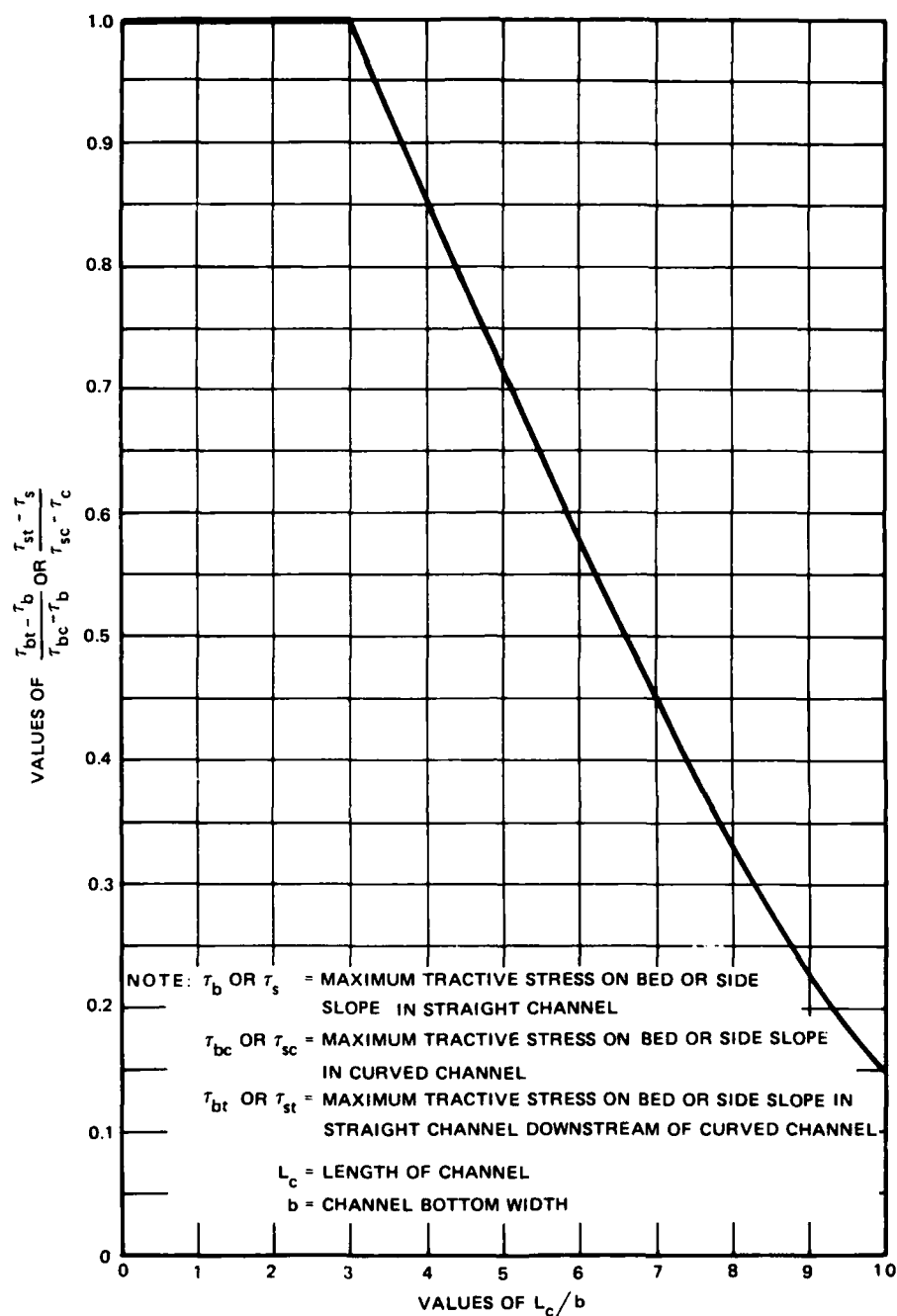


Figure 3. Relation of maximum shear to curvature ratio (Apmann 1972)

- a. The maximum shear increases with curvature ratio.
- b. Surface roughness increases maximum shear by about 15 percent.
- c. Upstream conditions play a significant role in amplifying maximum shear if in successive curves there is a reversal of direction; this increase was on the order of 30 percent.
- d. Combining these influences indicates that in a bend, maximum shears might be 50 percent above the smooth trend line drawn in Figure 3.

Also shown in Figure 3 are Apmann's (1972) results of the field studies on a reach of Buffalo Creek, New York, where cross sections and water-surface profiles were measured to compute the maximum shear stress (averaged over the cross section) for the sharpest bends. These values agree closely with the laboratory results and appear to be consistent with Ippen et al. data points for curves with a rough bed.

9. The variation of tractive stress downstream of channel bends (Soil Conservation Service 1977) is shown in Figure 4. This curve is



REFERENCE: NECE, R.E., GIVLER, G.A., AND DRINKER, P.A., MEASUREMENT OF BOUNDARY SHEAR STRESS IN AN OPEN CURVE CHANNEL WITH A SURFACE PITOT TUBE: M.I.T. TECH NOTE (NO 6), AUG. 1959.

Figure 4. Tractive stresses downstream of channel bends

based on limited data and does not reflect the effects of depth of flow or angle or curvature.

10. Wylie, Alonso, and Coleman (1977), Simons, Li, and Schall (1979) and others have set the groundwork for understanding the stochastic properties of turbulent tractive forces but field application of results to flow in channel bends is not yet possible.

11. Parsons (1960) has conducted field studies of the complete or partial failure of established protection measures. Figure 5 was presented by Parsons to describe the limits of attack in a channel bend. The reference line A-B is drawn along the eroding down-valley bank. Instability of the bank represented by line A-B immediately alters the situation in the downstream bend. Stabilization of bank line A-B should precede the bend under study.

The position of deposition point C in Figure 5 is an important consideration since it is logically associated with the beginning point of need for a rugged type of revetment. A rapidly migrating stream would leave the bank in this area in a raw condition. This superficially indicates the need for strong revetment much farther upstream than is truly the case. Common misjudgments in streambank-protection works are torevet this bank too far upstream and fail to go far enough downstream into the bend on the opposite side.

Parsons observed that the erosive forces begin to become severe at point B and reach a maximum one stream width away from reference line A-B.

12. Model tests were conducted to see if the limits of severe attack in a channel bend could be defined and compared with the results by Parsons. This would allow minimization of the amount of revetment required in each bend. The first series of tests were directed at determining the limits of attack along the stream. The second series of tests were directed at determining the minimum height of revetment required in the channel bend.

13. In studying the limits of attack in the channel model, a riprap revetment was placed along the concave bank at different distances both upstream and downstream from the channel bend in order to determine

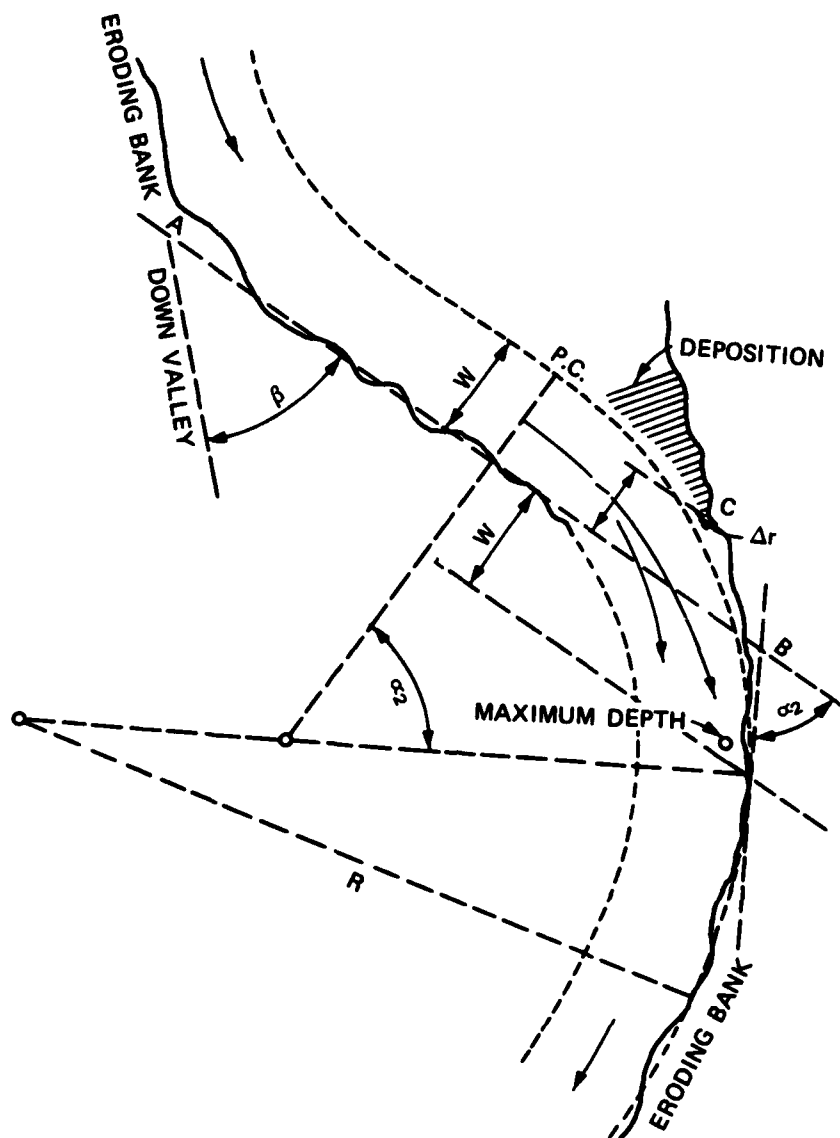


Figure 5. Flow in channel bends after Parsons (1960)

the minimum required for stability. The model bend had a water-surface width of 7 ft in the approach channel and turned an angle of approximately 110 deg. The combinations that were tested are shown in Plates 4-8. The distance W shown in the plates refers to the average water-surface width in the approach channel. The reference line shown on each curve for locating the upstream end of the revetment represents the concept of Parsons. The distance to the downstream end of the revetment is referenced to the end of the channel bend. The result of

terminating the revetment too soon on the downstream end is shown in Figure 6 (corresponds to Plate 6) where the right bank has eroded downstream of the revetment. The result of not extending the revetment far enough upstream is shown in Figure 7 (corresponds to Plate 7) where considerable erosion occurred upstream of the revetment and flanking might eventually fail the revetment. The minimum distances for extension of bend revetment found to be stable in the model were an upstream distance of $1.0W$ and a downstream distance of $1.5W$. Revetment downstream of the bend should possibly be extended to the crossover of flow to the opposite bank rather than some function of the channel width. These results are only qualitatively indicative of one condition and should be used with caution because of the many site specific factors involved in even one bend and flow condition. The significant finding of these tests is that money spent on protection techniques is better spent extending the protection downstream rather than upstream.



Figure 6. Limits of attack showing effect of terminating revetment too soon on downstream end



Figure 7. Limits of attack showing effect of not extending revetment far enough upstream

14. Tests were conducted to determine the minimum height of revetment required for stability in the sand model. Revetments were placed at 40, 60 and 80 percent of the depth of flow at the maximum discharge above the toe in the sand model. A cross section is shown in Figure 8. The four hydrograph cycles were run through the model and only 80 percent H revetment resulted in a rate of erosion that was

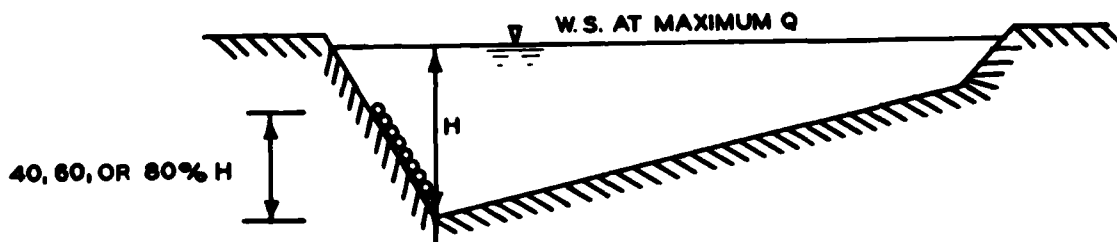


Figure 8. Cross section of sand model

acceptable. However, the required revetment height would be greatly affected by soil type, level of vegetal cover, and shape of the hydrograph. Use of a reduced height of protection would not apply where wave action (wind or navigation) was present. This concept is essentially the same as the riprap toe protection or reinforced revetment.

15. Riverbed scour during passage of floods is a severe threat to protective measures in an alluvial river. Many protective measures fail not because of high velocity or tractive force but due to undermining of the toe of the structure. Design guidance for scour protection generally states that protection should be extended to the maximum depth of scour but no one has an accepted method for predicting scour depth. Leopold, Wolman, and Miller (1964) reference several case histories of riverbed scour during flood passage. The Colorado River near Lees Ferry experienced a flood during which the discharge went from approximately 5,000 to 63,000 cfs; the bed scoured a maximum of 7 to 8 ft during the flood. The San Juan River experienced a flood in 1941 during which the discharge ranged from 635 to 59,600 cfs; the bed scoured a maximum of 10 ft during the flood passage.

16. Blench (1957) states that maximum scour in channel bends measured below the water surface of the peak flood is 1.7 times the regime depth of the approaching or upstream channel. This applies to a freely meandering channel without obstacles that interfere in any way with normal meander curvature. Regime depth is used by Blench as the depth at the annual flood.

17. Foley (1975) reports on a model and field investigation of scour in ephemeral streams. He concluded that scour during floods that is generally attributed to general scour over a long reach is likely due to bed-form migration in the stream. Measured scour depths in the field by Foley showed a maximum scour of 24 cm below the normal bottom for a bank-full depth of 23 cm above the normal bottom. In a second runoff event a maximum scour of 66 cm occurred for a bank-full flow depth of 34 cm. These measurements were compared with the amplitude of antidunes and shown to be within the range of computed antidune height.

18. Crews (1970) reports on a commonly used rule which probably

has some basis in past experience of placing protection down to 5 ft vertically below the existing bed.

19. Alvarez (1977) reported an analysis of scour in channel bends based on very limited field data or application. Alvarez gives the equation for the maximum depth of flow in the bend as:

$$H_{\max} = \epsilon H_{re}$$

where H_{\max} = maximum depth of flow in the bend

ϵ = coefficient depending on width/radius ratio (see tabulation below)

H_{re} = maximum depth in the straight reach

	B/R*					
	0.5	0.333	0.25	0.20	0.166	0
Coefficient ϵ	3.0	2.57	2.2	1.84	1.48	1.27

* B = channel water-surface width in upstream straight reach.

R = channel bend center-line radius.

This approach is similar to the regime approach discussed by Blench.

20. Apmann (1972) investigated the relation between the maximum depth/mean depth in a channel bend as a function of the width/radius ratio. Results from 18 different cross sections on Buffalo Creek, New York, are shown in Figure 9 along with predictive equations by Chatley (1931), Boussinesq, and Apmann (1972). The Apmann equation is:

$$\frac{h_m}{\bar{h}} = \frac{(n+1)(w/r_o)}{1 - (1 - w/r_o)^{n+1}}$$

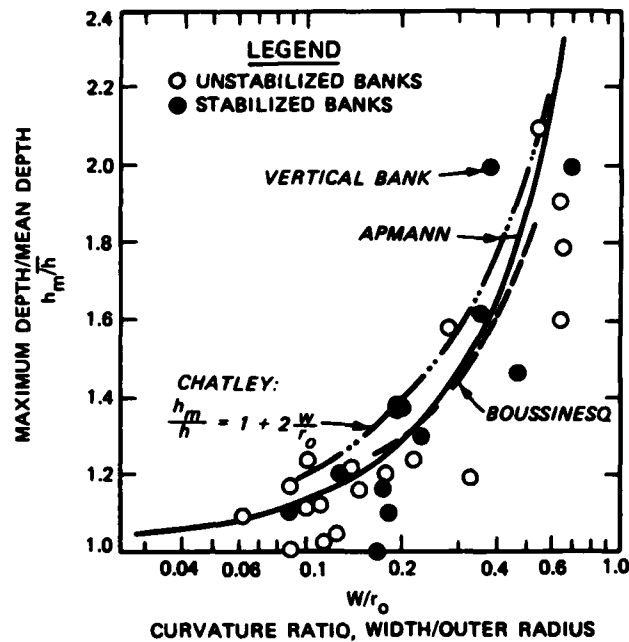
where

h_m = maximum depth

\bar{h} = mean depth

r_o = outer radius of curve
 w = width of channel
 n = coefficient

Figure 9. Relation of maximum depth to curvature ratio (Apmann 1972)



The coefficient n was found to be 2.5 for Buffalo Creek bends. Apmann suggests that the value n can be determined for a given stream for use in predicting maximum depths for flows larger than those for which data were collected. This maximum depth will then aid in the design of the depth of the toe of the bank protection required to prevent undermining.

Grid

21. The next protection technique tested in the model was the grid or honeycomb concept which would have an open bottom and top that could be square, rectangular, triangular, or possibly hexagonal. The inside of the grid could be empty, backfilled with native bank or bed material, or filled with rock much smaller in size than that required for a standard revetment. Anchoring of the grid might be necessary if the material used to construct the grid was lightweight. This concept has been used in the USSR (Balanin and Bykov 1965) to protect a

navigation channel from wave attack of passing ships. The insides of the grids used were filled with small rock. The idea behind the grid is that the sides will withstand and break up the forces generated by wave or channel flow. The key element in using the grid is finding a construction material that will satisfy strength and cost requirements. Webster and Watkins (1977) reported on the use of plastic to construct a grid for providing a stable base for roadway construction.

22. A plastic grid unit (Figure 10) was placed in the channel model to demonstrate and evaluate this concept. The grid was placed

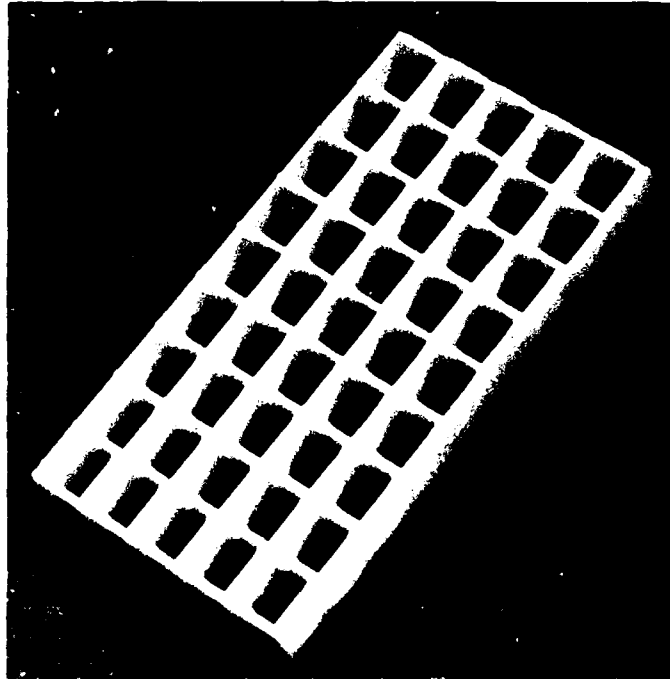
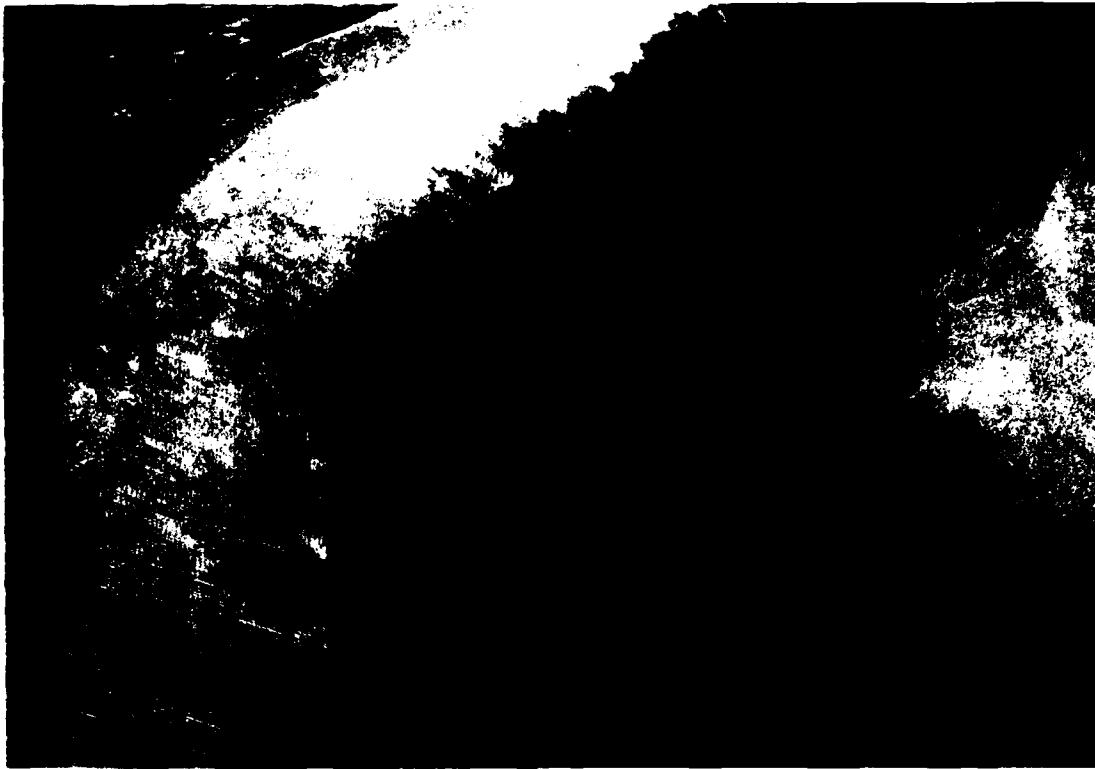


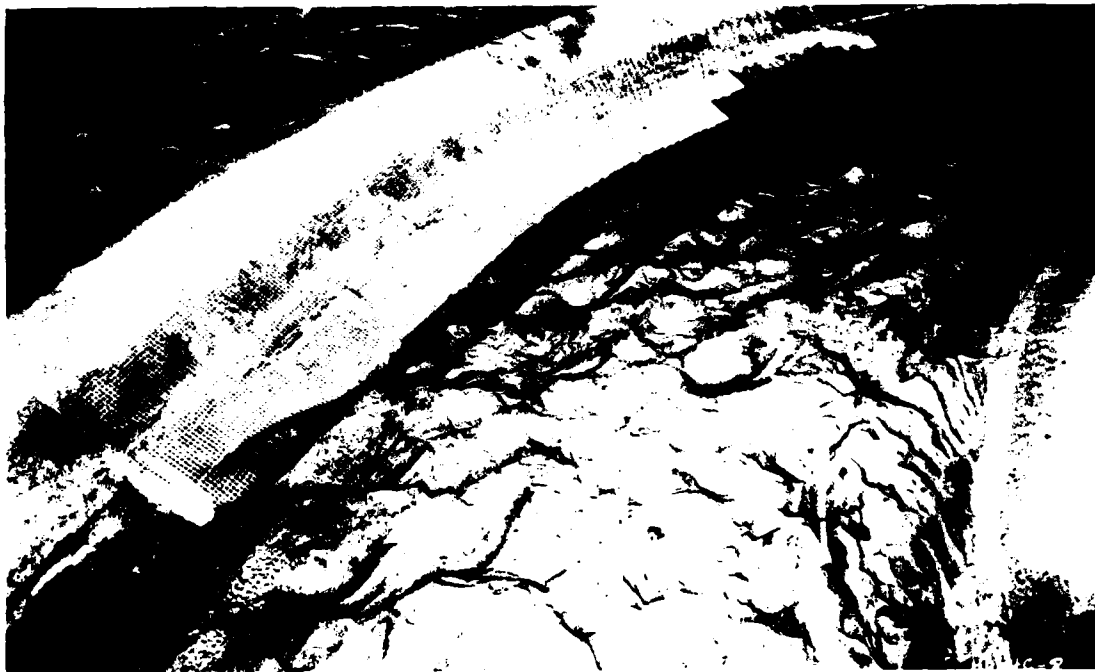
Figure 10. Plastic model grid unit

along the outer bank of the channel bend (Figure 11a) and the openings were filled with sand. The hydrograph was run through the model four times and the conditions after flow are shown in Figure 11b. The sand was removed from the individual cells and many of the grid units were moved off the bank. The greatest attack and resulting failure of the grid occurred at the toe of the slope.

23. Next, the grid units were anchored to the bank and backfilled with small rock at the upstream section of the bend and sand at the downstream section (Figure 12). The hydrograph was run through the



a. Before flow



b. After flow

Figure 11. Grid placed on concave bank

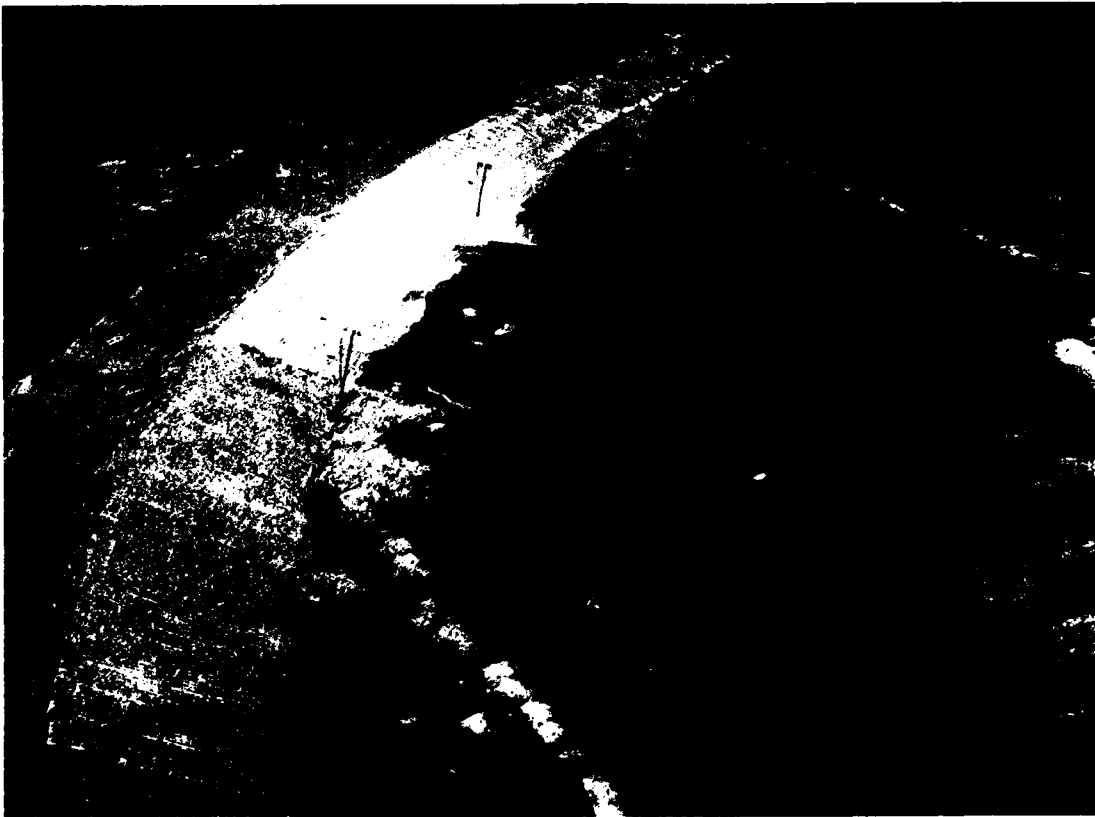


Figure 12. Anchored riprap-filled and sand-filled grids, before flow

model four times and the sand-filled section received the most severe damage. Units on the upper portions of the bank were relatively stable with only some of the sand removed from the individual cells. Units on the lower bank failed because all the sand was removed from the individual cells and because the toe was undermined. The riprap-filled section was stable on the upper bank and only a small amount of stone was removed from the lower bank units. However, failure resulted because of undermining of the toe of the bank. The grid concept also has potential for stabilizing banks subjected to wave attack, and wave tests were conducted under the Section 32 Program to evaluate the grid concept (Appendix B-8).

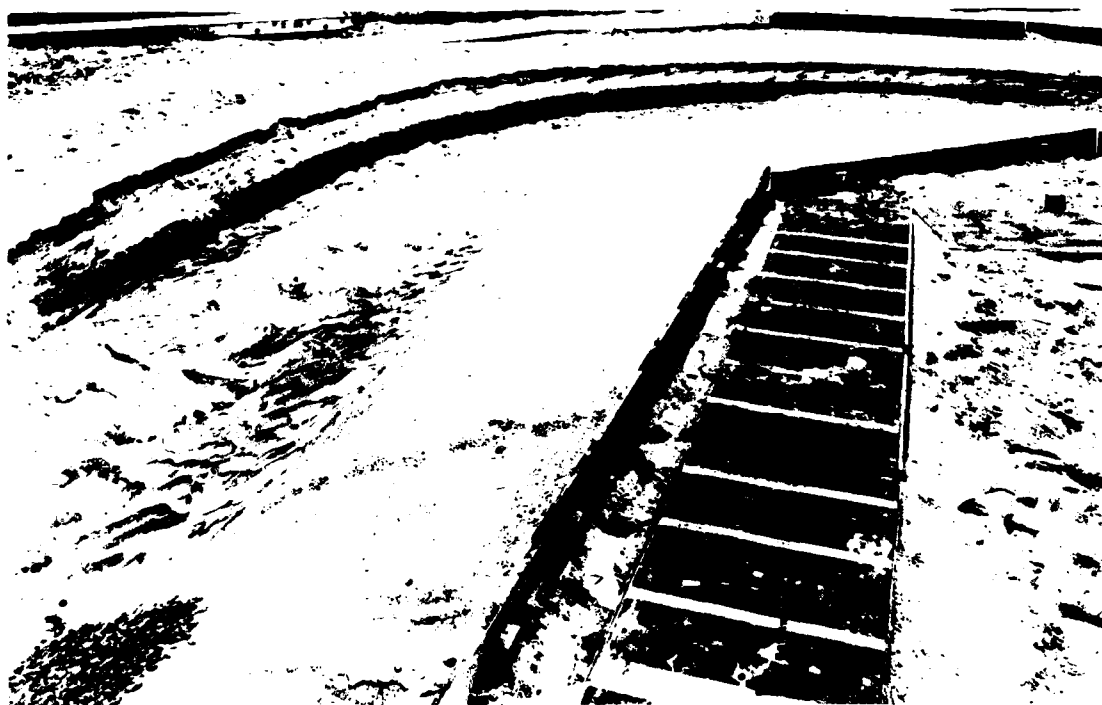
Riprap Toe Protection

24. The next protection technique evaluated was riprap toe protection or longitudinal stone dikes which is a component of reinforced revetment. This technique was used on several demonstration sites of the Section 32 Program. Riprap toe protection has potential for lower cost because only the lower portion of the streambank is protected. In one prototype installation on Batupan Bogue, Mississippi, bank shaping was not done and the riprap toe protection was installed after only clearing the bank. The idea behind this protection method is that the riprap placed at the toe will protect against the more frequent low flows and withstand the high-intensity attack that occurs at the toe of the bank. The upper bank could be vegetated to withstand the less frequent and less severe attack that occurs on the upper bank. Tiebacks are recommended with the toe protection to prevent flanking. The rock toe should have an amount of rock sufficient to launch to the maximum depth of scour. Unfortunately, generalized criteria for determining the maximum depth of scour for a given flood event are not available (paragraphs 15-20). Rock amounts used on streams in Mississippi have ranged from 1-1/2 to 4 tons per linear foot of bank. Criteria on the height of the toe are also limited. The observed or predicted annual flood stage is one possibility for sizing the toe.

25. Riprap toe protection was placed in the sand model (Figure 13a) to evaluate performance and compare with several prototype sites located in the Yazoo River Basin, Mississippi. The rock toe was placed approximately at the same height as the stage corresponding to the low flow (0.6 cfs) in the model. Four hydrograph cycles were run through the model and the after-flow condition is shown in Figure 13b. Considerable toe degradation and launching of the stone occurred during the flow. Without tiebacks substantial erosion of the upper bank occurred which eventually flanked the toe protection in the model. This erosion is similar to that observed in a Section 32 demonstration site located on Batupan Bogue, Mississippi, where riprap toe protection was used in a channel bend without tiebacks. The upper bank was graded but



a. Before flow



b. After flow

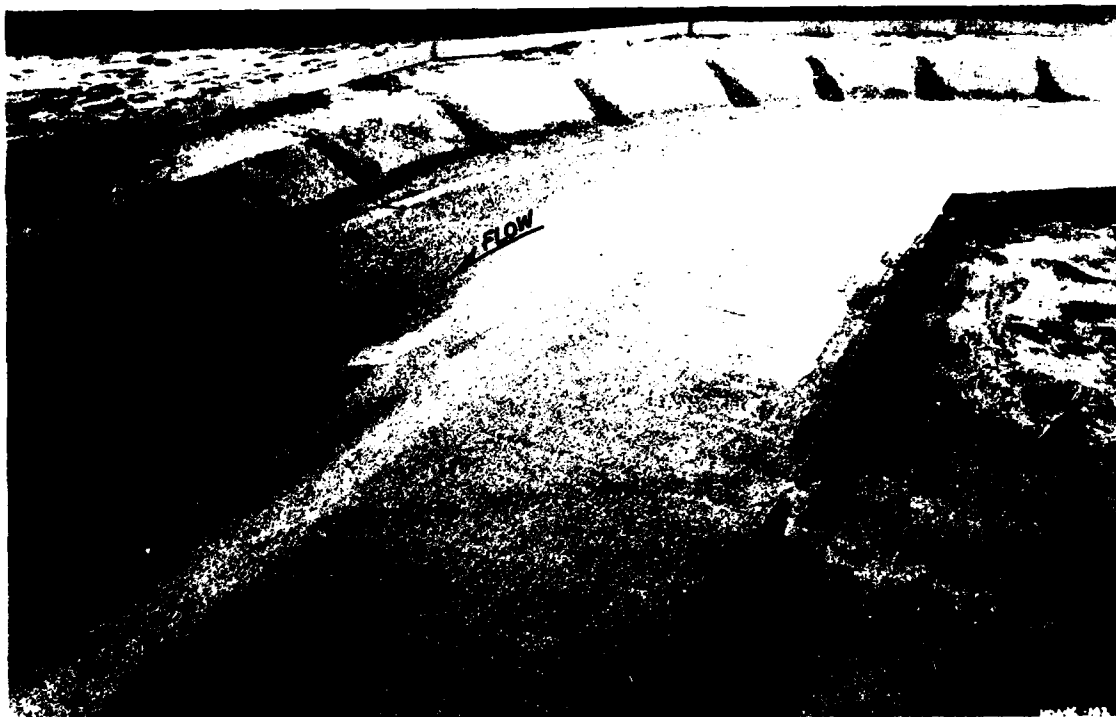
Figure 13. Riprap toe protection

vegetation had not established before a peak discharge occurred and severe erosion of the upper bank occurred.

Riprap Hard Points

26. Riprap hard points are a protection technique designed to provide erosion resistance points that keep the higher velocities away from the channel boundary. Limited erosion is expected between the hard points but the proper spacing is achieved when this erosion reaches an equilibrium condition before flanking the hard point. Hard points have an advantage in that bank grading is not necessary and rock can be dumped over the existing bank to form the hard point. Research has been conducted by the MRD Mead Hydraulic Laboratory investigating the required spacing of hard points in straight or mildly curved reaches. Past field experience has indicated that hard points may not be effective in sharp channel bends because the increased angle of attack requires a close hard-point spacing to prevent flanking. One prototype site on the South Fork, Tillatoba Creek, Mississippi, had hard points in a sharp channel bend and significant erosion had taken place between the hard points and flanking was a possibility.

27. Limited model evaluation of hard points in a sharp channel bend was conducted to supplement field observations. A series of hard points were installed in the sand model in a 100-deg channel bend as shown in Figure 14a. The spacing of the hard points was two times the depth of flow at the maximum discharge at the upstream end of the bend and three times the depth of flow at the downstream end of the bend. The four hydrographs were run through the model and the after-flow condition is shown in Figure 14b. The bank experienced minor erosion between the closely spaced hard points at the upper end of the bend. More severe erosion occurred between the hard point at the downstream end of the bend which was caused by the greater hard-point spacing and possibly more severe attack at the downstream portion of the bend. Considering the relatively large amount of rock required for each hard point, a riprap revetment would probably require less rock than hard points for protecting sharp channel bends.



a. Before flow



b. After flow

Figure 14. Riprap hard points

B-1-21

Wire Fence Retards

28. Wire fence retards are not a new idea for bank protection but have been used in the Section 32 Program because of the relative low cost and potential for use by landowners.

Retards are placed parallel to erodible banks of channels on stable gradients where the prime purpose is to lessen the tangential or impinging stream velocities sufficiently to prevent erosion of the bank and to induce deposition. As a remedial measure, the prime purpose may be deposition near the bank in deep channels or restoration of an eroded bank by accretion (Soil Conservation Service 1977).

Fence-type retards are used on smaller streams of less frequent and shorter duration flood-flow attack. All-metal types, such as pipe-and-wire or rail-and-wire, are preferred over wire and wooden posts due to fire loss of wooden posts from vandalism or brush fires.

The principal difference between fence retards and ordinary wire fences is that the posts of retards must be driven sufficiently deep to avoid loss by scour. Permeability can be varied in the design to fit the requirements of the location. For single fences, the factor most readily varied is the pattern of the wire mesh. For multiple fences, the mesh pattern can be varied or the space between fences can be filled to any desired height. Making optimum use of local materials, this fill may be brush ballasted by rock, or rock alone. (California Highway Department 1970).

One problem observed by Bondurant (1977) was the formation of random gravel bars by high flows so that intermediate and low flows are diverted through the fence to attack the bank. Ilk (1963) reported that a single wire fence with 6-in. mesh was used on the lower Colorado River. Initially these structures were reasonably successful, because the river was still carrying a fairly high sediment concentration. However, as the channelization activities began to reduce the sediment load of the river, it was found that these structures no longer performed satisfactorily. It soon became evident that with the velocities of 3 to 6 fps encountered along these banks, the sediment concentration in the flow

had to be about 700 parts per million to obtain adequate deposition. Steinberg (1960) reported a successful application of a single wire fence retard used on the Russian River. The 4-in. wire mesh fence was placed along the toe of a 10- to 15-ft-high bank and brush was placed between the bank and fence. Acheson (1968) reports that the height of the fence should be at about the annual flood level. O'Brien (1951) reported on both field and laboratory investigations of a pervious fence for bank protection. The following conclusions resulted from both the model and field studies:

- a. The amount of protection provided by a fence will vary with the size of the mesh of fencing, depth of water, location of fence in channel, amount of debris present, etc.
- b. A fence covered with debris or backed up with brush can be expected to give much more protection to the banks than the fence alone.
- c. Vegetation planted on the channel banks should add considerably to their protection.
- d. Tiebacks of impervious construction should give much more protection than those constructed of pervious material.
- e. Tiebacks of impervious construction placed at a 45-deg angle to the flow and pointing downstream are better than those placed normal to the flow.

The model study indicated that a fence of about half the water depth in height proved as effective as one extending well above the waterline. However, no prototype experience relative to fence height was obtained in the field study.

29. Several fencing schemes were evaluated in the sand model. A single-row wire fence retard with tiebacks is shown in Figure 15a. The tiebacks are used to prevent flanking and promote deposition behind the fences. The four hydrograph cycles were run through the model and the after-flow condition is shown in Figure 15b. Substantial toe scour took place at the base of the fence. This scour and the deposition and sloughing behind the fence resulted in failure of several sections of the fence.

30. Next a double-row wire fence similar to that used in prototype sites on both Tillatoba Creek, Mississippi, and Gering Valley Drain, Nebraska, was placed in the sand model. The test reach is shown



a. Before flow

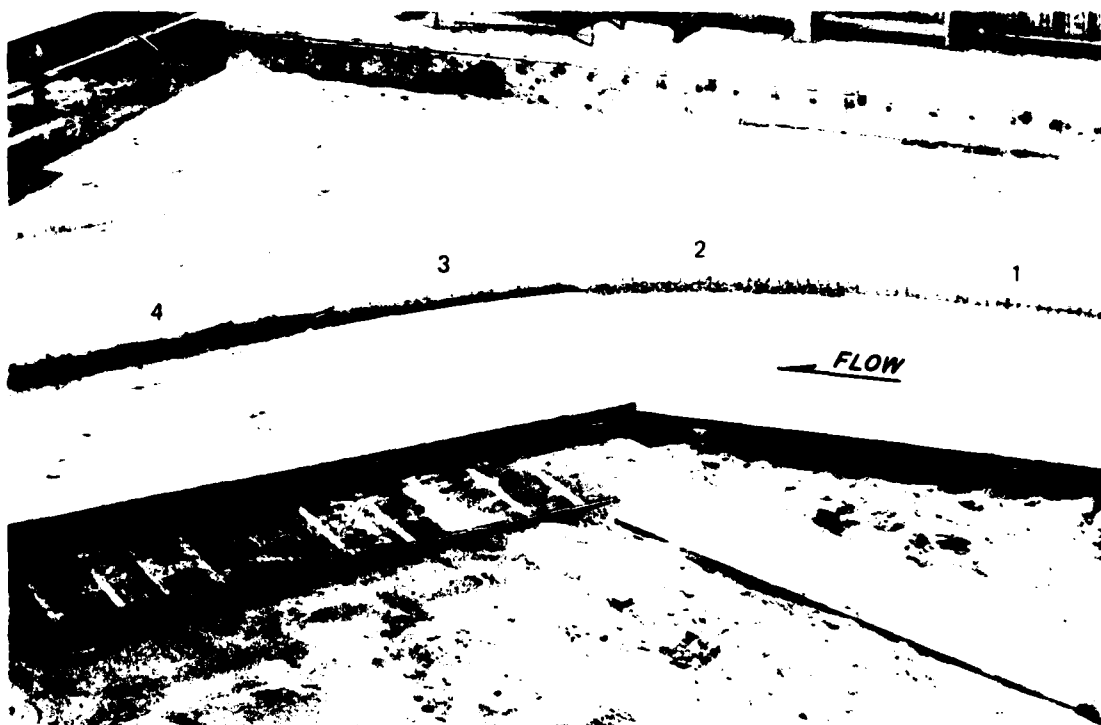


b. After flow

Figure 15. Single-row wire fence retard

B-1-24

in Figure 16a and consists of four different types. The first (upstream) section consists of a double-row wire fence without toe protection. The second section consists of a double-row wire fence with riprap placed on the channel side of the fence to provide toe protection. The third section consists of a double-row wire fence with riprap placed inside the fencing to provide toe protection. The fourth section consists of trees and debris anchored to posts at the toe of the slope. The hydrograph was run through the model four times and after-flow conditions are shown in Figure 16b. The unprotected fencing experienced degradation at the lower end of section 1 which would have ultimately failed the fence. Section 2 was in the area of most severe attack and considerable degradation occurred at the toe of the fence but the riprap launched and protected the toe from undermining. The third section suffered minor attack at the toe and rock launched to protect the toe from undermining. The fourth section remained stable but did not experience as severe attack as sections 2 and 3.



a. Before flow



b. After flow

Figure 16. Double-row wire fence retard, anchored debris

PART IV: SUMMARY AND DISCUSSION OF RESULTS

31. Maximum velocities along the concave bank of channel bends can range up to 1.8 times the average channel velocity based on observations in several California rivers and the sand model used in this investigation.

32. The maximum shear or tractive force that occurs in channel bends depends upon curvature ratio, surface roughness, and upstream conditions. Maximum values can range up to three times the average shear in the approach channel.

33. The limits of attack in a channel bend were shown to begin at a point 1.0 channel width upstream of the reference line A-B in the sand model tests. The downstream limit was found to be 1.5 channel widths downstream of the end of the bend but this distance is probably related to the point of crossover rather than some function of channel width.

34. Riverbed scour in channel bends is probably one of the more prevalent causes of failure of protective works placed in the prototype. The literature reveals several methods for computing the maximum depth in channel bends but none of these methods has been verified in the field to the extent that they may be used for design.

35. The key to successfully using the grid concept is finding a construction material that will satisfy strength and cost requirements. Lightweight materials used in the model required anchoring. The grid concept is particularly useful when rock of an adequate size is not available and small rock is inexpensive and readily available.

36. Toe protection with tiebacks was used successfully at many Section 32 sites. The required height of the toe and the volume of material required to prevent undermining are key design parameters that are being addressed in the field demonstration projects. Vegetation should be used to provide stability between tiebacks on the upper bank. Both riprap and gabions were used as toe protection in the model.

37. Riprap hard points require close spacings in sharp channel

bends to prevent flanking but have the advantage of not requiring any significant bank preparation.

38. Fencing is a low-cost method of bank protection that has been used for many years. Toe protection is essential and can be provided by rock placed at the toe of the fence or by extending the support post well below the anticipated scour. Regular maintenance is required.

REFERENCES

- Acheson, A. R. 1968. "River Control and Drainage in New Zealand," Ministry of Works, New Zealand, p 95.
- Al-Shaik, H. K. 1964. Flow Dynamics in Trapezoidal Open Channel Bends, Ph. D. Dissertation, Colorado State University, Fort Collins, Colo.
- Alvarez, J. A. M. 1977. "Scour in River-Beds," Research Institute of Engineering, UNAM, pp 53-55.
- Apmann, R. P. 1972 (May). "Flow Processes in Open Channel Bends," Journal, Hydraulics Division, American Society of Civil Engineers, Vol 98, No. HY5, Proceedings Paper 8886, pp 795-810.
- Balanin, V. V., and Bykov, L. S. 1965. "Selection of Leading Dimensions of Navigation Canal Sections and Modern Methods of Bank Protection," XXIst Permanent International Navigation Congress, Section 1, Subject 4, pp 151-170.
- Blench, T. 1957. "Regime Behaviour of Canals and Rivers," London.
- Bondurant, D. C. 1977. "Sedimentation Engineering," Chapter V, American Society of Civil Engineers M and R No. 54, p 537.
- California State Highway Department. 1970. "Bank and Shore Protection in California Highway Practice."
- Castle, G. H. 1956. "Attack Velocities Against Banks at River Bends," Office Memorandum, U. S. Army Engineer District, Sacramento, Sacramento, Calif.
- Chatley, H. 1931. "Curvature Effects in Alluvial Channels," Engineering, Vol 131, London.
- Crews, J. E. 1970 (Feb). "Bank Stabilization in Susquehanna River Basin," Journal, Waterways and Harbors Division, American Society of Civil Engineers, Vol 96, No. W1, Proceedings Paper 7061, pp 87-95.
- Einstein, H. A., and Harder, J. A. 1954 (Feb). "Velocity Distribution and Boundary Layer at Channel Bends," Transactions, American Geophysical Union, Vol. 35, No. 1, pp 114-120.
- Foley, M. G. 1975 (Nov). "Scour and Fill in Ephemeral Streams," Report No. KH-R-33, California Institute of Technology, Pasadena, Calif.
- Illk, F. K. 1963. "Methods and Criteria for Bank Protection on the Lower Colorado River," Proceedings of the Federal Interagency Sedimentation Conference, Miscellaneous Publication 970, U. S. Dept. of Agriculture, pp 366-372.
- Ippen, A. T., et al. 1960 (Oct). "The Distribution of Boundary Shear Stresses in Curved Trapezoidal Channels," MIT Technical Report No. 43, Cambridge, Mass.
- Leopold, L. B., Wolman, M. G., and Miller, J. P. 1964. "Fluvial Processes in Geomorphology."

O'Brien, J. T. 1951. "Studies of the Use of Pervious Fence for Stream-bank Revetment," Report No. A-70.1, U. S. Dept. of Agriculture, SCS; prepared by California Institute of Technology, Pasadena, Calif.

Parsons, D. A. 1960 (Apr). "Effects of Flood Flow on Channel Boundaries," Journal, Hydraulics Division, American Society of Civil Engineers, Vol 86, No. HY4, Proceedings Paper 2443, pp 21-34.

Rozovski, I. L. 1957. "Flow of Water in Bends of Open Channels," Academy of Sciences of the Ukrainian SSR, Kiev.

Simons, D. B., Li, R. M., and Schall, J. D. 1979 (Sep). "Spatial and Temporal Distribution of Boundary Shear Stress in Open Channel Flows," Colorado State University; prepared for National Science Foundation.

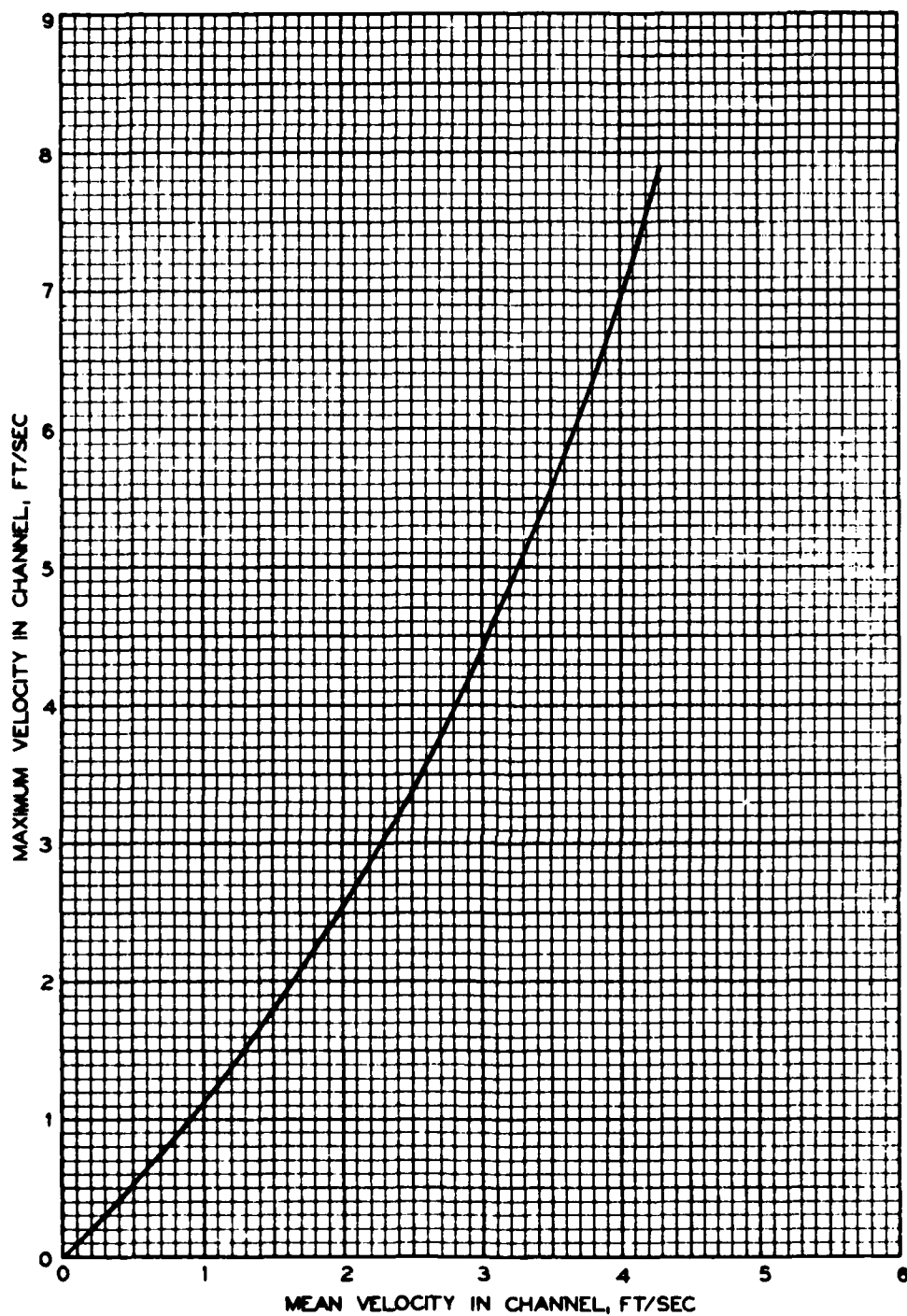
Soil Conservation Service. 1977 (Oct). "Design of Open Channels," Technical Release No. 25, U. S. Dept. of Agriculture.

Steinberg, I. H. 1960 (Nov). "Russian River Channel Works," Journal, Waterways and Harbors Division, American Society of Civil Engineers, Vol 86, No. WW4, Proceedings Paper 2647, pp 17-32.

Webster, S., and Watkins, J. E. 1977 (Feb). "Investigation of Construction Techniques for Tactical Bridge Approach Roads Across Soft Ground," Technical Report S-77-1, U. S. Army Engineer Waterways Experiment Station, CE, Vicksburg, Miss.

Wylie, K. F., Alonso, C. V., and Coleman, N. L. 1977. "Some Stochastic Properties of Turbulent Tractive Forces in Open-Channel Flows," paper presented to Turbulence in Liquids Conference, Rolla, Mo.

Yen, B. C. 1965. "Characteristics of Subcritical Flow in a Meandering Channel," Institute of Hydraulic Research, University of Iowa, Iowa City, Iowa.



**RELATION BETWEEN MEAN
AND MAXIMUM VELOCITIES
IN RIVER BENDS
(AFTER CASTLE (1956))**

PLATE 1

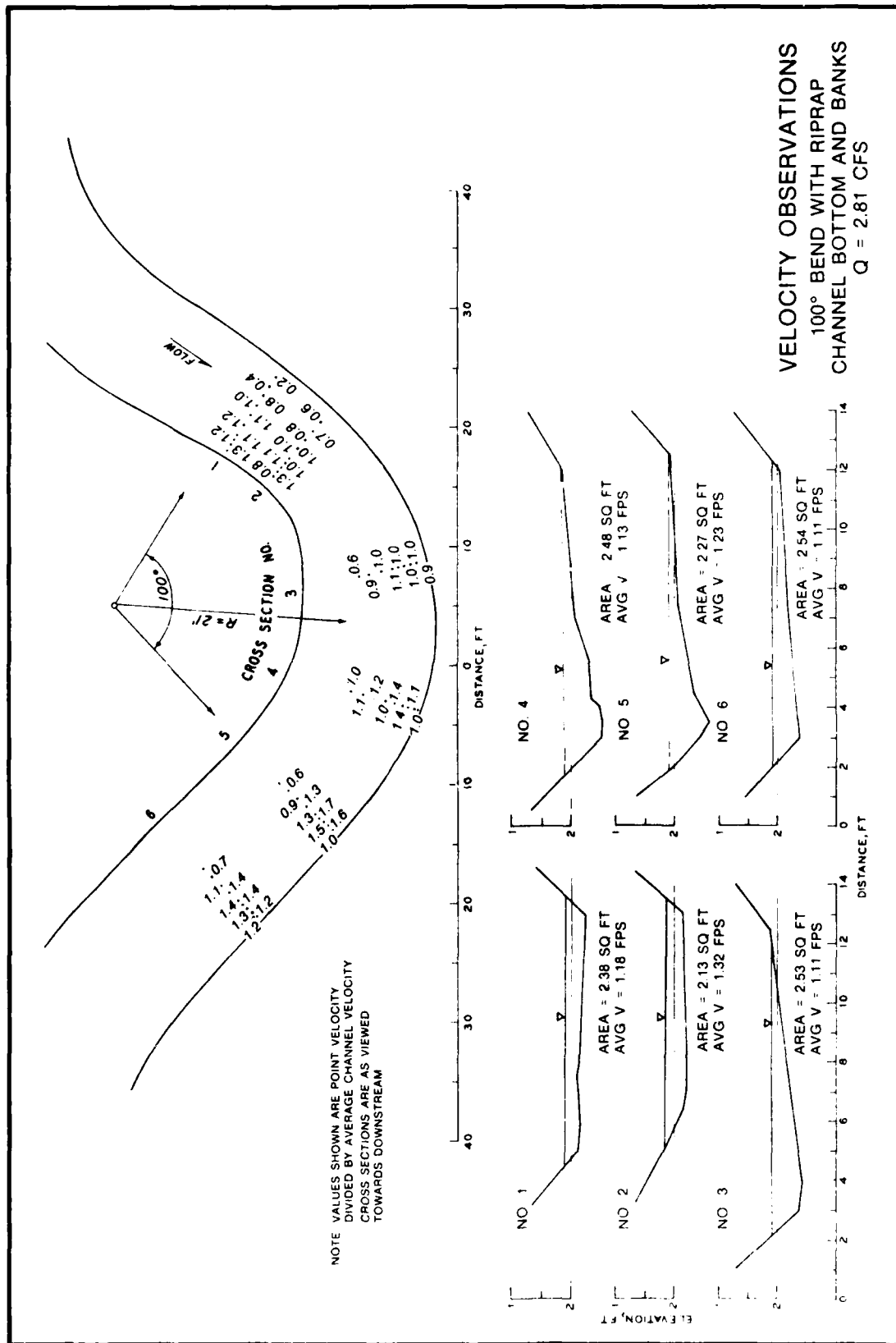
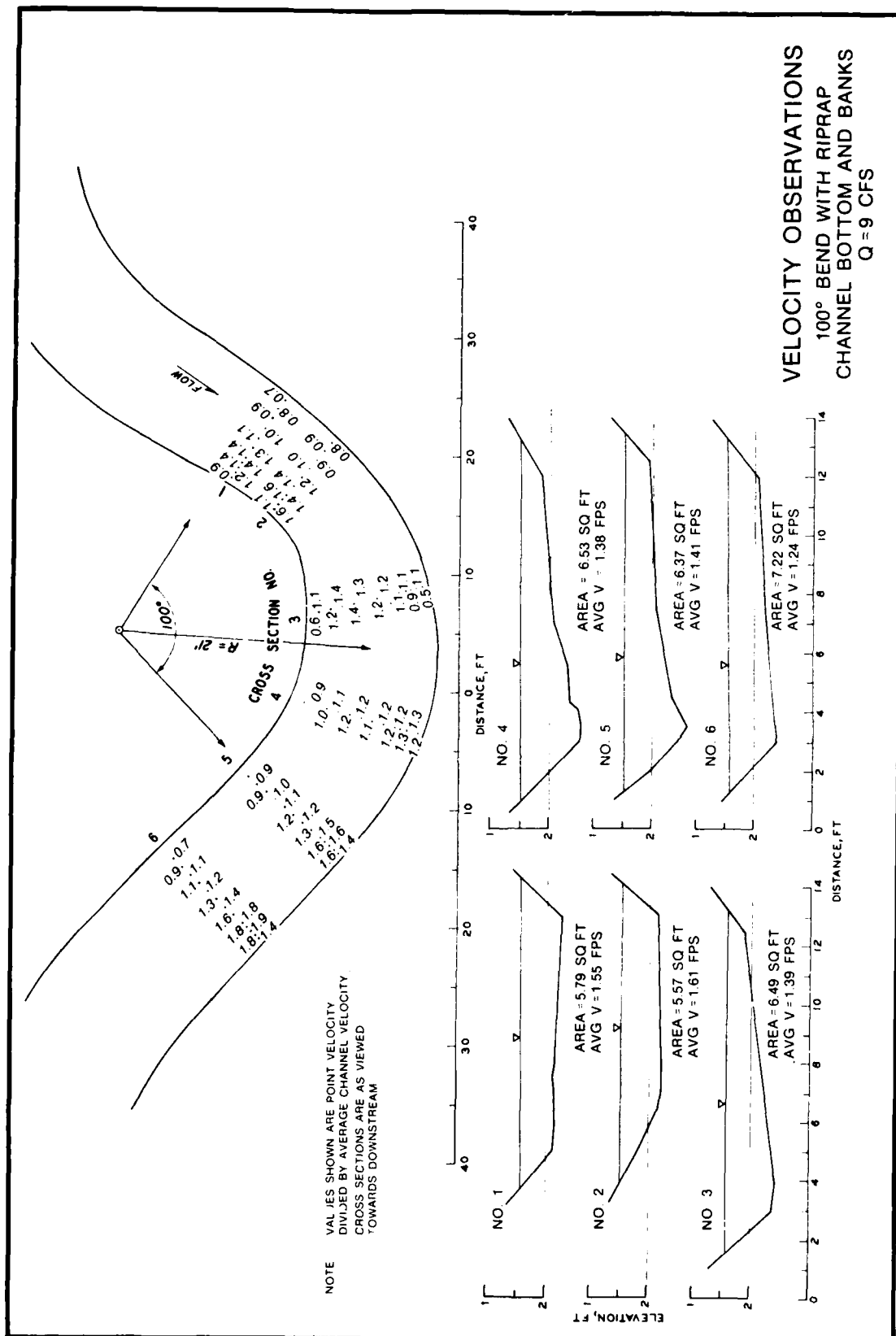


PLATE 2



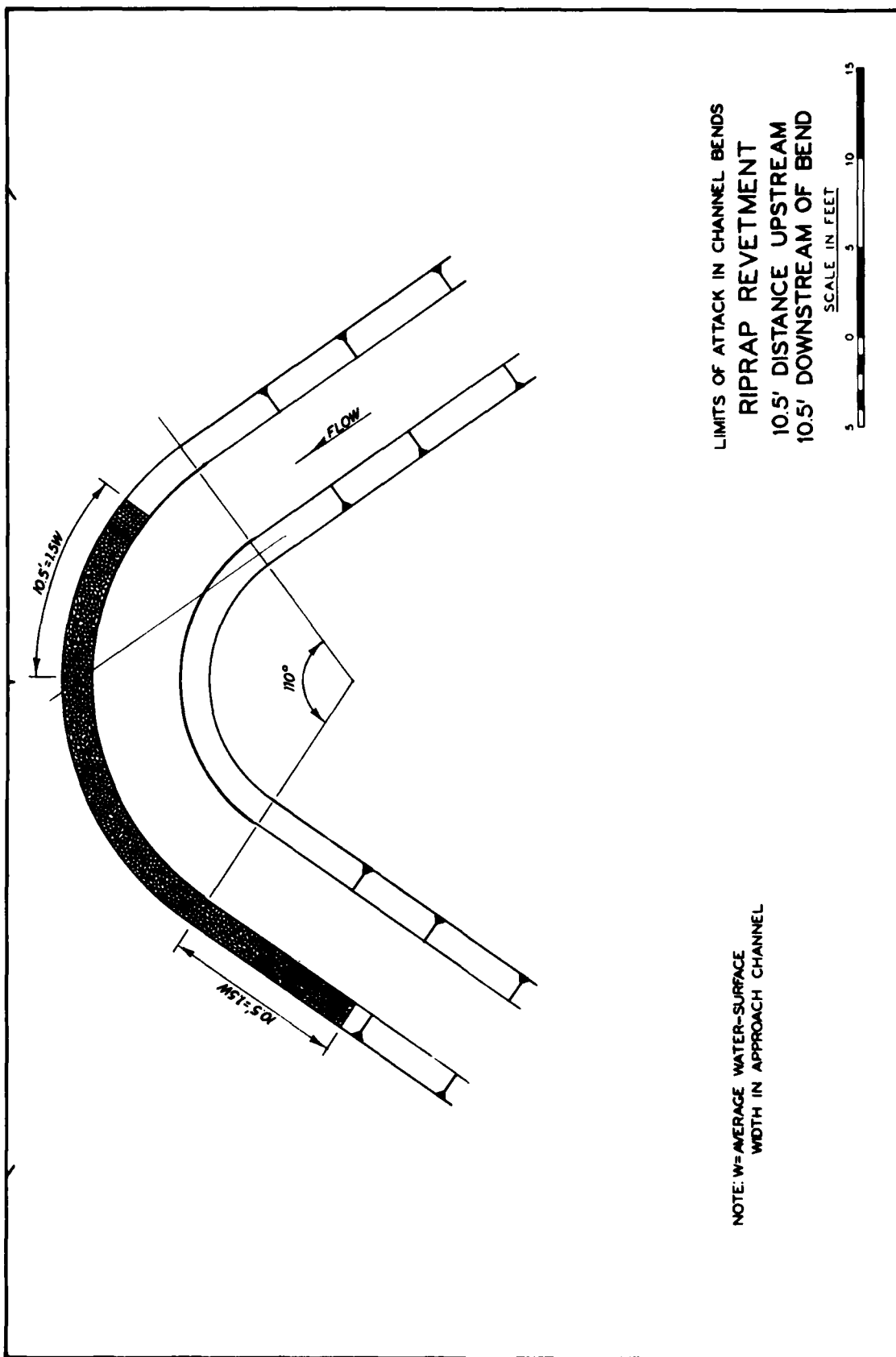


PLATE 4

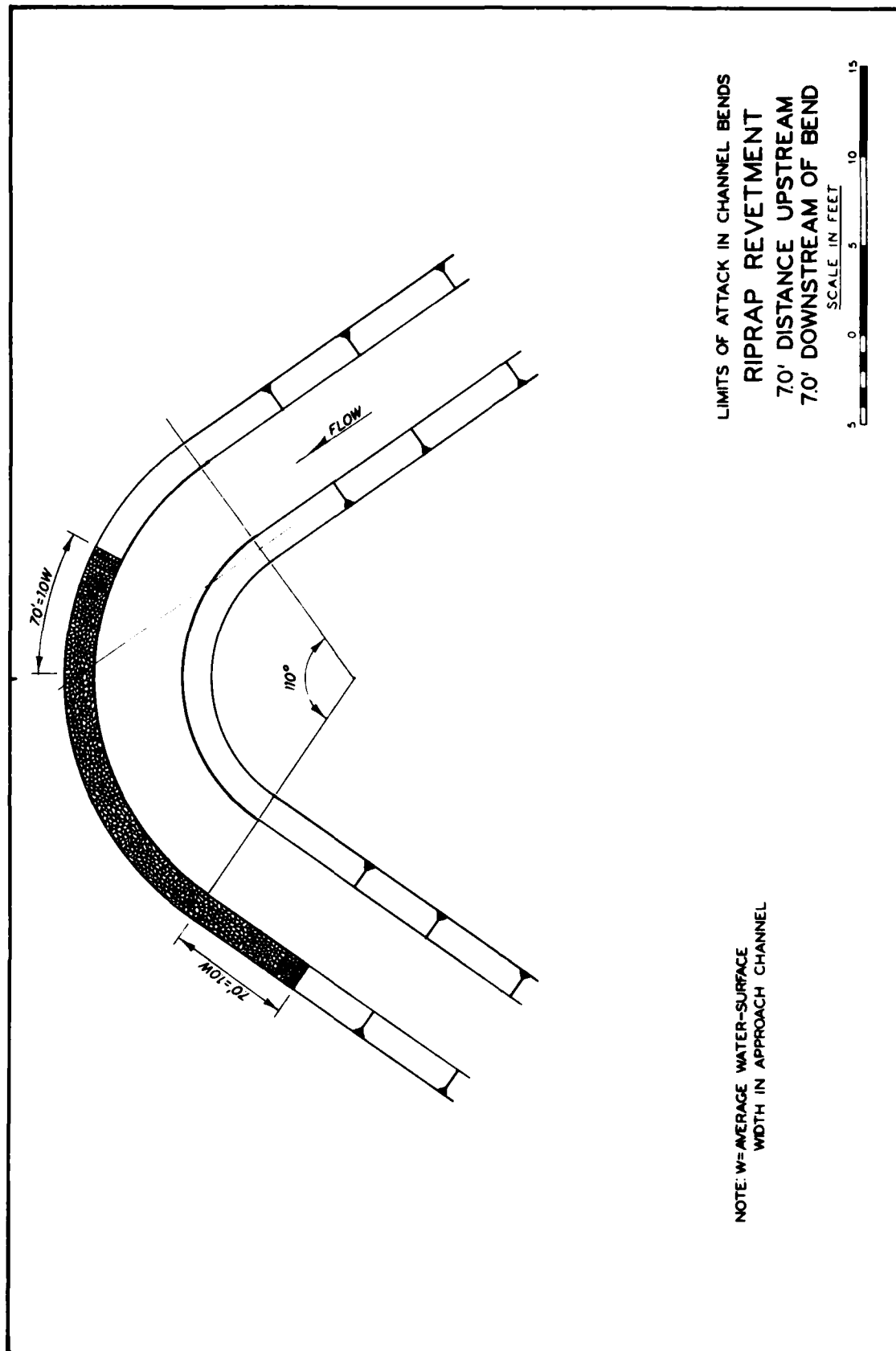


PLATE 5

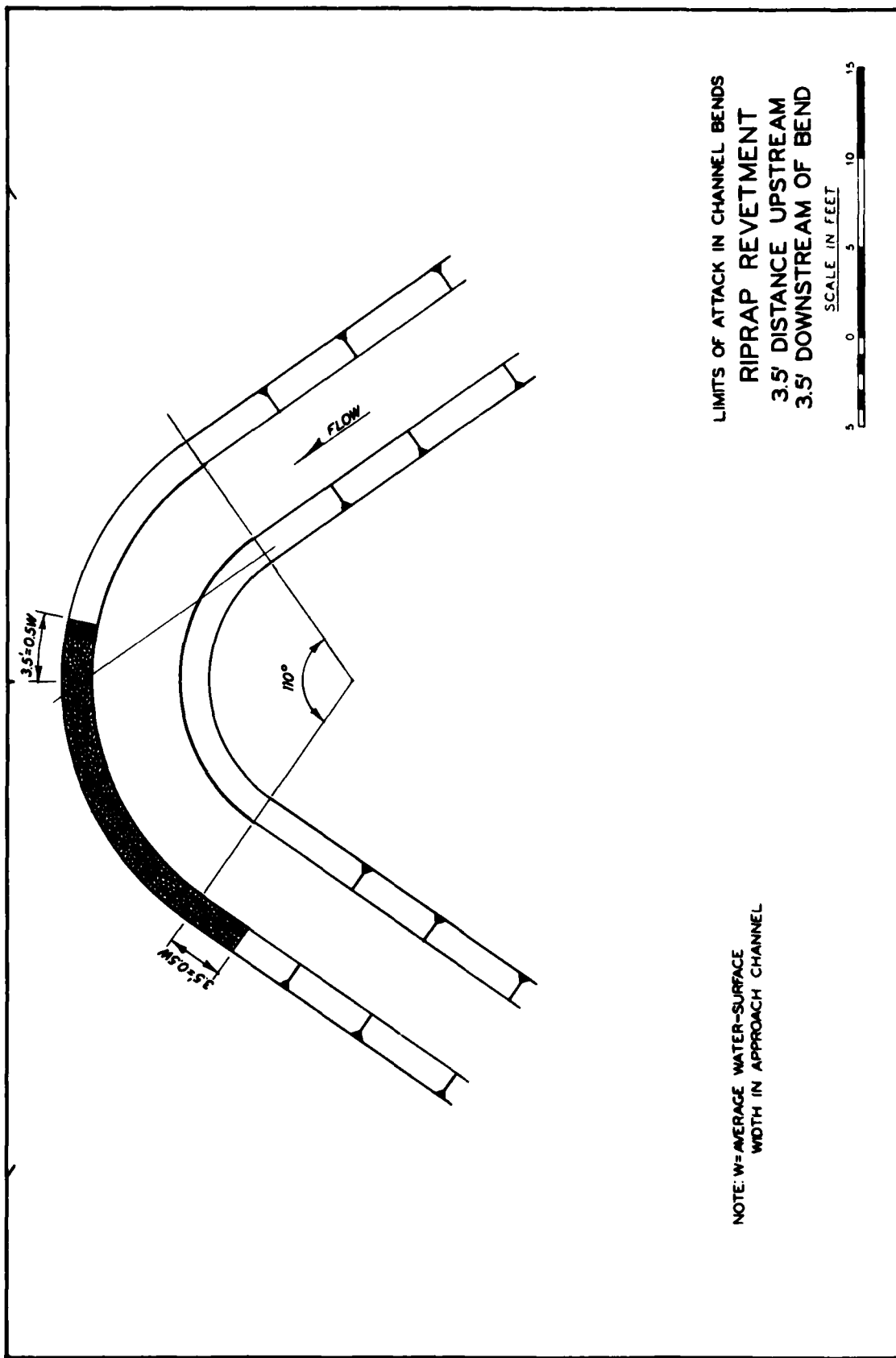


PLATE 6

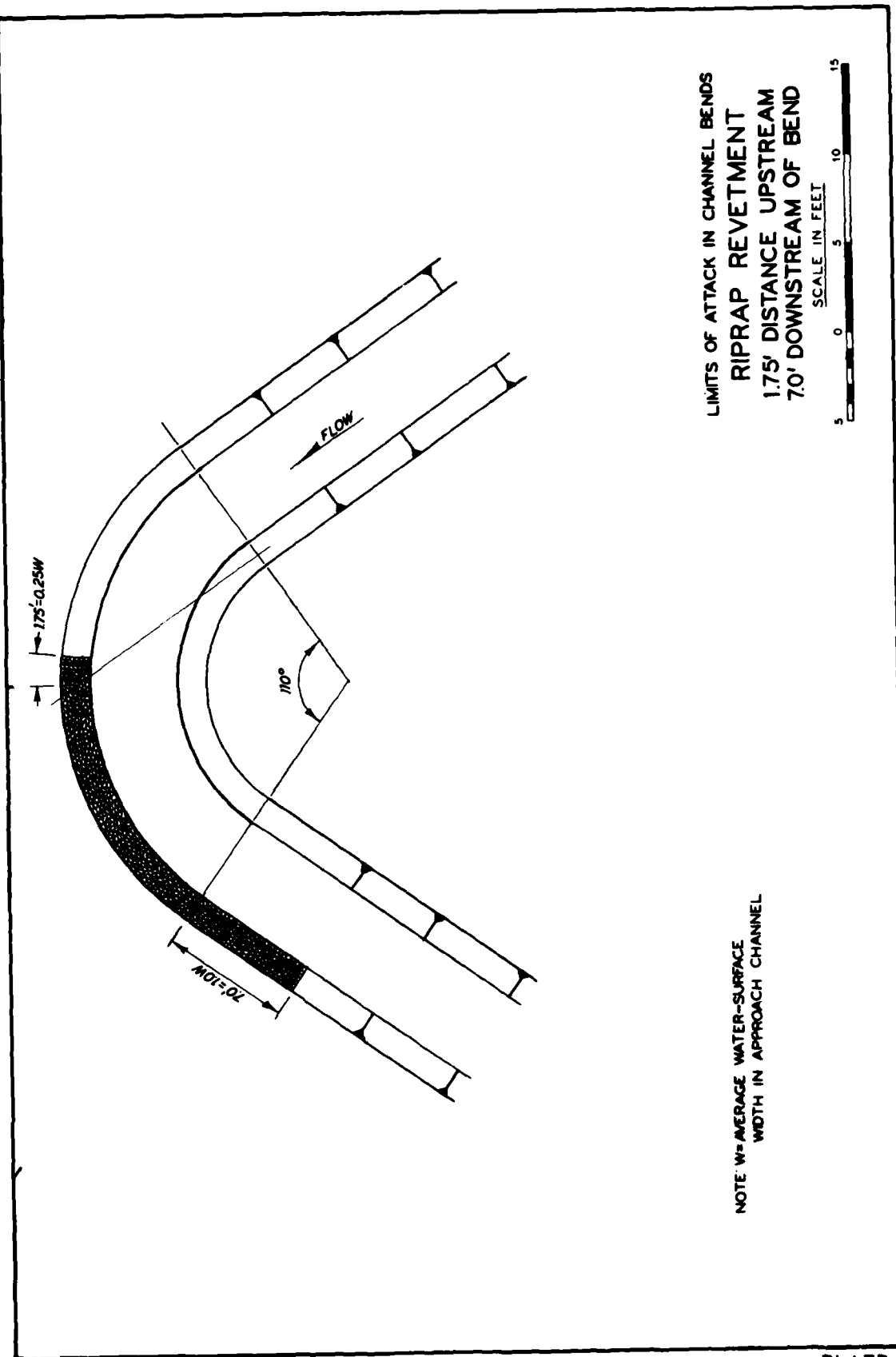


PLATE 7

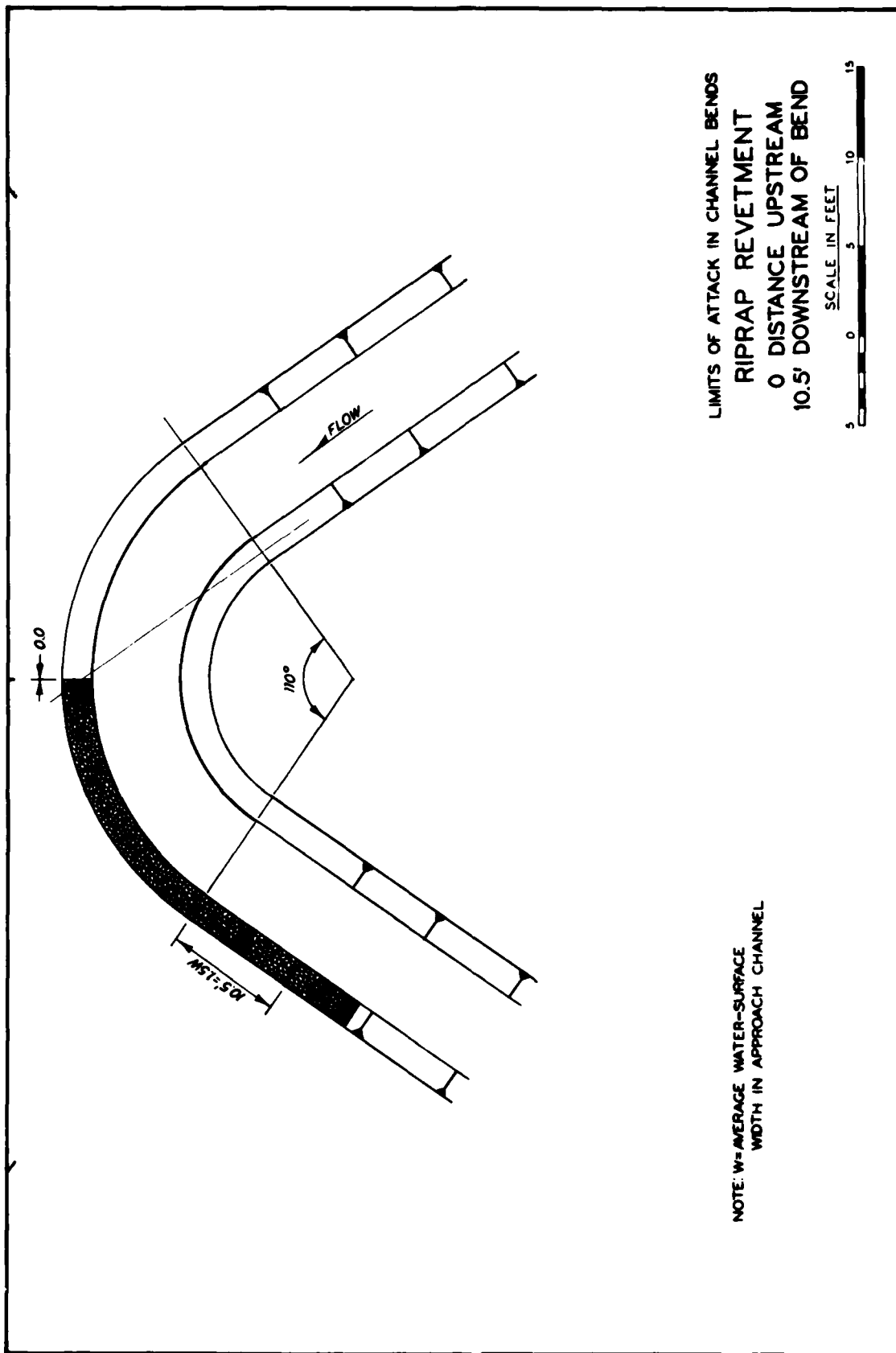


PLATE 8

BANK PROTECTION TECHNIQUES USING SPUR DIKES

SECTION 32 PROGRAM
STREAMBANK EROSION CONTROL EVALUATION AND DEMONSTRATION
BANK PROTECTION TECHNIQUES USING SPUR DIKES

Introduction

1. Spur dikes have been used extensively in all parts of the world as river training structures to enhance navigation, improve flood control, and protect erodible banks. A spur dike can be defined as an elongated obstruction having one end on the bank of a stream and the other end projecting into the current. It may be permeable, allowing water to pass through it at a reduced velocity; or it may be impermeable, completely blocking the current. Spur dikes may be constructed of permanent materials such as masonry, concrete, or earth and stone; semipermanent materials such as steel or timber sheet piling, gabions, or timber fencing; or temporary material such as weighted brushwood fascines. Spur dikes may be built at right angles to the bank or current, or angled upstream or downstream. The effect of the spur dike is to reduce the current along the streambank, thereby reducing the erosive capability of the stream and in some cases inducing sedimentation between dikes.

2. Although the use of spur dikes is extensive, no definitive hydraulic design criteria have been developed. Design continues to be based primarily on experience and judgment within specific geographical areas. This is primarily due to the wide range of variables affecting the performance of the spur dikes and the varying importance of these variables with specific applications. Parameters affecting spur dike design include: width, depth, velocity, and sinuosity of the channel; size and transportation rate of the bed material; cohesiveness of the bank; and length, width, crest profile, orientation angle, and spacing of the spur dikes.

3. This report is concerned with the use of impermeable spur dikes as a bank protection technique in a concave bend of a meandering stream. Design guidance drawn from several sources and reviewed herein

is generally based on experience and judgment on a variety of rivers throughout the world. A model study was conducted to evaluate several parameters relating to spur dike design. This study was not a scale model of any particular stream and was intended to demonstrate qualitatively the effect of various parameters on bank protection. These parameters include the spacing-to-length ratio and the orientation angle. The effect of an apron or mattress at the toe of the dike was also demonstrated.

Development of Spur Dike System Layout

Angle of dike to bank

4. The orientation of spur dikes (which is generally defined by the angle between the downstream streambank and the axis of the dike) has typically been determined by experience in specific geographical areas and by preference of engineers. There is considerable controversy as to whether spur dikes should be oriented with their axis in an upstream or downstream direction. Proponents of an upstream orientation claim that flow is repelled from dikes pointed upstream while flow is attracted to the bank by dikes slanted downstream. Sedimentation is more likely to occur behind spur dikes angled upstream so that less protection is required on the bank and on the upstream face of the dike. Advocates of a downstream orientation argue that turbulence and scour depths are less at the end of the spur dike when it is angled downstream. In addition, the more a spur dike is angled downstream the more the scour hole is angled away from the dike. Trash and ice are less likely to accumulate on dikes angled downstream. To date there has not been a sufficiently comprehensive series of tests either in the field or by model to settle this controversy. Therefore, it is often recommended that spur dikes be aligned perpendicular to the flow lines.

5. After reviewing spur dike applications in the rivers of Europe and America, Thomas and Watt (1913) concluded that the various alignments were probably of slight importance. Franzius (1927) reported that spur dikes directed upstream are superior to normal and downstream-oriented

spur dikes with respect to bank protection as well as sedimentation between the dikes. Water flowing over downstream-oriented spur dikes and normal to the axis is directed toward the bank, making submerged dikes with this alignment especially undesirable. A less adamant position was taken by Strom (1941), when he reported that the usual practice in New Zealand was to incline impermeable groins slightly upstream, but that downstream-oriented spur dikes had also been used successfully. Strom states that a spur dike angled downstream tends to swing the current below it toward midstream; this has a reflex action above the dike which may induce the current to attack the bank there. Thus, downstream-oriented dikes should only be used in series so that the downstream protection afforded by each dike extends to the one below it. The United Nations (1953) reported that the present practice was to construct spur dikes either perpendicular to the bank or to orient them upstream. This publication states that downstream-oriented dikes tend to bring the scour hole closer to the bank. An upstream dike angle varying between 100 and 120 deg was recommended for bank protection. The Indian Central Board of Irrigation and Power (1956), in their manual for river training, strongly discouraged the use of downstream-oriented dikes stating that a dike with such an orientation "invariably accentuates the existing conditions and may create undesirable results." Dikes with angles between 100 and 120 deg are recommended. Mamak (1964), reporting primarily on river training experiences in Poland, stated that dikes are usually set perpendicular to the flow or set upstream at angles between 100 and 110 deg. Lindner (1969), reporting on the state of knowledge for the U. S. Army Corps of Engineers, recommended perpendicular dikes except in concave bendways where they should be angled sharply downstream. Neill (1973) recommended using upstream-oriented dikes. After reviewing much of the literature on spur dikes Richardson and Simons (1973) recommended perpendicular spur dikes, suggesting that dikes with angles between 100 and 110 deg could be used to channelize or guide flow. Reporting on model tests and field experiences in Mexico, Alvarez recommended spur dikes with angles between 70 and 90 deg. In sharp or irregular curves the angle should be less, even as low as

30 deg. His studies indicated that upstream orientations called for smaller separations between spurs to achieve the same degree of bank protection. In the United States, the U. S. Army Corps of Engineers (1978) has generally oriented its spur dikes perpendicular or slightly downstream. On the Missouri River, dikes are generally oriented downstream with an angle of 75 deg. On the Red and Arkansas Rivers, dikes were placed normal to flow or at angles of 75 deg. The Memphis and Vicksburg Districts use perpendicular dikes. The St. Louis District uses both perpendicular and downstream-oriented dikes. The Los Angeles District (1980) uses dikes with an angle of 75 deg. As late as 1979, Jansen (1979) concluded that there is no definite answer as to whether spur dikes should be oriented upstream or downstream, and recommended using the cheapest solution--that being the shortest connection between the end of the dike and the bank. This corresponds with Lindner (1969) who stated that there has not been a sufficiently comprehensive series of tests either in the field or by model to conclude that any acute or obtuse angle for the alignment at dikes is superior or even as good as perpendicular to flow.

Spacing of spur dikes

6. The spacing between spur dikes has generally been related to the effective length (perpendicular projection) of the dike, although the bank curvature, flow velocity, and angle of attack are also important factors. The ratio of spur dike length to spacing required for bank protection is less than that required for navigation channels, as the primary purpose is to move the eroding current away from the bank and not necessarily to create a well-defined deep channel. Design guidance from several sources for spacing of spur dikes for bank protection is given in Table 1.

Local Scour at Spur Dikes

7. Intense vortex action is set up at the streamward end of a spur dike. Intermittent vortices of lesser strength occur along both the upstream and downstream faces of the dike. This turbulence causes

Table 1
Spur Dike Spacing for Bank Protection

Spacing	Type of Bank	Reference	Comment
1L	Concave	United Nations (1953)	General practice
2 to 2.5L	Convex	United Nations (1953)	General practice
4 to 6L	Concave	Richardson and Simons (1973)	Bank may need riprap
3L	Concave	Grant (1948)	
5.1 to 6.3L	Straight	Alvarez	
2.5 to 4L	Curves	Alvarez	
2 to 2.5L		CBIP (1956)	
1.5	Concave	Los Angeles District (1980)	Levee protection with riprap
2.0	Straight	Los Angeles District (1980)	
2.5	Convex	Los Angeles District (1980)	
2		Neill (1973)	If two or more dikes
4		Neill (1973)	
3 to 5L		Strom (1941)	

bed material to be suspended, where it becomes easier for the current to carry it downstream. The depth of the scour hole that develops around the spur dike and the angle of repose of the bed material are the primary factors which determine the extent of bank erosion in the vicinity of the dike (Figures 1 and 2). Thus, it is necessary to make an estimate of anticipated scour at the nose of the spur dike in order to provide for a spur dike length that is greater than the length of the scour hole.

8. Currently an established procedure for predicting scour depths at the nose of spur dikes is lacking. The most reliable design procedure would be to estimate scour depths based on experience with

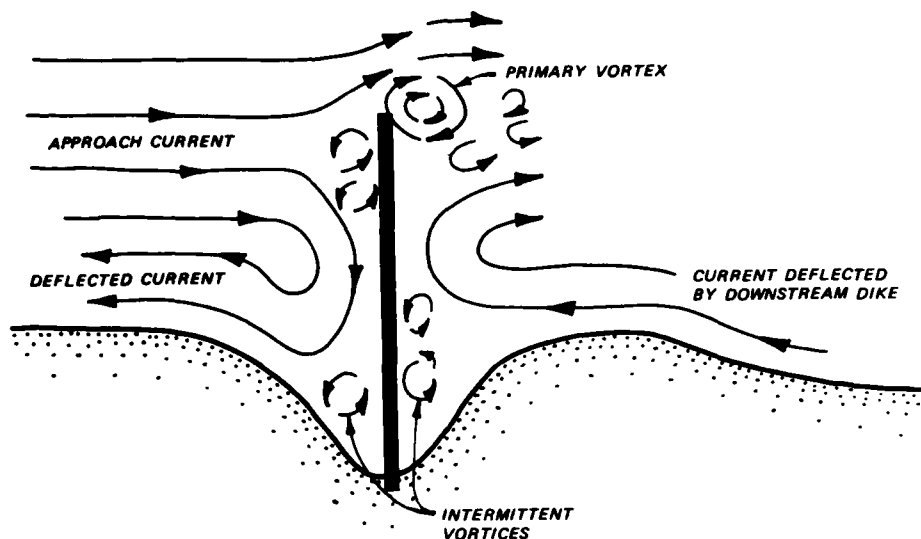


Figure 1. Flow patterns at spur dike

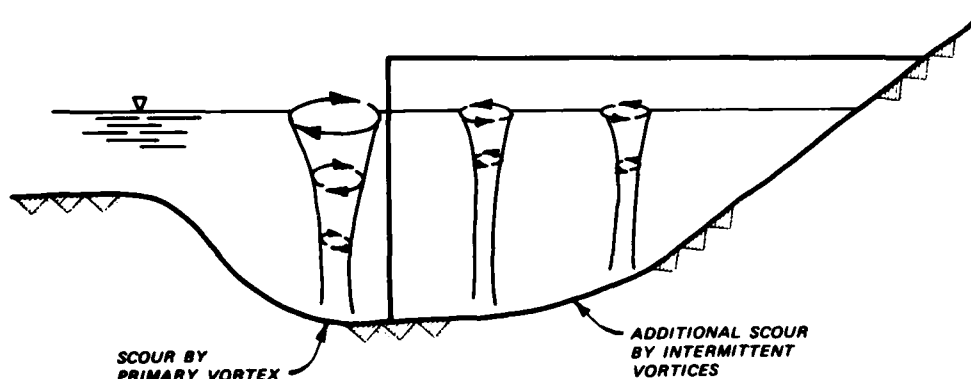


Figure 2. Scour hole profile along spur dike

similar situations in the stream in question. Movable-bed models may be used to give indications of relative scour depths. In the absence of any guidance from the field or models, one of several predictive equations may be used to obtain a rough estimate of scour depth.

9. Several investigators have proposed equations for predicting scour depths at the nose of spur dikes. These equations were derived from tests in laboratory flumes with limited verification by prototype testing. Prototype data are very difficult to obtain due to filling of the scour hole on the recession limb of flood hydrographs, and the

general unpopularity of obtaining data at high river stages when uncomfortable and dangerous working conditions prevail. Some of these equations are listed below; see various references for details and limits of applicability.

$$1. \quad y_s = k \left(\frac{Q}{f} \right)^{0.33} \quad \text{Inglis (1949)}$$

k varies between 0.8 and 1.8

$$2. \quad y_s = k \left(\frac{q^2}{F_{bo}} \right)^{0.33} \quad \text{Blench (1969)}$$

k varies between 2.0 and 2.75

$$3. \quad y_s = kq^{0.67} \quad \text{Ahmad (1953)}$$

$$4. \quad y_s = yK \left(\frac{B_1}{B_2} \right) F_n^n \quad \text{Garde et al. (1961)}$$

$$5. \quad y_s = y + 1.1y \left(\frac{L}{y} \right)^{0.4} F_n^{0.33} \quad \text{Liu et al. (1961)}$$

$$6. \quad y_s = 8.375y \left(\frac{D_{50}}{y} \right)^{0.25} \left(\frac{B_1}{B_2} \right)^{0.83} \quad \text{Gill (1972)}$$

$$7. \quad \frac{L}{y} = 2.75 \frac{y_s - y}{y} \left\{ \left[\frac{1}{r} \frac{(y_s - y)}{y} + 1 \right]^{1.70} - 1 \right\} \quad \text{Laursen (1962a)}$$

B_1 = original channel width

B_2 = constricted channel width

$$C_D = \text{drag coefficient} = 1.33 \frac{\Delta \gamma_s D_{50}}{\omega^2 \rho}$$

D_{50} = median grain size

F_{bo} = Blench's "zero bed factor" = function of grain size

$$F_n = \text{Froude number} = \frac{v}{\sqrt{gy}}$$

$$f = \text{Lacey silt factor} = 1.59 \sqrt{D_{50}} (D_{50} \text{ in mm})$$

g = acceleration due to gravity

k = function of approach conditions--varies with investigator

K = function of C_D --varies between 2.5 and 5.0

L = effective length of spur dike

n = function of C_D --varies between 0.65 and 0.9

Q = total stream discharge

q = discharge per unit width at constricted section

r = assumed multiple of scour at dike compared with scour in a long contraction--taken to be 11.5 by Laursen

v = average velocity in unconfined section

y = average depth in unconfined section

y_s = equilibrium scour depth measured from the water surface

$\Delta \gamma_s$ = difference in specific weight between sediment and water

ρ = mass density of water

ω = settling velocity of sediment

10. There is a general lack of agreement among investigators as to which parameters are most important in determining scour depths. Early investigators found that the contraction ratio and velocity were the most significant parameters. Laursen (1962b) maintains that when

there is sediment movement upstream of the spur dike (which would be true for most alluvial streams but not necessarily true for many laboratory flumes) the scour depth is independent of the contraction ratio and velocity and is primarily a function of the upstream depth and the length of the dike. Liu et al. (1961) and Cunha (1973) also determined that the contraction ratio was not important once sediment movement was established; however, Liu et al. considered velocity to be an important parameter with or without sediment movement. Confusing the issue, in recent studies by Garde et al. (1961) and Gill (1972) it was determined that the contraction ratio was an important parameter, with or without sediment movement. Gill concluded that velocity was not an important parameter; Garde concluded that it was. There is an equal division of opinion on the importance of bed material size. Inglis (1949), Blench (1969), Garde et al. (1961), and Gill (1972) found grain size to be important. Laursen (1962b), Liu et al. (1961), and Ahmad (1953) determined sediment size to be insignificant. These equations are based primarily on results from laboratory testing on a single spur dike in a straight flume. Thus, the effect of current attack angle is generally neglected. Inglis, Blench, and Ahmad provided for a variable coefficient to account for severity of attack, and Laursen and Garde provided for adjustments to account for the orientation angle of the spur dike axis. None of the predictive equations presented herein has attained any widespread acceptance, and it is likely that the contestable issues will remain unsettled until sufficient prototype data are obtained.

Demonstration Model Study

11. Model tests were conducted in a 130- by 50-ft sand bed flume. A meandering stream with three bends was molded in the flume as shown in Figure 3. The channel top width was 8 ft with an average depth of 0.24 ft. The stream sinuosity was 1.6 and the slope was 0.0012. A constant discharge of 2.7 cfs was recirculated through the model except for one test when a discharge of 4.6 cfs was used. There was bed-load movement in the model but no suspended load. The bed material was a

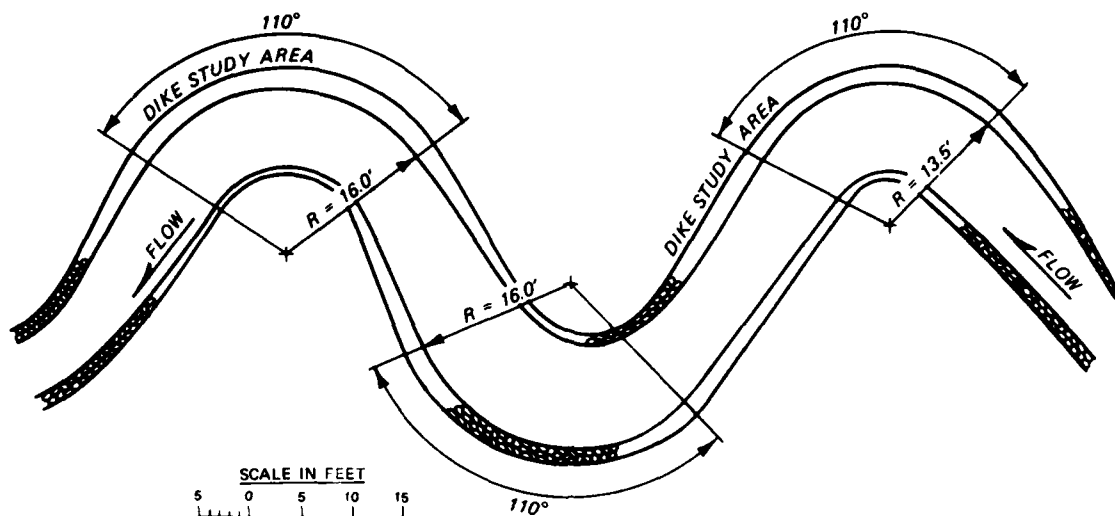


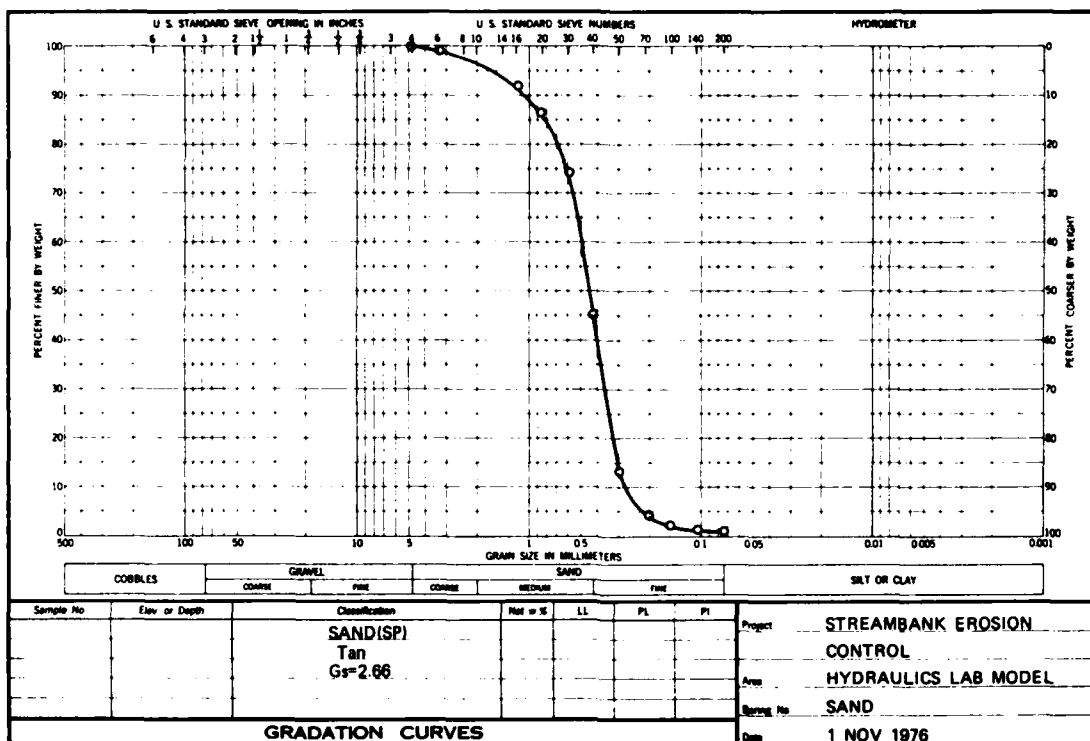
Figure 3. Streambank erosion test facility

medium sand and was recirculated. Velocities were measured at middepth with a paddle-wheel velocity meter. The spur dikes were made of sheet metal representing any relatively narrow impermeable structure. The stream was returned to approximately its original shape at the beginning of each test. Lines, 0.4 ft apart, were spray-painted along the bank for reference. A constant discharge was then run for 24 hr through the model. Most of the significant scour and bank erosion had occurred at the end of 8 hr, after which additional changes occurred slowly so that essentially equilibrium conditions had been achieved by the end of the test period. Effects of various spur dike spacings and orientation angles were then compared.

Effect of the Coarse Fraction of the Bed Material

12. The sand used in the model study was a uniform medium sand ($D_{50} = 0.45$ mm). Gradation curve of the sand was obtained by standard methods (Figure 4). The sand was not sieved prior to being placed in the model and thus may be assumed to represent a typical river sand deposit.

13. At the conclusion of each series of tests an armor layer of coarse material was observed in the scour holes formed at the spur dikes. The grain diameters of the material in these scour holes, as shown in Figure 5, varied between 3 and 30 mm. Thus, all of the armor



ENG FORM 2087
1 MAY 63

Figure 4. Gradation curve

Figure 5. Armor layer in
scour hole



B-2-11

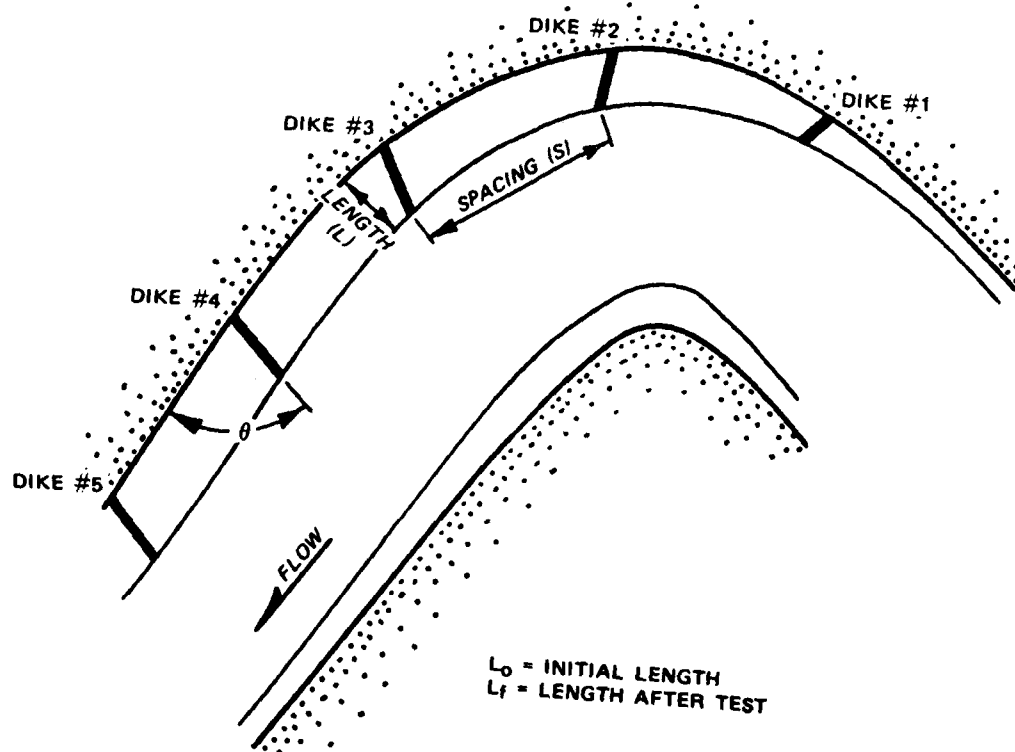
material is larger than d_{95} and much of the material is larger than the maximum size determined in the original gradation analysis. Since the development of this armor layer will affect the potential for scour, it is important that the very coarse fraction of streambed material be identified and considered in the design of spur dikes and other structures subject to extensive local scour.

Effect of Dike Angle

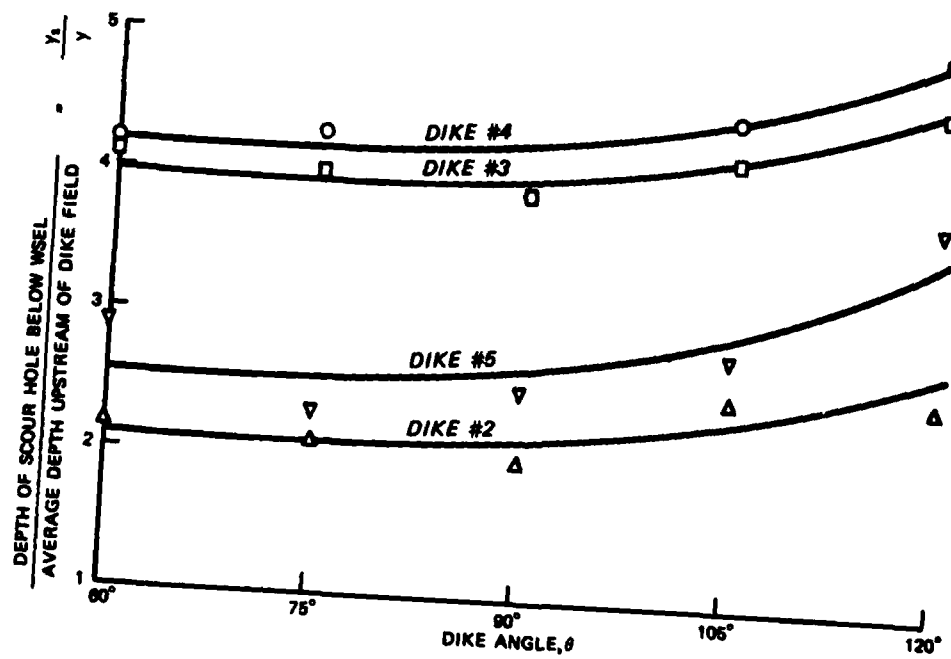
14. Spur dikes with a constant length of 2.2 ft and spacing of 9 ft were set at different angles in order to demonstrate the effect on bank erosion in a concave bend. Tests were run with dike angles of 60, 75, 90, 105, and 120 deg (angle defined in paragraph 5 and Figure 6). Effects of dike angle on scour depth, bank erosion, and deflection of flow were analyzed.

15. The scour depth was found to be more severe for spur dikes with an upstream orientation than for those with a downstream orientation. There was some variability in the extent of armor layer development in the various tests, so that smooth design curves were not developed. Results are shown in Figure 6 and conform to the generally accepted trend as reported by Tison (1962), Laursen (1962b), Ahmad (1953) and Garde et al. (1961). Scour holes for spur dike angles at 60, 75, 105, and 120 deg are shown in Figures 7-10, respectively. These figures indicate that short spur dikes with upstream orientations are just as susceptible to scour as those with downstream orientations. Also, there is no indication that the scour hole is closer to the bank for spur dikes pointed downstream.

16. The effect of spur dike angle on surface flow patterns was demonstrated. These patterns are shown in Figures 11-14 for angles of 60, 75, 105, and 120 deg, respectively. It is apparent that larger eddies are present on the upstream side of spur dikes oriented upstream. This may afford some protection to the spur dike root. However, erosion at the spur dike root is also a function of the extent and depth of the scour hole. Since scour depths are greater for spur dikes with an



a. Dike location



b. Effect of dike angle on scour depths, $F = 0.4$, $S/L_0 = 4.5$
 Figure 6. Spur dike



Figure 7. Scour hole patterns; spur dike angle 60 deg



Figure 8. Scour hole patterns; spur dike angle 75 deg



Figure 9. Scour hole patterns; spur dike angle 105 deg



Figure 10. Scour hole patterns; spur dike angle 120 deg

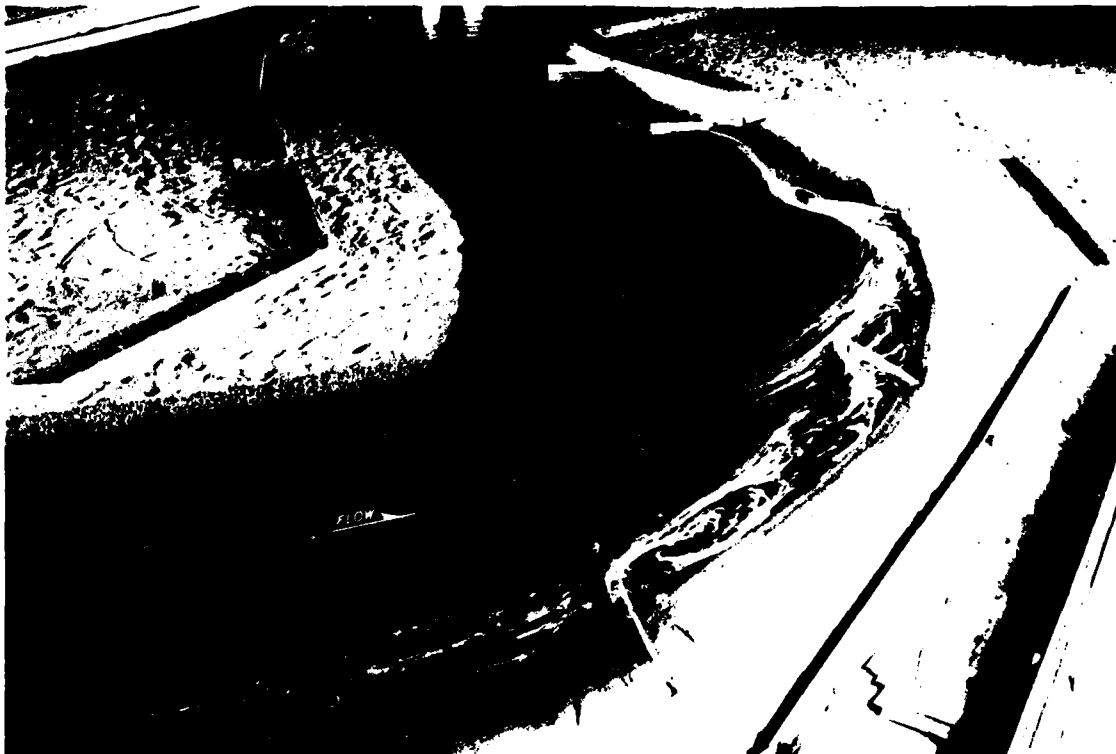


Figure 11. Surface flow patterns; spur dike angle 60 deg

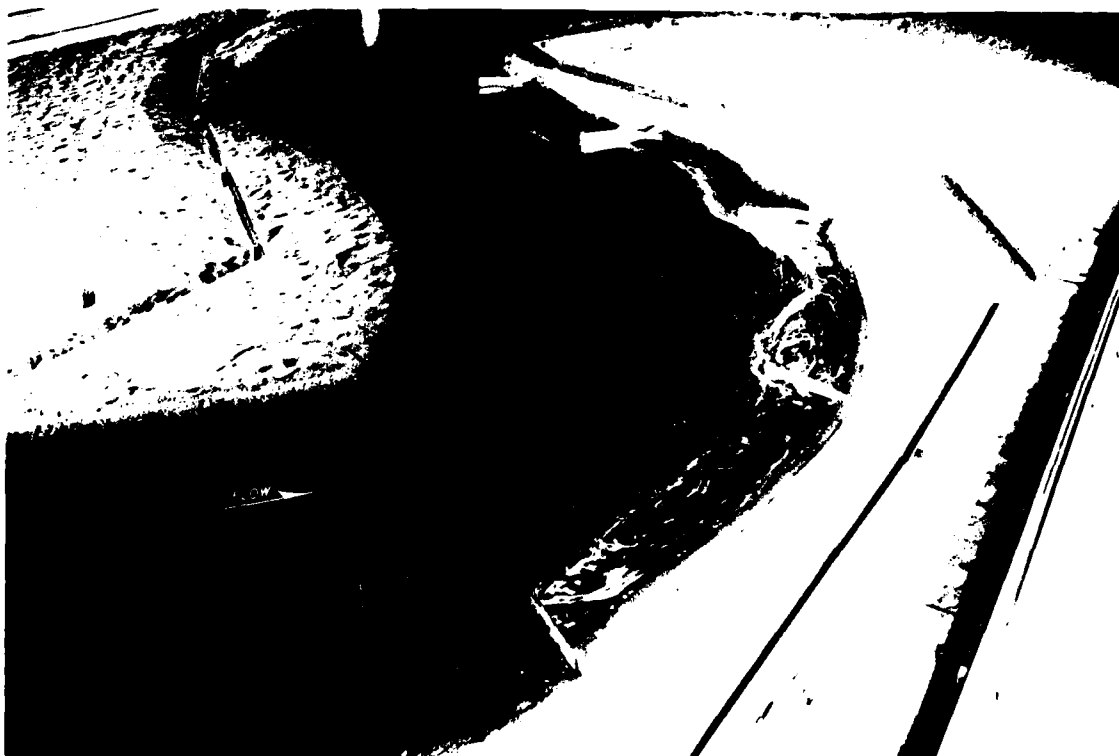


Figure 12. Surface flow patterns; spur dike angle 75 deg



Figure 13. Surface flow patterns; spur dike angle 105 deg



Figure 14. Surface flow patterns; spur dike angle 120 deg

upstream orientation, the potential benefit provided by the upstream eddy may be canceled out by the increased size of the scour hole. The spur dikes angled downstream were more successful in directing the flow toward the center of the channel, thus providing protection for a greater distance downstream.

17. The effective length (projection normal to the current) apparently is a more significant factor than the spur dike angle in providing bank protection. Figures 7-14 demonstrate that bank erosion is more severe with orientation angles at 60 and 120 deg than with angles of 75 and 105 deg. It may therefore be concluded that the spur dike should be oriented perpendicular to the bank to obtain the most effective bank protection.

Spacing-Length Ratio

18. In the demonstration model the riverward ends of the spur dikes were initially set a specific distance from the bank. As the testing proceeded, bank erosion occurred between the spur dikes. The rate of erosion was rapid at the beginning of the test but was fairly stable after 24 hr. At the conclusion of testing the distance from the riverward end of the spur dike to the eroded bank was measured and used to determine a relatively stable spacing-length ratio. The initial and maximum final spacing-length ratios for each test are plotted in Figure 15. Data indicated that for the conditions in the demonstration model ($Q = 2.7$ cfs, $F_n = 0.4$), the optimum spacing to length ratio was about 3 to 1.

19. The spacing-to-length ratio is a function of the approach velocity and discharge. This was demonstrated in the model by increasing the discharge from 2.7 to 4.6 cfs and allowing the model to run for 24 hr. With this higher flow the optimum ratio was reduced to about 2 to 1. These results serve to emphasize the need to study proposed bank protection with spur dikes on a site specific basis, using experiences in similar conditions or a model study.

20. The effectiveness of the spur dike in deflecting flow away

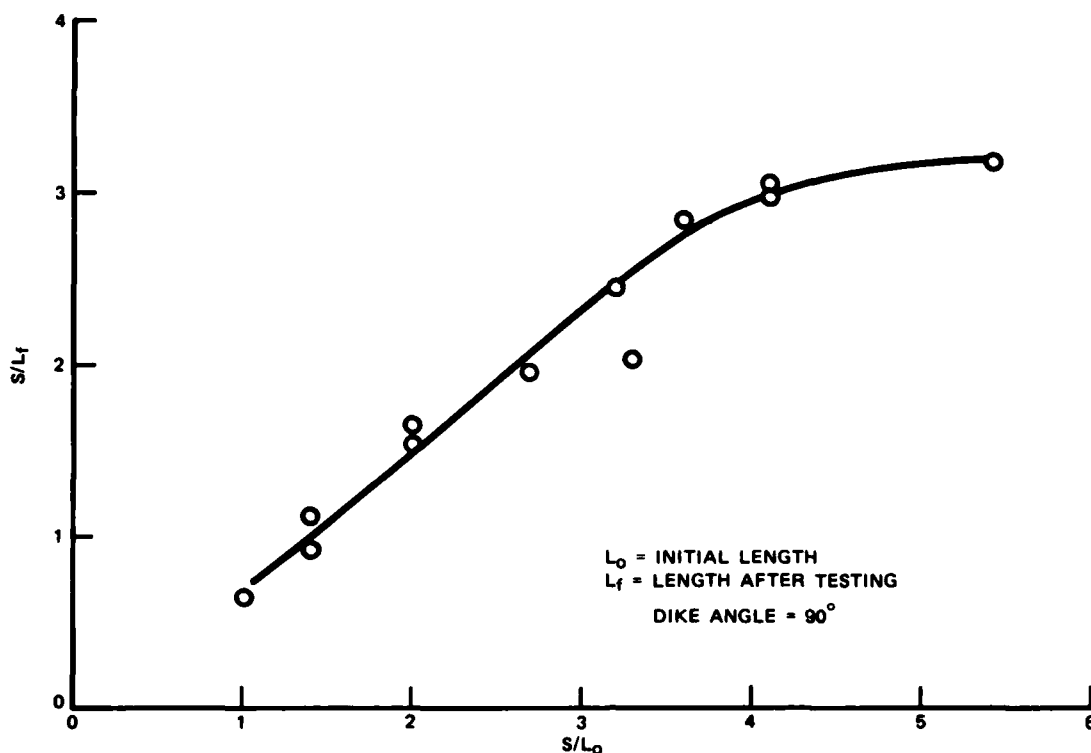
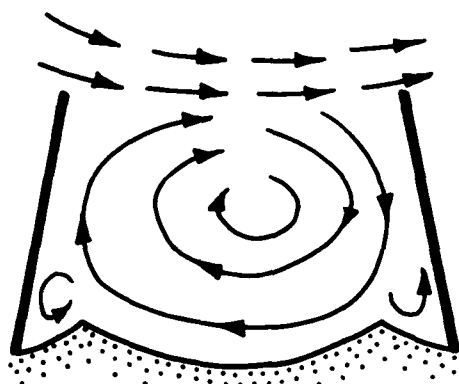
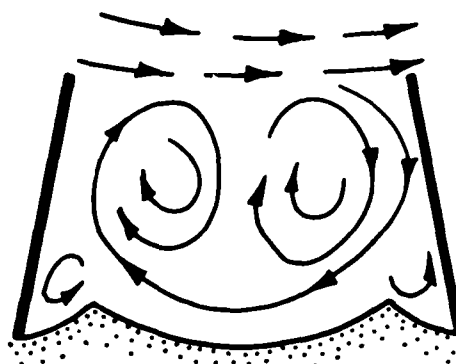


Figure 15. Spacing-length ratio; dike angle 90°

from the bank decreases as the length-spacing ratio increases. The eddy pattern set up between dikes is illustrated in Figure 16. With a type 1 circulation pattern the main current is deflected outside of the spur dike field, and a single eddy develops between the dikes. This pattern is optimum for navigation projects because a continuous deep channel is maintained along the face of the spur dike field. With a type 2 circulation pattern a second eddy appears, but the main current is deflected outside of the spur dike field. As the distance between the dikes increases, a type 3 pattern develops in which the main current is directed at the dike itself, creating a much stronger eddy behind the dike and greater turbulence along the upstream face and at the spur dike nose. When a type 4 pattern develops, the stability afforded to the upstream dike is washed out and a single strong reverse current develops. With a type 5 pattern the flow diverted by the upstream spur dike is directed at the bank between the dikes. Eddies form on both sides of



TYPE 1

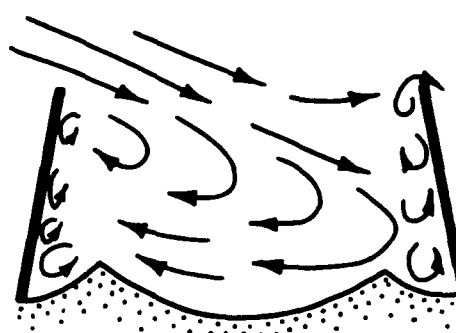


TYPE 2

MAIN CURRENT DEFLECTED OUTSIDE SPUR DIKE FIELD

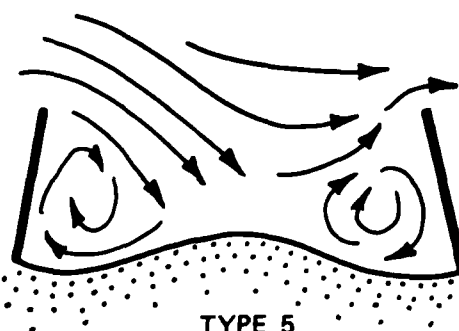


TYPE 3

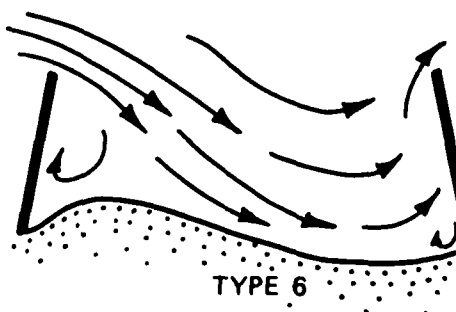


TYPE 4

MAIN CURRENT DIRECTED AT DIKE



TYPE 5



TYPE 6

MAIN CURRENT DIRECTED AT BANK

Figure 16. Flow patterns between dikes

this flow, providing some protection to the bank. As the spacing increases to type 6, the downstream eddy ceases to provide protection to the bank and the current attacks the bank directly. The flow pattern between the dikes is also dependent on the angle and velocity of the approach current.

21. In the demonstration model, the maximum velocity against the bank in the spur dike field was approximately 40 percent of the maximum velocity measured against the bank in a similar concave bend protected by riprap. This percentage was slightly lower when the spacing-to-length ratio was near 1.5 and slightly higher when the ratio was 3.0. This relationship is shown in Figure 17. The reduction of depth and velocity against the bank between the spur dikes may make additional bank protection requirements minimal or unnecessary altogether, depending on conditions at specific sites.

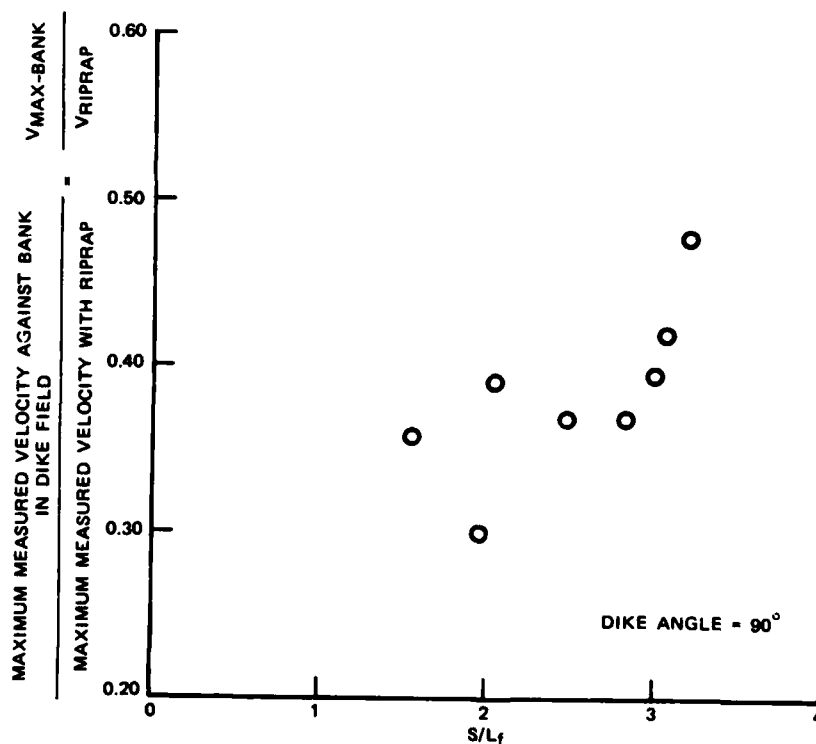


Figure 17. Velocity reduction in dike field;
dike angle 90 deg

Scour Prediction Equations

22. Data collected for two flow conditions in the demonstration model were used to compare several equations that have been proposed to predict local scour at spur dikes. In the model, scour at four dikes with an initial spacing to length ratio of 4.1 was evaluated for model discharges of 2.7 and 4.6 cfs. With a discharge of 2.7 cfs, the Froude number of the upstream channel flow was 0.4 and the average depth of flow was 0.24 ft; the maximum final spacing-to-length ratio was 3. With a discharge of 4.6 cfs the initial Froude number and depth of flow were 0.5 and 0.31 ft, respectively, and the maximum final spacing-to-length ratio was 2. Data from the model tests were used to calculate scour using several equations; results are tabulated in Table 2. These tests were not intended to verify or recommend any of the several equations for use, but to demonstrate the possible deviations that may occur between actual and predicted scour depths.

Table 2
Comparison of Predictive Equations for Scour
at Nose of Spur Dikes

Method	y_s/y	
	$Q = 2.7 \text{ cfs}$	$Q = 4.6 \text{ cfs}$
Demonstration model (4 dikes, $S/L_o = 4.1$)	2.0-3.9	2.9-5.2
Inglis (1949) ($0.8 < k < 1.8$)	4.5-10.2	4.2-9.4
Blench (1969) ($2.0 < k < 2.75$)	4.3-5.9	3.9-5.4
Ahmad (1953) (moderate bend)	3.7-4.3	3.8-3.9
Garde et al. (1961)	3.0	3.1
Liu et al. (1961)	2.9	2.8
Gill (1972)	3.2	2.7
Laursen (1962a)	5.3	4.8

Effect of Stone and Gabion Aprons

23. In order to minimize the severe scour that occurs at the toe of a spur dike, mattresses and aprons are often used. These may be constructed of willows, stone, or rock-filled wire baskets. The effect of a riprap apron was demonstrated in the model; the apron (of 5/8-in. rock) was placed around the toe of the dike at a radius of 0.5 ft (approximately twice the initial average depth) at a thickness of 0.08 ft. Initial placement and conditions after 24 hr of testing are shown in Figures 18 and 19, respectively. The apron did not significantly affect the amount of bank erosion or the maximum scour depth. However, the point of maximum scour was moved away from the toe of the spur dike and slightly downstream, substantially improving the structural integrity of the spur dike.

24. Gabion aprons were also demonstrated in the model. The gabions in the model, 0.5 ft long, 0.12 ft wide, and 0.04 ft thick, were made of standard aluminum screen and filled with crushed rock passing and retained on No. 4 and No. 8 sieves, respectively. In the model the gabions were not tied together as they would be in prototype installations, so the separation of gabions that occurred in the model may not be representative of larger scale applications. Initial placement and conditions after 24 hr of testing are shown in Figures 20 and 21, respectively. As with the stone aprons, bank erosion and maximum scour depths were not affected significantly by the gabion aprons. However, even with separation of the gabion baskets the point of maximum scour was moved away from the toe of the spur dike.

Comparison of Scour Depths

25. In the demonstration model, a comparison was made of scour depths in a concave bend protected by riprap to the depths created with a spur dike field. As shown in Figure 22, scour depths are considerably greater at the toe of spur dikes. However, model tests by Liu et al. (1961) indicated that the scour depths at vertical wall dikes, such as

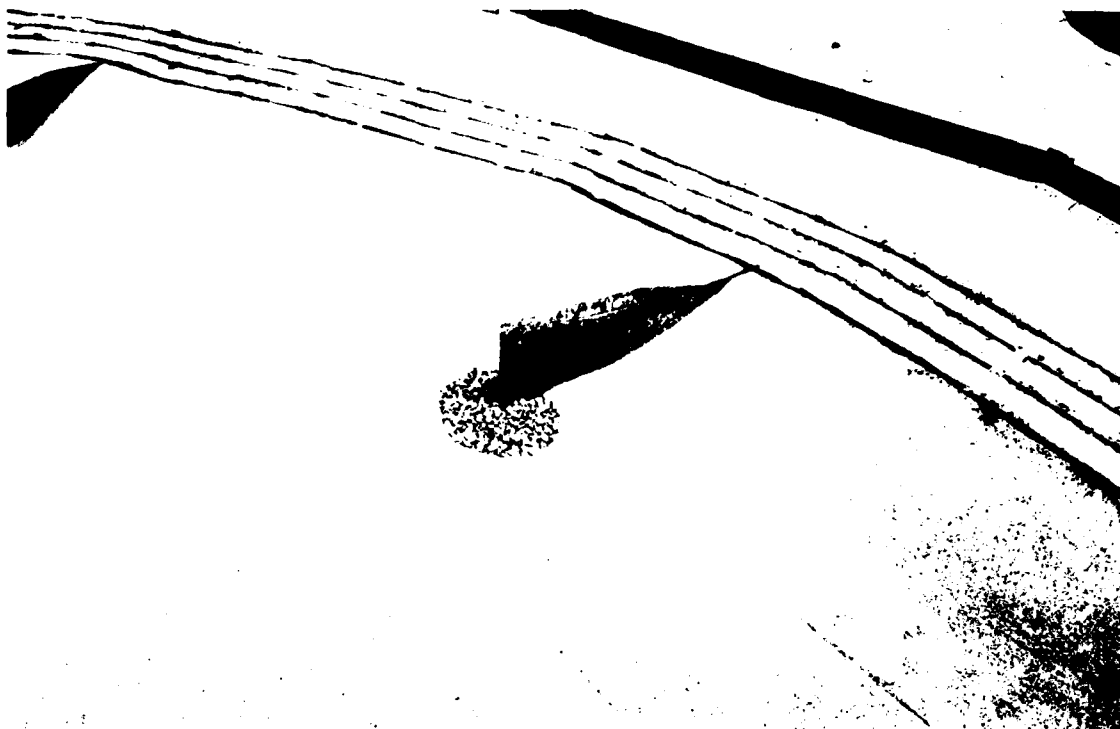


Figure 18. Initial placement of stone apron

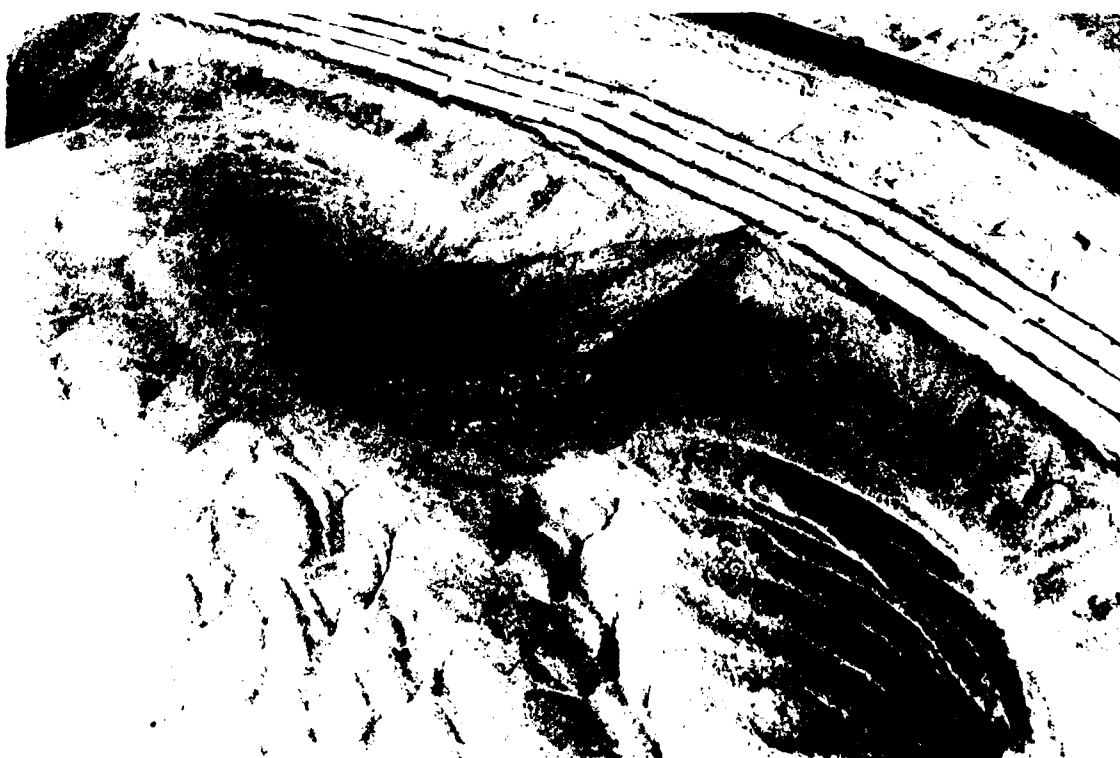


Figure 19. Final conditions for stone apron after 24 hr

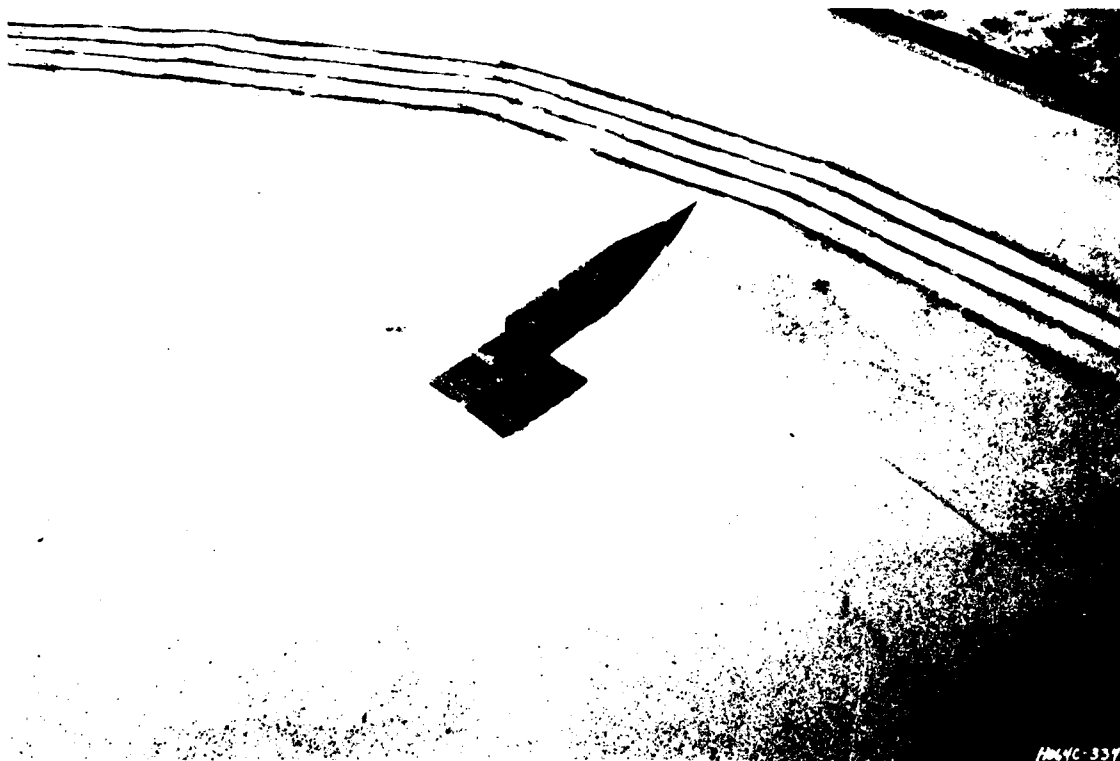


Figure 20. Initial placement of gabion apron



Figure 21. Final conditions for gabion apron after 24 hr

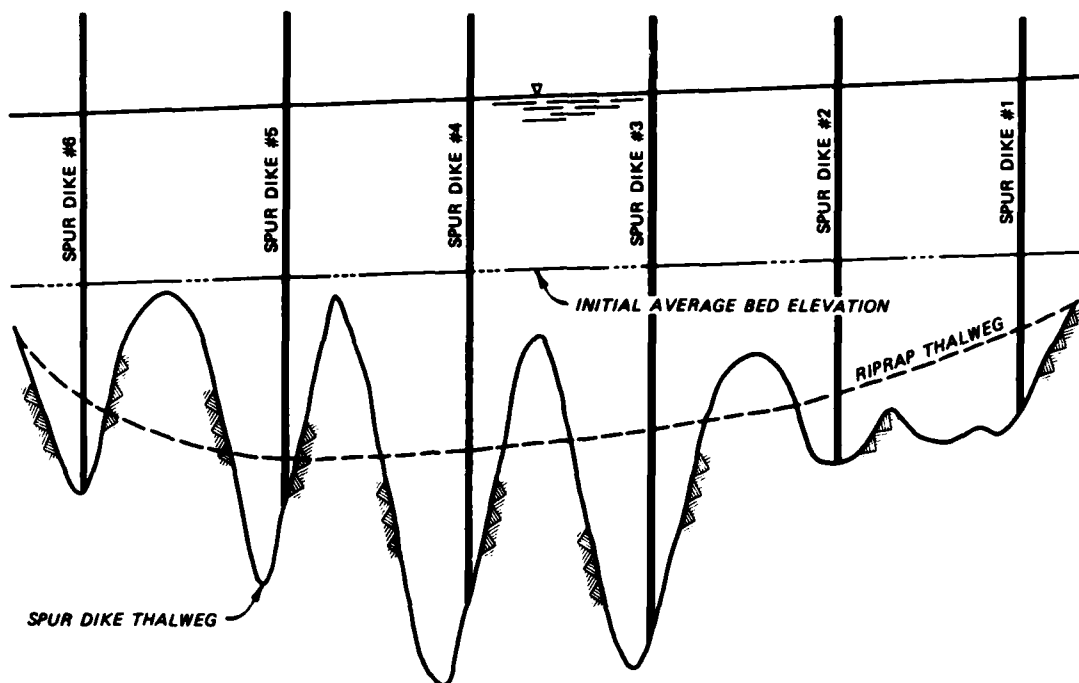


Figure 22. Comparison of thalwegs with riprap and spur dikes

those used in the demonstration model, are about twice the size of scour holes produced at spur dikes with sloping upstream and downstream sides and a rounded sloping nose. The sloping shape is typical of earth and rock-fill dikes with riprap protection.

26. Based on these investigations there was no apparent correlation between the spacing-to-length ratio and the maximum scour depth. Apparently the scour depth is primarily a function of the magnitude and direction of the approach current, discharge, depth of flow, and the orientation angle of the dike.

Conclusions

27. General design guidance cannot be developed from the demonstration model study. Limitations of the study included steady flow, with only two discharges, a single approach angle, and relatively uniform bed material and no suspended load. Keeping in mind these limitations,

several conclusions were reached as a result of the model study.

28. Spacing-to-length ratios as high as three may be effective in protecting concave banks with spur dikes; however, some type of minimal protection may be needed along the banks. Spacing-to-length ratios for specific projects are best determined by previous experiences in similar circumstances or site specific model studies.

29. Spur dike roots should be protected from scour caused by vortices set up along the upstream and downstream faces.

30. The spur dike should be aligned perpendicular to the bank or current. However, slight orientations upstream or downstream had little effect on bank erosion in the demonstration model.

31. Aprons are effective in limiting the depth of scour at the spur dike's toe; however, maximum scour depths and bank erosion in the demonstration model were similar, with and without aprons. Larger aprons may yield different results.

32. The development of a scour hole at the toe of the spur dike may be retarded by the formation of an armor layer. This armor may develop from the very coarse size fractions of the bed material, a size fraction that should not be neglected when bed material samples are taken and analyzed.

33. Site specific model studies will provide useful information with respect to velocity reduction against the bank and relative scour tendencies.

34. Existing equations for scour prediction at spur dikes are questionable when applied to dikes in concave bends.

REFERENCES

- Ahmad, Mushtag. 1953. "Experiments on Design and Behavior of Spur Dikes," Proceedings, Minnesota International Hydraulics Convention, International Association of Hydraulic Research, Minneapolis, Minn.
- Alvarez, Jose Antonio Maza. "Hydraulic Resources Design of Spur Dikes," University of Mexico.
- Blench, T. 1969. "Mobile-Bed Fluviology," University of Alberta Press, Edmonton, Alberta, Canada.
- Central Board of Irrigation and Power. 1956. "Manual on River Behavior, Control, and Training," Publication No. 60, pp 182-206, New Delhi, India.
- Cunha, L. Veiga da. 1973 (Sep). "Discussion of Erosion of Sand Beds Around Spur Dikes," Journal, Hydraulics Division, ASCE, Vol 98, No. HY9.
- Franzius, Otto. 1927. Waterway Engineering, Julius Springer, Berlin; translated by Lorenz Straub, 1936, Massachusetts Institute of Technology, Cambridge, Mass.
- Garde, R. J., Subramanga, K., and Nambudripad, K. D. 1961. "Study of Scour Around Spur Dikes," Journal, Hydraulics Division, ASCE, Vol 87, No. HY6, pp 23-27; and discussion, Vol 89, No. HY1, pp 167-175, Jan 1963.
- Gill, Mohammad Akram. 1972 (Sep). "Erosion of Sand Beds Around Spur Dikes," Journal, Hydraulics Division, ASCE, Vol 98, No. HY9, pp 1587-1602.
- Grant, A. P. 1948. "Channel Improvements in Alluvial Streams," Proceedings, New Zealand Institution of Engineers, Vol XXXIV, pp 231-279.
- Inglis, C. C. 1949. "The Behavior and Control of Rivers and Canals," Research publication No. 13, Parts I and II, Central Waterpower Irrigation and Navigation Research Station, Poona, India.
- Jansen, P. Ph., ed. 1979. Principles of River Engineering, Pitman, London, England.
- Laursen, Emmett M. 1962a. "Scour at Bridge Crossings," Transactions, ASCE, Paper No. 3294, Vol 127, Part I, pp 166-180.
- _____. 1962b. Discussion of "Study of Scour Around Spur Dikes," Journal, Hydraulics Division, ASCE, Vol 89, No. HY3, pp 225-228.
- Lindner, C. P. 1969. "Channel Improvement and Stabilization Measures," State of Knowledge of Channel Stabilization in Major Alluvial Rivers, Technical Report No. 7, G. B. Fenwick, ed., U. S. Army Corps of Engineers, Committee on Channel Stabilization.
- Liu, M. K., Chang, F. M., and Skinner, M. M. 1961. "Effect of Bridge Construction on Scour and Backwater," Report No. CER60-HKL22, Dept of Civil Engineering, Colorado State University, Fort Collins, Colo.

Mamak, Wiktor. 1964. "River Regulation," Arkady, Warszawa, Poland.

Neill, C. R., ed. 1973. "Guide to Bridge Hydraulics," published for Roads and Transportation Association of Canada by University of Toronto Press.

Richardson, E. V., and Simons, D. B. 1973. "Spurs and Guide Banks," Colorado State University, Fort Collins, Colo.

Strom, H. G. 1941. "River Control in New Zealand and Victoria," State Rivers and Water Supply Commission, Victoria, Australia.

Thomas, B. F., and Watt, D. A. 1913. The Improvement of Rivers, pp 135-242, Wiley, New York.

Tison, G. 1962. Discussion of "Study of Scour Around Spur Dikes," Journal, Hydraulics Division, ASCE, Vol 88, No. HY4, pp 301-306.

United Nations Economic Commission for Asia and the Far East. 1953. "River Training and Bank Protection," Flood Control Series No. 4, Bangkok.

U. S. Army Engineer District, Los Angeles CE. 1980. "Detailed Project Report for Flood Control and Environmental Assessment Sespe Creek at Fillmore, Ventura County, Calif."

U. S. Army Corps of Engineers. 1978. "Minutes of the Symposium on Design of Groins and Dikes," held at the U. S. Army Waterways Experiment Station, CE, Vicksburg, Miss.

BANK PROTECTION TECHNIQUES USING GABIONS

SECTION 32 PROGRAM
STREAMBANK EROSION CONTROL EVALUATION AND DEMONSTRATION
WORK UNIT 3 - HYDRAULIC RESEARCH

BANK PROTECTION TECHNIQUES USING GABIONS

1. A series of tests was conducted at the U. S. Army Engineer Waterways Experiment Station (WES) to evaluate the effectiveness of several schemes of using gabions for bank protection. Specifically, efforts were directed at evaluating the use of gabions for hard points or toe protection similar to the way riprap is used for hard points or toe protection at several prototype sites in the Vicksburg District.

2. The facility used in the tests is shown in Photo 1. The channel had a 5-ft bottom width, 1V-on-2H side slopes, and a depth of 0.8 ft. The test section in the channel was a 30° bend with a radius of 22.5 ft. A point bar was molded in the bend to concentrate the flow on the outside bank of the bend. The bend was preceded by a 40-ft-long straight reach having the same cross section. All test channels were molded in sand having a median diameter of 0.45 mm. Although no sand was fed at the entrance of the flume, the test section received substantial bed load due to scour in the straight reach preceding the test section.

3. Each design was tested at a series of runs with increasing discharges while the depth of flow was held constant at 0.5 ft. This resulted in an increase in the average stream velocity and total duration of exposure to flow. The ratio of depth of flow to material size was 340. Model discharges, time steps, and resulting average velocities were as follows:

<u>Run No.</u>	<u>Q cfs</u>	<u>Time hr</u>	<u>Average Velocity fps</u>
1	2.0	0- 4	0.67
2	2.5	4- 8	0.83
3	3.0	8-12	1.00
4	3.5	12-16	1.17
5	4.0	16-20	1.33
6	4.5	20-24	1.50

Photographs were taken before run 1 and after run 6.

4. The first test was conducted without any bank protection in order to establish a base condition with which to compare various

protective methods. The before-flow condition is shown in Photo 1 and the results after run 6 are shown in Photo 2. The unprotected channel experienced considerable erosion and became wider and shallower as a result of the flow.

5. The first protection tested was a series of gabion hard points connected with a row of gabions at the toe of the channel side slope. The gabions were wired together and the gabion hard points were anchored with cables at top of the bank. The approach channel and test section with gabions before flow are shown in Photo 3. The approach channel was protected with riprap toe protection to prevent excessive erosion of the channel banks. The test section with gabions in place and anchored is shown in Photo 4. The gabions were spaced at intervals of 1.6 ft ($2 \times$ bank height) at the beginning of the curve. The spacing was reduced to 1.2 ft ($1.5 \times$ bank height) in the area of maximum attack and increased to 1.6 ft downstream of the channel bend. This protection after run 6 is shown in Photo 5. The model gabions were not as flexible as they would be in the prototype, resulting in the "bridging" shown in Photo 5. This scheme of protection might be more effective if two or three rows of gabions were used instead of one for both toe protection and hard points.

6. The second protection tested was another series of gabion hard points spaced at greater intervals than in the first test series. The test section with gabions in place and anchored with cables to top of the bank is shown in Photo 6. The gabion hard points were spaced at intervals of 3 ft ($3.75 \times$ bank height) at the beginning of the curve. The spacing was reduced to 2 ft ($2.5 \times$ bank height) in the area of maximum attack and increased to 3 ft downstream of the channel bend. This protection after run 6 is shown in Photo 7. The greater spacing of the gabion hard points resulted in more severe erosion.

7. The third protection tested was a "toe protection only" scheme with four rows of gabions laid along the toe of the channel bank as shown in Photo 8. This protection after run 6 is shown in Photo 9. Because sand was used in the model bank, severe erosion took place on the upper bank. However, the gabions were effective in maintaining the integrity of the material at the toe of the channel bank and might work well in the prototype if the upper bank can withstand the infrequent attack that occurs during high runoff events. The upper bank stability would depend upon soil cohesiveness, vegetation, etc.

8. An innovative protection method similar to the "toe protection only" has been used on Antelope Creek and Dead Man's Run in Lincoln, Nebraska, by the Lower Platte South Natural Resources District. Both of these are major drainage channels located within the metropolitan area of Lincoln. A typical cross section illustrating the technique is shown in Figure 1.

9. No attempt was made to establish definite scale relations for use in these tests. This was because the ratio of depth of flow to material size was different in model and prototype and because of the problems involved in relating the rate of erosion of a model with sand bottom and bank to the rate of erosion of a prototype having bottom and bank with different characteristics. Therefore, no spacing for the gabion hard points or design velocities were determined from these tests. These tests were intended to demonstrate certain bank protection measures having the potential for low cost rather than to determine specific design criteria. The effectiveness of different hard-point spacing and flow velocities can be evaluated from specific prototype demonstration sites (existing or future). Gabion protection may be used as shown in WES TR H-75-19, "Fourmile Run Local Flood-Control Project; Alexandria and Arlington County, Virginia," in urban areas and where total bank protection is required.

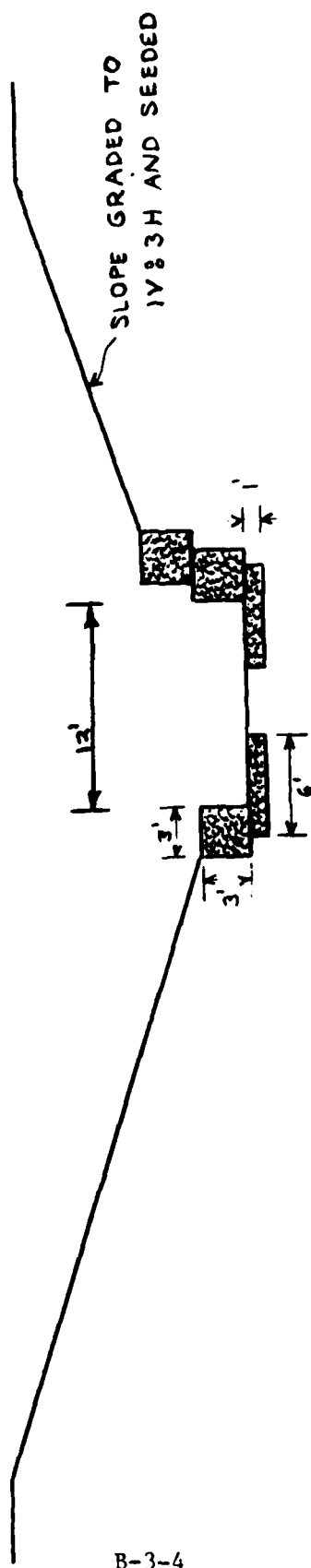


Figure 1. Typical cross section of Antelope Creek and Dead Man's Run, Lincoln, Nebraska

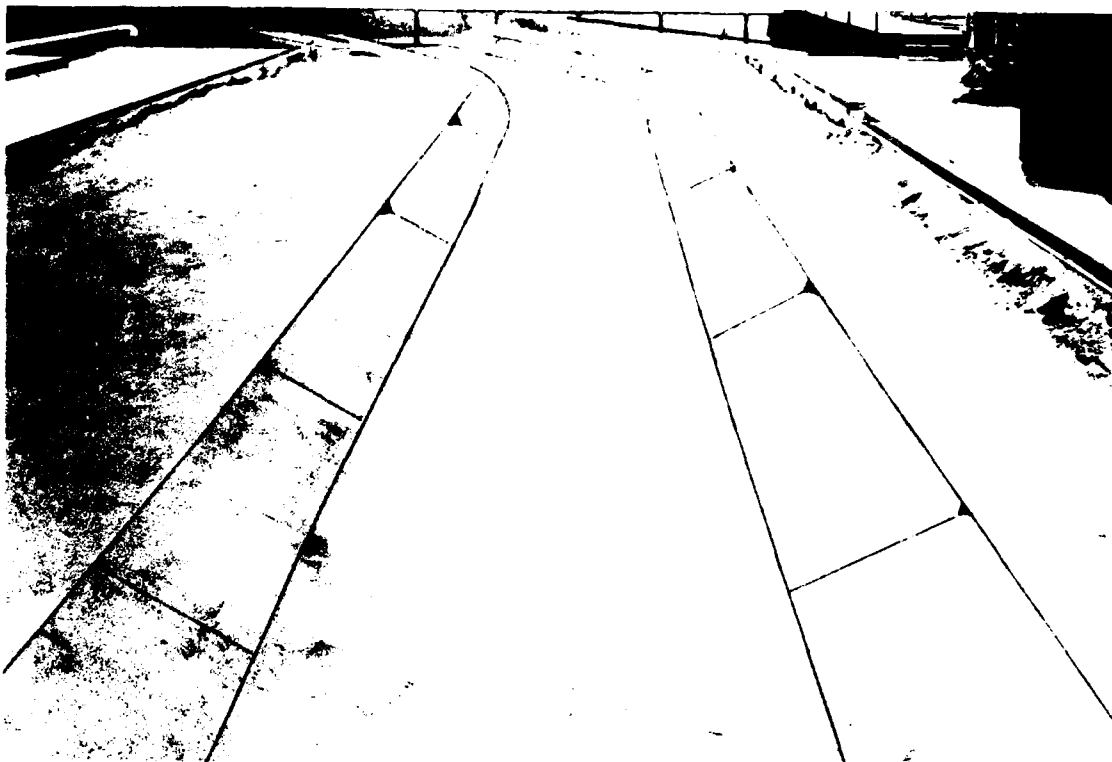


Photo 1. Test facility



Photo 2. Erosion of unprotected channel



Photo 3. Approach channel and test section with gabions before flow

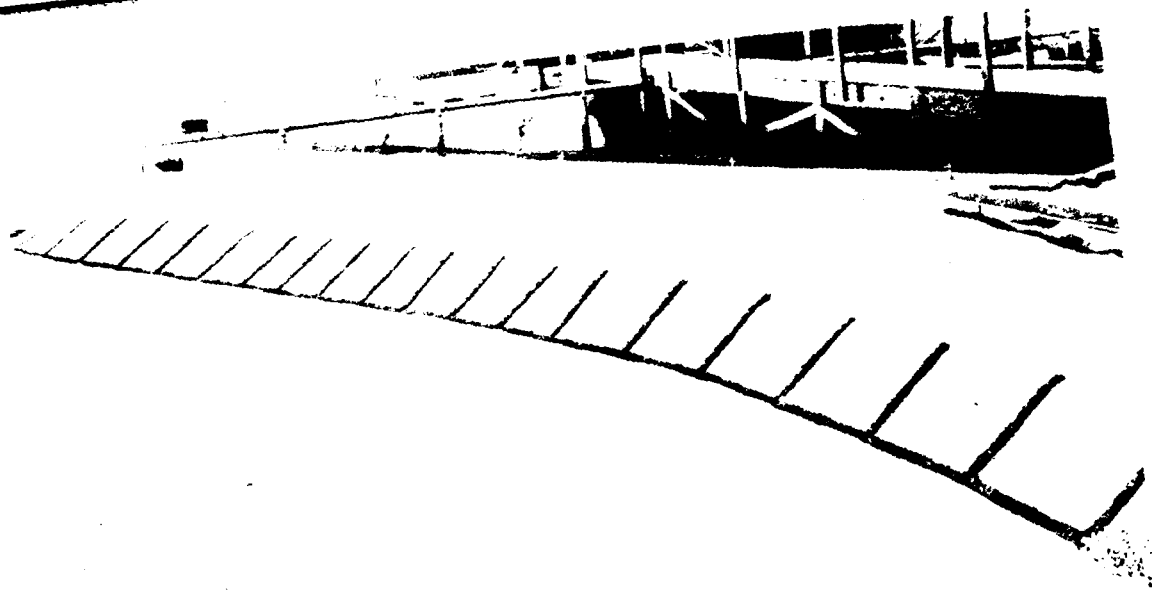


Photo 4. Gabion hard-point protection No. 1, before flow



Photo 5. Gabion hard-point protection No. 1, after flow

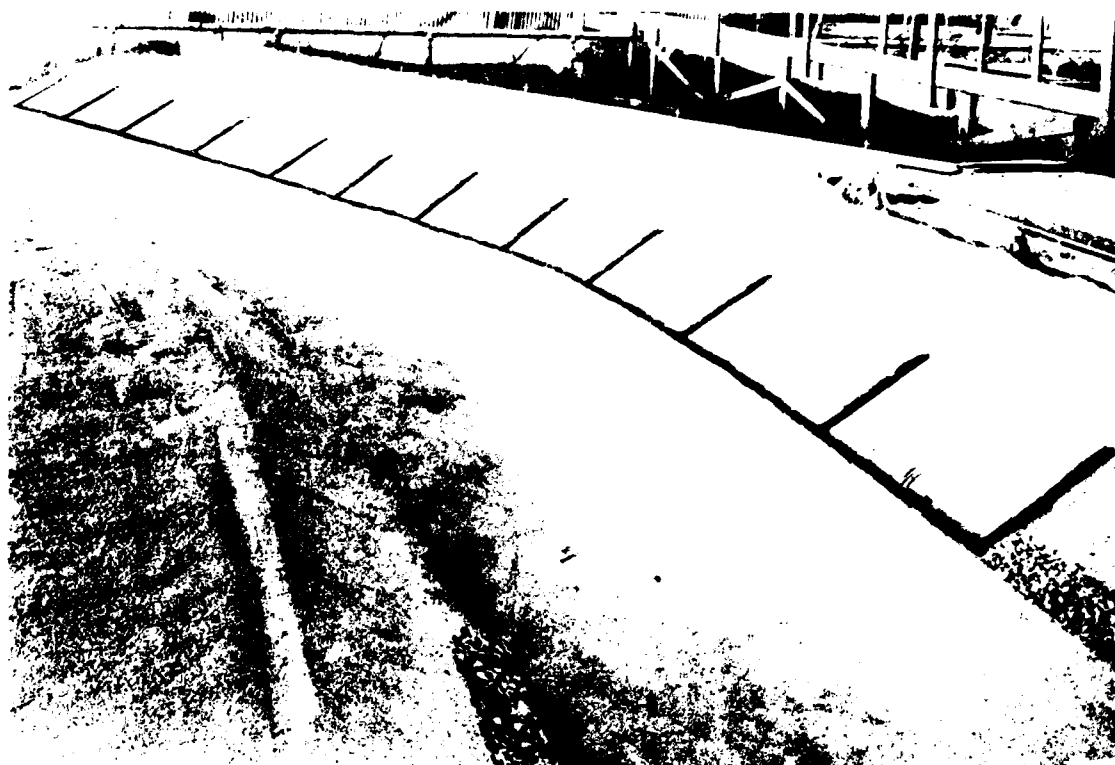


Photo 6. Gabion hard-point protection No. 2, before flow



Photo 7. Gabion hard-point protection No. 2, after flow



Photo 8. Gabion toe protection before flow



Photo 9. Gabion toe protection after flow

MOVABLE BED MODEL STUDIES

SECTION 32 PROGRAM
STREAMBANK EROSION CONTROL EVALUATION AND DEMONSTRATION
MOVABLE BED MODEL STUDIES

INTRODUCTION

1. Seven movable bed model studies were conducted at the Missouri River Division's Mead Hydraulic Laboratory under Work Unit 3 of the Section 32 Program. The purpose of the model studies was to obtain general information which would aid in the design and evaluation of the different methods and techniques for bank protection proposed for the Missouri River demonstration sites. Model studies were conducted on the following bank protection methods:

- a. Windrow revetment (2 model studies)
- b. Vane Dikes
- c. Hard Points (2 model studies)
- d. Reinforced Revetment (2 model studies)

2. The following sections of this report contain a general description of the Mead Facility and individual reviews of the model studies on the above four types of bank protection methods.

A. MEAD HYDRAULIC LABORATORY

3. The Mead Hydraulic Laboratory is located at the University of Nebraska Field Laboratory near Mead, Nebraska. It is operated as a joint use project under a special lease arrangement between the University of Nebraska and the U. S. Army Corps of Engineers. The primary facility consists of a model area and related equipment utilized by the Corps of Engineers for movable bed model investigations for the development and maintenance of the navigation channel of the Missouri River. This facility was designed specifically to permit rapid investigations of problem areas dealing with erosion or sediment deposition in the Missouri River.

4. The model facility is inclosed in a building 100 feet wide and 160 feet long. See Photo 1. Five miles or less of river can be modeled within these confines. Portable wall sections are used to form the interior boundaries of the particular river model under investigation. Lightweight ground walnut shells are used to simulate the stream bed and banks. Water and ground walnut shells are simultaneously recirculated through the model during testing thereby simulating both the water and sediment transport of a natural river system.

5. The portable wall sections forming the boundaries of the river model allow a large degree of flexibility in laying out various river shapes and alignments. These sections are inverted T-shaped lengths of pre-cast concrete, four feet long and two feet in height. The sections are equipped with necessary mountings to attach railings and auxiliary measuring equipment to the top or sides of the walls. See Photo 1. Once the general alignment of the prototype reach has been established, the sections are sealed to each other and to the floor with water proofing compound. At the completion of a study, they may be taken apart, and reused for the next model investigation. This method of construction permits rapid changes from one model



B-4-3

Photo 1. General view of the interior of the Mead Hydraulic Laboratory. The model shown in the photo is of the navigation channel at the junction of the Kansas and Missouri Rivers near Kansas City, Missouri. Model walls are formed from individual inverted T sections of pre-cast concrete. Bank and bed material of model is ground walnut shells. Bridge assembly for sonic sounder is shown in left center with X-Y plotter at right of bridge. Stilling well stand for water surface monitoring in center of photo. Water surface monitoring devices not visible through sediment laden water. Recirculation line in background with pump assembly at right.

layout to the next, thus cutting down considerably on the time between model studies.

6. The material normally used for the stream bed and channel banks at the Mead Laboratory are ground walnut shells which have a specific gravity of 1.3. This lightweight material is commercially available in various size gradations. The gradation selected for use at the Mead facility has a median grain size of 0.30 mm. The material has several operational advantages. Because of its relatively light weight, the length of time necessary for the model to reach an equilibrium condition is greatly reduced (about 8 hours). The material is suspended at rather low velocities, 0.3 fps, and thereby simulates suspended sediment transport. By controlling the gradation, the particle size distribution for the Missouri River sand and the ground walnut shells can be made almost identical, even though the specific gravity varies significantly between the two materials. Photomicrographs of the two materials illustrated in Photos 2 and 3 indicate the shape factors are similar.

7. The laboratory has two complete water recirculation systems, thus permitting two general investigations to be carried out simultaneously. Both systems are equipped with variable speed controls, and the discharge rate is controlled by adjusting the pump motor speed and a gate valve in the discharge line. Photo 4 shows a view of the pump assemblies. The water in a model is recirculated by one of the pumps through a piping system connecting the sump area of the downstream end of the model to a delivery point near the upstream entrance to the model. The sediment in the model is recirculated with the water. If necessary, sediment may either be added or extracted from the flow at some pre-determined rate near the upstream or downstream end of the model. Normally, no positive control of the sediment transport rate is attempted. The rate is then established by the relationship between the hydraulic characteristics present in the model at a given time. This last method of operation has been

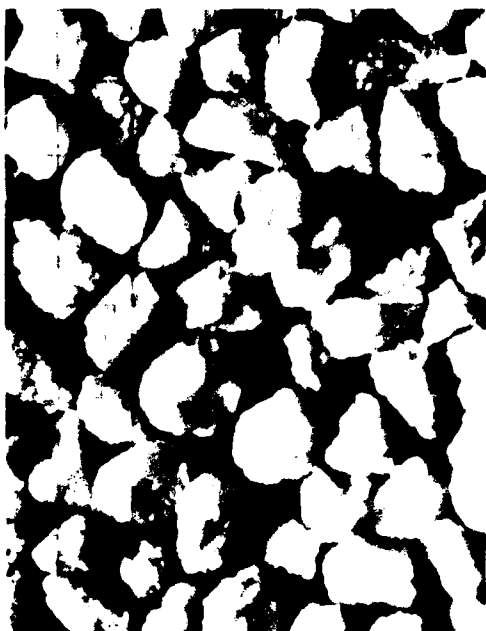


Photo 2. Photomicrograph of ground walnut shells. Grid size: 0.39 mm.



Photo 3. Photomicrograph of Missouri River sand. Grid size: 0.39 mm.

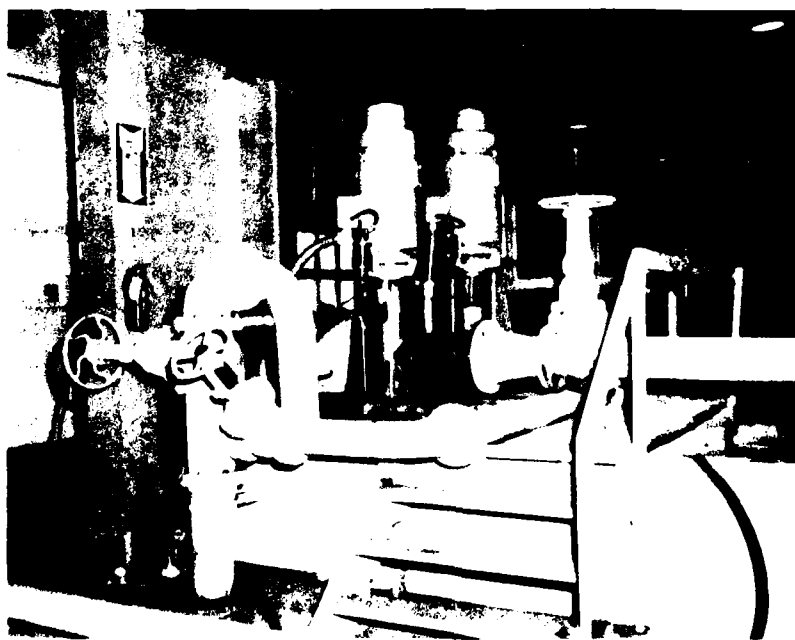


Photo 4. Two pumps, equipped with 15 and 20 H.P. motors, recirculate the water and sediment through the system. Gate valve at right of pumps used to adjust discharge. Water supply to facility furnished through pipe in foreground.

used almost exclusively in the studies performed to date, and has proved satisfactory for investigations involving problems associated with the bed configuration of alluvial channels.

8. There is no tailgate structure used in this system. Either one of two methods is used to control the water depth in the model. In the first method, the water surface elevation, and therefore the depth, at the midpoint of the model is held constant by adding or extracting water from the system. Many different flow velocities, water surface slopes, and bed slopes are obtainable for the same depth using this method. The second method imposes a predetermined water surface slope on the model by monitoring the difference between the water surface elevations at two locations. If this difference is greater than desired, water is added to the system. If the difference is less than desired, water is extracted. This method permits the model to react to changes in discharge much like a natural river, in that the depth of flow is a function of the discharge.

9. The total sediment transport rate is monitored while the model is in operation. A tube is inserted in the recirculation line and pointed into the flow. A variable speed pump is used to withdraw samples of water and sediment (walnut shells) at the same velocity as the average velocity in the recirculation line. The water and sediment mixture is pumped into an inverted cone where the sediment is allowed to settle to the bottom. The clear water overflow from the cone is drained back into the sump area. The material which settles to the bottom is extracted from the inverted cone and weighed. Several samples obtained over equal time increments are collected and model transport rates determined.

10. The water surface slope is measured with a series of monitoring devices spaced along the model channel. The monitoring devices are connected by plastic pipe, buried in the bed material, to a stand of individual stilling wells in which the water surface

elevation at each channel location is measured with a point gage. The difference in the water surface elevations through the model is usually less than 0.1 feet over 150 feet with velocities less than 0.6 fps. Photos 5 and 6 show a water surface monitoring device and the stilling well stand.

11. Point velocities are obtained at specified intervals across the model channel at key cross section locations during the tests. A standard "pigmy" meter is used to obtain these velocities. The distribution of the flow across the channel is then determined from the point velocities and compared to the distribution of flow similarly determined at the prototype locations. This information is used to adjust the model such that the flow distribution in the model is similar to that in the prototype and also to check the repeatability of the model during subsequent testing.

12. Cross sections in the model are obtained through the use of an echo-sonic depth sounder. This device uses high frequency water borne sound waves generated and received by a piezoelectric ceramic transducer. The time differential between transmission of sound and reflection of the sound wave or echo is used to indicate distances to specific reflecting surfaces. The transducer is mounted in the end of a three foot probe. The probe is attached to a moveable carriage which is traversed across a bridge spanning the width of the model. See Photo 7. The carriage containing the probe is pulled across the bridge by means of an endless cable powered by a variable speed motor. A potentiometer attached to the cable drum outputs a voltage proportional to the probe location on the bridge. The two output voltages, one from the transducer, and the other from the potentiometer serve as the inputs to an X - Y plotter and to an area integrator device. See Photo 8. As the carriage containing the transducer moves across the bridge, a complete cross section of the model channel is developed by the plotter. In addition the channel

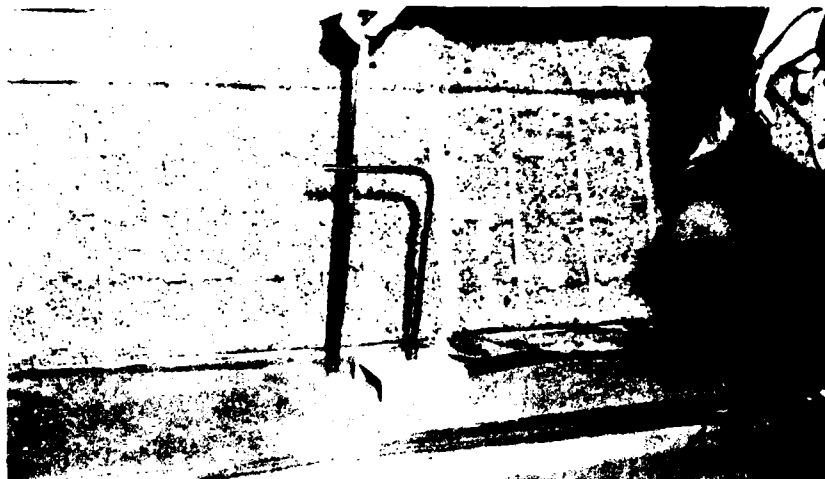


Photo 5. Water surface elevation monitoring devices such as shown in photo are normally located at 10-foot intervals throughout the model and are connected by plastic pipe to stilling wells at a central location.

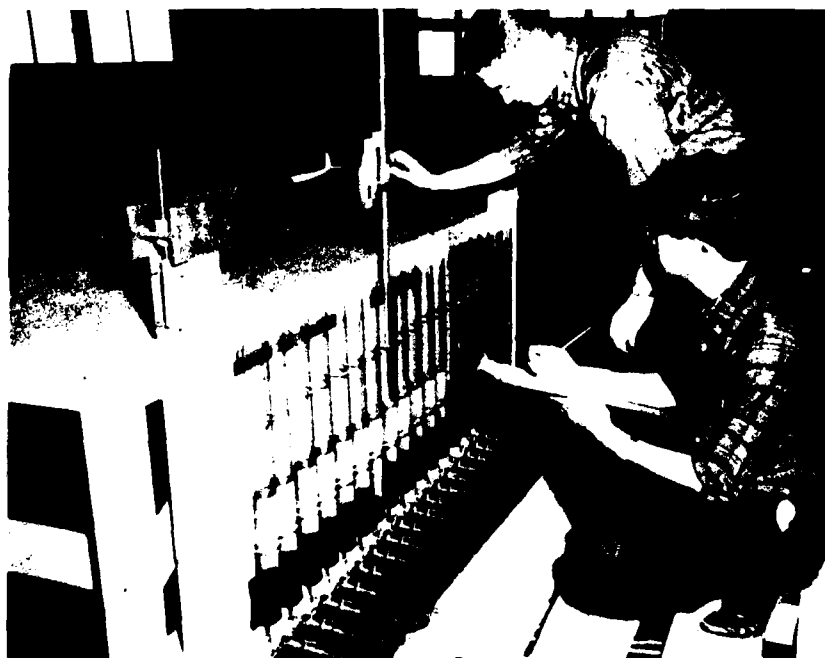


Photo 6. Stilling well stand where water surface elevations from model are measured with a point gage and recorded.

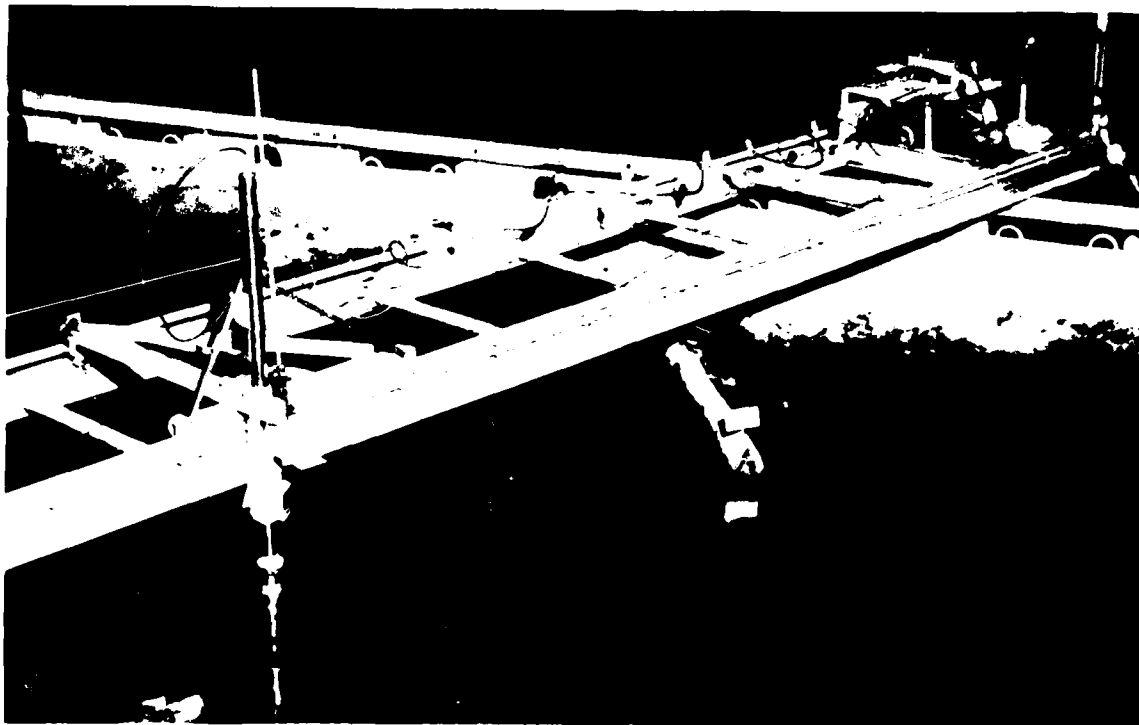


Photo 7. Depth sounding apparatus used to obtain model cross sections. Probe and carriage mounted on bridge at left in photo. Drive controls and assembly for endless cable to traverse probe and carriage are at upper right.

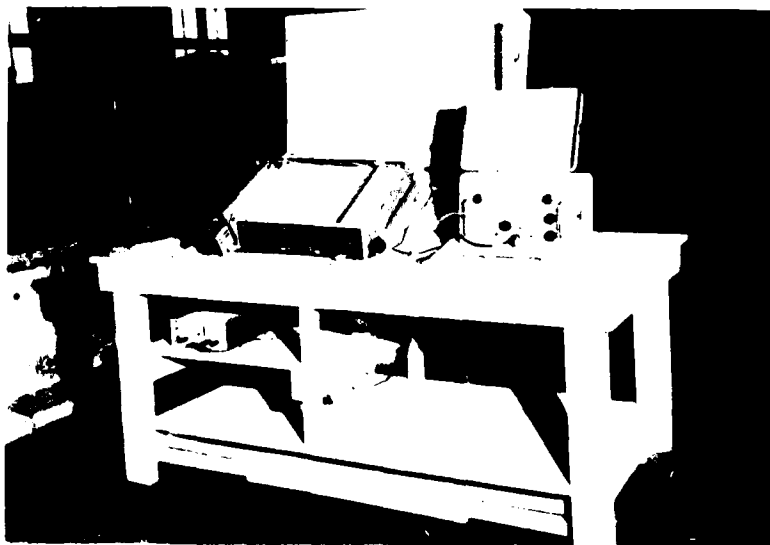


Photo 8. X-Y recorder and electronic equipment used to record model cross sections and area of model cross sections.

area below the water surface is calculated by an electronic integrator. Channel cross sections and areas at other locations are made by rolling the bridge assembly to other positions along the model.

13. Data from the cross sections are used to draw contour maps of the channel bed. These contour maps are then visually compared to a contour map of the prototype area. During the verification tests these contour maps are used in conjunction with the flow distribution data to show that the model is similar to the prototype. During the testing, the contour maps are used to illustrate the effect on the bed configuration of the various model changes.

14. Additional data and documentation of model tests are obtained from photographic techniques. These include:

- a. Before and after photos of the model to illustrate changes.
- b. Time exposure photos to show the magnitude and direction of surface velocities.
- c. Time lapse movies which compress many hours of testing into a few minutes for study and briefing purposes.

15. All of the above mentioned modeling techniques may not have been used during each of the Section 32 model studies. Modifications or additional techniques were required during some of the studies. These are discussed in the following sections.

B. WINDROW REVETMENTS

16. This section presents results of model studies on a windrow revetment erosion control structure. A windrow revetment is defined as a blanket of stone which forms when a windrow of stone, placed along a riverbank at or below the ground surface behind an eroding channel bank line, is undermined by erosion causing the stone to drop into the channel. See Plate 1. As long as a sufficient quantity of stone is available from the windrow, the stone will pave the bank thereby armoring the bank line against further erosion. More conventional bankline revetments are constructed by:

a. Digging a trench landward of the bank line and placing a blanket of stone on the side slope of the trench.

b. Dumping of stone directly into the stream.

17. The windrow revetment has the following advantages over the more conventional methods.

a. Complex site preparation is not required.

b. Stone may be added to or removed from the windrow as conditions dictate.

c. Manipulation of the stone is reduced.

d. A minimum amount of stone required to arrest the erosion process will be used.

18. Objectives. The objectives of the model tests were to determine:

a. The mechanics of the formation of the ultimate shape.

AD-A121 132

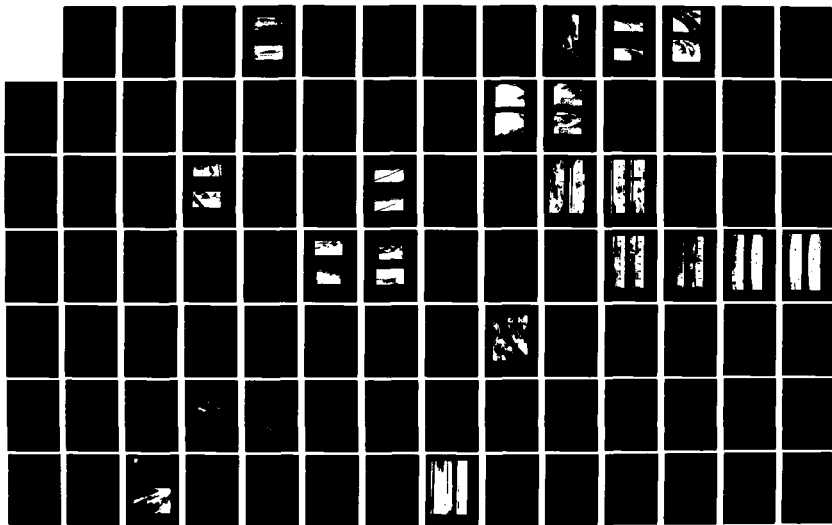
THE STREAMBANK EROSION CONTROL EVALUATION AND
 DEMONSTRATION ACT OF 1974 S. (U) ARMY ENGINEER
 WATERWAYS EXPERIMENT STATION VICKSBURG MS HYDRA.

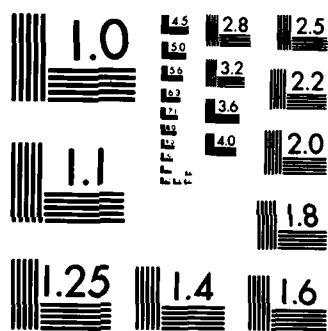
2/4

UNCLASSIFIED

H P KEOWN ET AL. DEC 81 WES/TR/H-77-9-APP-B F/G 13/2.

NL





MICROCOPY RESOLUTION TEST CHART
NATIONAL BUREAU OF STANDARDS-1963-A

b. A relationship for the minimum application rate or quantity of stone per foot of bank line required to form a permanent revetment.

c. The effect of different windrow cross sections on the final shape of the revetment.

d. The effect of stream velocities on the final shape of the revetment.

e. The effect of stone size and gradation on the formation of the revetment.

f. The effect of bank height on revetment formation.

g. The utility of using windrows of stone to develop segmented revetments as opposed to continuous revetments.

THE MODEL

19. This model study was of a general nature. The purpose of the model study was to provide general design information on the windrow revetment. Two different bed materials, fine sand and finely ground walnut shells, were used during the investigation. See Table 1.

TABLE 1

AVERAGE BED MATERIAL CHARACTERISTICS - MODEL

Material	Limits*	\bar{d}_b (ft)	Specific Gravity
Sand	#100 < d_b < #8	.0020	2.65
Ground Walnut Shells	#140 < d_b < #30	.00094	1.31

* U. S. Standard Sieve Size

20. Model Layout. The model was formed in a basin filled with bed material. See Plate 2 and Photos 9 and 10. Two bends of equal radii were used to form an "S" shaped model configuration. The "S" shape model was selected to simulate those flow characteristics encountered in natural alluvial streams. A radius of curvature was selected to represent one of the worst possible natural conditions, a forced bend, in order to insure that the model banks would erode. The average range of the ratios of the radii of curvature to the channel widths for forced bends varies from 2.5 to 3.0. Considering this type of bend and the space available, the model bends were constructed with a radius of 14.5 feet and a channel width of 5 feet. The bank lines in the upper bend and the right bank of the lower bend were armored to maintain a fixed channel geometry. The left bank in the lower bend was not fixed and was permitted to erode. This erodible section of the model was used to test the windrow revetment erosion control method.



Photo 9. Reconstruction of sand bed model. Horizontal bar in mid-section of photo fixed at left to center point of curve. Right end of bar free to slide along outside edge of basin. Person at right sliding end of bar while person in channel removing excess material from in front of template attached to bar.



Photo 10. Reconstructed sand bed channel prior to start of run 3. Flags were used initially to locate center line of windrow at 1 foot intervals.

21. Sediment Recirculation. A stilling basin was constructed in the sand bed model between the end of the model and the recirculation pump. A specially designed suction device, utilizing the Venturi principle, was placed in the stilling basin to recirculate the sand transported out of the model and deposited in the stilling basin. No stilling basin was required when ground walnut shells were used for the bed material as the ground walnut shells are non abrasive and were recirculated through the pump along with the water.

22. Model Stone Size. Four different windrow stone size "gradations" were used during the tests. See Table 2. Gradation 1 and 4 each contained stone ranging in size from a minimum to a maximum as indicated in Table 2. Gradations 2 and 3 essentially contained only one stone size.

Table 2

AVERAGE CHARACTERISTICS OF STONE (CRUSHED LIMESTONE) - MODEL

Gradation	Limits **		d_r ft
	Minimum	Maximum	
1	#4 < d_r < 1/2 inch		.0252
2	1/2 Inch < d_r < 3/4 inch		.0519*
3	#4 < d_r < #3		.0196*
4	3/8 Inch < d_r < 1 inch		.0449

*Geometric mean

** #4 + #3 refer to U. S. Standard Sieve Sizes

Specific gravity of limestone = 2.62

TESTING PROCEDURES

23. Reconstruction of Model. The model test area was reformed before each run. See Photo 9. A male template, mounted on a horizontal bar, was used to preshape the model to the desired form. The horizontal bar was fixed at the pivot point of the curve but was free to move along guide rails on the outside basin wall. The concave bank in the test area was formed to a slope of 1.0H to 1.0V, and the top of the bank for a distance of 2.0 feet landward was constructed to a constant elevation.

24. Windrow Construction. Three windrow shapes were tested; triangular, trapezoidal, and rectangular. The construction technique for all three was similar. A scribe was attached to a horizontal bar and used to etch lines parallel to the channel on top of the bank in the test area. These lines were used to define the windrow alignment, limits, and centerline. The centerline was divided into 1-foot segments which were extended radially. A given amount of stone, equal to the application rate to be tested, was weighed and placed within each 1-foot segment.

25. The triangular shape windrow was constructed by simply dumping the required quantity of stone to be tested along the centerline. The landward and riverward extent of the windrow was governed by the angle of repose of the material and the quantity of stone applied. The trapezoidal shape windrow was constructed by uniformly spreading the stone within the 1-foot limits of the segment, producing different windrow thicknesses. Construction of the rectangular shape windrow was similar to the trapezoidal except a trench was cut into the top of bank to the required depth and width. If the windrow layout was different than any previous run, overhead photos were taken to document the setup. Additional documentation was obtained for runs using the walnut shell bed material through the use of time-lapse photography.

26. Start-up Procedures. The model was slowly filled with water so as not to damage the test area, and the recirculation pump started. The discharge and water elevation at a control point were constantly monitored and adjusted until the desired water elevation and discharge were obtained. After that time, the controls were monitored and adjusted as necessary.

27. Monitoring Procedure. Periodically, during each run, samples of the recirculated sediment material were obtained, the water temperature recorded and water surface elevations measured at 10-foot centers through the model basin. The following measurements were obtained at selected cross-sections within the test reach. See Plates 1 and 2.

- a. The radius point of the eroded edge of the windrow, r_1 .
- b. The radius point of the top edge of the revetment, r_3 .
- c. The radius point of the toe of the revetment, r_2 .
- d. Water surface elevations and radii measurements at the left and right water's edge.
- e. Point velocities in the vertical above the revetment toe.
- f. A profile of the cross section.

28. End of Run Procedure. The recirculation pump was stopped and the water was slowly drained from the model at the end of the run after the last set of data had been obtained. Overhead photos and samples of the revetment were then taken to document the final model conditions.

29. Windrow Revetment Sampling Procedure. Five samples of the windrow revetment were obtained at each of the pre-selected cross-sections. See plate 3. First the bed material covering the toe of the revetment was carefully removed. The length of the revetment from the toe to the location of the water's edge was then measured. Using a guide, stone samples were then obtained within a 1-foot length of revetment alternately at the top, middle, and bottom of the revetment. The guide dimensions were 0.5 foot by 0.5 foot. All the stone within this guide area was removed, then the stone remaining within the 1-foot length of revetment was removed. Similarly all the stone within the 1-foot length remaining on the bank in the windrow was removed. The purpose of this procedure was to provide a check on reliability of the sampling procedures. The sum of the five samples taken from within the 1-foot length should equal the original quantity of stone placed in the windrow at the beginning of the test. The samples were then spread on the floor and left to dry. After they had air dried a sufficient length of time, they were weighed.

30. Special Procedures. During some of the tests, the above procedures were modified or other methods employed. Colored stone was placed at specific locations in the windrow of some tests to observe the movement of the stone. See Photo 11. Insufficient quantities of stone were used in several tests to determine how the stone would disperse in a failure situation. See Photos 12 and 13. Extensive point velocities were obtained at certain cross sections during some of the tests. The velocity and/or depth of flow was also varied during several tests. The bank height was increased in two runs, see Photo 14, and noncontinuous windrows were tested in two runs, see Photo 15.

CONCLUSIONS AND RECOMMENDATIONS

31. Mechanics of Windrow Revetment Formation. The windrow revetment in concept is simple. Stone is placed along an eroding



Photo 11. Looking down on model test area at end of Run 9. Colored stone placed in windrow to observe movement of stone. Note that except for toe zone, stone moved down the slope with no downstream component.



Photo 12. End of run 40 conditions looking upstream. Insufficient supply of stone in windrow. Note revetment continued to move into scour at toe zone exposing bank near water's edge. Upper bank zone eroded and revetment was overtopped.

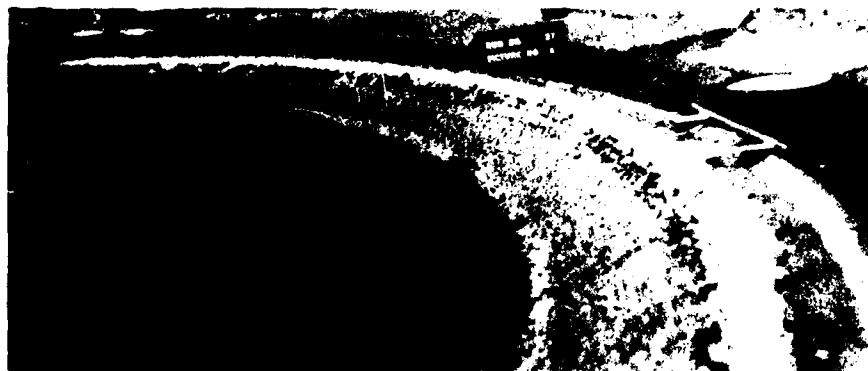


Photo 13. End of Run 27 conditions looking upstream. Normal appearance of windrow revetment.



Photo 14. End of run 41 conditions with high bank. Note slightly ragged appearance of bank line.

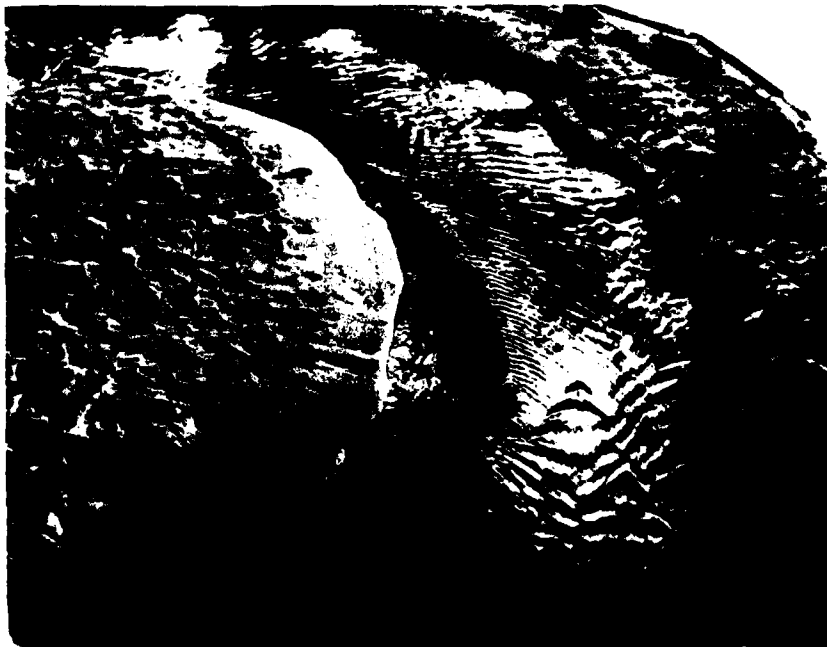


Photo 15. Looking upstream during testing of noncontinuous windrows.
Note scalloped bank line.

bank line which is eventually undercut by the stream. The stone then moves down the bank line to form a blanket which halts further erosion. In reality, the formation of this type of revetment is complex. Initially, the lateral erosive force of the stream undermines the windrowed stone causing some of the stone to drop into the stream. This stone slows the lateral erosion of the bank but causes an increase in the vertical erosion along the leading edge or toe of the newly forming revetment. This vertical erosion is believed to be caused both by turbulence around the individual stones and by a diminished supply of bed material from the bank. The initial quantity of stone which drops into the stream forms an unstable revetment which during the vertical erosion process is constantly adjusting itself as the toe of the revetment advances into the scour area, and results in a riverward movement of the stone. If a sufficient supply of stone is available from the windrow, a semi-stable revetment will eventually be formed as dictated by the intensity of the erosive forces of the stream. It should be noted that the riverward movement of the stone causes a thinning of the revetment blanket. If no riverward movement of stone occurred, the vertical thickness of the revetment blanket would simply be the same as the windrow height and there would be no design problem. It is important that the designer have some knowledge of the amount of scour which might be expected to occur. It is suggested that this be ascertained from other structures in the vicinity of the proposed windrow revetment, or by evaluating maximum scour depths existing upstream and downstream of the proposed revetment.

32. Application Rate. The application rate is the weight of stone applied per length of bank line. The amount of stone in the windrow dictates the degree to which the lateral erosion will occur, however, it is important to realize that a certain amount of lateral erosion has to occur in order to permit the stone to feed down the bank slope. If all the windrow is within this erosion zone, all of the stone may be undermined and the revetment overtopped and failure

will occur because of insufficient horizontal supply. Equation 1 defines the relationship between the amount of stone needed in a windrow to provide a blanket configuration for various slopes and thicknesses. See Plate 1 for a definition sketch and symbols.

$$X_1(\bar{h} L \gamma') = P_r(\bar{t} L \gamma'') \quad (1)$$

X_1 = lateral width or eroded windrow

P_r = Slope length of revetment

L = Downstream length of revetment

\bar{h} = Average height of used portion of windrow

\bar{t} = Average thickness of revetment normal to slope

γ' = Bulk unit weight of windrow material

γ'' = Bulk unit weight of in place revetment material

33. Windrow Cross Section. The shape of the windrow as originally placed on the upper bank is important only insofar as the average height, \bar{h} , of the segment of windrow used is concerned. A triangular shape will produce an average height which will vary from a maximum value equal to the initial height to half this value if the entire windrow is used. The average height of a trapezoidal shape will be constant throughout all but the last portion of the windrow, where it will behave similar to a triangular shape. A rectangular shape will function basically the same as the trapezoidal, except that an initial surge of stone is released from the containment trench when the eroded bank can no longer sustain it.

34. Generally speaking, the rectangular shape was found to be the best windrow shape. This shape supplies an initial surge of stone which counters the thinning effect of the scour in the toe zone of the forming revetment. The remaining portion of the windrow then provides a steady supply of stone to produce a uniform paving. The second best windrow shape was the trapezoidal shape. It has one advantage over the rectangular shape in that no trench is needed to contain the windrow stone. This shape supplies a steady supply of stone similar to the rectangular shape. The triangular shape was probably the least desirable shape. This shape supplies more stone initially, but the quantity of stone diminishes as the windrow is undercut.

35. Stream Velocity. The velocity and characteristics of the stream dictate the minimum size stone that should be used in the revetment. The stream velocity was found to have a strong influence on the magnitude of the ultimate stabilized revetment side slope. It was found that the initial bank slope was on the average about 15% steeper than the final revetment slope. No definite relationship could be established to predict the initial bank slope. The magnitude of the side slope appears to be a function of the bank material and the stream flow velocity, and has no direct relationship with the characteristics of the windrow stone. The initial side slope can best be estimated from field measurements at the location where the windrow revetment is planned.

36. A good relationship was found between the settling angle of the stone, the stream velocity, and the bed material. See Plate 1. This relationship was:

$$\Delta/Y_t = 0.68 (Z)^{1.4} / [V^2 / (SG-1)gd_b]^{0.085} \quad (2)$$

Δ = distance stone moves riverward after being eroded from windrow.

Y_t = water depth above toe of revetment

Z = cotangent of underwater bank slope

V = average channel velocity

SG = specific gravity of bank material

d_b = representative size of bank material

g = constant, equals 32.2 ft/sec²

37. Stone Gradation. None of the windrow revetments tested using either stone gradation 1 or 4 of table 2 failed by leaching even though very high velocities were used. Tests using single stone sizes gave conflicting results. Tests with gradation 3 failed, but tests with gradation 2 did not. However, the nonfailure of gradation 2 was attributed to mechanical blockage resulting from the size of the stone in respect to the model bed material. It is recommended that a well graded stone gradation be used for windrow revetments.

38. Stone Size. The size of the stone used in the windrow appears to be of no serious consequence as long as it is large enough to resist being transported by the stream. A change in stone size will impact on the thickness, \bar{t} , of the revetment, but this may not change the value of the relative thickness, \bar{t}/d_r . It should be noted that larger stone sizes require more weight per unit area than smaller stone sizes to produce the same relative thickness.

39. Bank Height. No definite conclusions were formulated on the effect of bank heights. The only noticeable difference in tests using high banks was a slightly ragged alignment. In the time lapse photos of these runs it was noted that the high banks have a tendency for large segments of the bank to break loose and rotate slightly, whereas the low banks simply melt or slough into the stream. The slight rotation of the high bank segment probably induces a tendency for ragged alignment. Compare Photos 13 and 14.

40. Windrow revetments constructed on high river banks may lead one to believe that some of the stone is wasted or more stone needs to be added to the windrow because quantities of stone will be scattered from the top of bank down to the water's edge. This stone is not wasted and additional quantities do not have to be added to the windrow to pave this zone. This stone is part of the supply and simply has not been used as yet. In the case of a low bank most of this stone would remain in the windrow, but because of the greater distance between the windrow and the water's edge for high river banks, it takes more time for the final quantities of stone to move into the water. Eventually, if this stone is needed, it will work its way down. The object of the revetment is to protect the bank from the erosive force of the water and not to armor the entire bank line top to bottom.

41. Noncontinuous Revetment. The use of noncontinuous windrow revetments appears to be feasible. However, because of numerous additional variables associated with this method, only runs demonstrating the applicability of the technique were made. See Photo 15.

42. Sample Calculation. The following example is included to demonstrate the design of a windrow revetment.

Example

Given:	Remarks
Average Stream Depth $D = 20 \text{ ft.}$	From field surveys
Assumed Scour Depth $Y_s = 10 \text{ ft.}$	From field observations at nearby structures
Average Stream Velocity $V = 4 \text{ fps}$	From field surveys
Mean diameter of bank material $d_b = 0.001 \text{ ft.}$	From mechanical analysis
Specific gravity of bank material $SG_b = 2.65$	From analysis
Assume cotangent of revetment slope $Z = (1.3)(1.15) = 1.5$	From field surveys of under- water bank slopes, Initial Slope = 1.3H to 1.0V (Final slope 15% flatter than initial slope)
Mean diameter of windrow stone $d_r = 1.0 \text{ ft.}$	From other calculations
Desired revetment thickness $\bar{t} = 1.5 d_r = 1.5 \text{ ft.}$	As required
Specific gravity of windrow stone $SG_r = 2.5$	From analysis

Given:

Remarks

Void ratio of windrow stone

From analysis

$$e = 0.30$$

Computations

Toe depth

$$Y_t = D + Y_g = 20 + 10 = 30 \text{ ft.}$$

Base width of revetment

$$X_o = Z Y_t = (1.5)(30) = 45 \text{ ft}$$

Influence of stream velocity and bank material

$$\frac{v^2}{(SG-1) g d_b} = \frac{(4)^2}{(2.65-1)(32.2)(0.001)} = 301$$

Cotangent of settling angle

$$\frac{\Delta}{Y_t} = \frac{0.68(Z)^{1.4}}{[v^2/(SG-1) g d_b]^{0.085}}$$

Equation 2

$$\frac{\Delta}{Y_t} = \frac{0.68 (1.5)^{1.4}}{(301)^{0.085}} = 0.74$$

Riverward movement of stone

$$\Delta = (0.74)(30) = 22 \text{ ft.}$$

Eroded width of windrow

$$X_1 = X_o - \Delta = 45 - 22 = 23 \text{ ft.}$$

Revetment slope length

$$P_r = Y_t(Z^2+1)^{0.5} = 54 \text{ ft.}$$

Bulk unit weight of revetment material

$$\gamma'' = \frac{(SG)(s)}{1+e} = \frac{(2.5)(62.4)}{1.3} = 120 \text{ lb/ft}^3$$

Weight of stone in revetment per foot of bank line

$$W_r = P_r \bar{t} \gamma''$$

$$W_r = \frac{(54)(1.5)(120)}{2000} = 4.9 \text{ tons/ft.}$$

Since this is an average value, the quantity of stone and windrow width should be increased. It is suggested that this be $1.25 W_r$ and $1.25 X_1$. Then

$$X_4 = 1.25 (23) = 29 \text{ ft.}$$

$$W_w = \frac{1.25 (29) (4.9)}{(23)} = 7.7 \text{ tons/ft. placed uniformly within a 29 ft. wide windrow}$$

where:

$$X_4 = \text{Base width of windrow as constructed.}$$

$$W_w = \text{Application rate of windrow as constructed.}$$

C. VANE DIKES

43. This section of the report presents results of model studies on river training structures called vane dikes. Vane dikes are defined as river training structures which are not attached to the river bank nor to each other. See Photos 17, 18, and 19. Some advantages of a vane dike system over conventional river training works are as follows:

(a) They are effective in directing the river flow away from channel banks subject to bank erosion, thereby creating and preserving shallow water areas.

(b) They use less construction material than continuous dikes and revetments.

(c) They lend themselves to "stage construction." Installing one structure at a time, beginning at an upstream location, allows the river to indicate the best location and orientation of subsequent structures.

44. The purpose of this investigation was to determine the relative effects of vane dikes on the flow distribution and bed configuration of a typical Missouri River bend. Items investigated included:

(a) The angle of the vane structure to the flow.

(b) The relative length of the vane structure.

(c) The ratio of the length of vane to the length between vanes (gap length).

The Model

45. Yankton Bend, located near Yankton, South Dakota, approximately five miles downstream from Gavins Point Dam on the Missouri River was selected as the prototype to be modeled. This bend was considered to be a typical Missouri River bend and field data were available. See Plate 4. The bend extends from the U. S. Highway 81 Bridge at Missouri River mile 840.4 to river mile 843.1 (1941 year mileage), the banks of which are basically uncontrolled except for a kicker structure at river mile 842.9. See Plate 5. The bend represents a typical river bend with an erosion zone along the concave bank and a point bar along the convex bank.

46. The model layout of Yankton Bend is shown on Plate 5 and Photos 16 through 19. It represents the prototype bend as shown on Plate 4. The model was constructed using a scale ratio of 1:25 in the vertical and 1:150 in the horizontal. The graduated boundary shown on Plate 5 is the same as that indicated by the solid line in Plate 4 and represents the outer basin walls of the flume. The graduations are reference marks which were placed on the outer basin walls to aid in the construction layout and stationing of structures within the flume. The solid inner lines represent the river bank line. This inner boundary was constructed from sheet metal covered with a textured material to simulate the prototype bank roughness. This was fixed in place, thus creating a nonerodible bank line. The bed material consisted of finely ground walnut shells. Water surface monitoring (WSM) devices were located on 10 foot centers through the middle of the design channel as shown in Plate 5. The water surface elevation at the mid-point of the model was regulated by a water control device located near the midpoint. This device controlled the elevation of the water in the model flume. The water and sediment were recirculated from a pump at the end of the basin to the upper end of the basin. The distribution of water was controlled through louvers at the flume inlet. The vane dike structures were fabricated

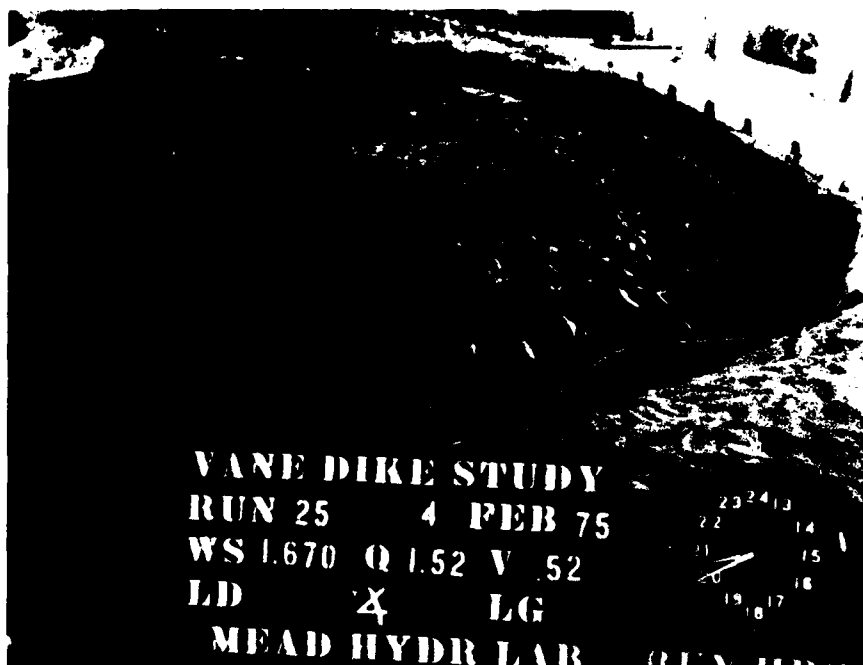


Photo 16. View upstream in model from River Mile 841.0 showing bed configuration of verification run after 20.7 hours. Note point bar in upper left of photo and deep channel identified by ponded water along bank line at right of photo.

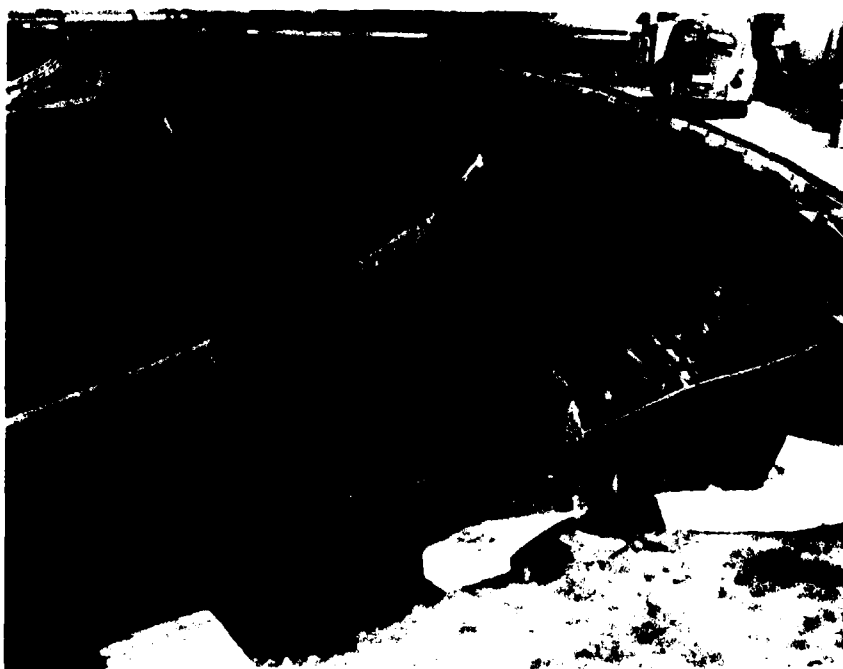


Photo 17. View from River Mile 841.0 at end of run 12 showing bed configuration resulting from 5 foot vane dikes at 0° placement angle and 5 foot gaps. Note minimum influence by vane dikes on bed configuration.

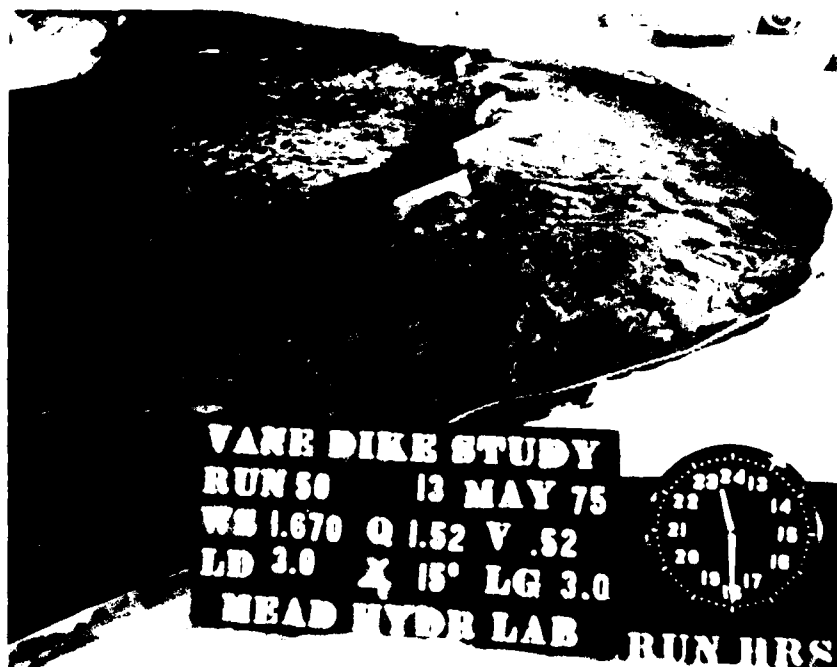


Photo 18. View from River Mile 841.0 at end of run 50 showing bed configuration resulting from 3 foot vane dikes at 15° placement angle and 3 foot gaps. Note channel riverward of vane dike system identified by ponded water.

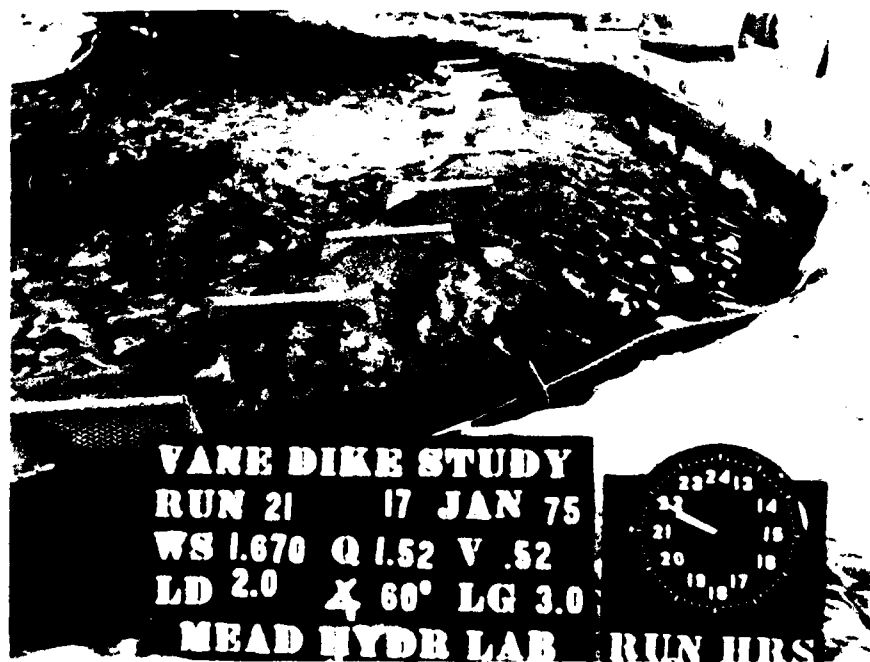


Photo 19. View from River Mile 841.0 at end of run 21 showing bed configuration resulting from 2 foot vane dikes at 60° placement angle and 3 foot gaps. Even though sediment accumulated between the vane dikes, this arrangement had minimal influence on flow distribution. Note deep channel along bankline at right of photo.

from sheet metal to three different lengths, 2', 3' and 5'. They were also covered with a textured material to simulate the prototype roughness of the stone.

TEST PROCEDURES.

47. In the first series of tests and prior to each test, the bed of walnut shells was leveled. This insured similar starting conditions at the beginning of each test and permitted comparison of tests of different structure configuration, quantitative measurements, and observation of scour and deposition. Vane dike structures were then placed in predetermined locations. See Photos 16 through 19. The model was slowly filled with water to eliminate any possible surging effect which could have altered the bed. The model was usually set up and started in the afternoon and run overnight. This insured sufficient time to enable the bed configuration and sediment transport to reach equilibrium.

48. During the last series of tests, the procedure was changed in order to be more representative of natural prototype processes. Tests were initiated only after the verification condition (left bank flow with point bar in the center of the test area) had been duplicated. See Photo 16. Placement of individual vanes then proceeded at 2-hour intervals, starting at the upstream end of the test area.

49. During each run, time lapse movies were taken of the test area. At the end of each run, channel cross sections were taken using a sonic sounder and X-Y plotter. The data from the channel cross sections was used to make contour maps of the bed. See Plate 6. Velocity measurements were taken during selected runs at different cross sections throughout the test area in order to determine the percent of flow both landward and riverward of the structures. At the end of each run all vane dikes were removed and the bed of walnut shells was leveled in preparation for the next run.

cross sections throughout the test area in order to determine the percent of flow both landward and riverward of the structures. At the end of each run all vane dikes were removed and the bed of walnut shells was leveled in preparation for the next run.

CONCLUSIONS.

50. During the first series of tests, efforts concentrated on determining the effect of various placement angles of the vane dikes on such things as the flow distribution and bed configuration. The placement angles were measured from the tangent of the stream line, as indicated in Plate 5. The next series of tests investigated varying the distance between vane dikes (gap length) and various lengths of the vane dikes themselves. The gap length is illustrated on Plate 5. For the first series of tests, a 5-foot vane length and a 5-foot gap length were used. The vanes were rotated with respect to the design channel alignment through angles varying from 0° to 180° . The purpose of these tests was to determine which structure placement angle was the most effective in diverting flows riverward of the structures. One measure of the effectiveness of the vane dikes was the development of the channel riverward of the vane dike structures. It was concluded from this series of tests that the most desirable channel alignment conditions for the bend studied was produced by a placement angle of 15° to the flow. Table 3 summarizes the findings from the first series of tests.

TABLE 3.

STRUCTURE PLACEMENT ANGLE RESULTS

Placement angle	Comments
0°, and 180°	Very little influence on channel flow.
7°	Minor influence on channel flow with some sediment deposition landward of vanes.
15°	Channel flow riverward and parallel to vane alignment with considerable sediment deposition landward of vanes.
30°	Flow around both sides of vanes in upper portion of model. Combined influence of vanes forced channel flow toward the convex bank in lower portion of model.
60° - 150°	Flow disrupted. Vanes acted as obstacles to flow with no apparent desirable effects.

51. The objective of the second series of tests on the vane dikes was to determine:

(a) The effect of different vane dike lengths.

(b) The effect of different gap lengths (distance between vane dike structures).

(c) The effectiveness of the vane dike structures on removing the existing point bar along the convex bank.

(d) Variations in the deposition landward from the vane dikes for various combinations of dike and gap lengths.

52. Velocity measurements and channel cross sections were taken at selected locations throughout the model in order to evaluate the above conditions. For all of these runs, a constant 15° vane placement angle was used.

53. The operating procedure was changed for this series of tests. For example, vane dike structures were placed in the model only after the model had developed the prototype bed configuration. Tests were made with 2' and 3' vane lengths and vane to gap length ratios of 1:1, 1:1.5, and 1:2. Table 4 shows the influence of different vane length to gap length ratios on the percent of total flow landward of the structures at the midbend point in the model and at the end of the model test area.

TABLE 4

Run No.	Channel* Depth ft.	Length of Vanes - Ft.	Length of Gaps - Ft.	Length Ratio	Flow Landward of Vanes	
					At Midbend %	At End %
52	0.13	3	6	1:2	55	46
49	0.13	2	4	1:2	51	25
51	0.14	3	4.5	1:1.5	40	23
48A	0.14	2	3	1:1.5	36	1
50	0.15	3	3	1:1	1	1

*Average Channel Depth computed starting 1-foot riverward of Design Channel Alignment in order to exclude scour adjacent to vane dike.

The runs shown in Table 4 are ranked from least effective at diverting the flow riverward to most effective.

54. Runs 52, 51, and 50 and Runs 49 and 48A had the same respective vane lengths but different gap lengths. It is apparent that by holding the vane length constant and narrowing the gap length, less flow will pass landward of the structures. This decrease in landward flow is apparent midbend in the model, and at the end of the test area. A reduction of the vane length (and gap length since the ratio is fixed) resulted in a minor decrease in the amount of landward flow at midbend, but substantially decreased the landward flow at the end of the test area.

55. It is apparent that the amount of material required to construct the vane dikes increases as the vane length to gap length decreases. Reducing the length of the vane while maintaining the same vane length to gap ratio, significantly influences the overall flow and bed configuration landward of the vane dikes; however, essentially the same quantity of material will be used to construct the vanes.

56. The model investigation on vane dikes indicated that a high degree of channel control can be achieved using this technique and one can successfully manage the river flow distribution and the bed configuration through judicious selection of vane lengths and gap lengths. A ratio of vane length to gap length of one tended to encourage the greatest amount of deposition in the landward zone. Increasing the gap length, irrespective of the vane length to gap length ratio, increased the amount of flow landward while decreasing the amount of deposition. Similar results were obtained by increasing the length of the vane. It was also determined that a placement angle for the vane structure of about 15° to the flow produced the most desirable results.

D. HARD POINTS

57. This section presents the results of model studies conducted on the Hard Point erosion control technique. Hard Point erosion control structures are two-part structures consisting of a spur which projects into the stream and a root which ties back into the bankline. See Plate 7. The spur consists of erosion resistant material extending from the bank into the river to retard bankline erosion. The root, which consists of erosion resistant material placed in an excavated trench on the overbank, is tied into the spur, thus preventing the structure from being flanked by the flow.

58. The specific objectives of this model study were to:

- a. Develop design criteria for hard point erosion control structures.
- b. Determine the effect of overtopping flows on the structures.
- c. Determine if the structures were equally effective in both curved and straight channel reaches.
- d. Determine the effect of structure alignment on the extent of erosion between structures.
- e. Determine the effects of varied spacing on the extent of erosion.
- f. Determine the effects of stream velocity and water depth on the extent of erosion.

THE MODEL

59. Model Setup. This model investigation was a generalized study of a typical eroding bankline, thus no particular prototype region was modeled. Model dimensions and criteria used were similar to those developed from previous model studies of the Missouri River.

60. The model test area was a straight channel reach about 40 feet long between two curves with different radii of curvature. The basin used is shown in Photo 20 and on plate 8. The upstream approach, the left bankline, and downstream exit portions of the test reach were controlled regions lined with permanent revetment. Erosion in the test reach could only occur in the channel bed or along the test bank of the model.

61. The channel shape was trapezoidal with a 5-foot top width and 1.5H to 1V side slopes. The average channel depth was 0.25 foot, typical of previous Missouri River model studies. The channel bank along the test reach was reformed before each test using a male template as shown in Photo 21.

62. Procedure for Testing. Model tests were conducted to determine the extent of bank erosion that would occur in the test reach for a variety of hard point structure spacings. The tests were conducted with constant discharge and water surface gradient control parameters. A preliminary model study indicated that model discharges averaging between 0.40 and 1.00 c.f.s. would provide sufficient flow for bank erosion and bed material movement with a depth of approximately 0.25 foot. The water surface gradient was held constant using an instrument called a "slope control device" which monitored water surface elevations at two control stations and maintained a desired water surface differential between the two

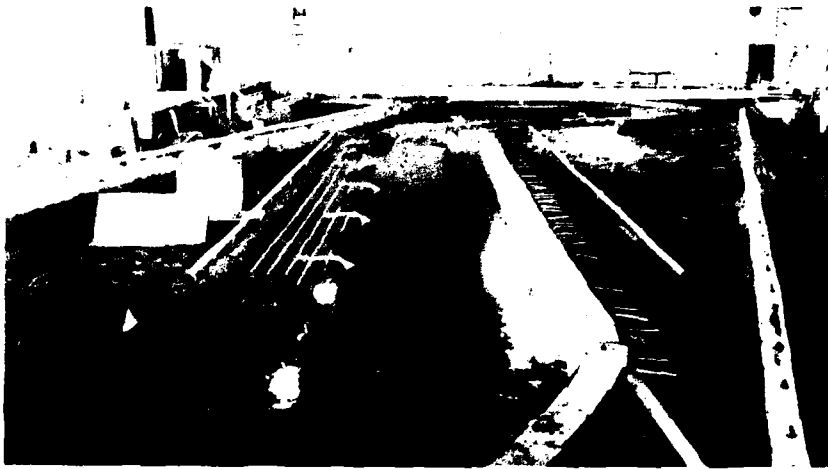


Photo 20. General view of the basin flume after a typical test looking upstream.

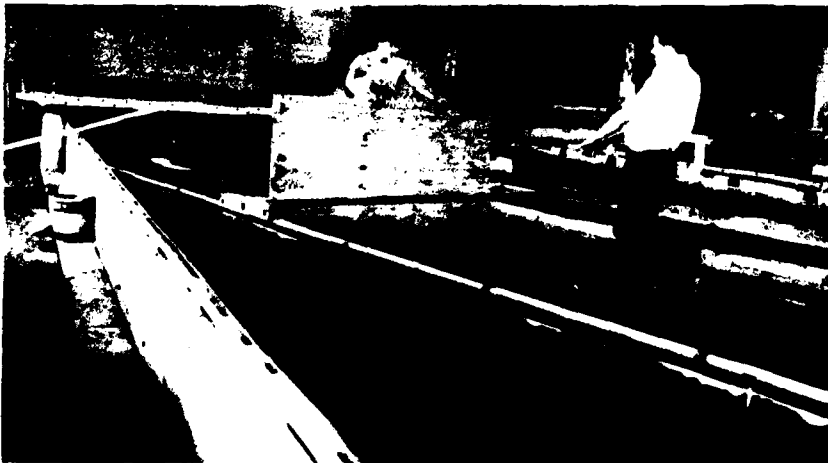


Photo 21. Formation of the test bank using a male template fixed to a carriage on a rail traverse.

stations. The device adjusted the volume of water in the basin to provide and maintain the desired water surface gradient.

63. Typical model tests lasted approximately 21 hours, beginning in late afternoon and continuing through the night and into the next morning. The testing was usually completed and remaining data obtained by noon.

64. The channel was reformed prior to the start of each test run. The bank material lost during the previous test was replaced with material from the channel bed and shaped to provide a uniform configuration by pulling a male template across the material. Longitudinal lines, spaced 0.4 foot apart along the test area, were formed by placing thin deposits of light colored walnut shells on the overbank. The lines were used as a horizontal reference for evaluation of the erosion pattern. See Photo 22.

65. The selected hard point spacing interval was measured off and the locations prepared for stone placement. Hard point structures require two types of stone placement, the root and the spur. A rectangular root trench was cut into the bank lines with the dimensions dictated by the preselected quantity of stone to be used. The root trench was cut about a foot into the bankline, 0.2 foot deep, and 0.4 foot wide. The trench was then filled with the required quantity of stone per foot. The stone spur of the hard point was formed by dumping the stone directly onto the channel bank and transitioned into the stone root. See Photos 22 and 23. The gradation for the stone used in modeling the hard point structure ($d_{50} = 10\text{mm}$) was scaled from the stone gradation currently being specified for hard points on the Missouri River ($d_{50} = 1.3\text{ ft}$).

66. With the physical construction of the model completed, the basin was filled slowly, to preclude bank sloughing, and the test run was started. Each run was made at a predetermined discharge, slope,

and spacing interval. The channel flow velocity and depth were allowed to develop subject to the constraints imposed by the pre-selected parameters. The maximum extent of erosion usually occurred after about 10 hours of running. The test basin was drained after completion of the model test.

67. Data Collection. The following data were obtained during the duration of each run.

a. Prior to each test, photographs were taken of the initial model setup from overhead positions. The pictures for each test were taken from the same overhead location and height so that the photographic scale would be constant. These pictures were used to show the bank before erosion.

b. When the erosion process had reached an apparent equilibrium condition, point velocity readings were taken at a control section, which was located as shown on Plate 8. The data obtained were used as a check on the selected control parameters.

c. Point velocities were obtained at 1-foot intervals across the channel at each structure location. The point velocities were used to obtain the average depth and velocity for that location.

d. At the end of each run, photographs were taken of the final bank erosion pattern with water flowing past the structures. These photos included time exposures showing the typical channel streamflow lines and eddy action around the hard points.

e. The basin was drained and photographs were taken of the bed formation and used for channel configuration comparisons.

f. Time lapse movies were taken throughout the duration of each test, and used for examination of the erosion process.



Photo 22. Excavation of the root trench into the right bank.



Photo 23. Placement of the stone used for the hard point structure formation.

68. The analysis of each run involved reviews of both the time lapse movies and photographs along with measurements of the erosion patterns from the still photographs. The amount of area eroded between structures, the spacing between structures, the average maximum lateral extent of erosion into the bank, and the angle of the erosion expansion were parameters required for the analysis. See Plate 9. The measurements were taken directly from enlarged photographs and adjusted to the proper scale.

REVIEW OF TESTS

69. The model study proceeded in two phases. In the first phase, tests were run at a constant slope of .0008 ft/ft and discharge of 0.65 c.f.s. with various hard point structure configurations. The tests were run to obtain critical design effects for situations involving various channel alignments, flood stage overtopping, and structural alignment to the channel banks.

70. The initial tests involved placement of hard point structures in the upstream curve and straight reach of the test area at 5 and 7.5 foot intervals respectively. The initial tests used 4 lbs of stone in the spur and 3.5 lb/ft of stone in the root of each structure. This quantity of stone for the indicated discharge resulted in failure of the structures in both regions. The volume of stone was insufficient to protect against the resulting scour. A typical structure failure is shown in Photo 24.

71. The hard point structures were then tested using 8 lbs of stone in each spur with the stone in the root remaining at 3.5 lb/ft and tested under the previous conditions. The spur portion of the structures in this case was stable in the straight reach. However, because of the angle of attack in the curved region, the structures failed completely indicating that the hard points should not be recommended for use in sharp bends. The banks in the curved region

were then fixed so that the approach geometry would remain constant. It was also necessary to fix the first hard point structure to insure that flow would be directed toward the straight portion of the model. The 8-lb quantity of stone for the spur proved to be adequate for the remainder of the study.

72. The effects of root alignment on the erosion pattern were observed with a 7.5-foot hard point spacing and alignment angles of 60° and 30°. The angles were measured from a line perpendicular to the channel. The erosion patterns for the tests are shown on Photos 25, 26, and 27. A comparison of the pictures shows the erosion patterns for the 30° and the perpendicular alignments to be essentially the same. Erosion in the 60° alignment is less than that for both the 30° and the perpendicular alignment because in the 60° alignment much of the root is, in effect, used for bank erosion protection.

73. Phase II of the model testing evaluated the impact of channel depth and velocity, on observed lateral erosion patterns for hard point spacings of 2.5, 4.0, and 7.5, as well as tests with no hard points. The resulting investigations concluded that the erosion between hard points was related to the structure spacing by the Froude Number, $F = V / \sqrt{g D}$. The relationship is as follows:

$$\bar{Y}/D = 59.5 F^{1.2} (10^{-8.2} D/L) \quad (3)$$

where:

D = average channel depth, ft.



Photo 24. Failure of the hard points in the curve due to insufficient quantity of stone in the nose. The stone migrates to the bottom of the channel.

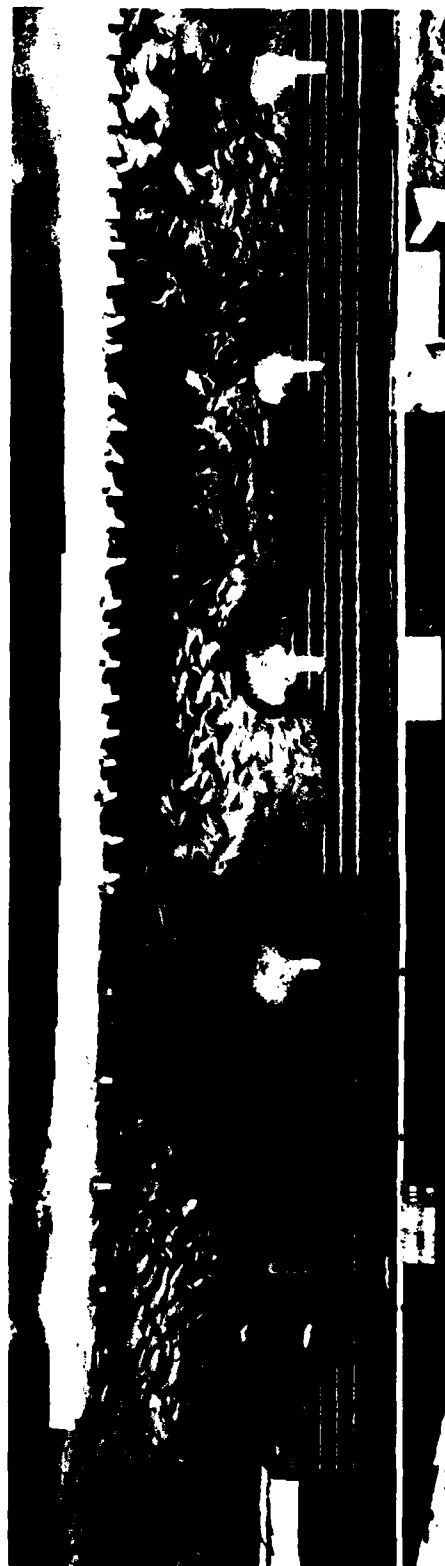


Photo 25. Development of erosion pattern with hard point roots aligned perpendicular to the channel bank.



Photo 26. Development of erosion pattern with hard point root alignment at 30 degrees upstream from the perpendicular position. (Note the deterioration of the root.)



Photo 27. Development of erosion pattern with hard point root alignment at 60 degrees upstream from the perpendicular position. (Note the deterioration of the root.)

\bar{Y} = average maximum lateral extent of erosion between structures, ft.

V = average velocity in the test reach, f.p.s.

L = spacing length between hard point structures, ft.

A graph for the relationship is shown on Plate 10.

74. The angle of erosion expansion downstream of each structure was found to be approximately 20.0 degrees. See Plate 11. Complete development of the expansion angle did not occur for hard point spacings less than 4.0 feet or average test reach velocities less than 0.5 f.p.s. Spacings less than 4.0 feet were so close that the structures interfered with one another's erosion development.

CONCLUSIONS

75. The following conclusions were reached from the model study on the hard point erosion control technique:

a. The spur or riverward end of the hard point is the principal design component for protection against failure of the system. The quantity of stone used in the spur of the hard point is critical to the stability of the system. If the spur of the hard point fails, the quantity of stone in the root would not be adequate to protect against the erosive forces of direct flows.

b. The root is the principal design component providing protection in the case of overtopping of the structure during flood stages. Flanking of the spur structure should be a major concern during the passage of flood flows. The design of the root should be sufficient to inhibit leaching of the soil from behind the spur section. The root should be designed to protect against flanking or eddy erosion.

c. Placement of hard points in various channel alignments can be accomplished and can be effective, however, placement along acute channel curves is not recommended. The extreme attack angle of flow in curves against the spur and root would necessitate excessive amounts of stone. In those cases, it would be more advantageous to design a continuous bank revetment or windrow revetment.

d. Alignment of the hard points involves only the root portion of the structures. Orienting the root upstream to the flow serves no apparent useful purpose. When the angle of the root is small, the erosion characteristics are similar to those with a perpendicular root. When the angle is large, the root tends to parallel the eroded bank and direct flow attack occurs on the root. The root is then utilized in a windrow type of situation. Since the roots are usually not designed for that purpose, they would be apt to fail.

e. Various spacings for the hard point structure placement had definable effects on the erosion pattern. There was no detectable optimum structure interval indicated from the erosion patterns in the model. The greater the spacing between structures, the more extensive the degree of bank erosion. The amount of bank protection to be provided would then depend upon the relationship between the cost of the proposed project and the value of the property protected.

f. A definable relationship was determined involving velocity, average channel depth, and the average maximum lateral erosion. A semilogarithmic plot relates the amount of lateral bank erosion to the structure spacing and the Froude number. An increase in the Froude number or the spacing length results in increases in the extent of lateral erosion.

76. The study indicated that the expansion angle of the erosion scallop downstream of each structure remained about constant at 20.0 degrees. Angles of erosion expansion of less than 20.0 degrees were found for situations in which the model velocity was less than 0.5 fps or the structure spacing was so close that the erosion scallop could not develop.

77. Sample Calculation. The following example illustrates the use of Plate 10 to evaluate equation 3.

Example

Given:	Remarks
Average Stream Depth (Design Flood Stage) D = 16 feet	From Field Surveys
Average Stream Velocity V = 6 f.p.s.	From Field Surveys
Longitudinal Hard Point Spacing L = 200 feet	

Computations

$$\text{Froude Number} = \frac{V}{(gD)^{0.5}}$$

$$\text{Froude Number} = \frac{6}{[(32.2)(16)]^{0.5}} = 0.26$$

$$\text{Spacing length ratio} = D/L$$

$$= 16/200 = 0.08$$

From graph, Plate 10

$$\frac{Y}{D} = 2.5$$

$$Y = (16)(2.5) = 40 \text{ feet}$$

Applying a safety factor of 1.5 gives:

$$Y = (40)(1.5) = 60 \text{ feet}$$

Therefore, the lateral extent of the root of each hard point should be at least 60 feet for longitudinal hard point spacings of 200 feet. The required quantities of stone for the spur and the root would depend on the local characteristics of the stream.

E. REINFORCED REVETMENT

78. This section presents results of model studies on reinforced revetment erosion control structures. A reinforced revetment (see Plates 12, and 13) is a 2-part structure consisting of:

a. A continuous stone toefill. The stone toefill is placed with the crown at or slightly below the normal water surface (NWS), and either against the eroding bankline or at a distance riverward from the high bank.

b. A series of stone fill tiebacks perpendicular to the bank line. The tieback is placed with the crown extending from the toefill crown back into the channel bank, sloping upward toward the top of the natural bank.

79. The toefill's purpose is to inhibit bank line erosion and undercutting of the bankline for flows at or below the NWS. During high stages when the toefill is overtopped, the tiebacks prevent flows from concentrating behind the toefill. Minor bank line erosion might occur between the tiebacks during high stages, but this eventually stabilizes.

80. The reinforced revetment erosion control technique lends itself to many design combinations and field situations, making it an ideal method to control streambank erosion and yet produce minimal impact on the environment and on the natural appearance of the area. Because of the versatility of the technique, five variations in the design have been developed. The particular design variation which the river engineer may choose will depend upon the field situation and the desired results.

81. The Type I Reinforced Revetment, see Plate 12, is constructed with the toefill stone placed adjacent to the high bank with the tieback stone fill placed in trenches excavated into the high bank. If the toefill crown is constructed to the normal water surface, the lateral extent of each tieback is 20 feet. This type lends itself to, but is not restricted to, perennial streams with well defined channels.

82. Types II through V, see Plate 13, are constructed with the toefill stone placed riverward of the high bank. The tieback stone fill extends from the toefill across a low elevation overbank area to the high bank and may extend into trenches excavated into the high bank. The low elevation overbank area between the toefill and the high bank may be a shelf extending under water some distance riverward of the high bank, a sand bar, a secondary channel, or a small flood plain. For construction purposes, the landward side of the toefill is divided into two zones; the lower bank zone, and the upper bank zone. The lower bank zone consists entirely of the low elevation overbank area adjacent to the toefill. The upper bank zone will contain varying proportions of the low elevation overbank area and the high bank, depending upon the irregularity of the bankline. The lateral extent of each tieback for the Types II and IV designs is 25 feet, at least 10 feet of which is constructed on the lower bank zone. In the Types III and V designs, the lateral extent of each tieback is 40 feet with at least 20 feet of each tieback constructed on the lower bank zone. In the Types II and III designs, the area between the toefill and the high bank is backfilled, whereas in the Types IV and V it is not. Each tieback in the Type II design is constructed with a crown slope of 1V to 5H, sloping upward from the toefill toward the high bank. For the Type III design this slope is 1V to 8H. In the Types IV and V designs, the slope may be varied depending upon site conditions. The Types II through V are more suited, but not restricted, to intermittent or braided streams in which the high bank is not strongly or constantly under attack by the stream flow.

83. The objectives of this study were to investigate the following design parameters:

- a. Longitudinal tieback spacings.
- b. Toefill crown height.
- c. Backfilling or not backfilling the region between the toefill and the high bank.
- d. Tieback structure crown slope.

THE MODEL

84. Two different model investigations were conducted during the Reinforced Revetment study; one of the Type I design (see Plates 14 and 15 and Photo 32), and a second on Types II, III, IV and V designs (see Plates 14 and 16 and Photo 36). Type II, III, IV and V designs are similar and therefore were tested as minor variations of one design. Both models were constructed to represent average river conditions typical of the Missouri River between Yankton, South Dakota and Sioux City, Iowa. A scale ratio of 1:40 was used in both models. Because of limitations on available space it was not practical to reproduce the entire prototype channel width (about 2,000 feet) in the model, therefore only a representative segment of the river adjacent to the bank line was constructed in the laboratory. The Type I model employed a 6 foot wide channel and a 2.8 foot wide high bank. The second model used a 5 foot wide channel with provisions for a 2 foot wide low elevation overbank zone flanked by a high bank. Both models were formed within inclosures filled with finely ground walnut shells. Crushed limestone (SG=2.5; $d_{50} = 6.5\text{mm}$) was used to simulate the stone for the tieback and toefill structures. Each model river segment consisted of a trapezoidal channel with a bend radius of 190 feet. The

right bank in each model was vertical and nonerodible. The left bank, through both model test areas, was molded from ground walnut shells and was erodible. Outside of the test area, the left bank in each model was fixed and nonerodible.

85. In each study the left bank of the test area was reformed prior to the start of each run. See Photo 28. Material was removed from the channel bed and mixed with the bank material to replace material eroded from the bank during the prior run. This material was thoroughly mixed prior to each test run to insure homogeneous physical properties. The bank was molded to the desired configuration with the aid of a male template. The template was mounted on a carriage which was manually traversed up and down the model along the top of concrete block walls parallel to the channel alignment thereby producing a bank with a uniform configuration. See Photos 28 and 29.

86. A construction reference plane was established in each model. The reference plane was identical to the normal water surface and was equal to an elevation of 1.375 feet at the midpoint in each model. The intersection of the reference plane and the left bankline was called the reference line. See Plate 14. In the Type I model the reference line was always 6 feet from the right wall, whereas in the second study it was always 5 feet from the right wall. See Plates 15 and 16.

87. A thin layer of dry ground walnut shells was spread on the surface of the bank berm. See Photo 29. These shells, light brown in color, contrasted with the moist dark brown shells and accentuated the berm area in the overhead pictures and time lapse movie photos. A grid, constructed from a white powder, also was placed on the overbank berm to aid in measuring and observing the extent of bank erosion. See Photos 30 and 31. The grid increments for the Type I model were 1 foot in the longitudinal direction and 0.4 foot in the lateral direction.



Photo 28. Reconstruction of left bank model test area. Template attached to horizontal bar was used to shape bank to desired dimensions and elevations.



Photo 29. Covering top of left bank area with dry ground walnut shells to highlight area for photos. Note horizontally mounted wheel on bar rides against right bank to aid in positioning template.



Photo 30. Placing grid and stone test structures in test area after constructing bank.



Photo 31. Overhead view of test area showing placement of graduated markers over grid at end of run to facilitate measurement of erosion. Note irregular white line placed to mark erosion boundary.

In the second model the longitudinal increments were increased to 2 feet, the lateral increments were maintained at 0.4 feet. The first longitudinal grid line always identified the reference line (See Plates 14, 15, and 16) and all lateral erosion values were measured from this line.

88. The crown of the toefill was always constructed at or below the NWS. The front face location or plane of the toefill structure did not change when the toefill crown elevation was changed. This caused the centerline station of the toefill crown to move riverward proportional to the difference between the NWS and the toefill crown elevation. See Plate 15. Subsequently during the evaluation of the data, it was determined that the lateral erosion as measured from the reference line had to be adjusted to measure instead from the centerline station of the toefill crown.

89. The toefill structures were constructed from either loose stone hand placed against the preformed bank slope, see Photo 30, or from sheet metal with stone glued to the metal.

90. During the Type I model study, trapezoidal trenches were cut into the bank similar in scale to prototype trenches, at the specified longitudinal tieback intervals. These trenches were backfilled with stone flush with the top of the bank. Additional stone was placed riverward from the trenches filling the zone between the trenches and the toefill crown. See Plates 12 and 15 and Photo 32. The face of each tieback was flush with the riverward face of the toefill, and the front slope of each tieback was at the angle of repose of the stone, assumed to be 1V to 1-1/4H. If there was no toefill being used in a given test, the additional stone filled the zone between the trenches and the stream bed. See Photo 33.

91. In the second model tests of reinforced revetments, the tiebacks were constructed of sheet metal with stone glued to the metal. The riverward face of the tiebacks for this model began at the crown of the toefill and projected landward back through the low elevation overbank zone and into the high bank. See Plates 13, and 16.

Test Procedures.

92. The principle objective of the model testing was to determine the impact of the following design parameters on the extent of bank erosion:

- a. Tieback spacings.
- b. Toefill crown height (relative to the channel bed and the normal water surface).
- c. Backfilling or not backfilling the region between the toefill and the high bank (Types II and III versus IV and V).
- d. Tieback structure crown slope.

93. Each test was conducted with the above parameters fixed. During the course of investigation, these parameters were varied from one test to another. A normal test run lasted about 21 hours. This length of time was more than sufficient for the model to develop an equilibrium condition. Each test started in the afternoon and continued through the night to the next morning. Discharge measurements, sediment samples, and water surface slope measurements were then obtained. Point velocities defining the flow distribution at specific cross sections were also acquired on most runs. Time lapse movies were made during each run to document the test. During some of the runs, slow motion movies were made toward the end of the run to record the

surface currents immediately adjacent to the reinforced revetments. At the completion of each run cross-sections were obtained by sonar sounding. These cross sections were used to measure the physical properties of the model channel and to supplement the erosion measurements obtained from overhead photos. The model was then slowly drained, taking care not to disturb the test results. A line of white powder was placed along the eroded bank line to accent the extent of erosion in the final set of overhead photos. To facilitate erosion measurements, markers with 0.1 foot gradations were placed on the bank grid extending out over the eroded area. See Photo 31. The final set of overhead photos were then obtained and the model prepared for the next run.

94. The interpretation of the data included reviews of both the time lapse movies and the overhead photos. The location of the maximum lateral erosion between each tieback and the extent of that erosion were obtained from the overhead photos. These values were then averaged to provide an average maximum lateral erosion value for each run. See plate 14.

Conclusions.

95. In accordance with the objectives stated in paragraph 83, the following conclusions were formulated:

a. Different Tieback Spacings. The principle purpose of the tieback is to prevent overtopping flows from concentrating behind the toefill and thereby causing the reinforced revetment system to fail. Tieback spacings greater than about 15 channel depths should be avoided because they encourage scour landward of the toefill crown. This scour causes the toefill structure to degrade allowing more severe scour to occur landward. Special attention should be given to the region near



Photo 32. Overhead view of test area at the end of Run 58, Type I. Tieback spacings of 4 feet (160 feet prototype), toefill crown was at elevation 0.18 foot below NWS, and stage at NWS (unprotected depth of 0.18 foot).

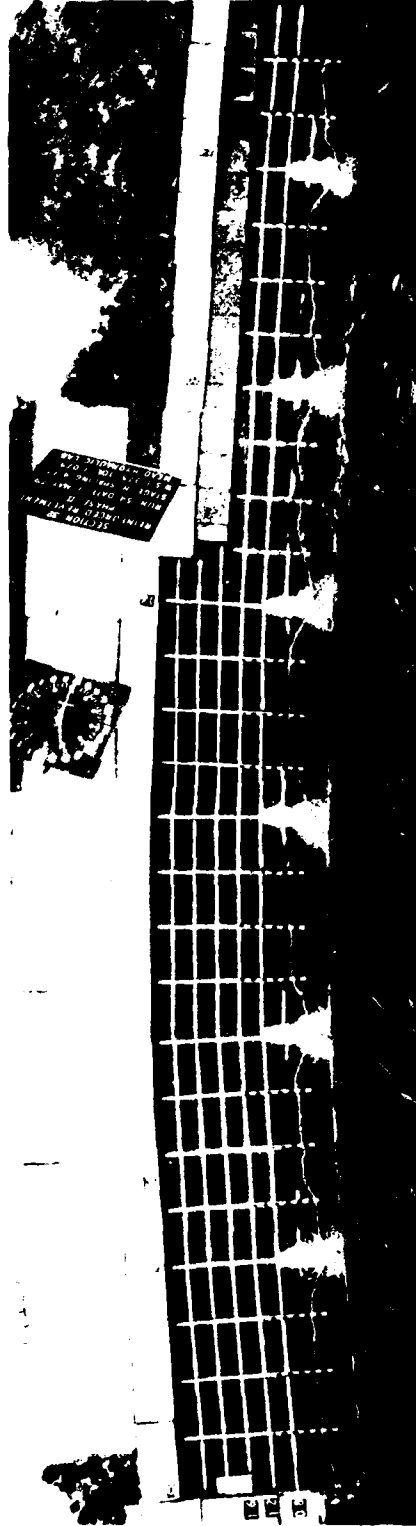


Photo 33. Overhead view of test area at the end of Run 54, Type I. Tieback spacings of 4 feet (160 foot prototype). No toefill. Stage at NWS (unprotected depth of 0.28 foot).



Photo 34. Overhead view of test area at the end of Run 60, Type I. Tieback spacings of 4 feet (160 feet prototype), toefill crown elevation 0.18 foot below NWS, and stage 0.18 foot above NWS (unprotected depth of 0.36 foot).

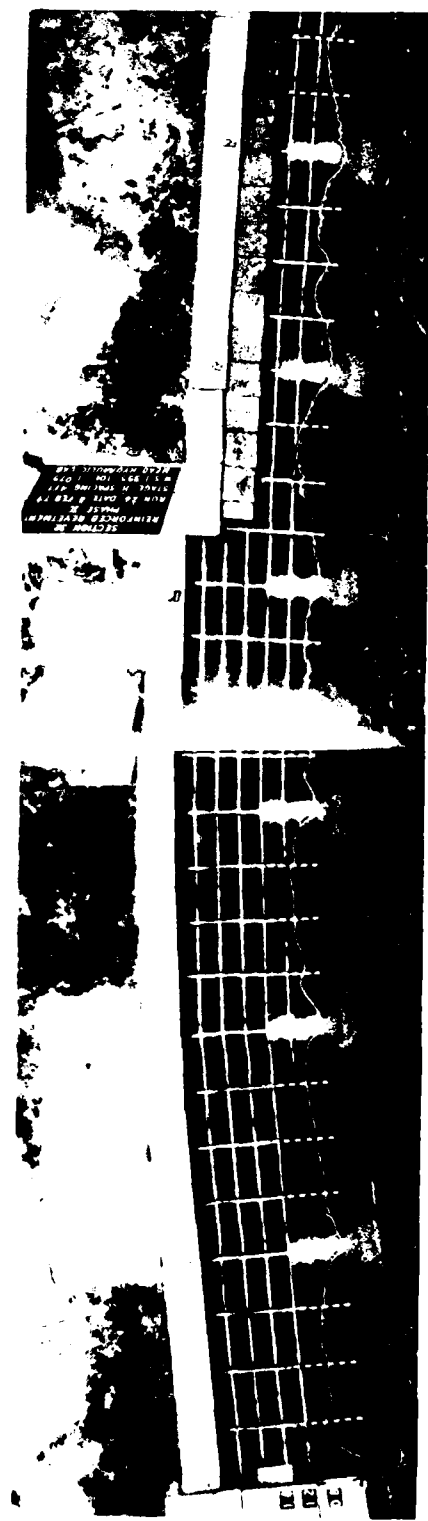


Photo 35. Overhead view of test area at the end of Run 26, Type I. Tieback spacings of 4 foot (160 foot prototype). No toefill. Stage 0.18 foot above NWS (unprotected depth of 0.44 foot).



Photo 36. Overhead view of test area at end of run 7, Types II, III, IV and V. Tieback spacing of 4 feet, (160 feet in prototype), toefill crown elevation 0.2 foot below NWS, and stage 0.2 foot above NWS (unprotected depth of 0.4 foot), tieback crown slope = 0.4. No backfill placed between structures, fill from sediment deposition.

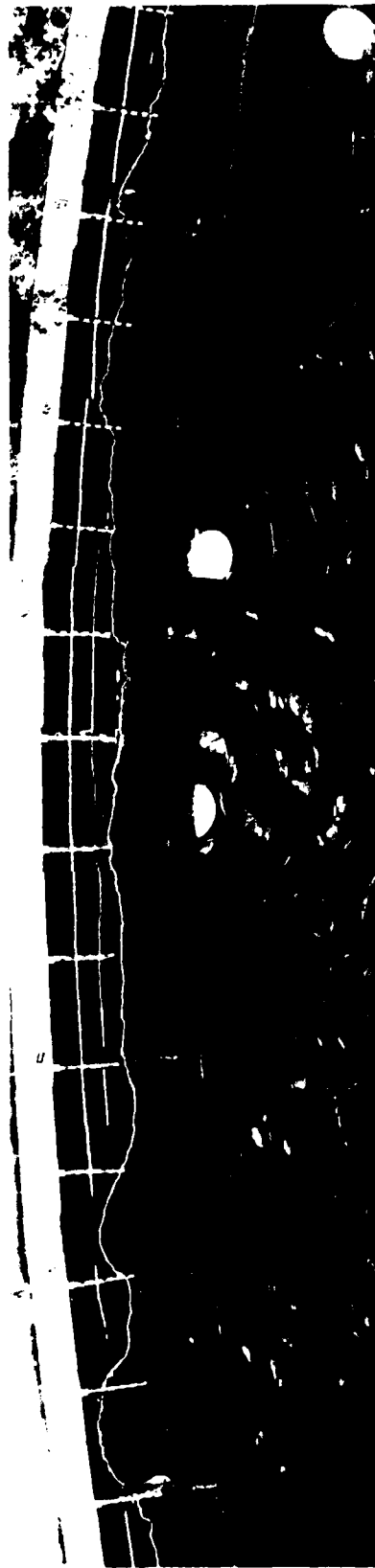


Photo 37. Overhead view of test area at end of run 28, Types II, III, IV, and V. Tieback spacing of 4 feet, (160 feet in prototype), toefill crown elevation 0.1 foot below NWS, and stage 0.2 foot above NWS (unprotected depth of 0.3 foot), tieback crown slope = 0.2. Note scour around tieback at left edge of photo.

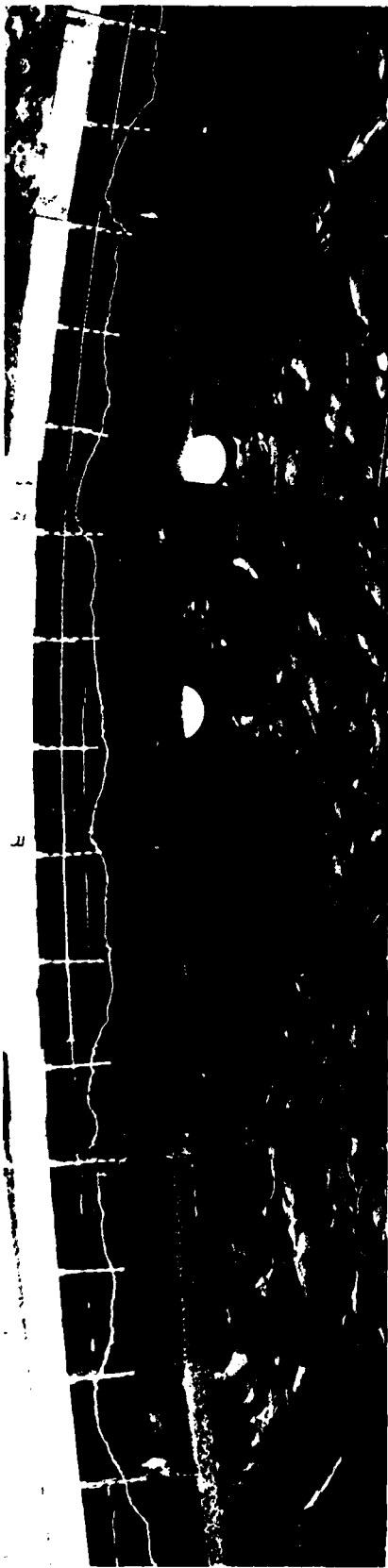


Photo 38. Overhead view of test area at end of run 27, Types II, III, IV and V. Tieback spacing of 6 feet, (240 feet in prototype), toefill crown elevation 0.1 foot below NWS, and stage 0.2 foot above NWS (unprotected depth of 0.3 foot), tieback crown slope = 0.2. Note scour around first 2 tieback structures.



Photo 39. Overhead view of test area at end of run 35, Types II, III, IV, and V. Tieback spacing of 6 feet, (240 feet in prototype), toefill crown elevation 0.1 foot below NWS, and stage 0.2 foot above NWS (unprotected depth of 0.3 foot), tieback crown slope = 0 (flat). Note scour around first 2 tieback structures.

the downstream end of the reinforced revetment system. If a tieback is located at this point, the volume of stone in this tieback must be increased over that used in the upstream tiebacks. In the model an eddy always formed off the trailing edge of the downstream end of the revetment and caused erosion of the bankline at this point. The increased volume of stone in the end tieback is needed to prevent failure of the end tieback. An alternative approach found to be satisfactory in the model was to extend the toefill downstream from the end tieback by at least two channel depths.

b. Different Crown Slopes On The Tieback Structures. The slope of the crown of the tieback is important as it impacts on the amount of streambank erosion that occurs along the plane of the front face of the tiebacks. To prevent flanking of the tieback by the flow, the lateral extent of the tieback (tieback length) must be as great as the anticipated lateral erosion, and the tieback at some point landward must rise above the maximum flood flow elevation. These studies indicated that a flat crown slope (slope = 0) should be avoided unless some provision is made at the intersection of the tieback and the high bank to prevent the high bank from eroding. See Photo 39. It was also noted that scour developed upstream and downstream of the tiebacks with crown slopes of 0.4 or flatter and appeared to become more severe for the flatter slopes. See Photos 37, 38, and 39.

c. Different Toefill Crown Heights. The toefill material was found to have a significant influence on the degree of streambank erosion for relatively shallow flows over the toefill (prototype depths less than 4 feet). It was found that for these shallow flows, the roughness of the toefill stone retarded the overbank velocities. Consequently bankline erosion was almost nonexistent. The lateral extent of erosion became significant as the depth of flow over the toefill increased past this depth. See Photos 32 through 35.

d. Backfilling Between The Toefill And The High Bank. No significant difference was observed between runs in which the zone between the toefill and the high bank was backfilled and runs in which this zone was not backfilled. During the runs with no backfill, the zone between the toefill and the high bank slowly filled with sediment and the end result was similar to runs in which this zone had been backfilled. See Photo 36. Since the types IV and V encourage deposition in the shallow overbank zones they should be more economical to construct than the types II and III.

96. In general the extent of the lateral erosion between tieback structures is governed by the tieback spacing, the slope of the tieback crown, and by the depth of flow over the toefill. See Photos 33 through 39.

97. A relationship defining the average maximum erosion for the Type I design was obtained from the test results. The extent of lateral erosion between tiebacks for the Types II, III, IV, and V designs was generally limited to a line connecting the points of intersection between the water surface and the tieback crown. The relationship for the Type I was found to be:

$$Y = K D^{-0.25} S^{0.44} I^{0.61} y_u^{1.2} \quad (4)$$

where

Y = The average maximum lateral erosion as measured from the toefill crown. ft.

K equal to a value of 27 for model and 4.6 for the prototype (length ratio = 40, slope ratio = .5)

D = The average channel depth, ft. (Design flood stage).

S = The water surface slope, ft/ft.

I = The tieback interval, ft.

y_u = The depth of flow over the toefill, ft.

98. It should be noted that equation 4 is not homogeneous. Consequently the "K" value in equation 4 must be adjusted if the equation is to be used to predict prototype erosion. Equation 4 must therefore be used with caution until sufficient prototype data becomes available to either substantiate or modify this relationship. It is suggested that the results of equation 4 be increased 50% to provide for a factor of safety.

99. It was also determined that the location of the point of maximum erosion for the Type I design occurred at a mean distance, ℓ' , downstream from each tieback at

$$\ell' = 0.6I \quad (5)$$

100. Sample Calculation. The following example illustrates the use of equation 4 for a Type I reinforced revetment.

Example

Given:	Remarks
Average Stream Depth (NWS)	From Field Surveys
D = 10 feet	
Average Stream Depth (Design flood Stage)	From Field Surveys
D = 16 feet	

Given:	Remarks
Toefill Crown 2 feet below NWS	Some initial bankline erosion permissible at NWS
Depth of flow over toefill $y_u = 8$ feet	$(16-10)+2$
Water Surface Slope $S = 0.0002$ ft/ft	From Field Surveys
Longitudinal Tieback Interval $I = 200$ feet	Want $I < 15 D$

Computations

$$Y = 4.6 (D)^{-0.25} S^{0.44} I^{0.61} y_u^{1.2} \quad \text{Equation 4 with "K" equal 4.6 for prototype values}$$

$$Y = 4.6 (16)^{-0.25} (0.0002)^{0.44} (200)^{0.61} (8)^{1.2}$$

$$Y = 4.6 (0.5) (0.024) (25) (12)$$

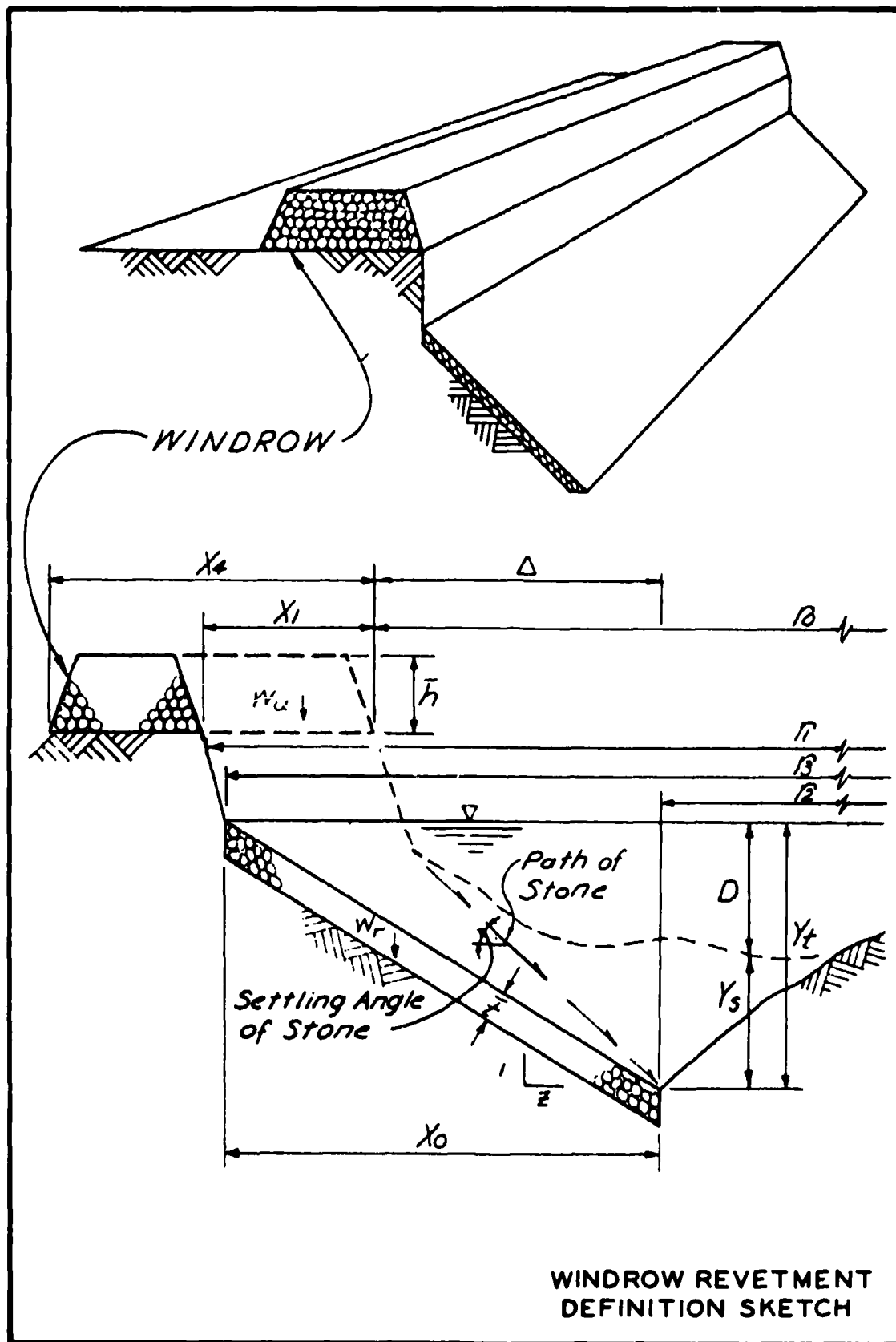
$$Y = 17 \text{ feet}$$

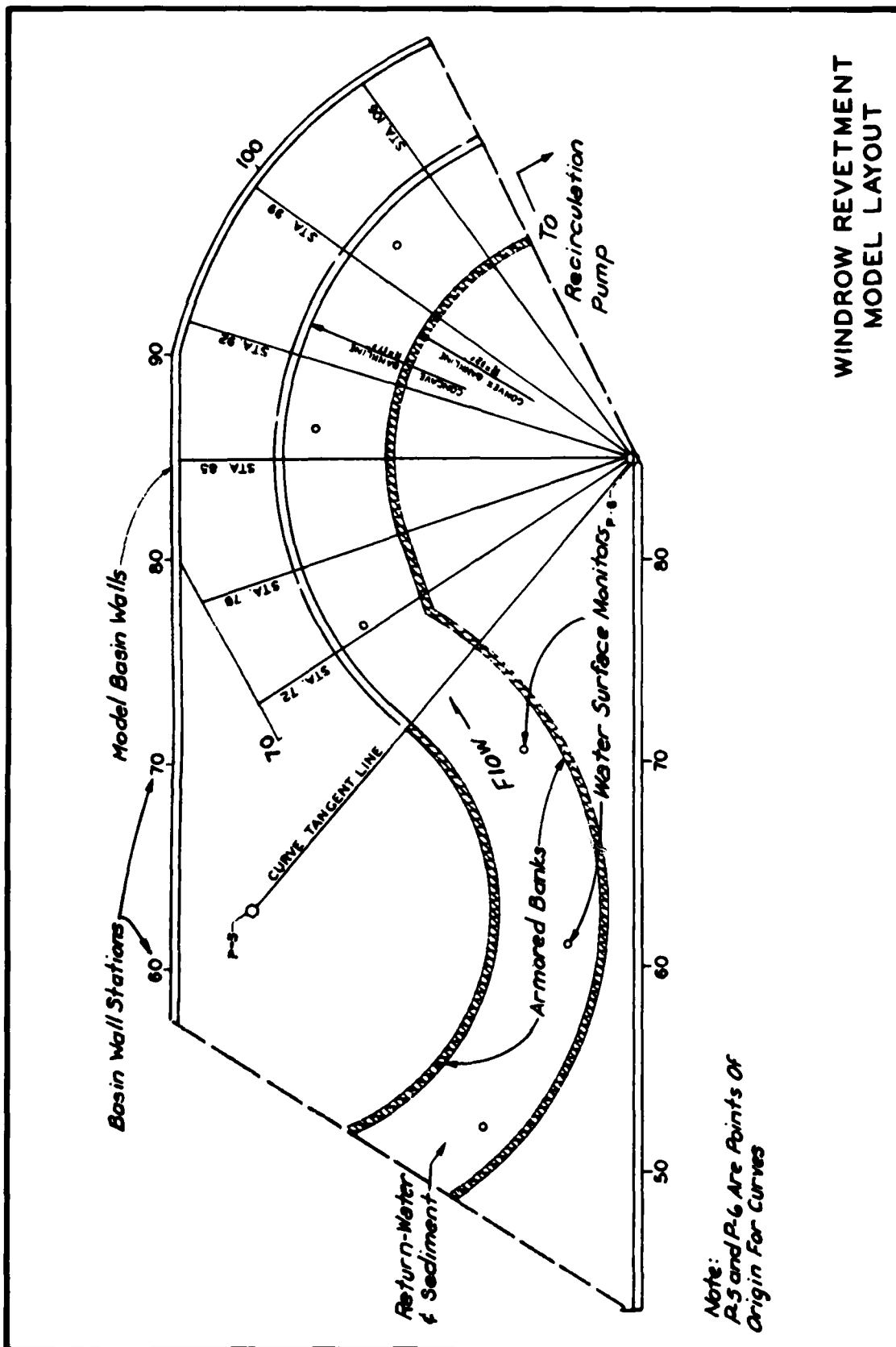
with safety factor

$$Y = 17(1.5) = 26 \text{ feet}$$

Therefore, the reinforced revetment system would be constructed with the crown of the toefill 2 feet below the normal water surface with tiebacks located along the toefill at 200 foot intervals. The tiebacks should extend laterally from the toefill back into the bank a

distance of 26 feet. The required quantities of stone for the toe-fill and the tiebacks would depend on the local characteristics of the stream, i.e. the bend radius, the anticipated scour along the toefill, and the composition of the bank material.





WINDROW REVETMENT MODEL LAYOUT

PLATE 2

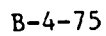
B-4-72





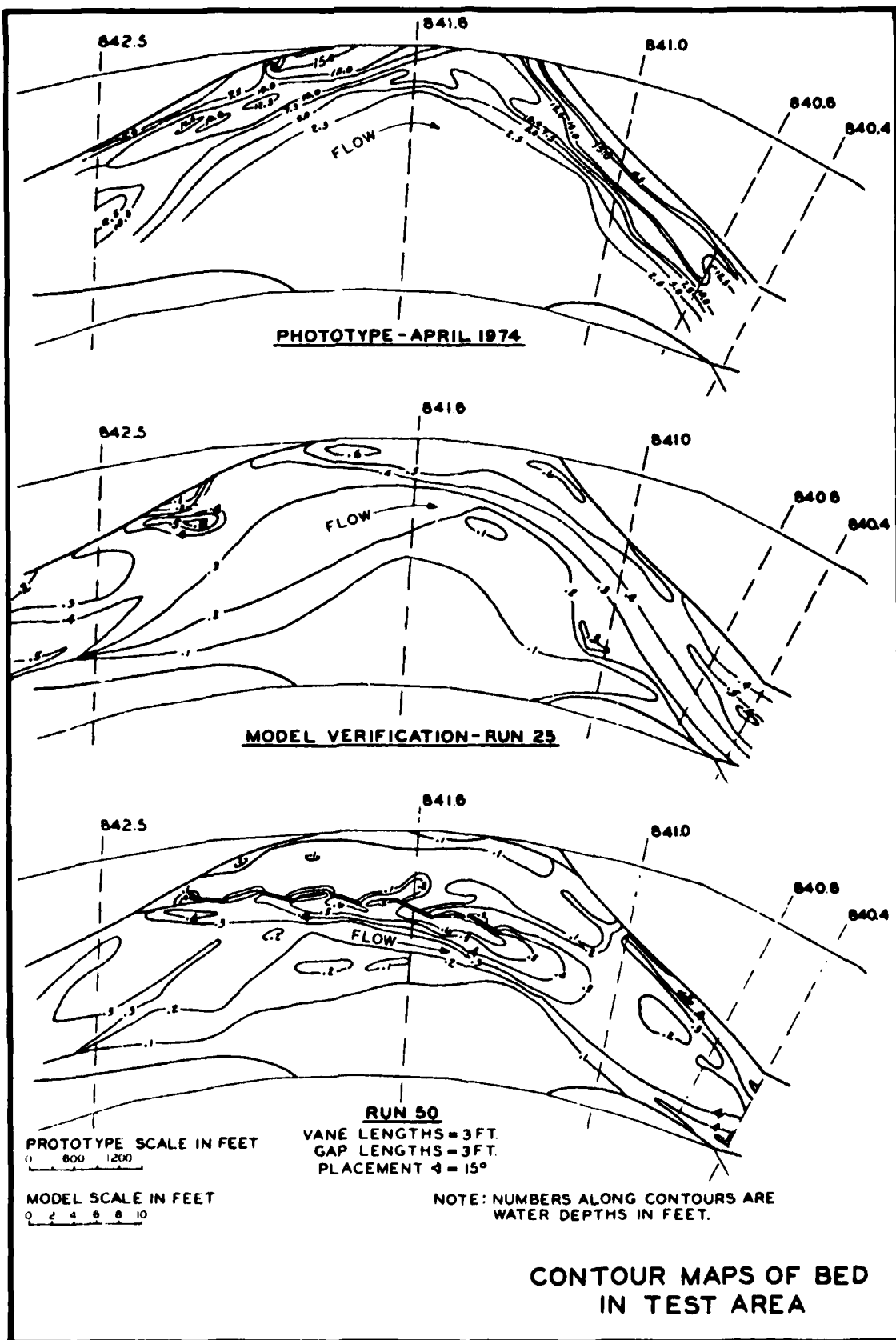
PLATE 4

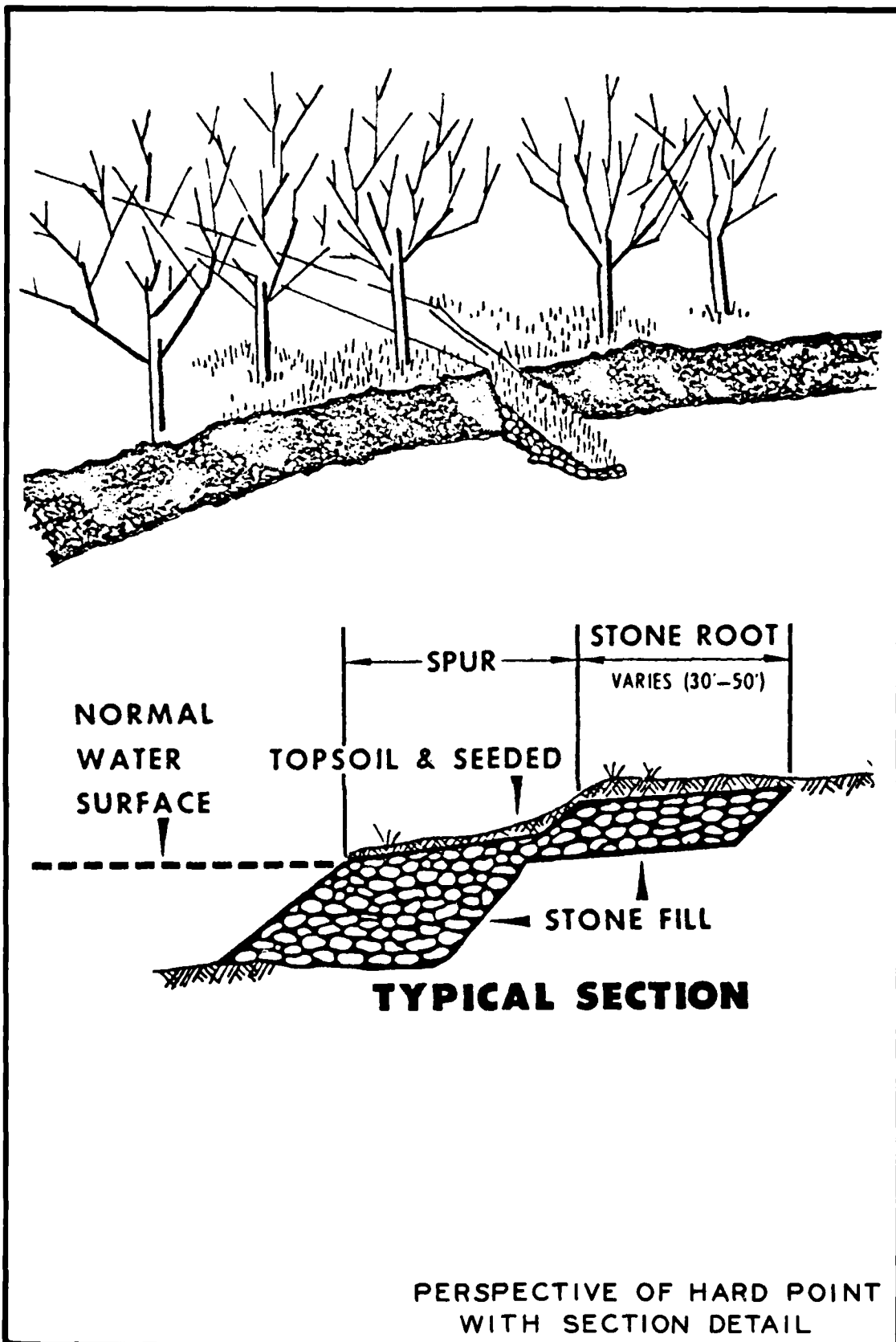
B-4-74

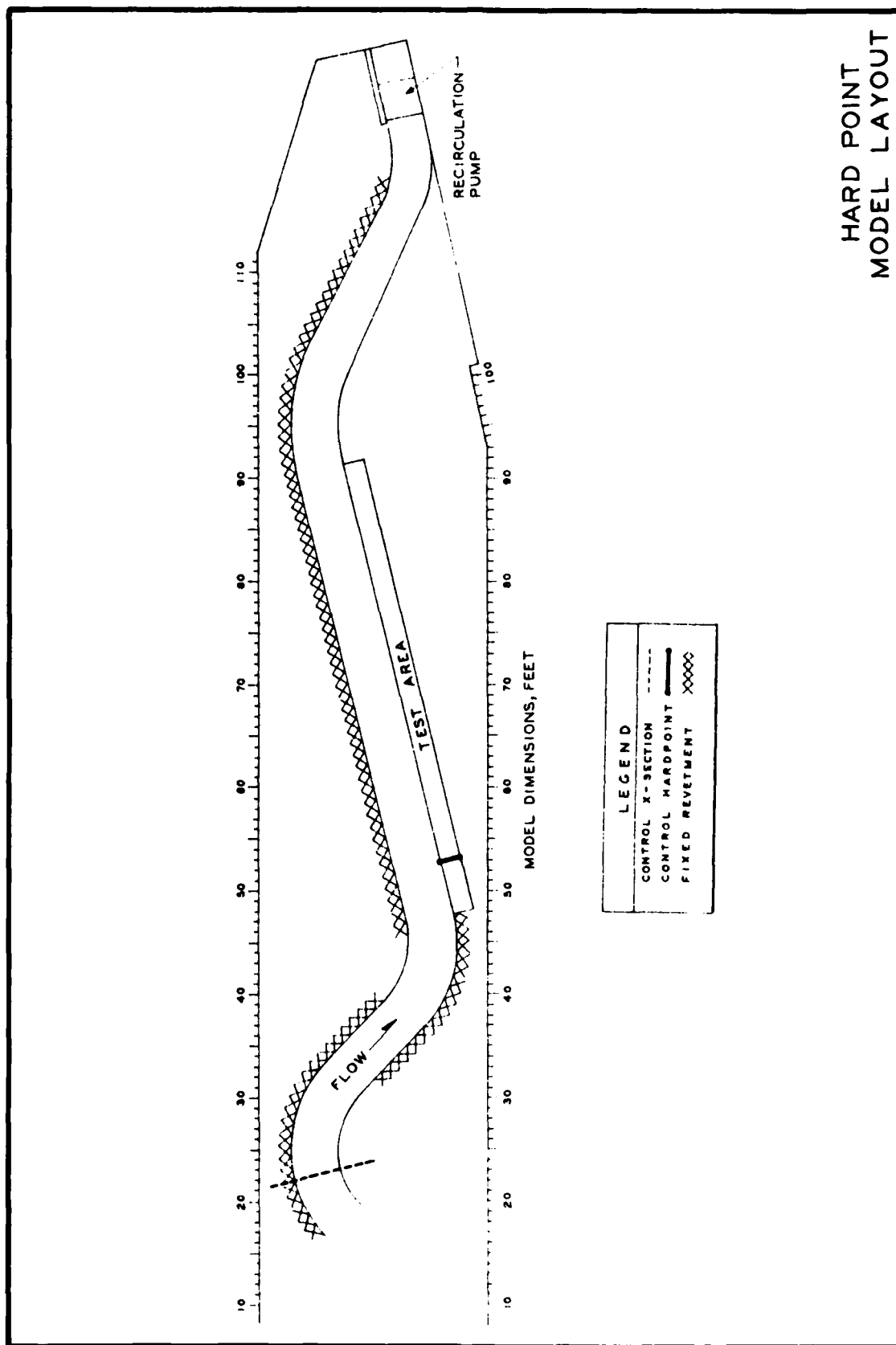


MODEL LAYOUT AND VANE DIKE PLACEMENT DETAILS

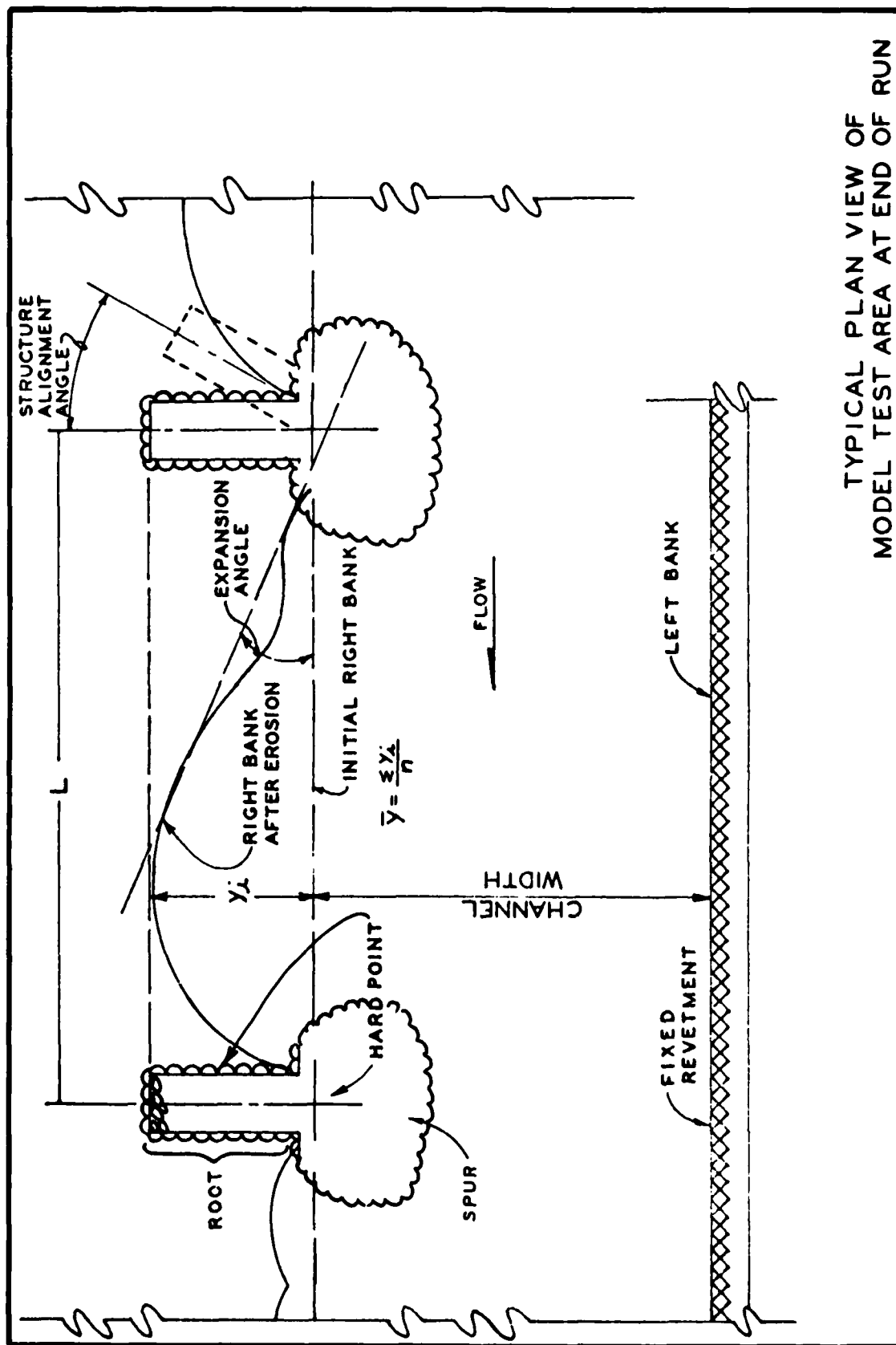
PLATE 5



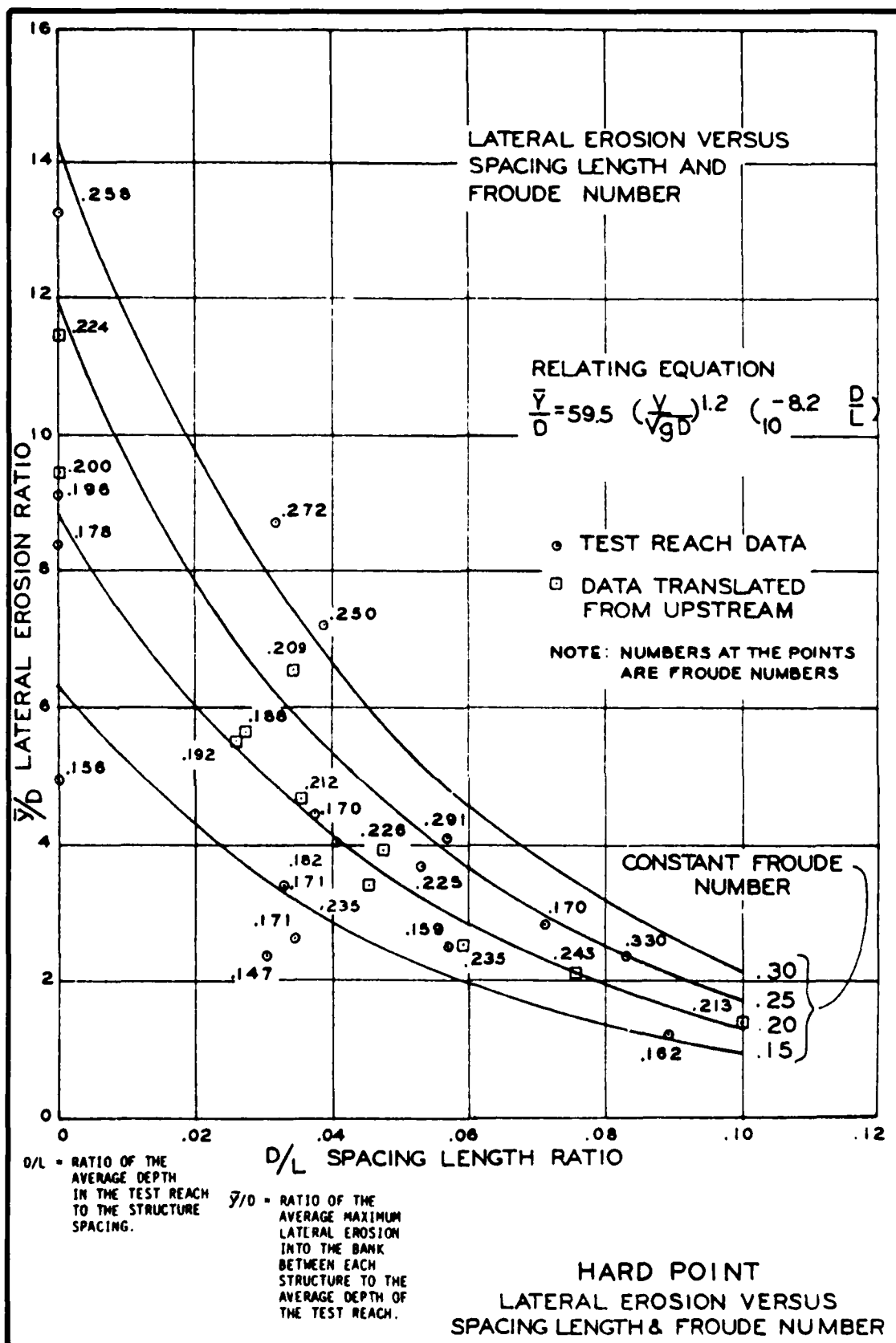


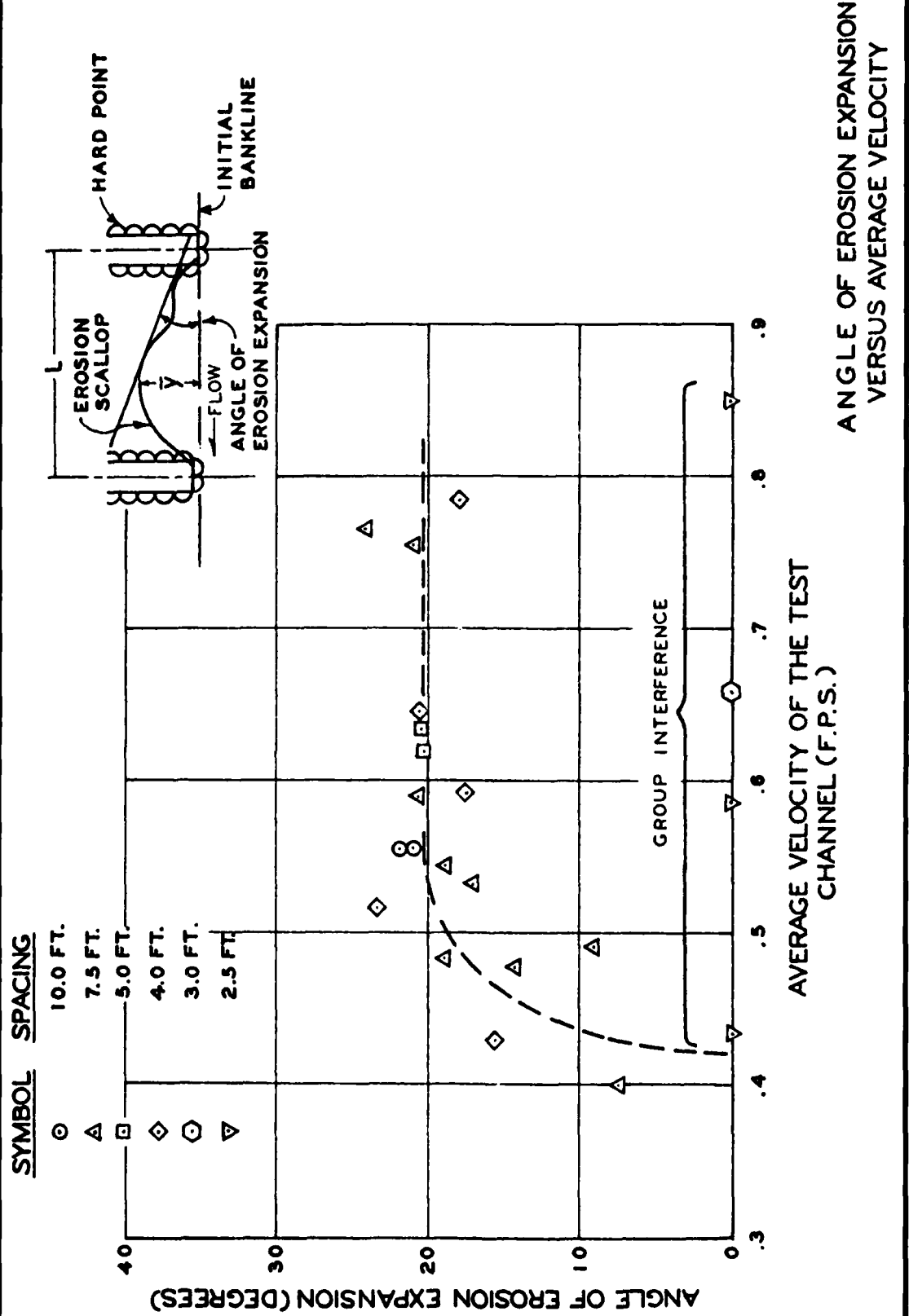


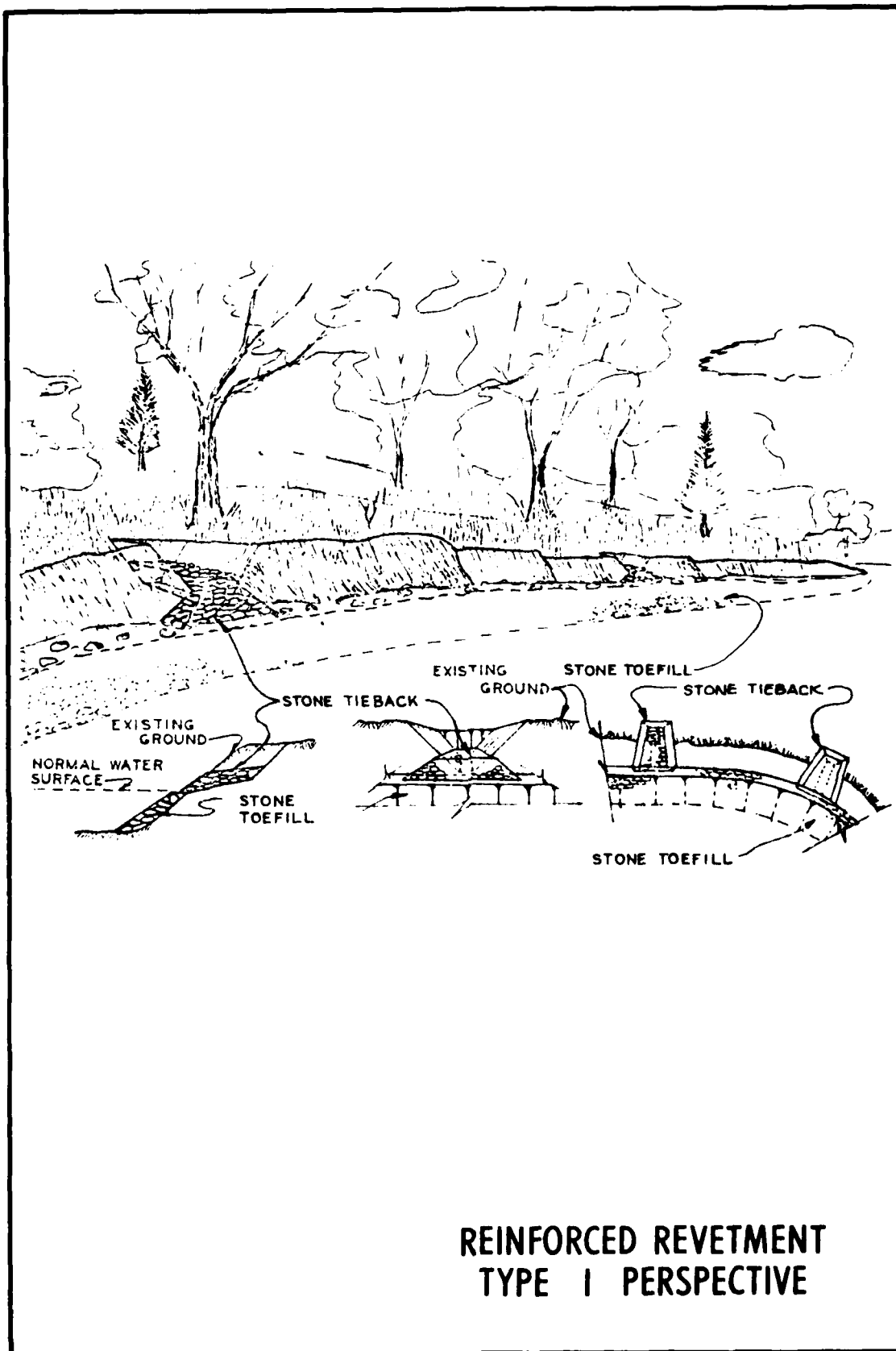
HARD POINT
MODEL LAYOUT



TYPICAL PLAN VIEW OF
MODEL TEST AREA AT END OF RUN







REINFORCED REVETMENT
TYPE I PERSPECTIVE

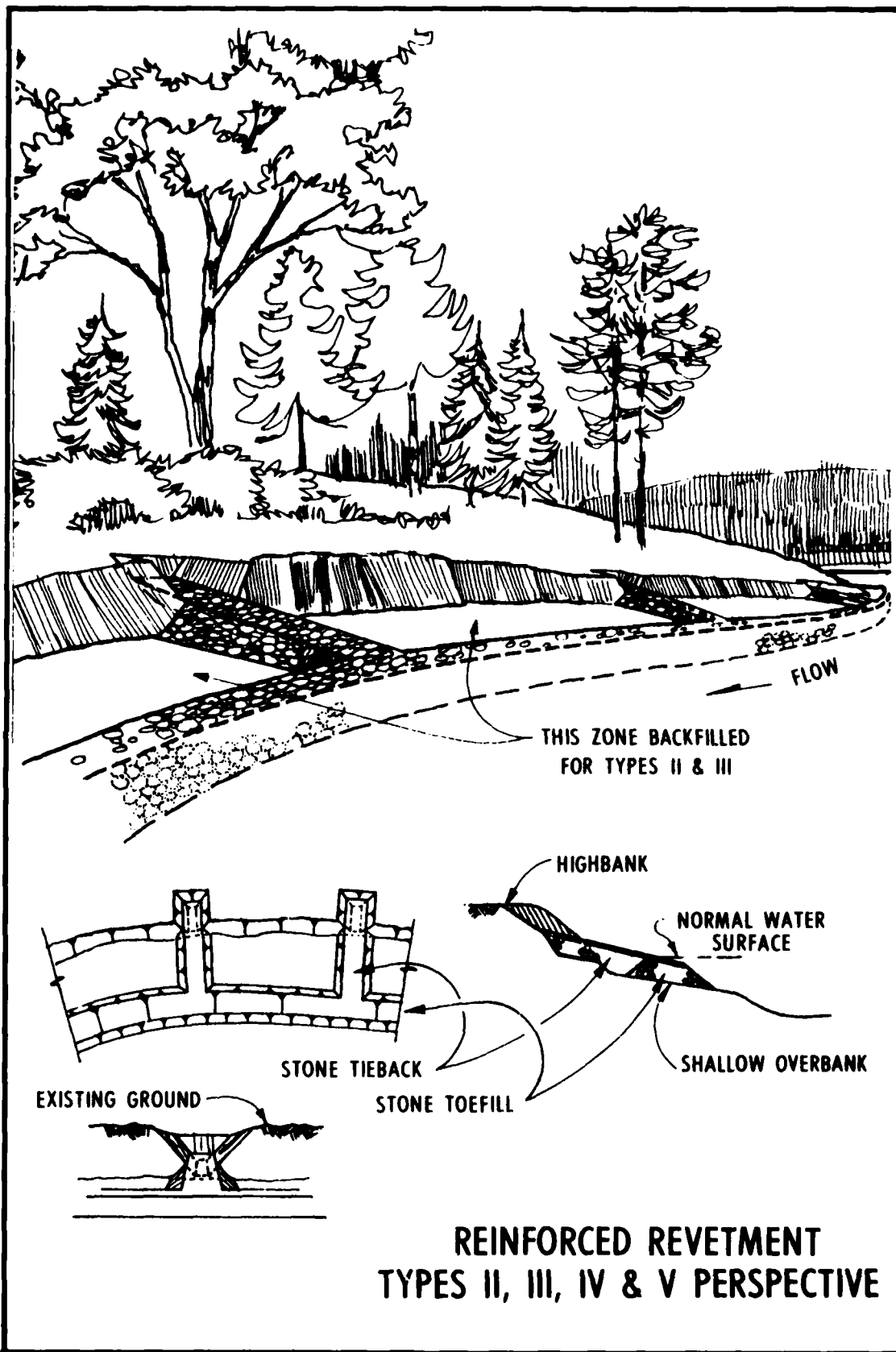


PLATE 13

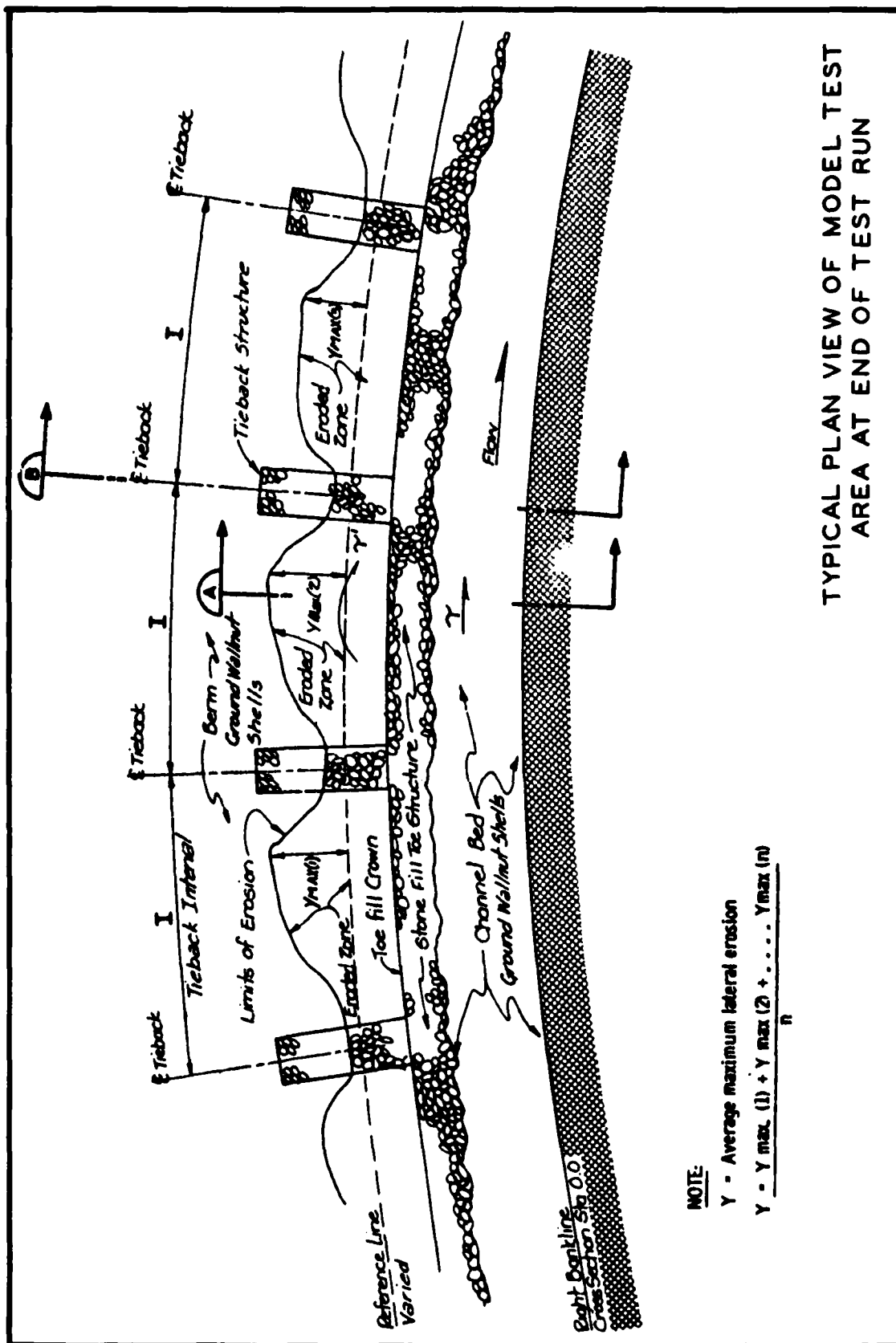
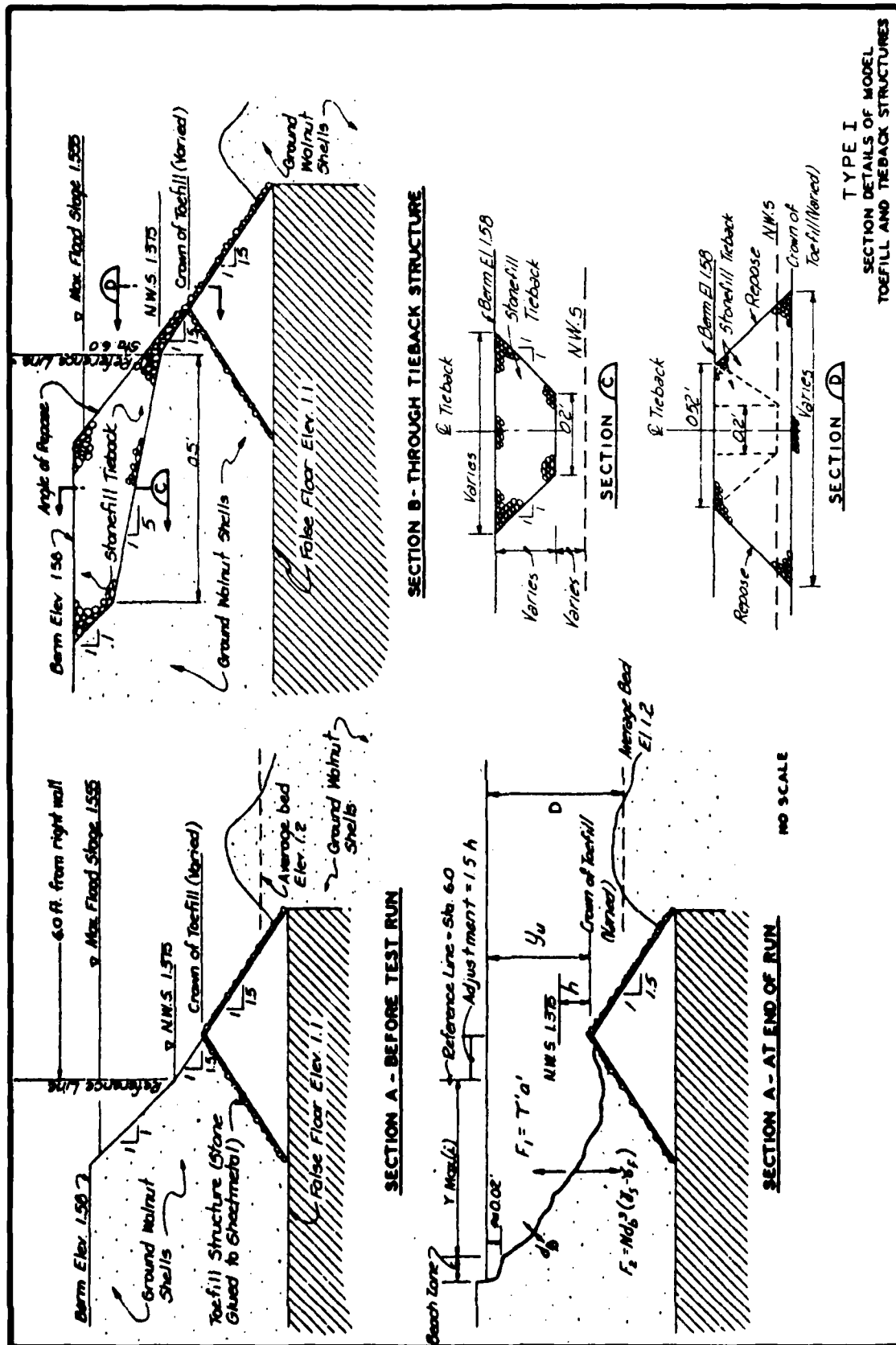
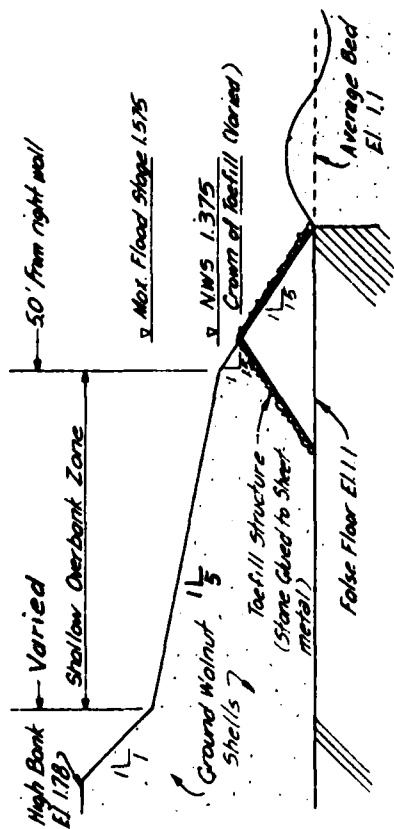
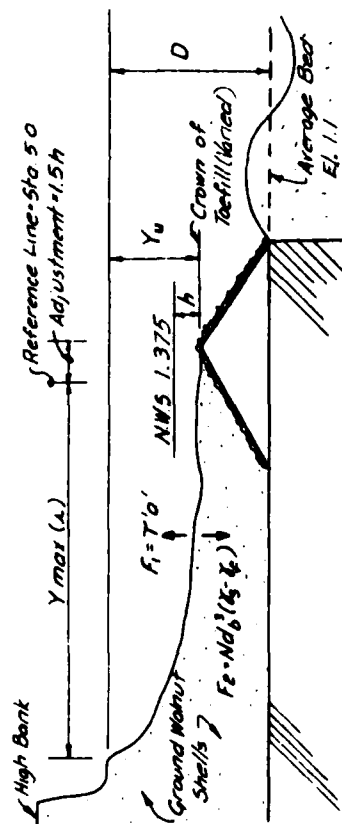


PLATE 14

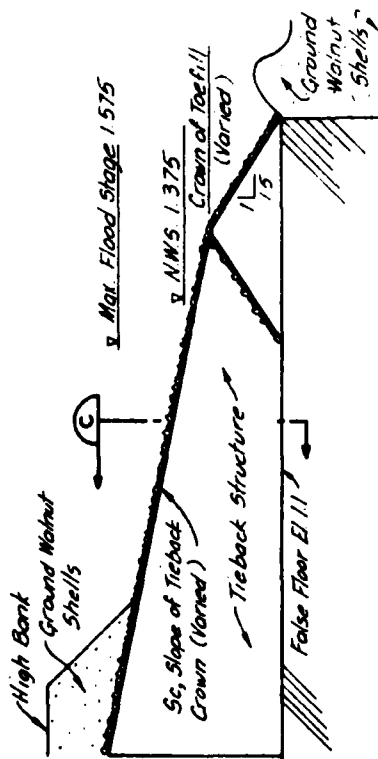




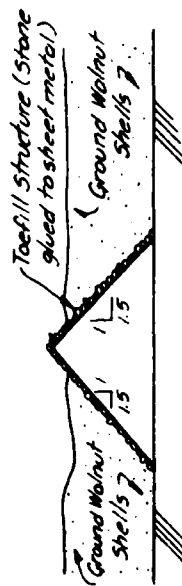
SECTION A - BEFORE TEST RUN



SECTION A - AT END OF RUN



SECTION B - THROUGH TIEBACK STRUCTURE



SECTION C

SECTION DETAILS OF MODEL TOEFILL AND TIEBACK STRUCTURES TYPES II, III, IV, & V

**EFFECTS OF NAVIGATION ON BANK STABILITY
IN CONFINED WATERWAYS**

PART II: THE PROTOTYPE

2. A site specific 1:30-scale model study was conducted of a reach of the Sacramento River Deep Water Ship Channel (SRDWSC) which has experienced several riprap failures along the levees of the channel. The SRDWSC has been in operation since 1963. Table 1 shows a sampling of vessels using the SRDWSC. Also shown in the last column of this table is the value of the cross-section ratio, η , which is the ratio of the waterway cross-sectional area to the submerged cross-sectional area of the ship. Many of the vessels using the SRDWSC result in a cross-section ratio as low as 4 with the average ratio being 4.8. Feuerhake et al. (1969) reports "tests with ship speeds up to 15 km/hr (9.3 mph) showed that the cross-section ratio, η , should be at least 7. Economic bank revetments then provide protection against forces."

3. A map of the SRDWSC is shown in Plate 1. The particular area of concern is along the east levee from about mile 18.6 to mile 21.0. The as-built (1963) channel cross section in this reach is shown in Plate 2. In May 1979, five cross sections were surveyed within the study reach and increases in cross-sectional area ranged from 13 to 35 percent with the average increase being 23 percent. Significant bank protection maintenance work has been required in this reach since 1967 as listed below:

Specification No.	Issue Date	Quarry Stone		Bedding Layer Thickness	Embankment Material	Replaced Under Later Spec
		Thickness in.	Max Size lb			
3418	1967	12	300	6 in.	Uncompacted	Yes
3572	1969	12	300	6 in.	Uncompacted	Yes
4010	1971	18	300	9 in.	Uncompacted	Yes
4284	1972	18	300	9 in.	Uncompacted	Yes
4851	1974	18	400	9 in.	Compacted	No
4958	1976	18	350	9 in.	Compacted	No
5296	1977	18	350	Filter cloth	Compacted	No

Note: From Jones (1980).

4. During spring inspections of 1979, damage was observed at the sites constructed in 1974 and 1976. According to Jones (1980), three possible failure mechanisms are indicated.

- a. Improper gradation of quarystone versus filter material. This allows wave action to remove filter material and expose the embankment to wave and seepage erosion which leads to stone failure.
- b. Saturation of uncompacted embankment material. Saturation by waves and tidal action resulting in subsequent seepage moving embankment material through the filter material which leads to stone protection failure.
- c. Inadequate design wave. If stone protection is being subjected to larger waves than presently designed for (design wave \approx 4.0 ft); then the stone layer may not be adequate to withstand the wave force.

5. In the summer of 1979 the U. S. Army Engineer Waterways Experiment Station (WES) was asked to review the bank protection design relative to:

- a. Quarystone gradation and layer thickness.
- b. Filter material gradation and layer thickness.
- c. Embankment material selection and compaction.

After review by WES and discussion with the U. S. Army Engineer District, Sacramento, a design was developed and has been included in a contract that is now being advertised for bids. This design consists of a compacted embankment overlaid with 6 in. of masonry sand which in turn is overlaid with a 12-in.-thick granular filter. The entire system is covered with a 27-in.-thick stone protection layer all placed on a 1V-on-3H slope. The maximum size stone was increased to 1300 lb. The design was developed using the following design guidance:

- (1) EM 1110-2-2300, 1 Mar 1971, updated by ETL 1110-2-222 dated 10 July 1978.
- (2) EM 1110-2-1901, Part CXIX, Chapter 1, February 1952.
- (3) Shore Protection Manual, 1977, Volume 2.

The gradation limits for the recommended replacement stone and for specification No. 4851 (placed in 1974) which experienced damage are as follows:

	Weight lb	Finer by Weight Percent
Specification No. 4851	400	100
	200	70-90
	100	30-70
	50	20-50
	20	10-30
	5	0-10
Replacement gradation	1300	100
	1000	80-90
	500	50-70
	100	10-30
	50	0-10

6. The existing speed limit within the study reach for all ocean-going craft is as follows:

- a. When going against a current of 2 knots or more, the maximum speed over the bottom shall not exceed 5 knots (5.8 mph).
- b. When going with the current, in slack water, or against a current of 2 knots or less, the maximum speed through the water shall not exceed 7 knots (8.05 mph).

Past speed surveys have shown that the average speed of all vessels was 8.4 mph.

PART III: PURPOSE OF THE MODEL STUDY

7. The purpose of the model study was to determine the mode of failure of the existing riprap along the SRDWSC and to evaluate the adequacy of the rock to be used in repairing the damaged sections. A side benefit of this study is the opportunity for future model-prototype correlation of results. Results of this study are applicable specifically to the SRDWSC and generally to similar confined waterways.

PART IV: PERTINENT LITERATURE

8. The study of navigation effects such as drawdown, surges, and waves created by ships in a confined waterway has received considerable attention in the literature. Cases similar to the SRDWSC having a horizontal berm have received limited attention, but much of the research based on trapezoidal channels without berms can yield information pertinent to the berm situation.

9. Passage of large ships in confined channels results in significant drawdown levels but relatively small waves compared with the smaller but much faster vessels that induce very little drawdown. Prototype measurements on the St. Lawrence Seaway are reported (Gelencser 1977) which confirm and quantify these observations. A plot of the time-history of the water surface for a relatively large ship is shown in Plate 3. The cross-section ratio for the trapezoidal channel and vessel was 5.3 and the speed of the vessel was 7.6 mph. Maximum drawdown below the static water level was 2.1 ft.

10. Model experiments were also reported (Gelencser 1977) which were directed at bank stabilization. "... the cost studies preconcluded have shown that the riprap protection is the cheapest one and therefore became the only protection investigated in the model." These tests showed that a design vessel of 730-ft length traveling at 14 to 15 mph would fail riprap as large as 5 ft in diameter. They also found that by limiting speeds to 10 mph, riprap material of 30 in. (maximum size) would not be damaged. The cross-section ratio for these tests was 7.0.

11. Various studies have addressed the drawdown that occurs with ship passage (Gelencser 1977, Balanin et al. 1977, Dand and White 1977, Kao 1978, and Lee and Bowers 1947). Most relate drawdown as a function of channel depth, ship speed, and cross-section ratio.

12. Research connected with the design of the Kiel Canal in Europe revealed that the final channel size was more dependent on bank and bed stability than on navigability requirements (Wiedemann 1978).

13. Dand and White (1977) report on surge waves that result from

drawdown effects in the Suez Canal. The following excerpt is from Dand and White (1977):

The present western side of the Suez Canal has a horizontal berm which runs out from the bank at a level between 1 m and 2 m below water level. One disadvantage of a horizontal berm [see cross section, Plate 4] is that under certain circumstances surge waves can be created by vessels in transit. Conditions which increase the likelihood of surge waves include shallow depths of water over a berm, h_b , high speeds of transit, and significant drawdown of the water surface caused by the passing ship.

At slow speeds of transit there is a gradual and small fall in water level as the bow of the vessel passes and a gradual increase as the stern reaches the point under consideration. As the speed of transit increases, the amount of drawdown increases and at some stage a weak undular disturbance is initiated over the berm. At even higher speeds this weak undular disturbance is transformed into a surge wave which travels along the berm roughly in line with the stern of the vessel.

It is unwise to design new banks which will induce damaging surge waves under the operating conditions anticipated for the new canal. Hence it was desirable to be able to predict when these effects would occur and to develop design criteria which would avoid them.

A semiempirical approach to the problem, utilizing the observed drawdown characteristics, indicated a general relationship between the Froude number (based on the speed of the ship and the undisturbed depth over the berm), the blockage ratio and the type of wave disturbance. The plot is given in nondimensional form in [Plate 4].

Dand and White (1977) also verify "bank erosion is caused by drawdown from large vessels and free waves from small vessels moving at a higher speed."

14. Lee and Bowers (1947) report on restricted channel tests for the Panama Canal. Extensive drawdown measurements were made for a wide range of channel depths, widths, ship speed, and relative position in the cross section.

15. Helm (1953) states that:

The speed of return-flow gives us an idea of the attack on the bottom to be expected. It should be restricted by imposing a speed-limit on navigation, according to the nature of the soil. For the present report, the speed of the return flow has been fixed at 1 m/sec [3.3 ft/sec].

Helm (1953) states that the limiting speed of a ship in a canal is a function of the speed of the translation wave and the ratio of the water-way area to the submerged ship area (η).

16. Jansen and Schijf (1953) present curves in Plate 5 for determining the water-surface drawdown and the speed of return flow as a function of the reciprocal of the cross-section ratio and the ship Froude number.

17. Tenaud (1977) reports on the damaging effects of waves in a navigation channel. Extensive model testing was conducted over a wide range of channel shapes, rock sizes, ship sizes, and ship speeds. Techniques are presented for estimating the wave heights as well as the protective stone required.

PART V: THE MODEL STUDY

Description

18. A straight 0.5-mile-long reach of the SRDWSC was reproduced in the model at a scale of 1:30 (Figure 1). The as-built cross section (Plate 2) was used throughout the model study with the exception that the replacement rock was tested at a 1V-on-3H side slope as proposed for the prototype. Only the east berm (left side of channel) was reproduced in the model. The correct channel area was maintained by a small adjustment of the bottom width of the channel. The channel used in the study was a slack-water channel; therefore, the small tidal-induced velocities that occur in the prototype were not reproduced in the model. The berm and side slopes on the east bank were molded in concrete with sand used in the bottom of the channel.

19. The 1:30-scale model ship used in the study (Figure 2) represented a tanker having a prototype length of 660 ft, beam of 102.6 ft, and drafts up to 40 ft. The ship is self-propelled with an operator on board. The draft of the model ship was varied to represent different ship displacements. This allowed variation of the ratio η (channel cross-section area/submerged ship cross-section area) during the test program. The model ship was capable of prototype speeds up to 11 mph. Ship speeds were determined by measuring the time required for the ship to traverse the middle 0.25-mile length of the test reach.

20. Crushed limestone was sieved and mixed to the proper gradation to simulate the prototype riprap. The specific gravity of the crushed limestone used in the model was 2.67. Movement of riprap in the model was determined by inspection during and immediately following each passage of the model ship. The W_{50} 's simulated in the model were 90 lb and 340 lb for gradation No. 4851 and the replacement riprap, respectively.

21. A continuous recording water-level detector was used to monitor the water level over the berm at the midpoint of the test section as shown in Figure 2.

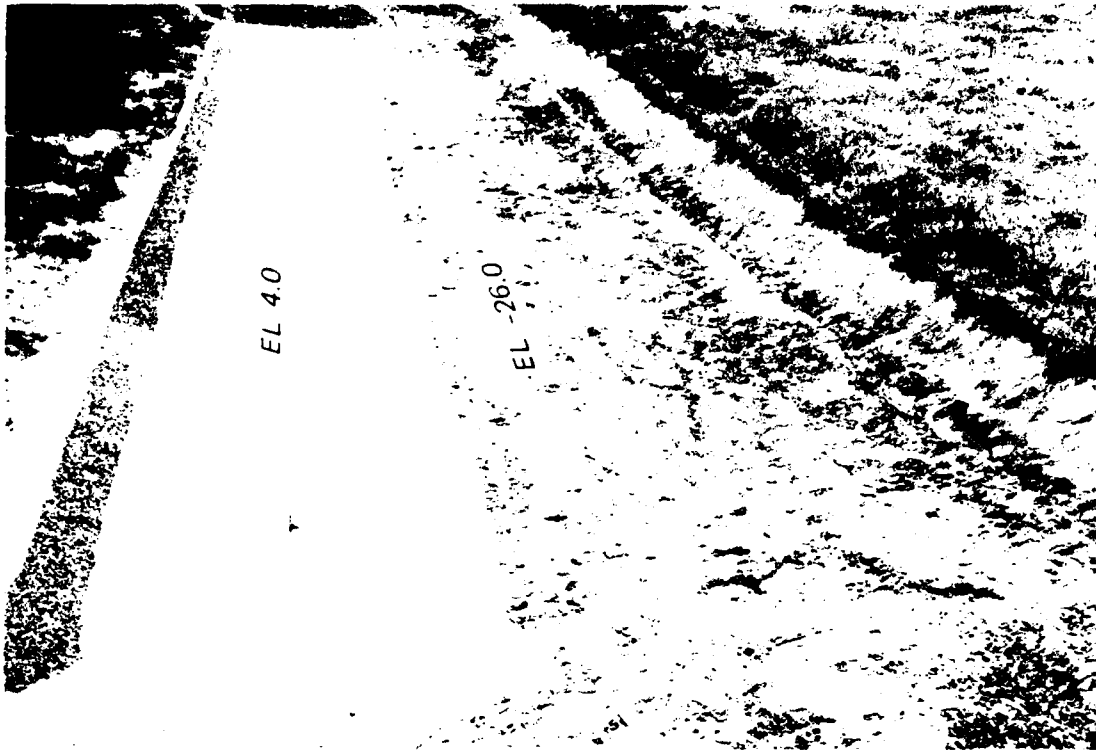


Figure 1. 1:30-scale model of 0.5-mile reach of SRDWSC



Figure 2. 1:30-scale ship in SRDWSC model

B-5-10

Scaling Relations

22. The equations of similitude based on Froude's law

$$\text{Froude No. Model} = \text{Froude No. Prototype} = \frac{V}{\sqrt{gL}}$$

where

V = velocity, ft/sec

g = gravity, ft/sec²

L = characteristic length, ft

were used to express mathematical relations between the dimensions and the hydraulic quantities of the model and prototype. The following relations were used:

<u>Dimension</u>	<u>Ratio</u>	<u>Scale Relations</u>
Length	L_r	1:30
Time	$T_r = L_r^{1/2}$	1:5.48
Velocity	$V_r = L_r^{1/2}$	1:5.48
Weight	$W_r = L_r^3$	1:27,000

However, frictional resistance of ships is dependent on Reynolds number

$$R = \frac{VL}{\nu}$$

where

R = Reynolds number

V = velocity, ft/sec

L = characteristic length, ft

ν = kinematic viscosity, ft²/sec

and the model and prototype Reynolds numbers are different when the same fluid is common to both model and prototype and the Froude criteria are used as the basis of similitude. Greater relative thrust must be applied in the model to overcome the greater friction in the model. The drag coefficient as a function of ship Reynolds number is shown in Figure 3. Also shown in this figure is the point on the curve for a

typical prototype and the point on the curve for the 1:30-scale model used in this investigation. Drag coefficients in the model are relatively close to those of the prototype, and only a small increase in thrust in the model was required. Water-level drawdown and return surge or a classical bore are the most likely failure mechanisms in the SRDWSC. Drawdown is a function of the cross-section ratio and the ship speed. The increase in thrust required in the model to simulate a given prototype speed should not affect the similarity of the drawdown phenomenon.

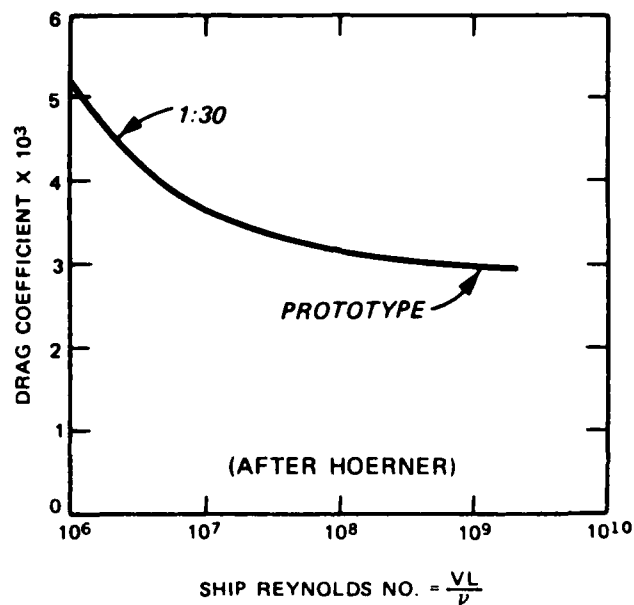


Figure 3. Drag coefficient as a function of ship Reynolds number (from Huval and Pickering 1978)

23. Other scale effects are present relative to the rock movement resulting from the return surge or wave occurring on the berm. Dai and Kamel (1969) compared rock stability of rubble-mound breakwater models constructed with a wide range of model Reynolds number. Their tests indicated that scale effects due to viscous forces were significant below a certain Reynolds number. Unlike the case of the breakwater, the speed of the surge on the berm affects the stability of the riprap. The mechanics of a moving surge or bore departs considerably from that of a

wave train. The forces generated by the surge moving parallel to the bank line are more analogous to forces generated by flow over a channel boundary than to wave-generated forces. Unfortunately, certain viscous scale effects are present when testing riprap stability in a channel flow environment in models not having sufficiently large Reynolds number. The particle Reynolds number is defined as

$$R = \frac{Vd_{50}}{\nu}$$

where

V = average velocity, ft/sec

d_{50} = 50 percent riprap size, ft

ν = kinematic viscosity, ft²/sec

O'Loughlin et al. (1970) recommends a particle Reynolds number greater than 2.5×10^3 to minimize Reynolds number scale effects. The particle Reynolds number for the model using a surge speed of 8 mph to represent the average velocity and the d_{50} for gradation No. 4851 is 7×10^3 , indicating minimal Reynolds number scale effects.

PART VI: TEST RESULTS

Existing Design

24. The riprap plan based on gradation No. 4851 was placed in the model for the initial test series. Two values of the cross-section ratio, η , were tested for each of three different water depths over the berm. For each test the speed of the ship was varied and the drawdown of water over the berm was monitored and recorded. This drawdown was the difference between the static water level and the minimum water level that occurred during the passage of the ship. Results are shown in Plates 6 and 7, for cross-section ratios of 6.1 and 4.3, respectively. A typical trace of the water level as a function of time for a 4-ft depth over the berm and a cross-section ratio of 4.3 is shown in Plate 8. The speed of the ship for this test was 8.8 mph. The speed at which the water surface falls can be a significant factor in the stability of the riprap on the levee. For the condition shown in Plate 8, a fall of 3.5 ft occurs in approximately 1 min in the prototype. This rapid drawdown can result in removal of bank material through the revetment if adequate filters are not installed. The drawdown over the berm is shown in Figure 4.

25. During these tests, the ship speed at which the riprap on the levee began moving was observed for each water depth over the berm and each cross-section ratio for gradation No. 4851. Results of these rock movement observations are shown in Plate 9. The surge or bore which caused the rock movement is shown in Figure 4.

Alternate Designs

26. Limited testing was conducted to evaluate the effects of gabion dikes on the levee riprap stability. Gabion dikes were placed along the berm (Plate 10) at 150-ft intervals. These dikes were 3 ft high and 40 ft in length. Tests were conducted for an η ratio of 4.3 and a 4-ft depth over the berm. Results of the drawdown measurements

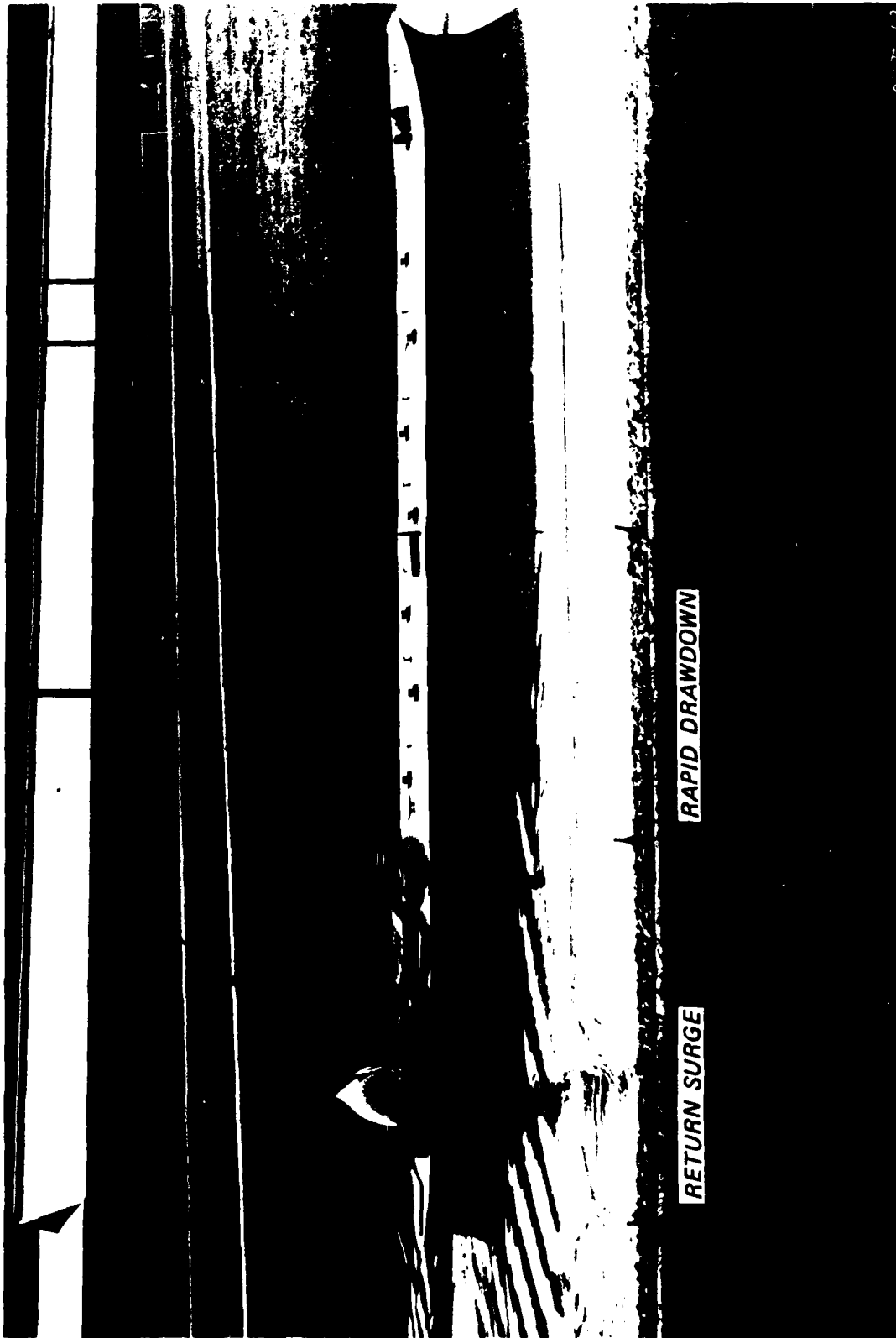


Figure 4. Rapid drawdown followed by return surge

are shown in Plate 11. Only a small decrease in drawdown was observed with the gabion dikes. However, the ship speed at which rock movement occurred was increased from approximately 7.8 to 9 mph with the 4-ft depth over the berm and the cross-section ratio of 4.3.

27. The gabion dike spacing was increased to 300 ft with the length and height remaining 40 ft and 3 ft, respectively. Rock movement tests were conducted with this design, and the ship speed at which rock movement began remained unchanged from the original design without dikes.

28. The third alternate design tested was an attempt to reduce the rapid drawdown occurring over the berm and particularly on the levee. A gabion fence was constructed in the model as shown in Plate 12. This design stopped the drawdown at the top elevation of the gabion fence and none of the rock was moved at speeds up to 9.8 mph. However, this design reduced the effective channel area and the cross-section ratio and resulted in more adverse conditions out in the channel, particularly at the toe of the gabion fence. One engineer observing tests noted that a gabion levee revetment could be constructed with the same amount of gabions required to construct the gabion fence and thus avoid any reduction in the channel area.

29. The fourth alternative tested was a 20 percent increase in channel area which changed the cross-section ratio with the largest ship from 4.3 to 5.2. The resulting drawdown plot as a function of ship speed is shown in Plate 13. Rock movement tests indicated only a small increase from 7.8 mph with the original design to $\cong 8.5$ mph with the increased channel area could be achieved. These tests were conducted with a 4-ft depth of water over the berm.

Proposed Replacement Design

30. The riprap design proposed for repair of the prototype was then placed in the model. Rock movement tests were conducted for a cross-section ratio of 4.3 with water depths over the berm of 2, 4, and 6 ft. The replacement rock was moved at ship speeds of $\cong 1.0$ mph faster than the speeds for the original No. 4851 gradation (Plate 9) for all depths over the berm.

PART VII: DISCUSSION OF RESULTS AND CONCLUSIONS

31. Model tests show that surging and rapid drawdown in the SRDWSC are caused by the low waterway to submerged ship cross-section ratio in conjunction with the typical speed of the using vessels. The average cross-section ratio for the channel and all ships sampled was 4.8. Model tests showed rock movement began along the levee with ship speeds as low as 8 mph for a cross-section ratio of 6.1. Model results are valid for the original as-built cross section. Results of model tests with a 20 percent increase can be used to estimate the effects of the altered prototype cross section (paragraph 3). Based on these tests, rock movement on the levee with the enlarged section will occur at ship speeds of 0.5 to 1.0 mph faster than with the as-built section.

32. The failure mechanisms observed in the model study were similar to those stated by Jones (1980). The rapid drawdown that occurs as the ship passes can lead to riprap failure if adequate filters are not provided beneath the revetment. At the highest ship speeds and ship displacements, the drawdown can be equal to the depth of water over the berm. The surge or bore that follows the rapid drawdown leads to rock revetment failure. The surge or bore height always exceeded the bow or stern waves coming off the ship. The surge moved along the berm approximately equal to the location of the stern of the ship. The rock movement curves approximate the point at which rock moved off the levee and onto the berm. For determining the speed at which revetment failure should not occur, a safety factor should be incorporated by selecting a speed less than the speed at which initial rock movement occurred.

33. The gabion dike (150-ft spacing) alternative did not solve the rapid drawdown problem but was effective in allowing an increase of ship speed at which rock movement was initiated. The gabion fence alternative solved both the rapid drawdown and the rock movement due to the surge or bore but reduced the cross-sectional channel area in an already critically confined channel.

34. The proposed larger replacement riprap will help solve the problem of riprap failure if past failures have been caused by the

action of the surge or bore. If past failures have been caused by rapid drawdown, the filters proposed for the replacement riprap may solve the problem of failure due to rapid drawdown.

35. Only a small increase (≈ 1.0 mph) in ship speed above the speeds shown in Plate 9 for gradation No. 4851 can be tolerated without movement of the replacement riprap. This is surprising since the average diameter of the replacement stone is 50 percent greater than the existing riprap. The reason for this small increase is the small cross-section ratio of the SRDWSC to the using vessels. The drawdown curves shown in Plates 6 and 7 show a large increase in drawdown (and therefore surge or bore height) for a relatively small increase in ship speed. Only an increase in channel area or a decrease in ship speed can result in favorable conditions within the channel and along the riprapped levees with the using vessels and the proposed replacement riprap.

36. According to research conducted on the Suez Canal a horizontal berm can result in severe surging if the depth over the berm is shallow or ships travel at high speeds. These breaking surge waves or bores occur in the SRDWSC and may result in rock failure along the levee at the higher ship speeds.

37. Drawdown, surge or bore height, wave action, and rock failure would be reduced by enforcement of longer travel times and/or lower speed limits.

38. Results of this study are valid quantitatively to only the specific channel dimensions of the SRDWSC. Results are valid qualitatively to other confined channels. Qualitative application of these results to large navigable waterways that cannot be considered as confined channels is not valid.

REFERENCES

- Balanin, V., et al. 1977. "Peculiarities of Navigation on Canals and Restricted Channels, Originating Hydraulic Phenomena Associated with Them and Their Effect on the Canal Bed; Measures Preventing Slope Deterioration," 24th International Navigation Congress, PIANC, Leningrad, Section I, Subject 3.
- Dai, Y. B., and Kamel, A. M. 1969 (Dec). "Scale Effect Tests for Rubble-Mound Breakwaters," Research Report H-69-2, U. S. Army Engineer Waterways Experiment Station, CE, Vicksburg, Miss.
- Dand, I. W., and White, W. R. 1977. "Design of Navigation Canals and Restricted Channels, Originating Hydraulic Phenomena Associated with Them and Their Effect on the Canal Bed; Measures Preventing Slope Deterioration," 24th International Navigation Congress, PIANC, Leningrad, Section I, Subject 3.
- Feuerhake, K., et al. 1969. "Les Forces S'exercent sur les Berge Des Voies Navigables," XXIInd International Navigation Congress, Paris, Section I, Subject 6.
- Gelencser, G. J. 1977. "Drawdown Surge and Slope Protection, Experimental Results," 24th International Navigation Congress, PIANC, Leningrad, Section I, Subject 3.
- Helm, K. 1953. "Conditions Requisites pour la Section Transversale de Navigation," 18th International Navigation Congress, PIANC, Rome, Section I, Communication I.
- Huval, C., and Pickering, G. 1978 (Apr). "Physical and Mathematical Models for Improved Navigation Channel Design," Symposium--Aspects of Navigability of Constraint Waterways, Including Harbour Entrances, Delft, The Netherlands.
- Jansen, P., and Schijf, J. 1953. "Conditions Requisites pour la Section Transversale de Navigation," 18th International Navigation Congress, PIANC, Rome, Section I, Communication I.
- Jones, D. R. 1980 (Aug). "Channel Design Considerations Summary Report, Sacramento Deep Water Ship Channel," presented at WES Deep Draft Channel Design Course, Vicksburg, Miss.
- Kao, E. 1978 (Apr). "Power and Speed of Push Tows and Canals," Symposium--Aspects of Navigability of Constraint Waterways, Including Harbour Entrances, Delft, The Netherlands, Vol 3.
- Lee, C., and Bowers, C. 1947 (May). "Restricted Channel Tests for the Panama Canal," Navy Department, David Taylor Model Basin, Bethesda, Md.
- O'Loughlin, E. M., et al. 1970. "Scale Effects in Hydraulic Model Tests of Rock Protected Structures," IIHR Report No. 124, February 1970, Iowa Institute of Hydraulic Research, Iowa City, Iowa.

Tenaud, R. 1977. "Trials Made with Reduced Models and a Scale Model for Studying the Passage of Motorized Ships in a Channel and the Protection of River Banks," Proceedings, 24th International Navigation Conference, Leningrad, Section I, Subject 3, pp 59-77.

Wiedemann, G. 1978 (Apr). "Design Procedures for Recently Constructed Canals, Channels, and Harbour Entrances," Symposium--Aspects of Navigability of Constraint Waterways, Including Harbour Entrances, Delft, The Netherlands, Vol 3.

Table 1
Sample of Vessels Loading at the Port of Sacramento
1976-79

DWT	Length		Beam		Design Draft		Sailing Draft		Tons Loaded	η Ratio
	ft	in.	ft	in.	ft	in.	ft	in.		
25,040	585	8	75	1	34	1	30	6	20,235	5.1
22,593	539	2	75	2	32	4	30	6	21,041	5.1
35,657	655	5	91	5	36	10	31	5	30,166	4.1
16,588	557	10	86	0	29	10	30	6	16,421	4.1
52,225	700	0	96	2	41	10	30	0	33,075	4.0
26,900	581	4	75	0	34	3	31	0	23,681	5.0
38,711	656	0	88	9	36	7	28	0	27,305	4.7
20,203	518	4	76	11	31	3	30	4	18,682	5.0
26,600	600	6	74	8	34	5	30	6	23,422	5.1
60,740	736	3	106	0	41	4	29	2	39,225	3.8
25,604	591	7	75	1	33	6	29	10	20,944	5.2
34,602	604	9	85	9	36	3	28	9	24,182	4.7
52,733	716	9	102	2	39	5	30	10	37,449	3.7
39,796	623	4	90	9	37	3	29	8	29,848	4.3
30,668	623	4	75	6	35	1	30	0	24,556	5.2
19,030	506	0	74	10	30	2	30	4	19,711	5.1
29,168	593	2	91	3	35	1	28	9	22,046	4.4
22,697	544	5	75	1	34	0	30	4	16,204	5.1
16,061	474	6	67	10	30	4	31	0	16,017	5.6
20,520	520	0	74	3	30	1	31	2	19,996	5.0
16,230	534	4	66	7	30	10	30	4	16,436	5.8
40,347	669	11	90	7	38	7	30	5	29,423	4.2
27,306	597	1	75	2	34	11	30	5	21,600	5.1
51,658	655	11	105	8	40	9	30	10	36,904	3.6
29,202	593	2	75	11	35	0	30	3	24,595	5.1
27,593	577	0	75	0	36	1	31	0	21,934	5.0
23,625	555	11	80	10	32	6	31	2	21,197	4.6
37,836	615	9	93	2	35	2	30	6	32,554	4.1
41,035	602	3	90	8	39	4	29	7	29,944	4.4
27,890	564	0	85	2	34	2	30	4	--	4.5
29,709	564	0	85	2	35	4	31	0	--	4.4
27,890	564	0	85	2	34	2	29	6	--	4.6
27,890	564	0	85	2	34	2	29	6	--	4.6
28,939	593	10	95	11	34	4	27	8	--	4.4
24,090	534	4	75	2	34	2	29	6	--	5.3
29,623	574	7	85	5	33	9	30	8	20,609	4.5
19,418	512	4	74	4	31	3	30	5	15,064	5.2
18,820	508	8	75	0	29	4	30	6	14,512	5.1
20,009	502	0	77	6	30	11	30	6	15,804	4.4
18,546	469	10	75	0	30	0	29	2	13,244	5.3
16,549	465	9	71	7	29	10	30	2	13,769	5.4
19,297	512	4	74	4	31	3	31	0	14,603	5.1
25,401	576	11	83	5	31	2	31	6	20,684	4.4
20,000	555	10	75	0	33	8	31	1	17,236	5.0

* Ratio of waterway cross-sectional area to submerged cross-sectional area of the ship.

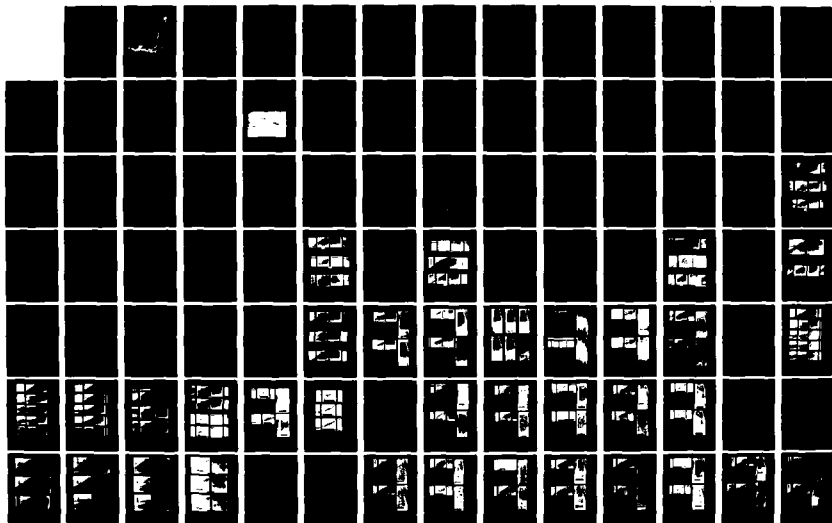
AD-A121 132

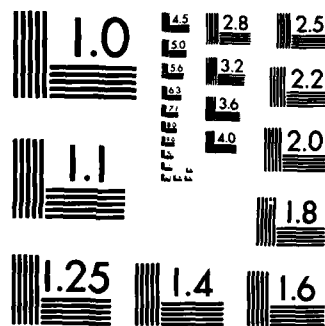
THE STREAMBANK EROSION CONTROL EVALUATION AND
DEMONSTRATION ACT OF 1974 S. (U) ARMY ENGINEER
WATERWAYS EXPERIMENT STATION VICKSBURG MS HYDRA.

UNCLASSIFIED

M P KEOWN ET AL. DEC 81 WES/TR/H-77-9-APP-B F/G 13/2

NL





MICROCOPY RESOLUTION TEST CHART
NATIONAL BUREAU OF STANDARDS-1963-A

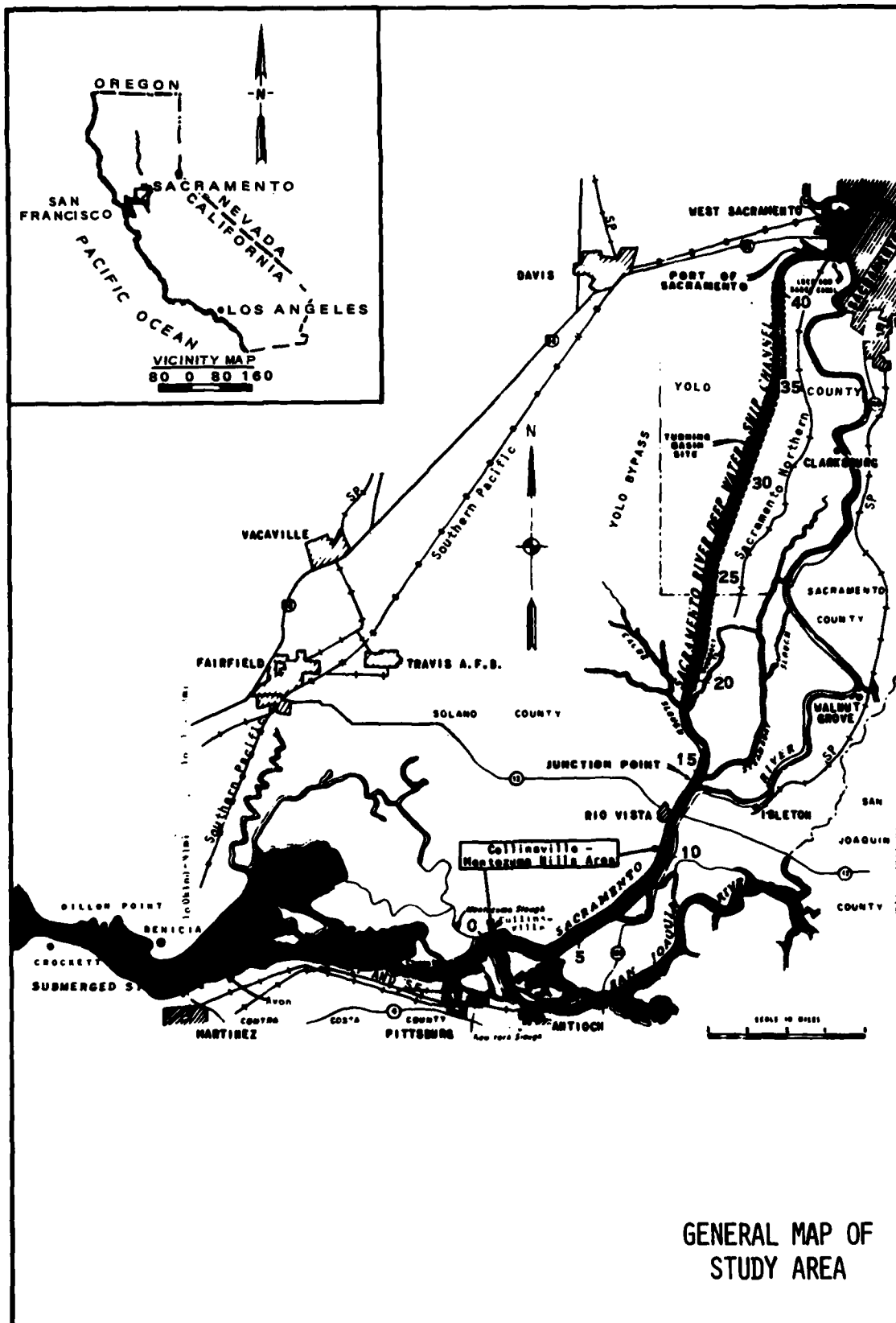
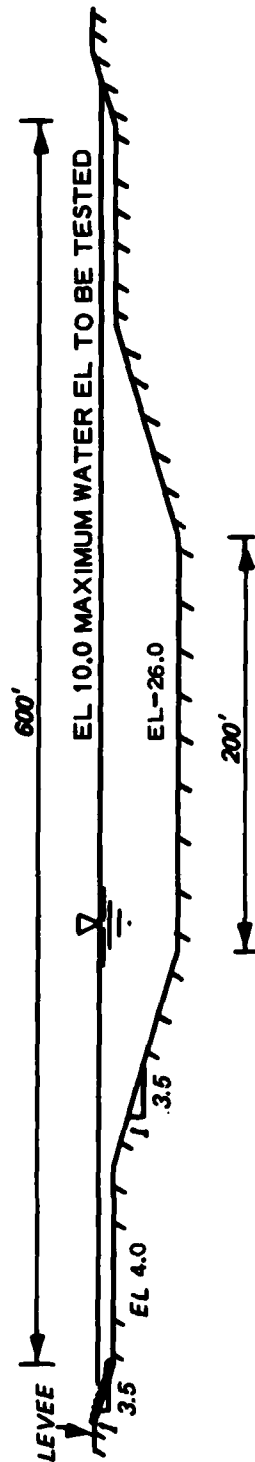


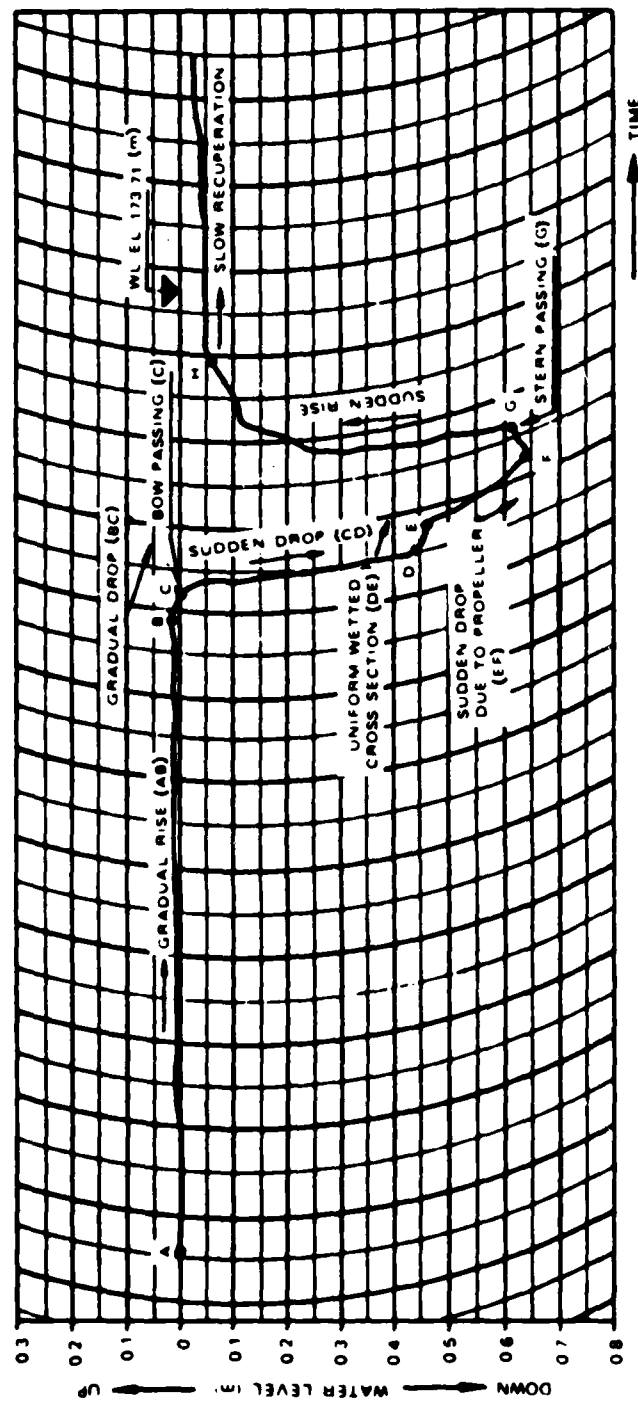
PLATE 1

B-5-23



SACRAMENTO RIVER DEEP WATER
SHIP CHANNEL
TYPICAL SECTION
MILE 18.6 TO 21.0

NOTE: ELEVATIONS IN FEET NGVD



NOTE: SHIP SPEED = 7.6 MPH

$\eta = 5.3$

MAXIMUM DRAWDOWN = 2.1 FT

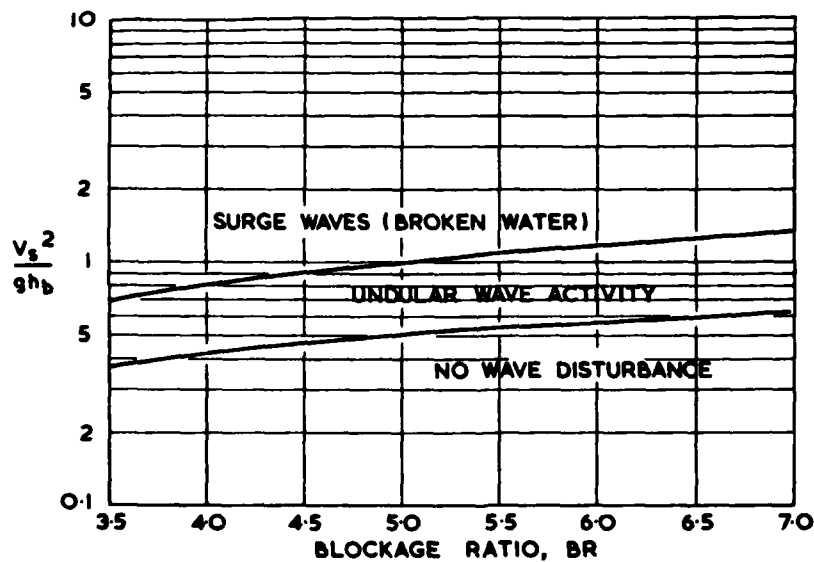
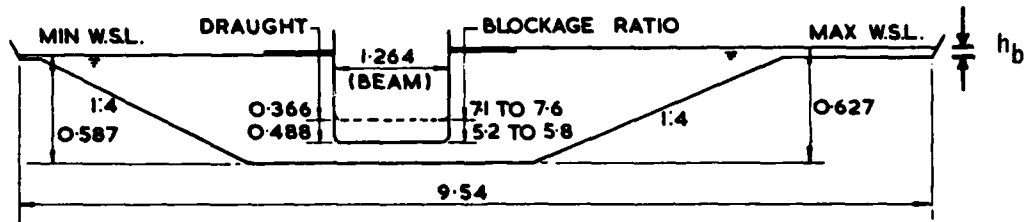
WATER-LEVEL DRAWDOWN
ST. LAWRENCE SEAWAY
PROTOTYPE MEASUREMENT

FROM GELENCSE (1977)

PLATE 3

1. ALL DIMENSIONS IN METRES (MODEL)
2. VERTICAL EXAGGERATION 2:1

CANAL CROSS-SECTION No.1



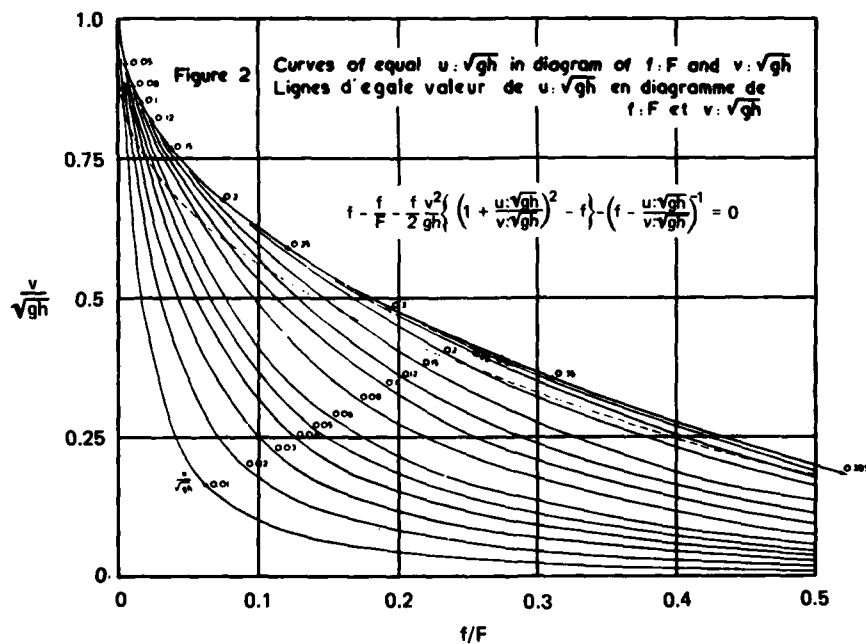
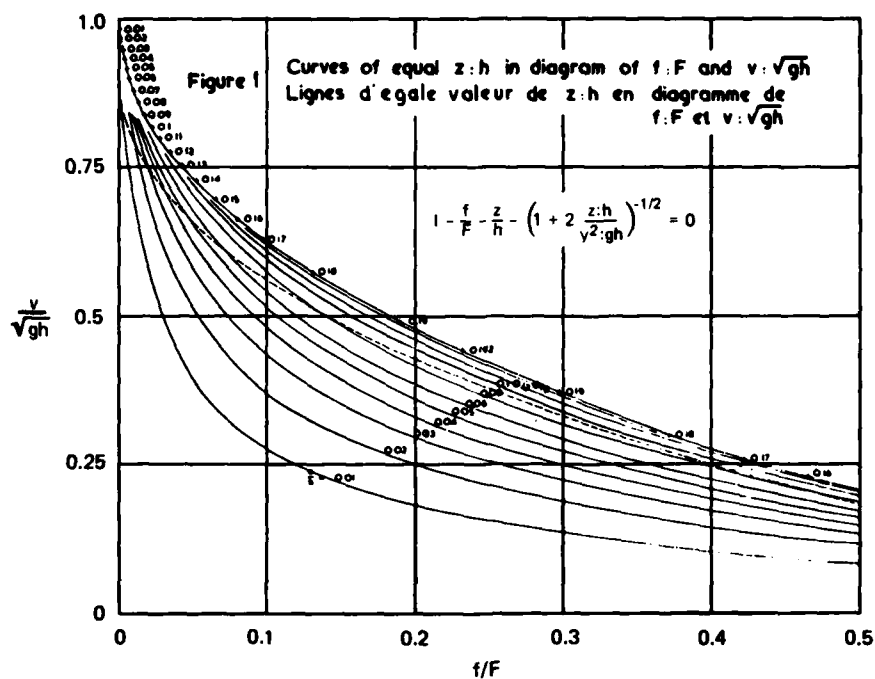
WAVE ACTIVITY ASSOCIATED WITH DRAWDOWN AT THE BERM

$$BR = \eta$$

V_s = SHIP SPEED

h_b = DEPTH OVER BERM

DRAWDOWN EFFECTS IN THE
SUEZ CANAL
(FROM DAND AND WHITE (1977))



z = WATER-SURFACE DRAWDOWN
 u = SPEED OF RETURN FLOW
 $f/F = 1/\eta$
 h = CHANNEL DEPTH
 v = SHIP SPEED

WATER-SURFACE DRAWDOWN AND
 SPEED OF RETURN FLOW
 (FROM JANSEN AND SCHIJF (1953))

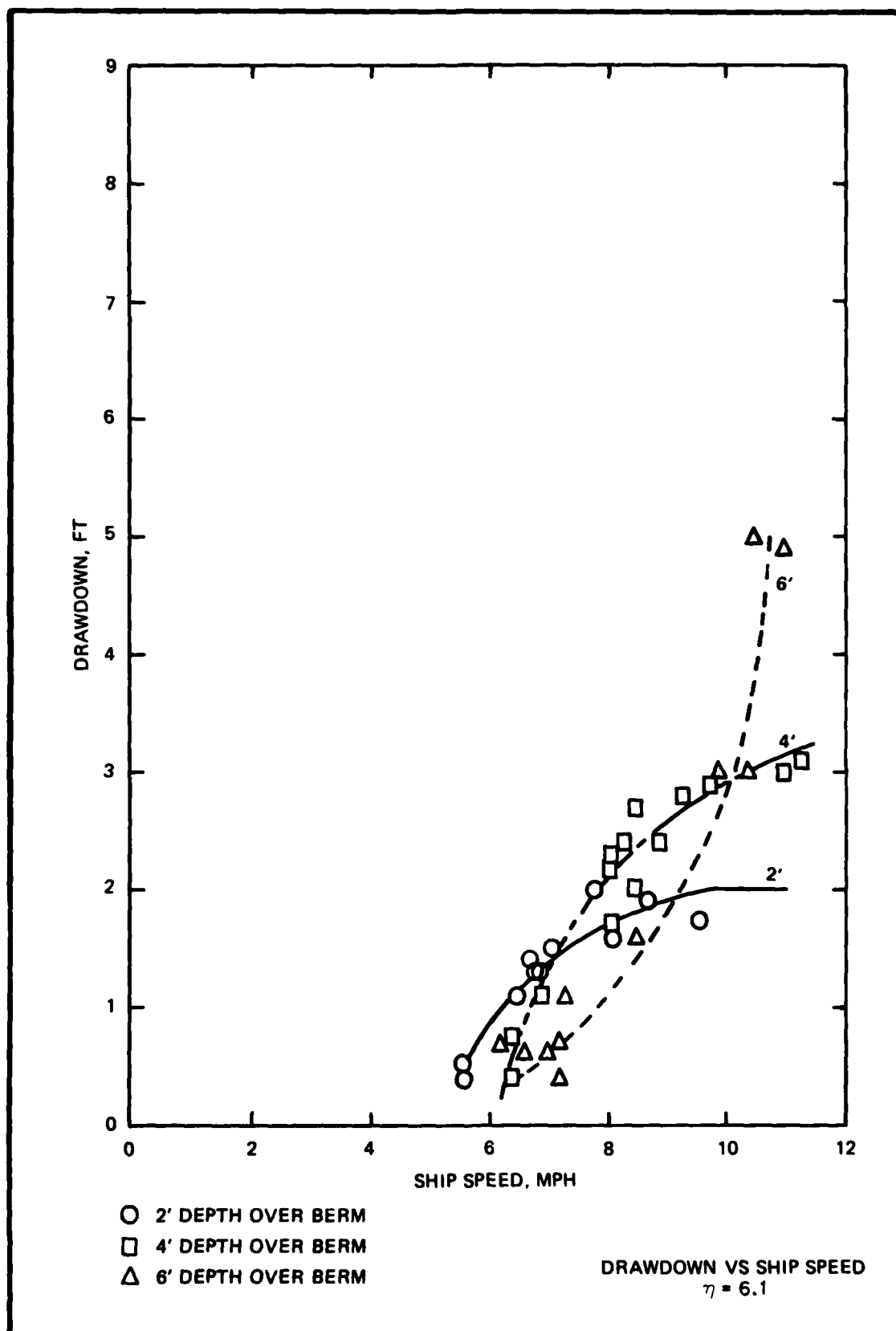
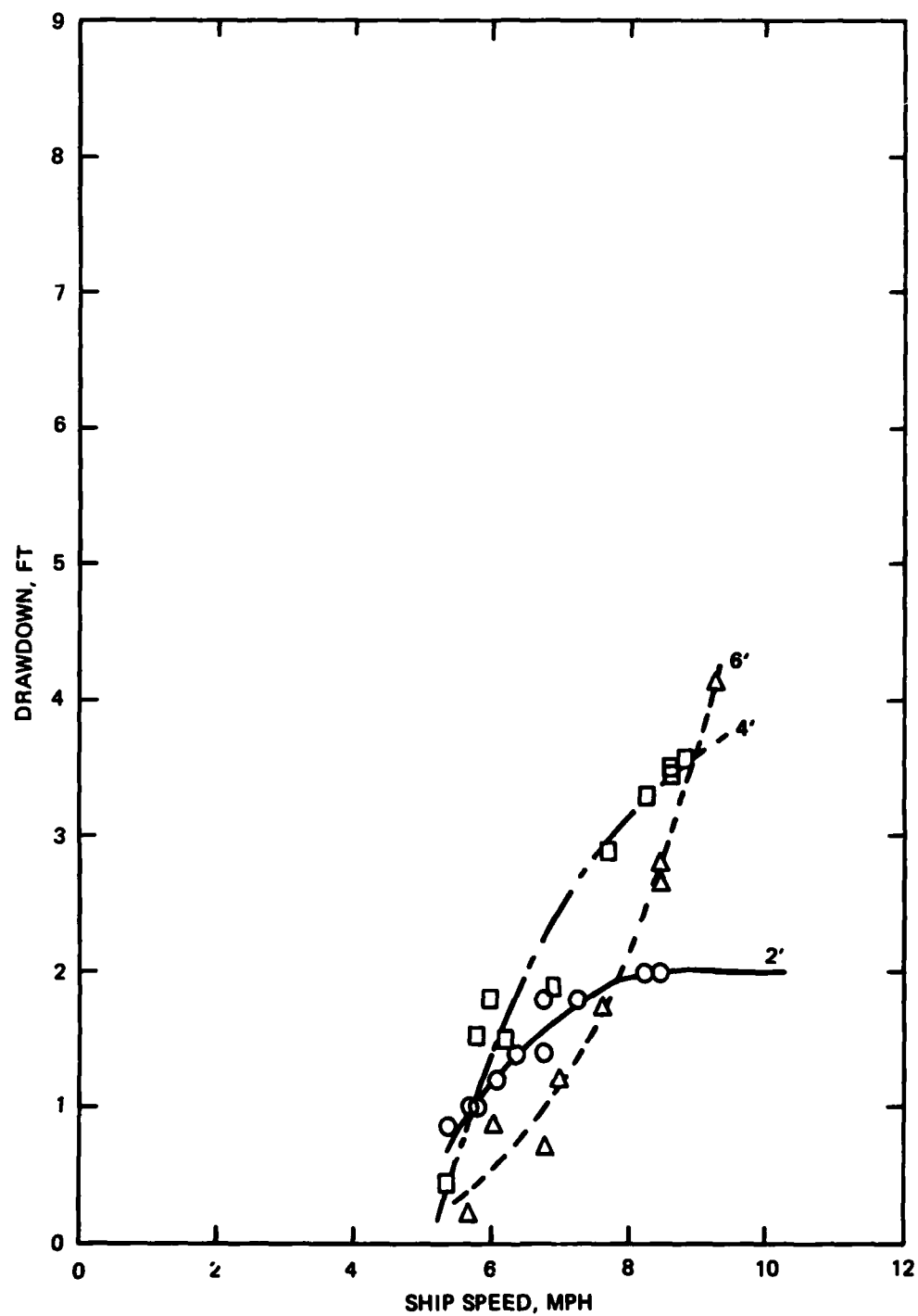


PLATE 6



○ 2' DEPTH OVER BERM
□ 4' DEPTH OVER BERM
△ 6' DEPTH OVER BERM

DRAWDOWN VS SHIP SPEED
 $\eta = 4.3$

PLATE 7

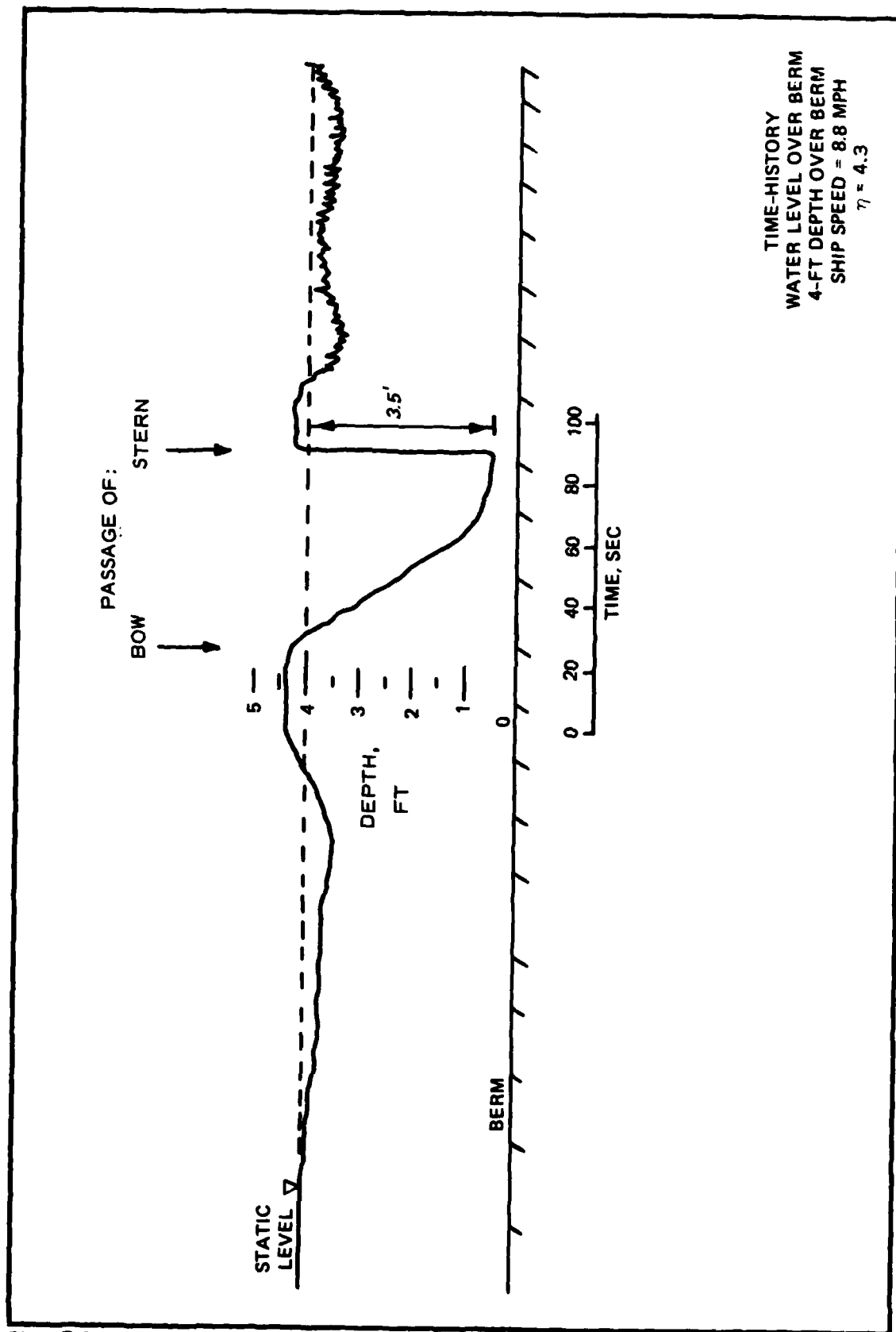


PLATE 8

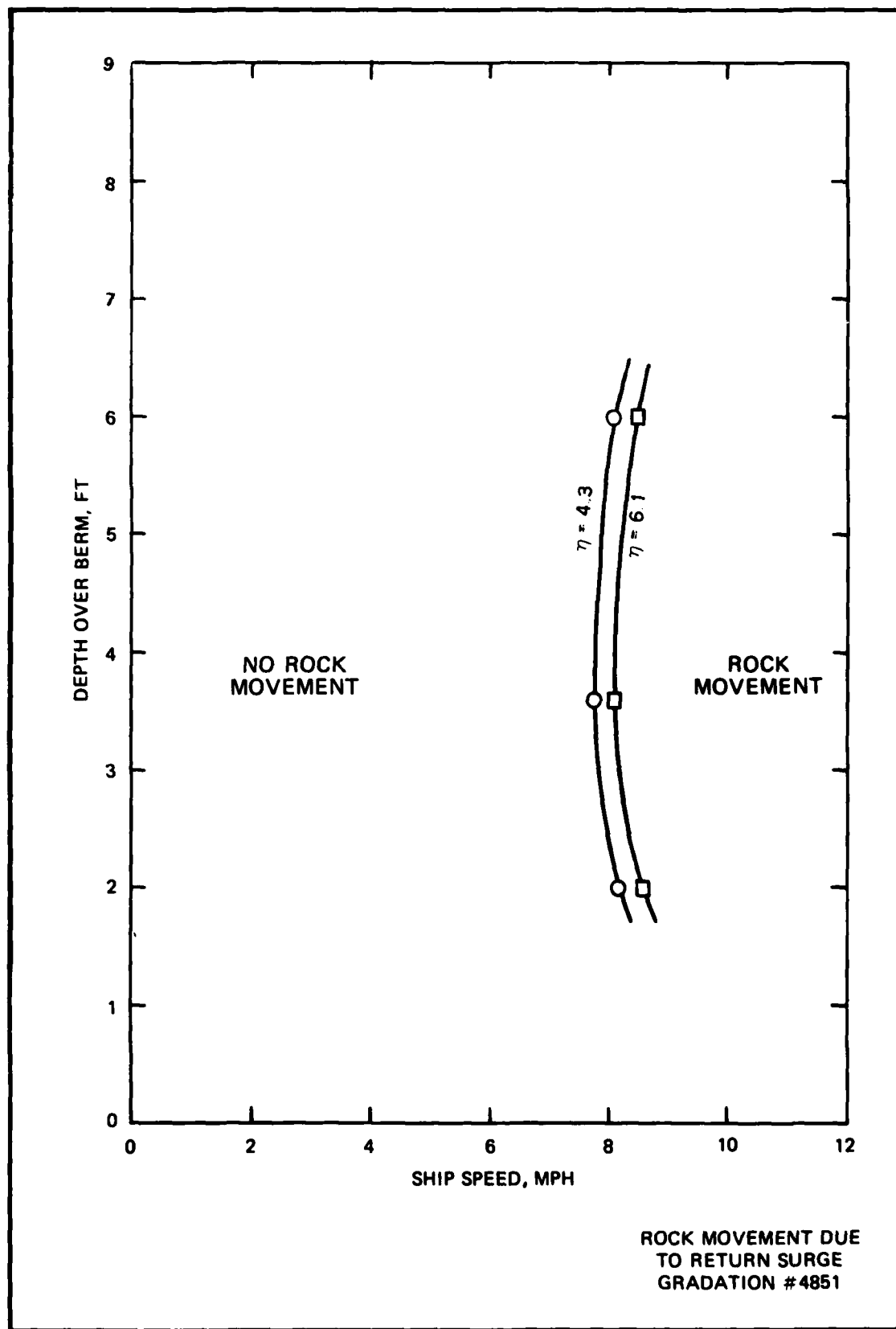


PLATE 9

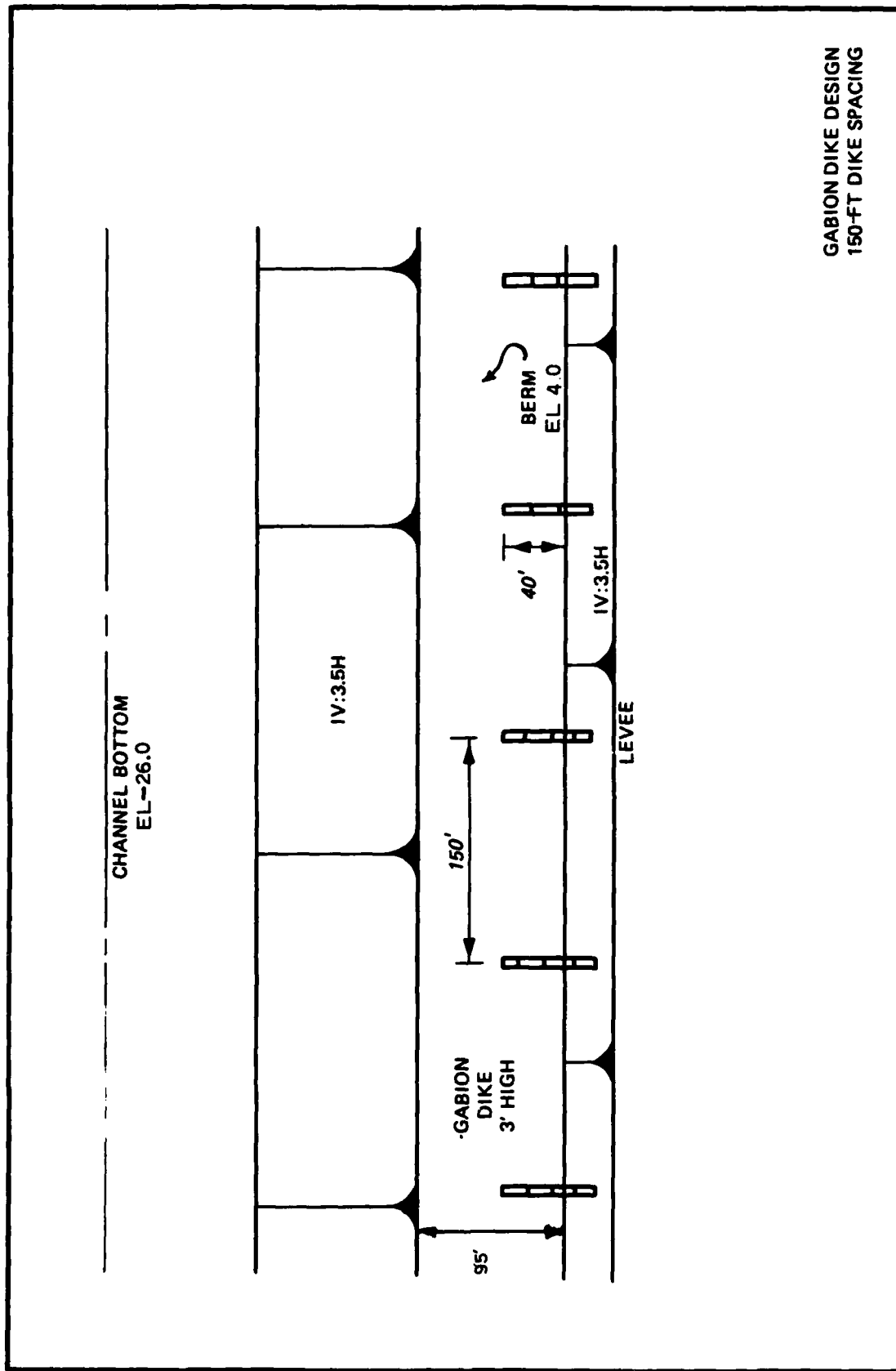
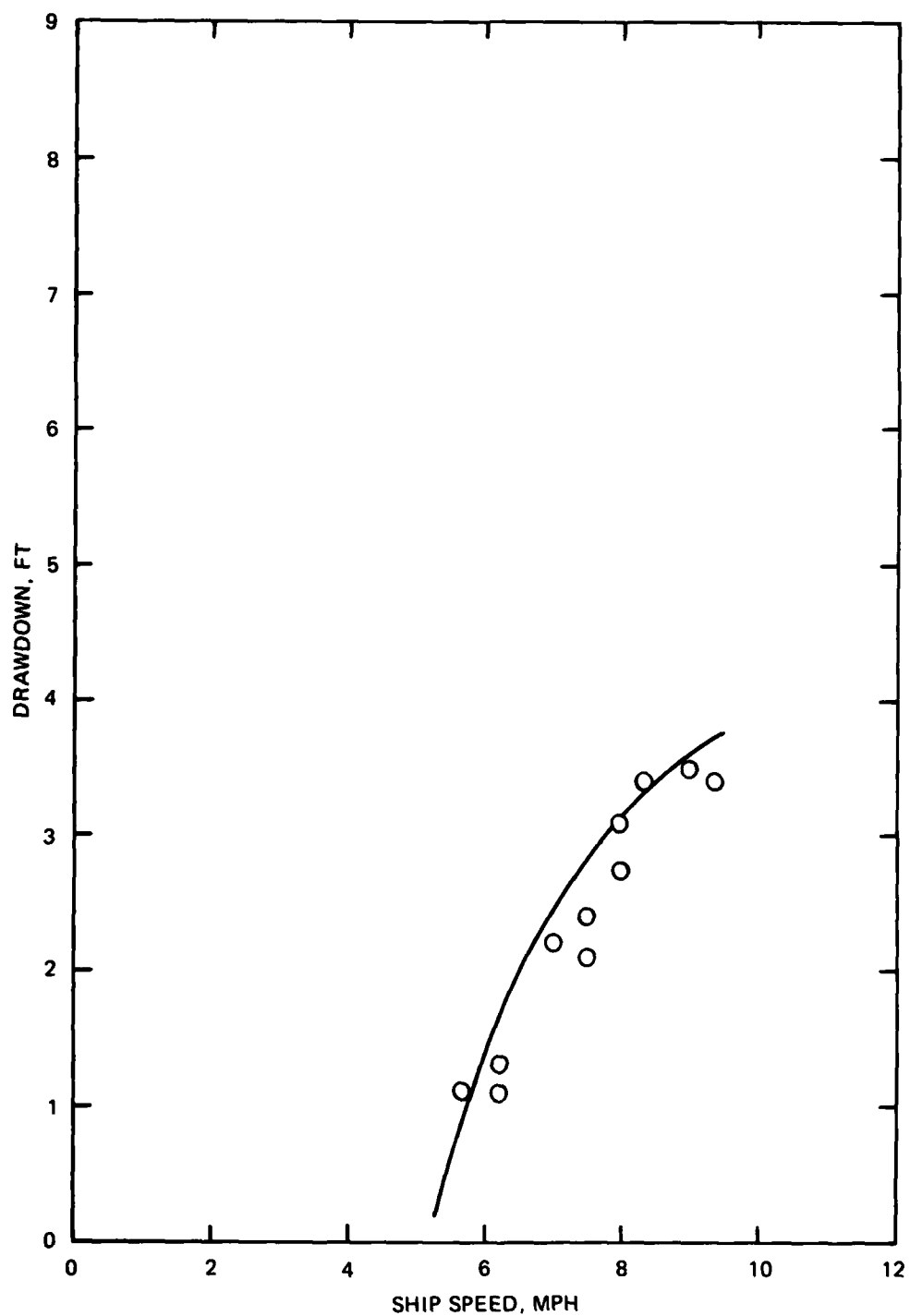


PLATE 10

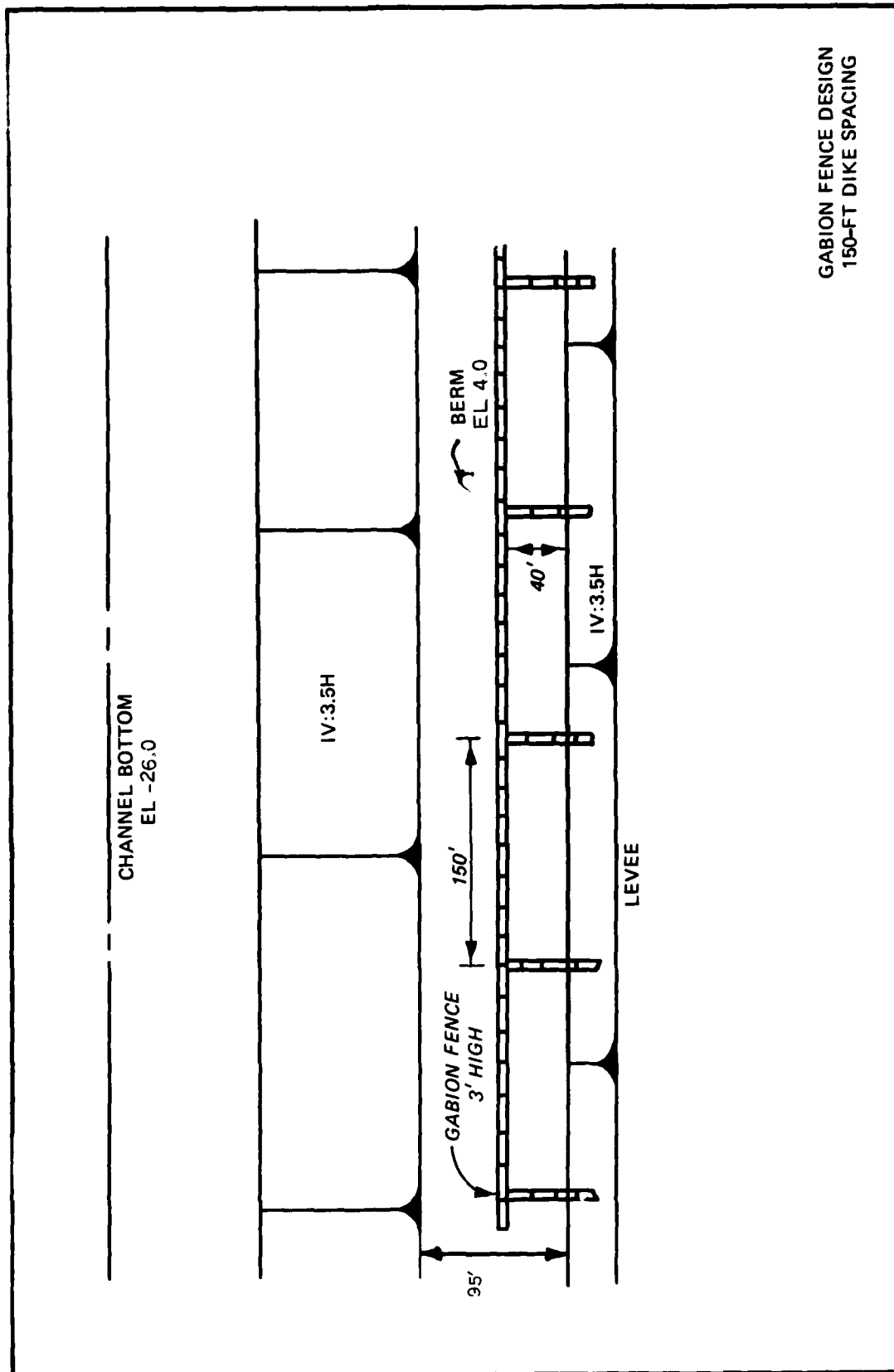


— ORIGINAL DESIGN
○ GABION DIKE

GABION DIKE DESIGN
DRAWDOWN VS SHIP SPEED
 $\eta = 4.3$ SHIP DISPLACEMENT
4-FT DEPTH OVER BERM
150-FT GABION DIKE SPACING

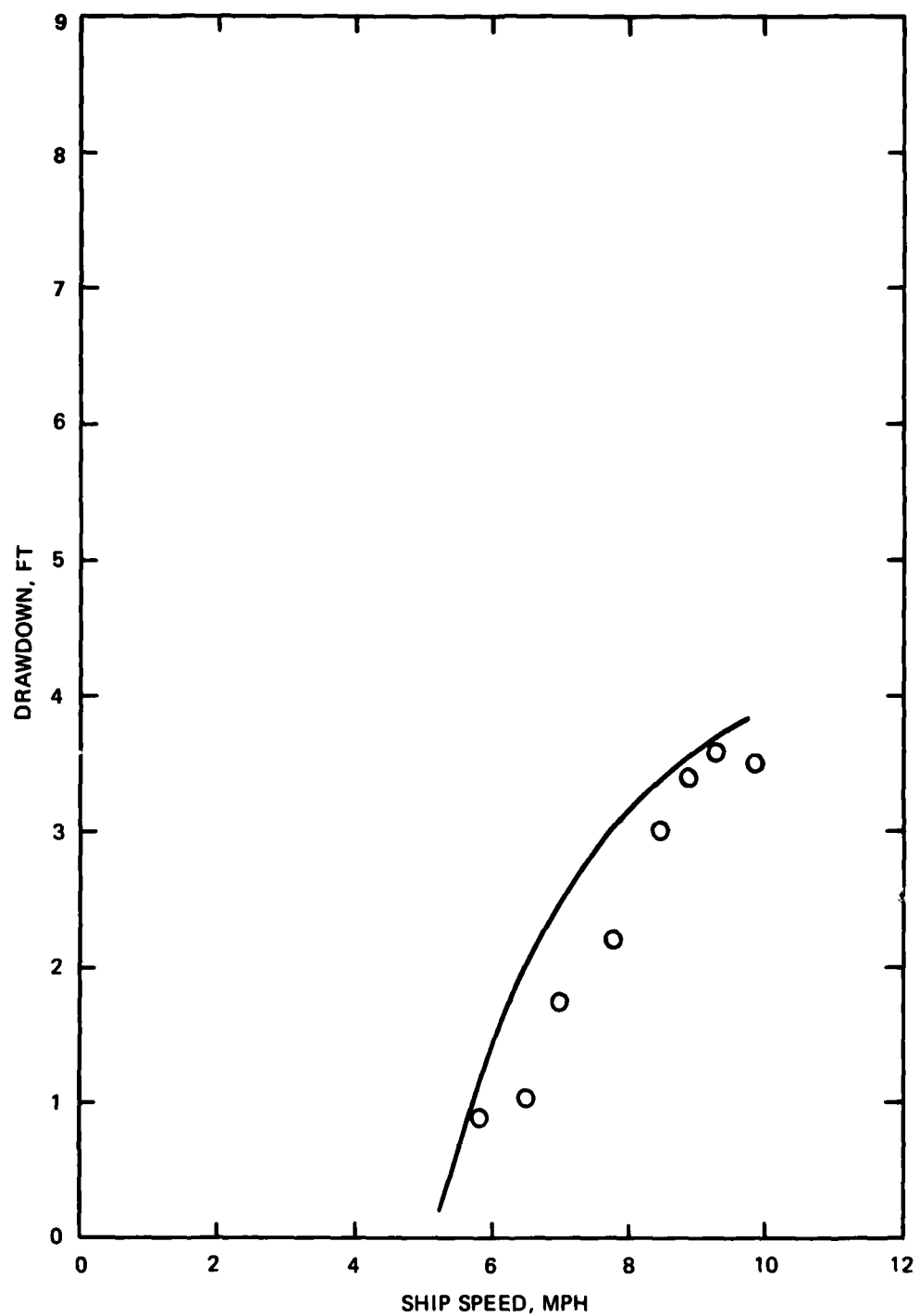
PLATE 11

B-5-33



GABION FENCE DESIGN
150-FT DIKE SPACING

PLATE 12



— ORIGINAL DESIGN

○ 20% INCREASE IN CHANNEL AREA

INCREASED CHANNEL AREA
DRAWDOWN VS SHIP SPEED
 $\eta = 5.2$ SHIP DISPLACEMENT
4-FT DEPTH OVER BERM

**EFFECTS OF PROPELLER WASH FROM INLAND NAVIGATION
ON CHANNEL BOTTOM STABILITY**

SECTION 32 PROGRAM
STREAMBANK EROSION CONTROL EVALUATION AND DEMONSTRATION
EFFECTS OF PROPELLER WASH FROM INLAND NAVIGATION
ON CHANNEL BOTTOM STABILITY
Hydraulic Model Investigation

Introduction

1. Under the Section 32 Program,* hydraulic research was conducted to study the effects of propeller wash from inland navigation on channel bottom stability. This research addressed the riprap size required in maneuvering areas such as docks and lock approaches where vessel speeds are low but the energy of propeller wash can be high. The increasing size of vessels and vessel horsepower has exposed inland waterways to increased hydraulic forces and previously stable maneuvering areas are experiencing problems with scour of the channel bottom. Engineers planning and designing rehabilitation of existing or construction of future inland navigation facilities requiring bottom protection can use the results of this research within the limits stated in paragraph 10.

Model Appurtenances and Test Procedures

2. A 1:20-scale model was used for the investigation and model quantities were converted to prototype quantities based on the Froudian similarity criteria. The scaling relations are as follows:

<u>Characteristic</u>	<u>Dimension</u>	<u>Model:Prototype</u>
Length	L_r	1:20
Area	$A_r = L_r^2$	1:400

(Continued)

* PL 92-251, Section 32, Streambank Erosion Control Evaluation and Demonstration Act of 1974.

<u>Characteristic</u>	<u>Dimension</u>	<u>Model:Prototype</u>
Volume	$Vol_r = L_r^3$	1:8000
Weight	$W_r = L_r^3$	1:8000
Time	$T_r = L_r^{1/2}$	1:4.47
Velocity	$V_r = L_r^{1/2}$	1:4.47
Thrust	$Th_r = L_r^3$	1:8000
Revolutions	$R_r = 1/L_r^{1/2}$	1:0.224

An outdoor slack-water channel with depths up to 25 ft (prototype) was used to represent the maneuvering areas. All references to sizes refer to the prototype unless stated otherwise. The channel bottom was sand having a median diameter of approximately 0.5 mm (model dimension) and the side slopes of the channel were covered with filter fabric (prototype). To form the model riprap test sections, filter fabric was placed over the horizontal sand bed and riprap was placed on the filter fabric to simulate 300-ft-long by 100-ft-wide (prototype) test sections. Riprap used in the model was crushed limestone having a specific gravity of 2.67 and d_{50} sizes used in the investigation simulated prototype stone with diameters up to 2.92 ft. Gradations of the prototype stone simulated in the different model riprap test sections are shown in Plate 1.

3. The 1:20-scale model tow (Figure 1) used in the investigation represents an inland waterway vessel having twin screws, main and flanking rudders for each screw, tunnel stern with twin rudder gear, and without Kort nozzles. Dimensions and other pertinent data for the simulated towboat are as follows:

Length = 208.8 ft
Width = 45.6 ft
Draft = 9 ft
Horsepower = 5600
No. of propellers = 2
Propeller diameter = 10 ft

(Continued)

No. of blades = 4
Propeller rpm = 190
 K_T , thrust coefficient at zero
ship speed = 0.36

4. Each test was conducted with the vessel held in a stationary position over the riprap test section in the slack-water channel and the required propeller speed was established in the model. Depths were gradually lowered until failure of the bottom riprap was detected. Each riprap size was subjected to a 9-min duration of the full thrust of the towboat at each depth before the test section was inspected for failure. Depths were measured with staff gages and riprap failure was determined by observing either rock movement or exposure of the underlying filter fabric. Tests were conducted with both forward and backward thrust and attack of the rock was similar in the slack-water channel.



Figure 1. 1:20-scale model tow

Test Results

5. A summary of tests conducted and results is shown in Table 1. A plot of rock size as a function of channel depth for the 5600-hp tow-boat is shown in Plate 2. These results are applicable to attack on the channel bottom without the effects of any lateral walls. Details of the rock gradations simulated and investigated are shown in Plate 1. These gradations represent very uniform riprap or capstone and do not address energy absorption or filter requirements between the riprap and soil. A rock gradation with a wide variation in sizes contains fine material that may be transported by the propeller wash and deposited in undesirable areas within the maneuvering zones.

Comparison of Model Results with Engineering Literature

6. A search of the literature was conducted to evaluate existing design information regarding bottom protection against propeller wash. A recent article by Fuehrer et al.* gives an excellent review of past work and presents a design procedure for protecting both the bottom and side slope of navigation canals. This procedure requires computing the induced jet velocity, V_o , defined as

$$V_o = 1.6 n D K_T \quad (1)$$

where

V_o = induced jet velocity at ship speed = 0, m/sec

n = propeller speed, rev/sec

D = propeller diameter, m

K_T = thrust coefficient, at ship speed = 0

* M. Fuehrer, K. Römisch, and G. Engelke. 1981. Criteria for Dimensioning the Bottom and Slope Protections and for Applying the New Methods of Protecting Navigation Canals," Permanent International Association of Navigation Congresses, 25th Congress, Section I, Volume I.

For the 5600-hp towboat, the induced jet velocity is $V_o = 9.27 \text{ m/sec} = 30.4 \text{ ft/sec}$. Many times the thrust coefficient may not be known and Blaauw and van de Kaa* present an equation for estimating V_o based on horsepower and propeller diameter

$$V_o = 1.48 \frac{(P_D)^{1/3}}{D^2} \quad (2)$$

where

P_D = installed engine power, kw (1 Hp = 0.746 kw)

D = propeller diameter, m

hp = horsepower

Based on Equation 4 for the 5600-hp towboat, $V_o = 9.0 \text{ m/sec} = 29.4 \text{ ft/sec}$ which is close to the value obtained by Equation 3. Next, the bottom velocity is determined as a function of V_o , propeller diameter, and depth by Fuehrer as

$$V_{B,max} = V_o \cdot E \cdot (hp/D)^{-1.0} \quad (3)$$

where

$V_{B,max}$ = maximum bottom velocity at zero ship speed, m/sec

hp = distance from center of propeller to bottom, m

E = a coefficient depending upon the stern shape and type of rudder arrangement; 0.25 for inland ship, tunnel stern, single screw, with twin rudder gear

This value of E was determined by Fuehrer using single screw vessels whereas the model vessel used in this investigation was a twin screw vessel. At the shallower depths, the propeller jet may attack the bottom before the jets intersect. At deeper depths, the jets may intersect before attacking the bottom and result in greater attack than with the single screw vessel. Comparison of the twin screw model results with the results of Fuehrer's design procedure should help resolve the

* H. G. Blaauw and E. J. van de Kaa. 1978. "Erosion of Bottom and Sloping Banks Caused by the Screw Race of Maneuvering Ships," Delft Hydraulics Laboratory, Publication No. 202.

difference between single screw-double screw ships. The final step is relating the maximum bottom velocity to the required stone size by Fuehrer's equation for $V_{B,max}$ defined as

$$V_{B,max} = B \sqrt{d_{50} g \left(\frac{\rho_s - \rho}{\rho} \right)} \quad (4)$$

where

d_{50} = average stone diameter, m

g = gravity = 9.81 m/sec²

ρ_s = stone density

ρ = water density

B = a coefficient depending upon the type of stern and type of rudder arrangement; 0.9 for inland ship, tunnel stern, and twin rudder gear

This value of B is the limiting condition or point at which rock movement would be incipient. For safe design the d_{50} size should be increased by an appropriate factor.

7. A comparison of the 1:20-scale model data and the Fuehrer, Römisch, and Engelke technique is shown in Plate 3 for the 5600-hp towboat. The curve represents incipient motion for bottom riprap protection without the effects of walls or flowing water which inhibit spreading of the flow and concentrate the attack.

8. According to Fuehrer, a significant reduction in the maximum bottom velocity occurs for normal navigation, i.e. navigation that is under way at a constant rate of speed. The maximum bottom velocity ($V_{B,max}$) for normal navigation is given by the relation

$$V_{B,max} = V_o \cdot E \cdot (hp/D)^{-1.0} \left(1 - \frac{V}{nD} \right)$$

where

V = ship speed, m/sec

n = propeller revolution, rev/sec

D = propeller diameter, m

Discussion of Results and Conclusions

9. The relation between rock size and water depth developed from the model tests is as expected; large rock required for small depths and small rock with large depths. Further, it appears that asymptotic limits of depth exist such that the size of stone required for stability increases and/or decreases at an infinite rate. For example, with a depth of 12.5 ft a significant increase in rock size does not permit any decrease in the depth allowed. This is not unexpected because at this condition there exists a jet of water approximately 10 ft in diameter with a velocity of about 30 ft/sec at a distance of only 3.5 ft from the riprap. The energy dissipation and velocity reduction at the boundary will be small for this condition. One preliminary conclusion from these tests is that riprap should not be used as protection with these small depths for the towboat size tested in this investigation. Stated differently, a greater depth of water would be necessary for use of riprap to protect the bottom of a berthing area or navigation channel, lock approach, etc.

10. Good correlation was found between the design procedure recommended by Fuehrer and the results of this investigation. These results, although more conservative than Fuehrer's, show that Fuehrer's design procedure for single screw vessels is applicable to the twin screw vessel used in this investigation. The curve shown in Plate 3 represents incipient motion of the bottom riprap protection and rock size should be increased to provide a stable design. This curve and the model results should not be used where adjacent lock or training walls limit spreading of the jet or in flowing waters. This occurs mainly when propeller thrust is angled toward a wall or upstream against flowing water which results in concentrated attack on the bottom.

11. Fuehrer's design procedure can be used to estimate the rock size required in maneuvering areas for various towboat sizes and water depths. Additional research is needed to determine the individual and collective effects of walls, angle of attack, depth, draft, horsepower, and velocity of vessel relative to riverflow. The capability to do

such research experiments has been demonstrated and such additional R&D would result in improved guidance and criteria for plan, design, operation, and maintenance of the nation's waterways.

Table 1
Summary of Test Results

<u>Gradation No.</u>	<u>d₅₀ ft</u>	<u>Depth ft</u>	<u>hp ft</u>	<u>hp/D*</u>	<u>Test Result</u>
1	2.92	15.6	11.6	1.16	Stable
	2.92	14.6	10.6	1.06	Stable
	2.92	13.6	9.6	0.96	Stable
	2.92	12.4	8.4	0.84	Failed
2	2.08	15.3	11.3	1.13	Stable
	2.08	14.2	10.2	1.02	Stable
	2.08	13.2	9.2	0.92	Stable
	2.08	12.2	8.2	0.82	Failed
3	1.46	18.0	14.0	1.40	Stable
	1.46	17.0	13.0	1.30	Stable
	1.46	16.0	12.0	1.20	Stable
	1.46	14.0	10.0	1.00	Failed
4	1.04	19.0	15.0	1.50	Stable
	1.04	18.0	14.0	1.40	Stable
	1.04	17.0	13.0	1.30	Failed
5	0.50	24.0	20.0	2.00	Stable
	0.50	22.0	18.0	1.80	Stable
	0.50	20.0	16.0	1.60	Stable
	0.50	18.0	14.0	1.40	Failed

* hp is the distance from the center of the prop to the channel bottom; D is the prop diameter.

B-6-9 / B-6-10

SIMULATED RIPRAP GRADATIONS

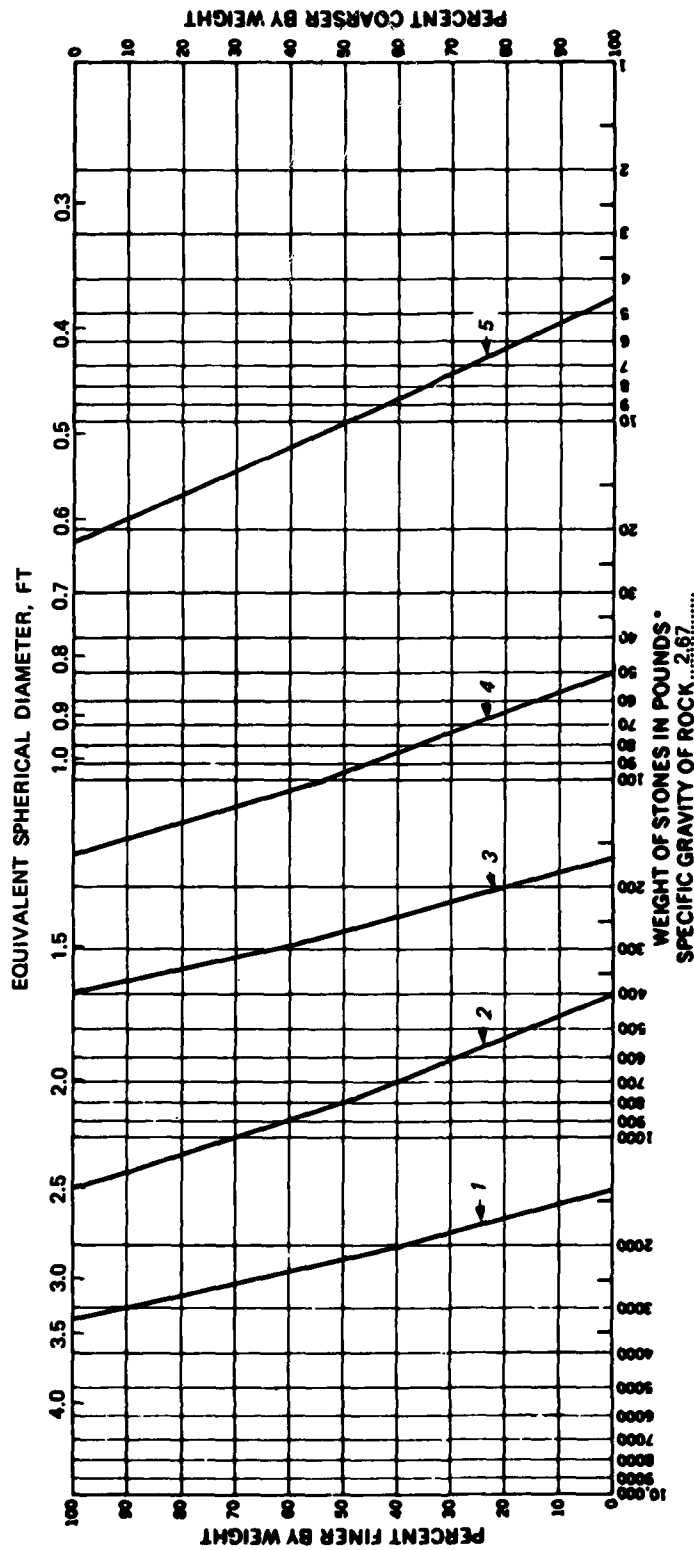
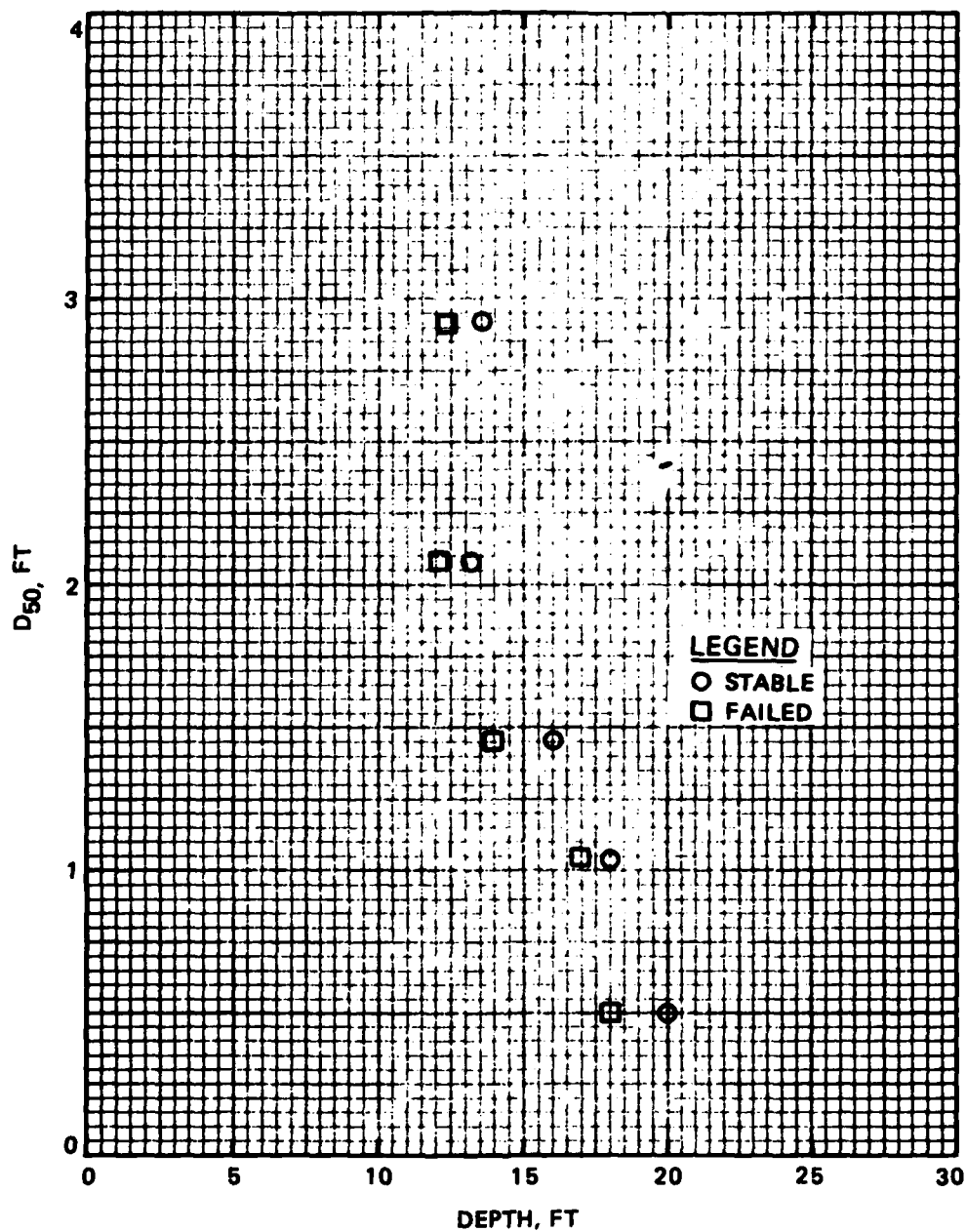


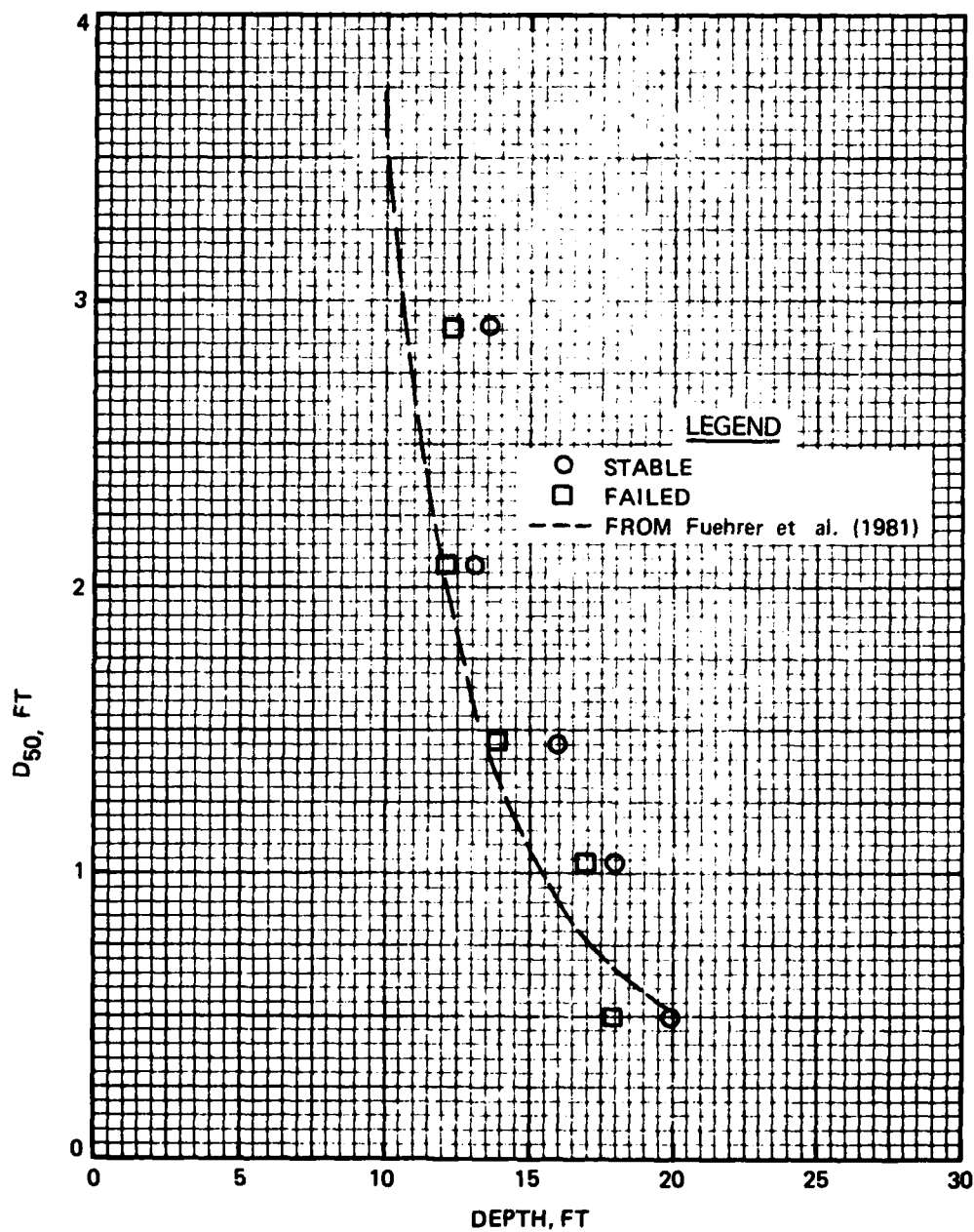
PLATE 1



ROCK SIZE VS DEPTH
MODEL RESULTS
5600-HP TOWBOAT
STRAIGHT ATTACK
W/O WALL EFFECTS
SLACK-WATER CHANNEL

PLATE 2

B-6-12



ROCK SIZE VS DEPTH COMPARISON OF
MODEL RESULTS WITH FUEHRER'S
DESIGN TECHNIQUE
5600-HP TOWBOAT
STRAIGHT ATTACK
W/O WALL EFFECTS
SLACK-WATER CHANNEL

PLATE 3

**WAVE AND SEEPAGE-FLOW EFFECTS ON SAND STREAMBANKS
AND THEIR PROTECTIVE COVER LAYERS**

SECTION 32 PROGRAM
STREAMBANK EROSION CONTROL EVALUATION AND DEMONSTRATION
WAVE AND SEEPAGE-FLOW EFFECTS ON SAND STREAMBANKS
AND THEIR PROTECTIVE COVER LAYERS
Demonstration Hydraulic Models

PART I: INTRODUCTION

The Prototype

1. Streambank erosion is a major problem along many miles of rivers and streams in the United States. In many instances, this erosion results in the loss of valuable land, flooding, and/or blocking of navigation channels. Streamflow velocities, wave action, overbank flow, and water-level drawdown, which induces seepage flows, are some of the major hydraulic factors that influence streambank erosion. Erosion can be initiated and sustained by any one or a combination of the above factors. This investigation addresses demonstration and documentation of waves, drawdown, and seepage-flow effects on a sand streambank with and without several types of protection.

Purpose of Demonstration Model Tasks

2. In many instances individuals are aware that they have streambank stability problems but are not certain as to the cause or causes of the instability. Many times the instability is due to more than one erosion-inducing process. Unless adequate protection is provided against all causes of local erosion, the streambank will continue to fail. One example would be a case of a streambank instability caused by the combined effect of wave action and seepage flow out of the streambank, the latter induced by the differential elevation between the stream and the groundwater table. If the streambank was covered with a solid concrete blanket it would be adequately protected from the wave-induced erosion

but the streambank protection might fail due to the buildup of hydrostatic water pressure caused by the higher groundwater table. Thus, the total problem needs to be understood before measures can be taken to provide adequate protection.

3. The purpose of these tests was not to establish any new protection techniques or design criteria for streambank protection. The main purpose of the test series reported herein was to demonstrate the effect of wave action, drawdown, and seepage flow on an unprotected streambank and then to demonstrate and compare the effectiveness of some of the state-of-the-art streambank protection techniques.

Tests Conducted

4. Wave- and seepage-flow-induced erosion are the two areas considered in this test series. Wave-induced erosion is obviously the result of the impingement of waves, which are short-period fluctuations in the still water level (swl), against the streambank slopes. Seepage flow is induced both into and out of the streambank by the periodic wave action and is induced either into or out of the streambank by static differential heads between the groundwater level and the water level in the river or stream. With the drawdown of the stream relative to the groundwater level or the raising of the water table relative to the stream level, seepage flow out of the embankment will result. The following tests were conducted to demonstrate both the individual and combined effects of waves, drawdown, and static-differential heads on both protected and unprotected streambank slopes:

- a. Static-differential heads across the streambank to induce seepage flow.
- b. Drawdown followed by static-differential heads across the streambank.
- c. Wave penetration without static-differential heads across the streambank.
- d. Wave stability without static-differential heads across the streambank.
- e. Wave stability with static-differential heads across the streambank.

Each of these tests will be explained in more detail in their respective sections of the report.

PART II: TEST FACILITY AND STREAMBANK

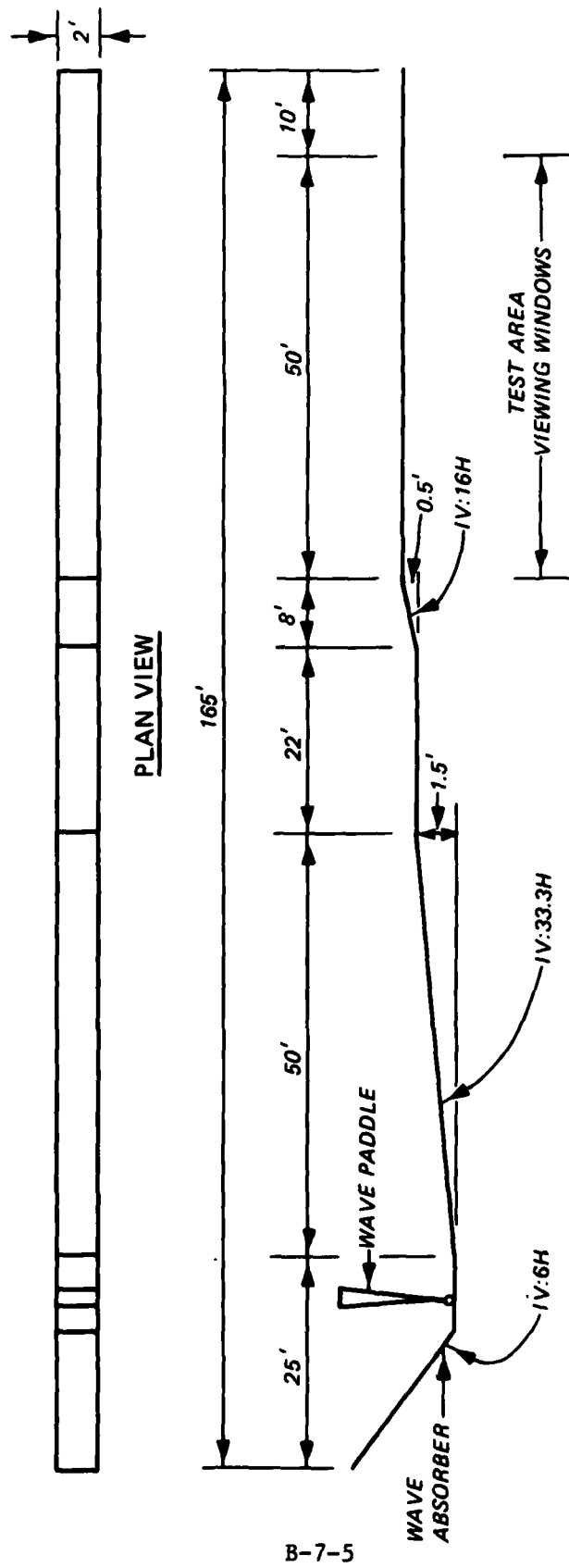
Selection of Test Scale

5. Laws of similitude have not been developed for accurate model reproduction of the interaction of fine streambank material and fluid mediums. Froude model laws are used for wave-stability tests where inertia and gravity are the predominant forces. Reynolds model laws are used for modeling flows where inertia and viscous forces predominate. The force ratios and scaling factors involved are different for these two laws of similitude for models and both cannot be satisfied simultaneously when water is the fluid in both the model and prototype systems. Therefore, to preclude any possible scale effects in the tests a prototype streambank was constructed in the available facility and tested at full scale (1:1, model to prototype).

Test Facility and Equipment

6. All tests were conducted in a 2-ft-wide and approximately 165-ft-long flume in which the depth varied from 4.5 ft in the test area to 6.5 ft at the wave paddle (Figure 1). The flume was equipped with a flap-type wave generator capable of producing monochromatic waves of various periods and heights. All test plans were constructed and tested within the flat bottom area of the test flume, labeled test area viewing windows in Figure 1. Changes in water-surface elevation (wave heights) as a function of time were measured by electrical wave-height gages and recorded on chart paper by an electrically operated oscillograph. The electrical output of the wave gage was directly proportional to its submergence depth in the water. All wave-height measurements were made prior to installing any of the test sections. The measurements were made where the toes of the streambank slopes would be located.

7. A system of bulkheads, overflow weirs, pumps, water supply hoses, and water-level control valves was installed in the flume test area to monitor and control the streamside and landside water levels for



ELEVATION VIEW

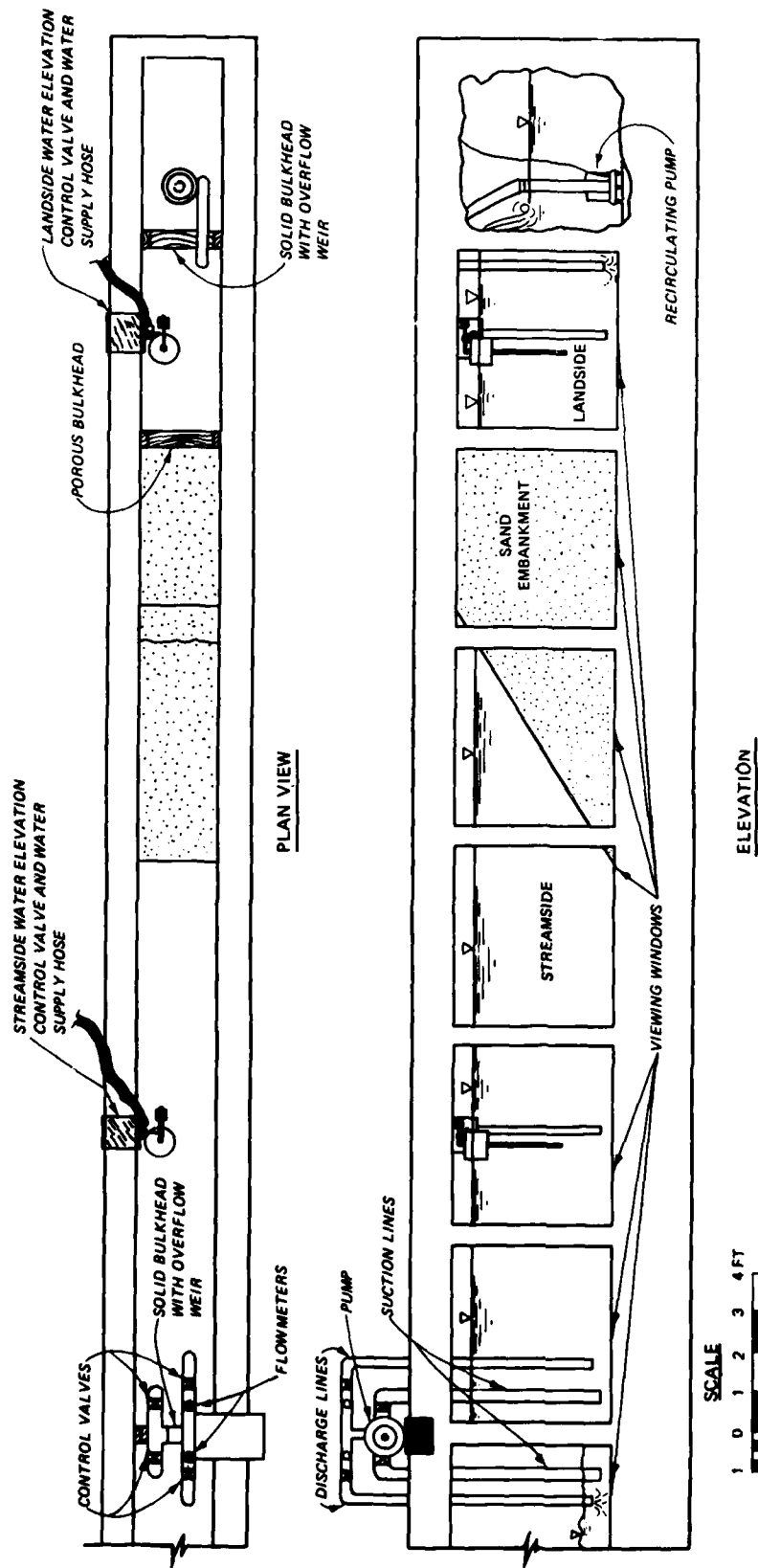
Figure 1. Test flume geometry

the drawdown and static differential head tests. The test area layout is shown in Figure 2.

8. For all but one of the test plans, a porous wooden bulkhead was used to support the vertical face on the landside of the streambank. The screen and cheese cloth used on the bulkhead were able to keep the sand from leaching out but were porous enough not to restrict the flow of water into or out of the sand streambank.

Selection of Streambank Material

9. Although the basic types of soils are generally finite in number, the combinations of soil types that occur along rivers and streams are almost infinite. Very seldom will a homogeneous streambank material be found along the entire reach of a streambank. In most all cases the streambank profile will be made up of layers of varying soil and/or rock types. It was not feasible to test all the naturally occurring soil types for all the proposed tests in this series. It was also necessary to reproduce the streambank as closely as possible, from one test to the next. Taking all this into account, it was decided to use a fine sand and one construction technique. This made it possible to closely reproduce the streambank properties, bulk density, porosity, etc., each time the streambank was rebuilt and thus allow the comparison of test results. The material used in all tests in this series was a uniform fine sand obtained from a source near the Big Black River about 7 miles south of Vicksburg, Mississippi. It is referred to locally as Reid-Bedford model sand. Materials laboratory tests indicated maximum and minimum dry unit weights of 104.2 and 87.2 lb per cu ft (pcf), respectively. Specific gravity of the sand was 2.65. Average grain size (D_{50}) was 0.24 mm, and the uniformity coefficient, D_{60}/D_{10} , was 1.5. Examination of sand grains under a low power microscope indicated that the predominant grain shapes were subrounded to subangular. The grain-size distribution, or gradation curve, is shown in Figure 3. Conventional consolidated drained, direct shear tests performed on laboratory samples prepared at 20 to 100 percent relative density indicated angles of internal friction



B-7-7

Figure 2. Test equipment and layout for drawdown and static-differential head tests

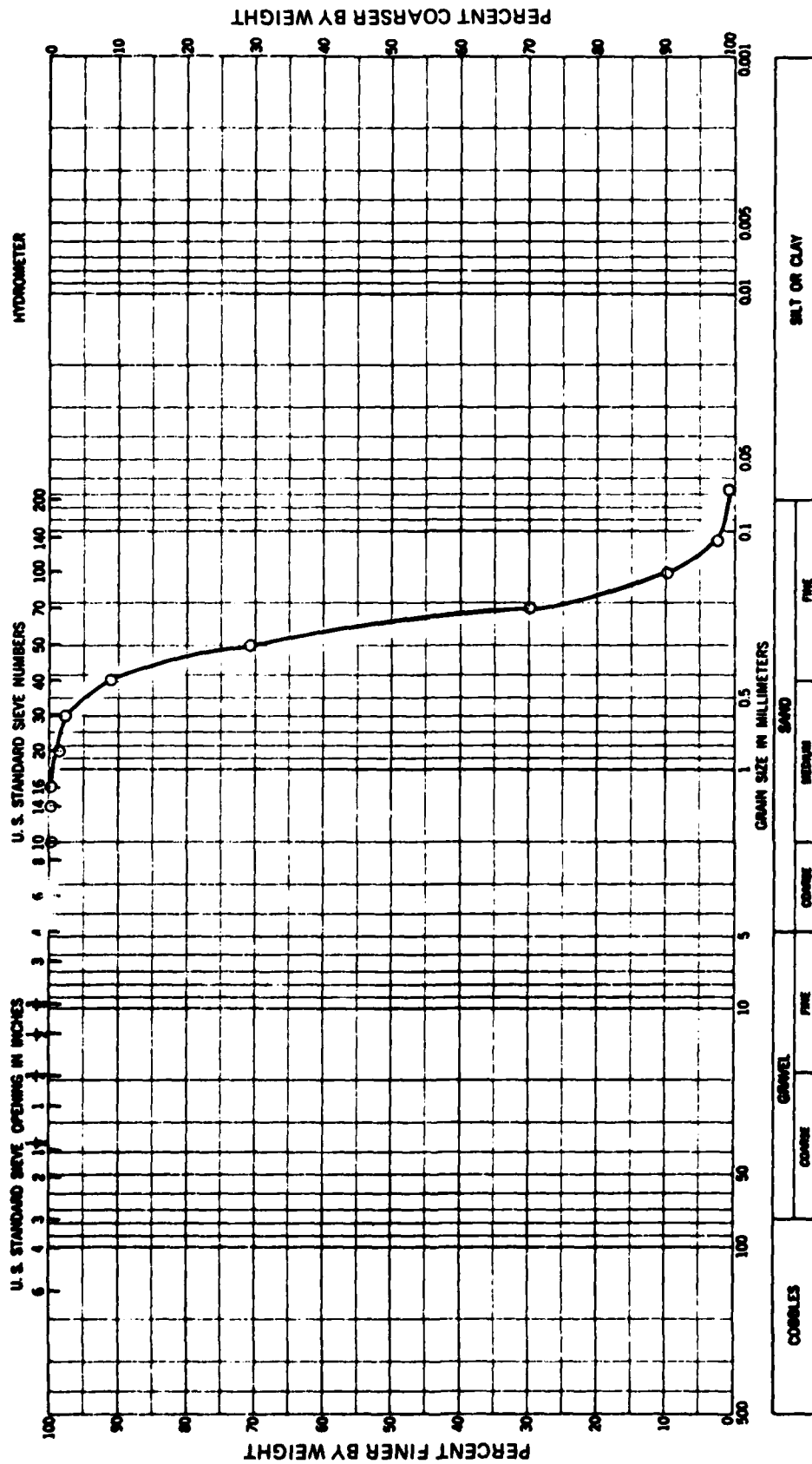


Figure 3. Gradation curve for streambank sand

of 29.2 to 32.3 deg, respectively, and cohesion equal to zero (Poplin 1965).

Construction of Model Streambanks

10. The sand was thoroughly dried and passed through a number 10 U. S. Standard sieve. To obtain as uniform density as possible, the sand was sprinkled from a shovel through standing water. The sand was added and let fall to its natural angle of repose, slope of 1V on 1.6H, until the sand mound slightly exceeded the size of structure that had been laid out on the test flume walls. The test flume was drained and the sand was allowed to drain thoroughly before the excess sand was screeded off. In all but one test series, the streambank sand was tested at its natural angle of repose. This closely simulated an alluvial sand deposit and was the steepest and thus most unstable slope that could occur naturally. For this reason any protective measures that successfully stabilized this slope would more than likely work on flatter slopes. In situ undisturbed sand samples were taken from several test sections. Laboratory tests showed dry unit weights ranging from 96.8 to 100.5 pcf with an average dry unit weight of 98.0 pcf. This corresponds to an average relative density of 67.5 percent.

PART III: TESTS AND RESULTS

Development of Plans

11. Three unprotected and fourteen protected sand streambank plans were used in all or a portion of the tests discussed in paragraph 4. All the sand streambanks were constructed using the procedures described in paragraph 10.

12. Plan 1, Figures 4 and 7, was an unprotected sand streambank 4 ft high with a 4-ft-crown width. The landside face of the structure was vertical while the streamside face was constructed with a 1V-on-1.6H slope.

13. Plan 2, Figures 5 and 8, was an unprotected sand streambank. The landside face of the structure had a vertical rise of 3 ft and the structure had no crown width. The streamside face of the structure used a 1V-on-1.6H slope between the base and the 1.0-ft elevation and a 1V-on-4H slope between the 1.0-ft elevation and the crown.

14. Plan 3, Figures 6 and 9-12, was a protected sand streambank. The streambank was constructed using the identical dimensions and geometry as Plan 1, paragraph 12. The streamside face was protected by a 0.5-ft-thick layer of riprap, a 0.17-ft-thick layer of filter B below the riprap, and a 0.04-ft-thick layer of filter A between filter B and the sand. Engineer Technical Letter 1110-2-222 (OCE 1978) was used as design guidance for the riprap. The sizing of the riprap was based on the following equations:

$$W_A = \gamma H_s^3 / 4.37 \cot \alpha (G-1)^3 \quad (1)$$

$$W_{\max} = 4W_A \quad (2)$$

$$W_{\min} = W_A / 8 \quad (3)$$

where

W_A = weight of median sized stone, lb

γ = unit of weight of stone, pcf

H_s = significant wave height, ft

α = angle streambank slope makes with the horizontal, deg

G = specific gravity of stone

W_{\max} = weight of maximum sized stone, lb

W_{\min} = weight of minimum sized stone, lb

A significant wave height of 0.75 ft, streambank slope of 1V on 1.6H ($\alpha = 32$ deg), and a 165-pcf unit weight of stone gave a W_A equal to 2.24 lb and this weight was used for all plans designed with riprap as the primary cover layer protection. The criteria call for the riprap to be well graded and the gradation curve should approximately parallel the gradation of the filter layer beneath it. The riprap gradation used is shown in Figures 10 and 11. The riprap layer thickness should be based on the following equation:

$$T = 20 (W_A/\gamma)^{1/3} \quad (4)$$

where T equals riprap layer thickness, in. Engineer Manual 1110-2-2300 (OCE 1971) states that a minimum riprap thickness of 12 in. should be used even if Equation 4 calls for a smaller thickness. Equation 4 called for a riprap thickness of 4.78 in. A thickness of 0.5 ft was used on a portion of the protected streambanks. This was well below the 12-in. minimum designated in the design criteria. It was felt that if this thickness proved to be adequate, then structures designed using Equations 1-4 should be more stable designs. Sizing and gradation of the two-layer filter system were based on the following equations from EM 1110-2-1913 (OCE 1978):

$$\frac{D_{15F}}{D_{85E}} \leq 5 \quad (5)$$

$$\frac{D_{50F}}{D_{50E}} \leq 25 \quad (6)$$

$$\frac{D_{15F}}{D_{15E}} \geq 5 \quad (7)$$

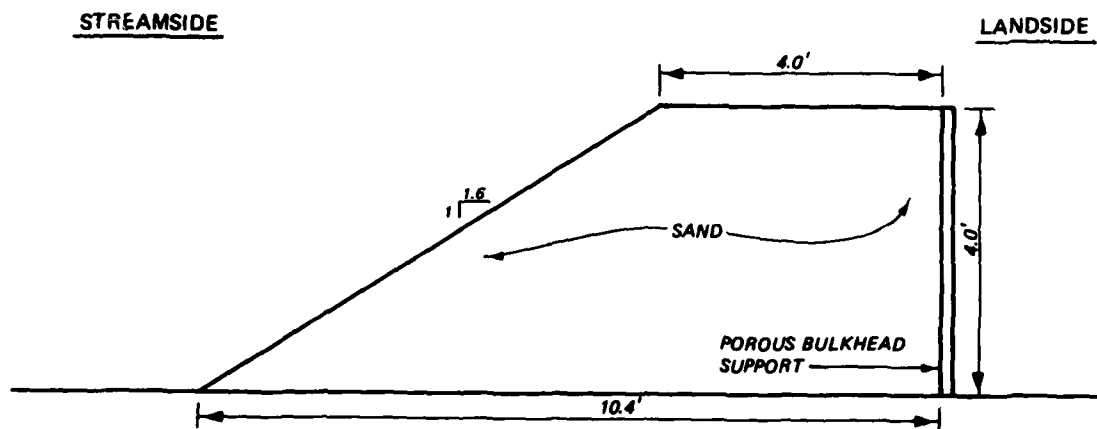


Figure 4. Plan 1, unprotected sand streambank

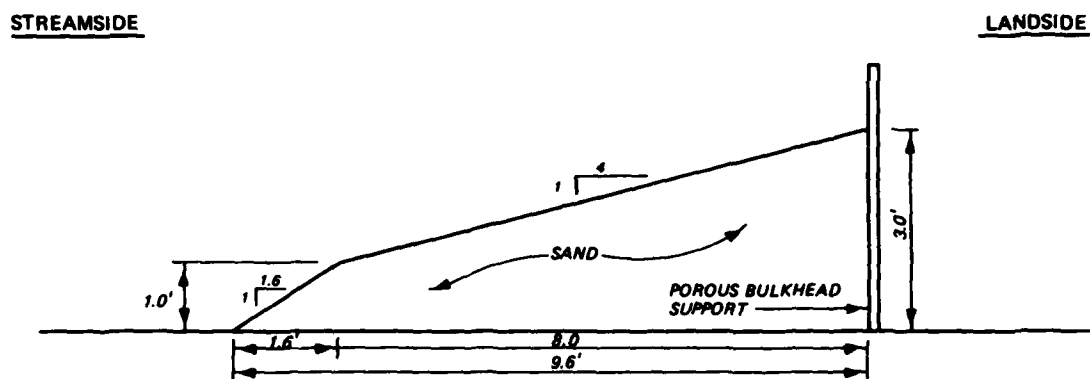
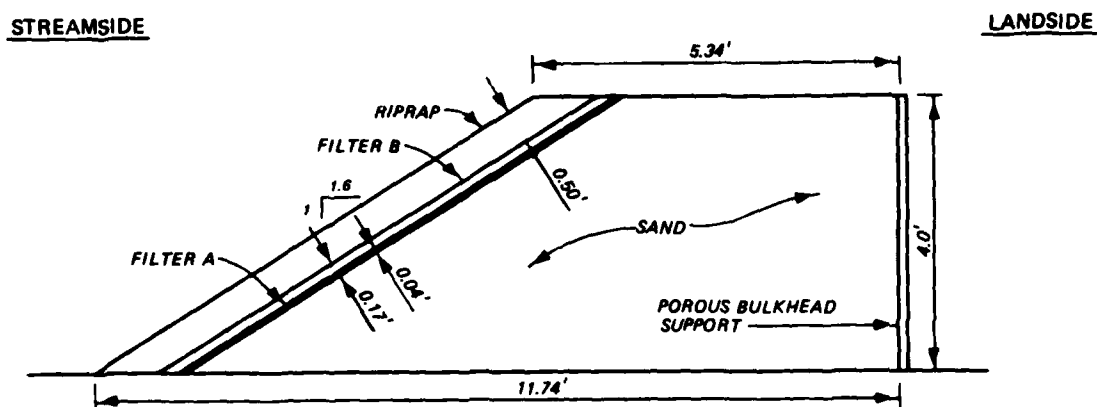


Figure 5. Plan 2, unprotected sand streambank



NOTE: FOR SIZE AND WEIGHT GRADATIONS OF RIPRAP AND FILTER LAYERS SEE FIGURES 10-12.

Figure 6. Plan 3, sand streambank with 0.5 ft of riprap and filter (two well-graded rock layers) protection

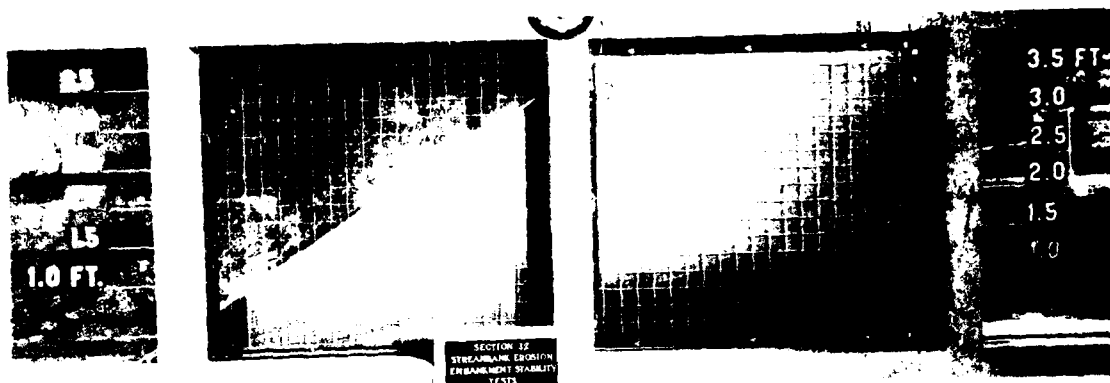


Figure 7. Plan 1

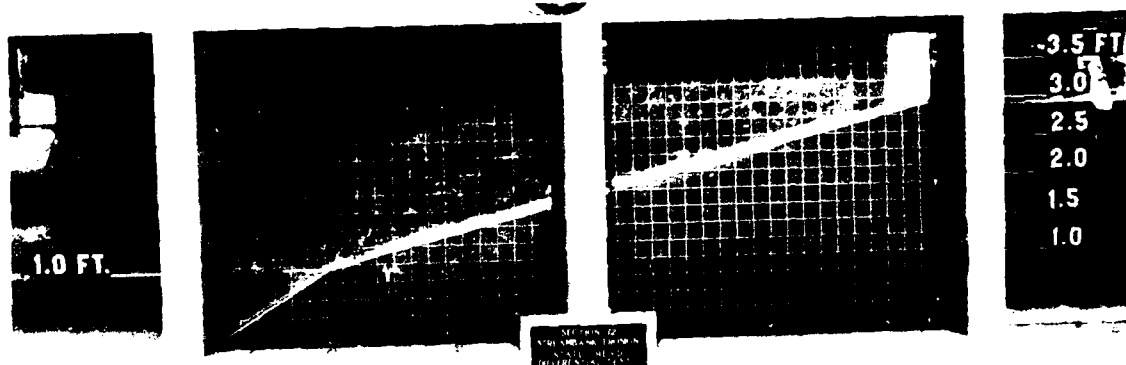


Figure 8. Plan 2

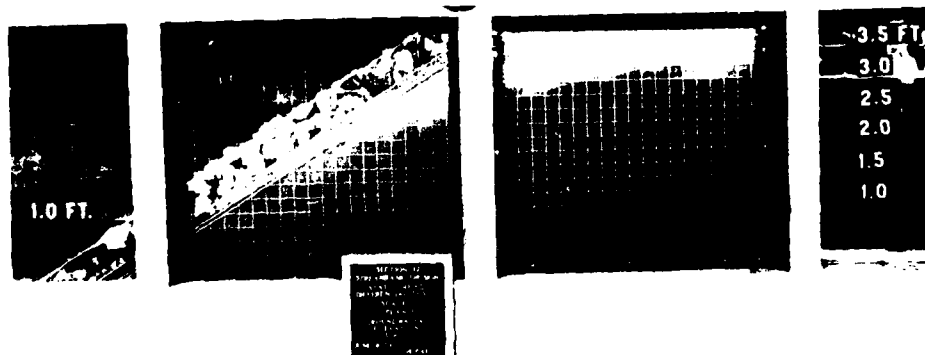


Figure 9. Plan 3

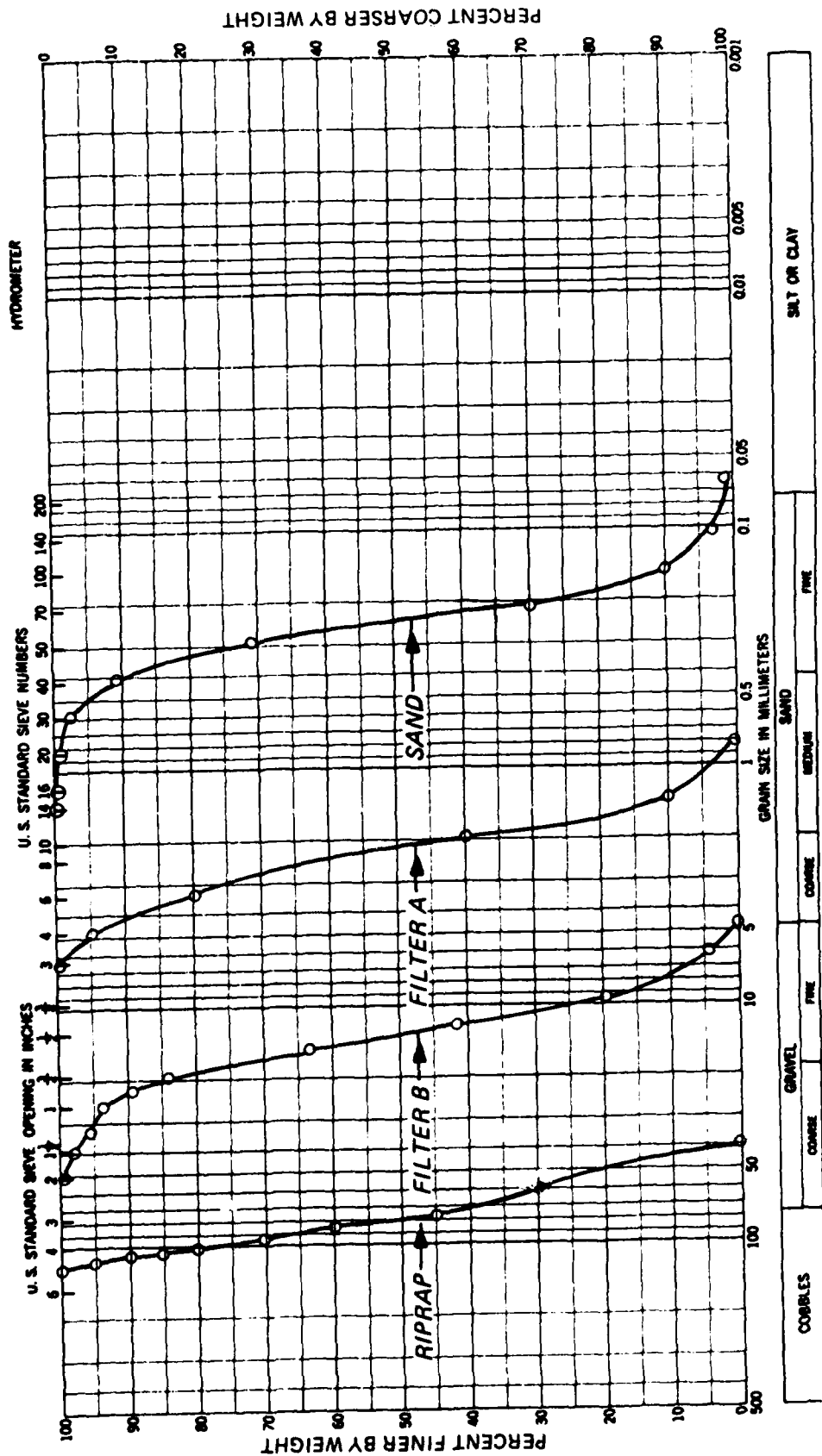


Figure 10. Size gradation curve for riprap, filter A, filter B, and sand

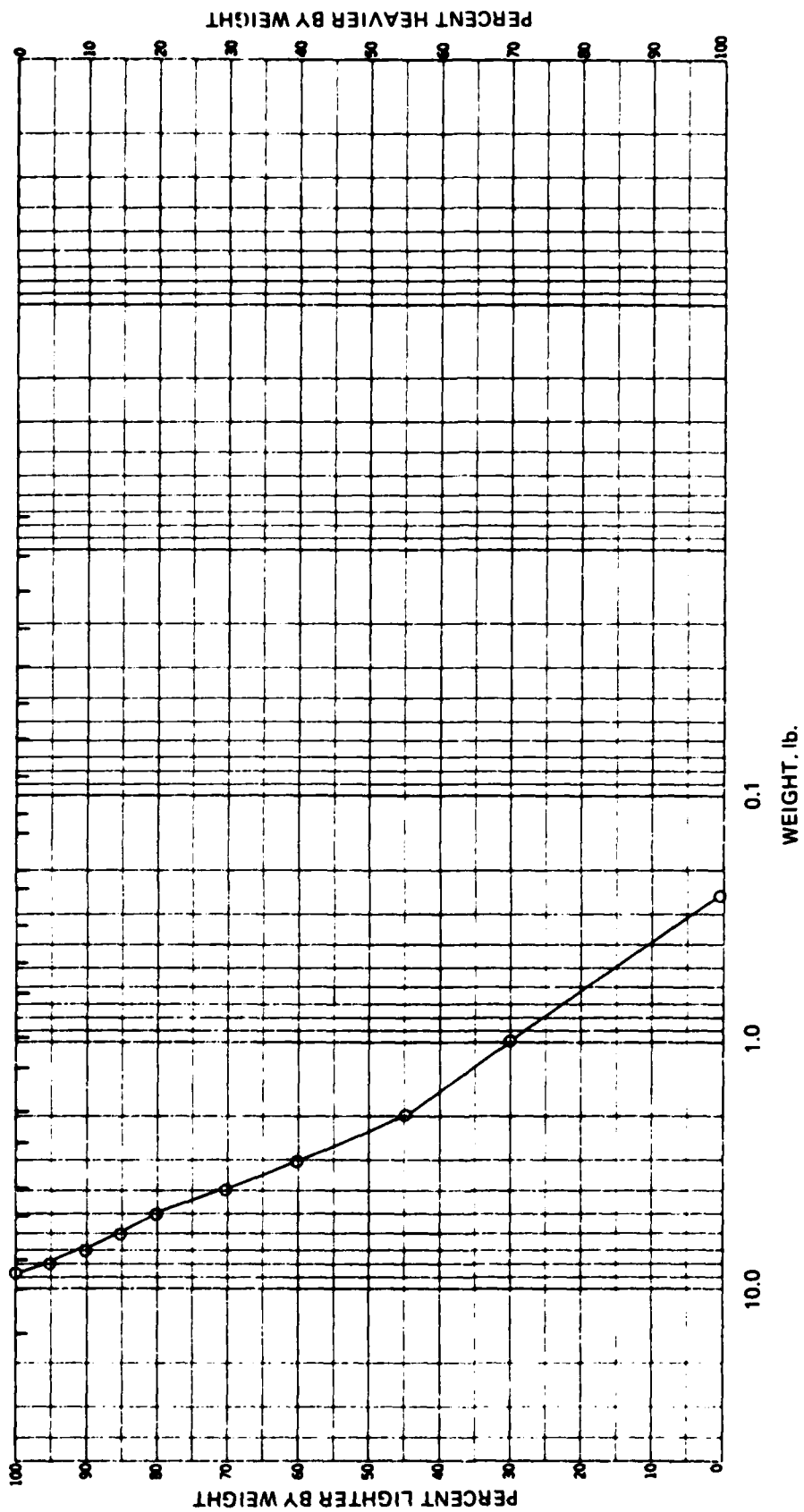


Figure 11. Weight gradation curve for riprap

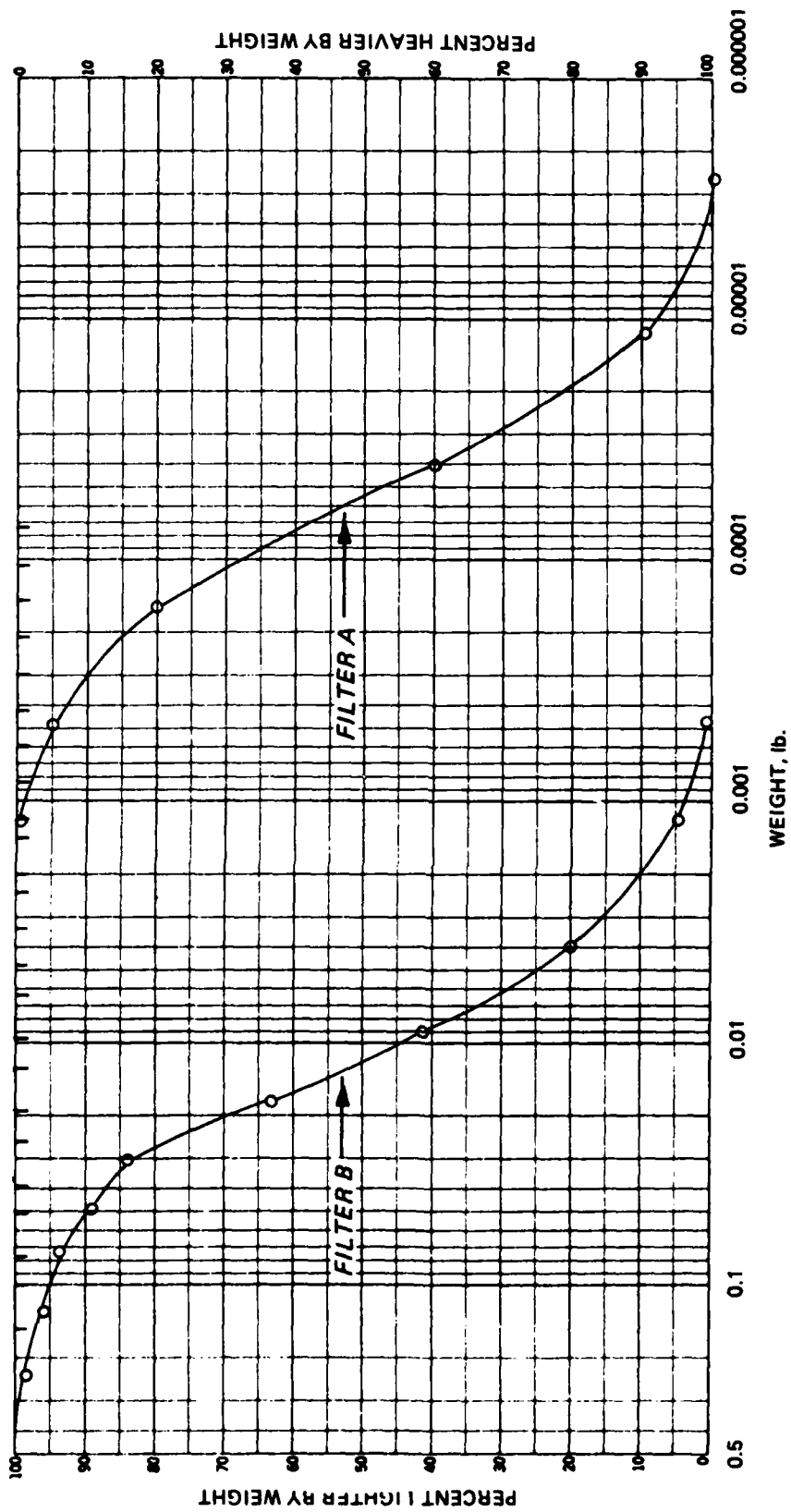


Figure 12. Weight gradation curves for filter A and filter B

where

D_{15F} = the 15 percent passing size of filter

D_{50F} = the 50 percent passing size of filter

D_{85F} = the 85 percent passing size of filter

D_{15E} = the 15 percent passing size of material under filter

D_{50E} = the 50 percent passing size of material under filter

Gradation curves for filters A and B are given in Figures 10 and 12.

The thickness of the individual filter layers was considerably less than the 9-in. minimum called for in the design guidance. If these thinner layers (1/2 and 2 in., respectively) proved to be adequate, prototype filter layers designed using the minimum thickness criteria should be adequate.

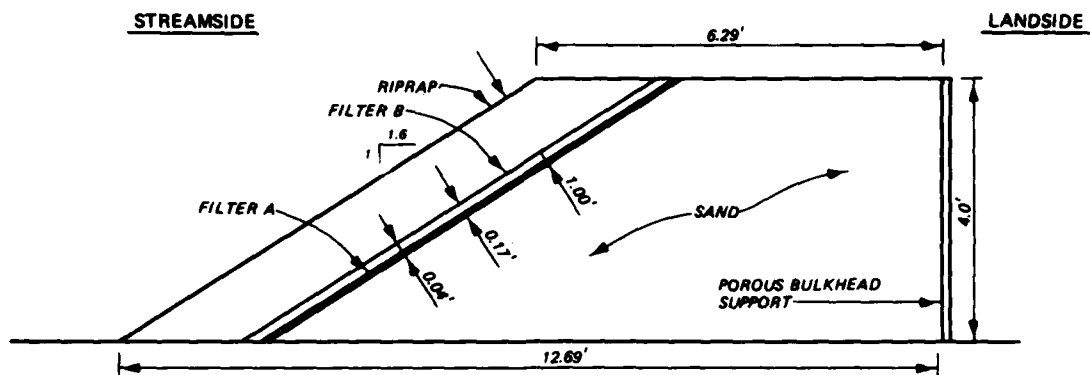
15. Plan 3A, Figures 13 and 16, was a protected sand streambank. Plan 3A was identical with Plan 3 except for the increased riprap layer thickness of 1.0 ft used in Plan 3A.

16. Plan 4, Figures 14 and 17, was a protected sand streambank using the same riprap design as Plan 3. The size and geometry of the sand streambank were identical with Plan 1. No filter was used between the riprap and sand.

17. Plan 4A, Figures 15 and 18, was a protected sand streambank. Plan 4A was identical with Plan 4 except for the increased riprap layer thickness of 1.0 ft used on Plan 4A.

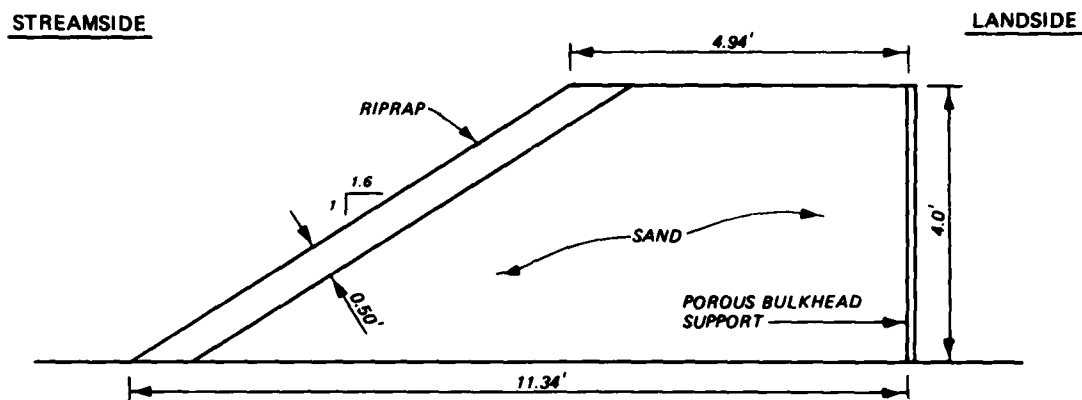
18. Plans 5 and 5A, Figures 19, 20, 22 and 23, were protected sand streambanks identical with Plan 4 except for the woven filter fabric that was placed between the riprap and sand in Plans 5 and 5A. Selection of the appropriate woven filter fabric was based on the design guidance given in the Civil Works Construction Guide Specifications for Plastic Filter Fabric, CW-02215 (OCE 1977). The woven filter fabric had an equivalent opening size (EOS) of 40, as determined by the procedures in CW-02215. The design guidance specifies the following:

$$\frac{\text{85 percent passing size of soil } (D_{85})}{\text{Opening size of EOS sieve}} \geq 1 \quad (8)$$



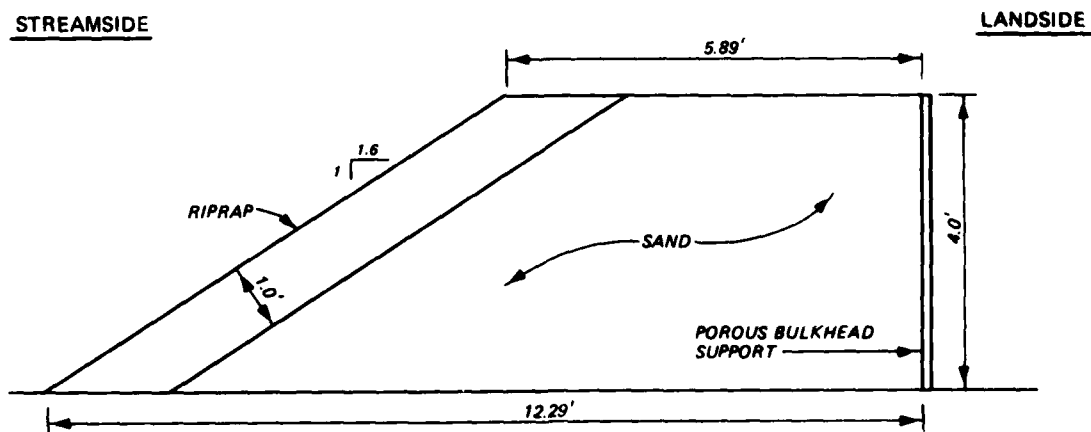
NOTE: FOR SIZE AND WEIGHT GRADATIONS OF RIPRAP AND FILTER LAYERS SEE FIGURES 10-12.

Figure 13. Plan 3A, sand streambank with 1.0 ft of riprap and filter (two well-graded rock layers) protection



NOTE: FOR SIZE AND WEIGHT GRADATIONS OF RIPRAP SEE FIGURES 10 AND 11.

Figure 14. Plan 4, sand streambank with 0.5 ft of riprap protection



NOTE: FOR SIZE AND WEIGHT GRADATIONS OF RIPRAP SEE FIGURES 10 AND 11.

Figure 15. Plan 4A, sand streambank with 1.0 ft of riprap protection

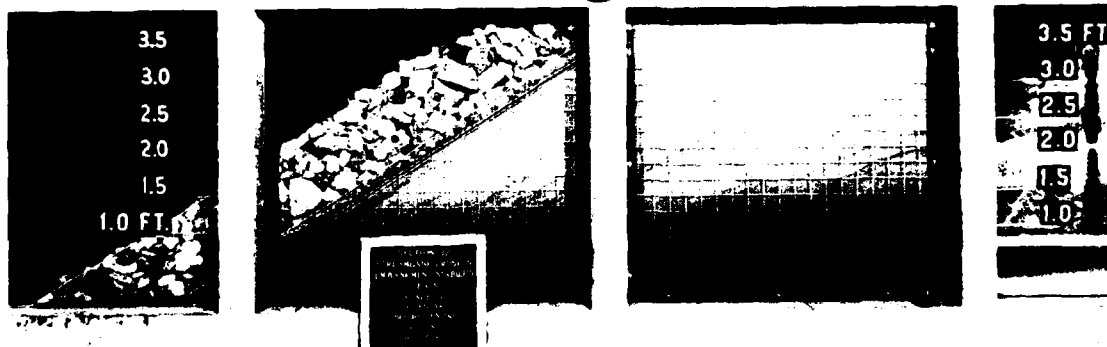


Figure 16. Plan 3A

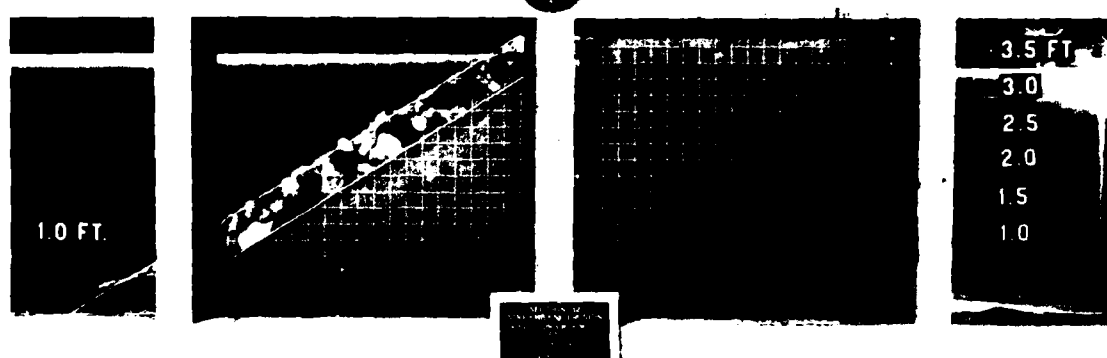


Figure 17. Plan 4

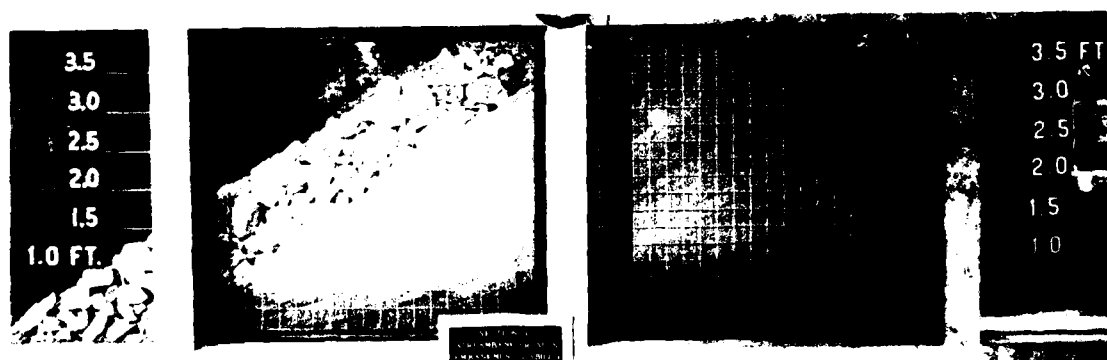


Figure 18. Plan 4A

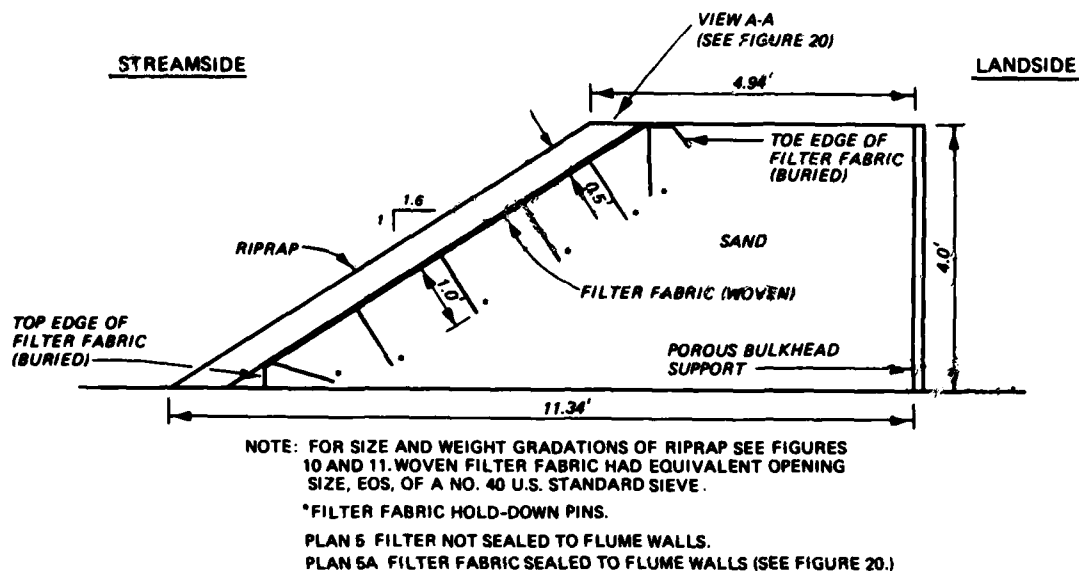


Figure 19. Plans 5 and 5A, sand streambanks with 0.5 ft of riprap and woven filter fabric protection

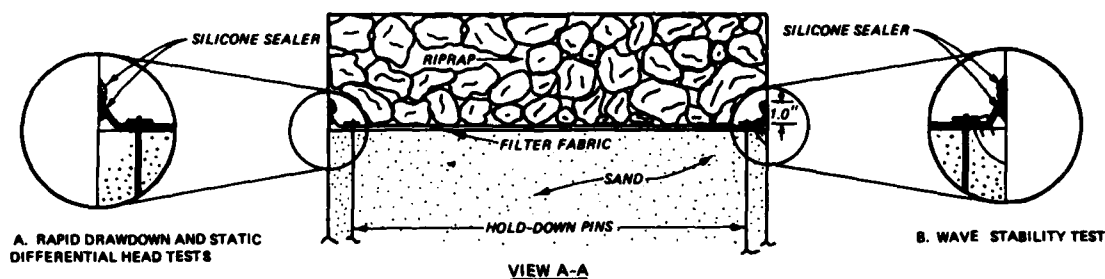


Figure 20. Details of filter fabric sealing used for drawdown, static differential head, and wave-stability tests

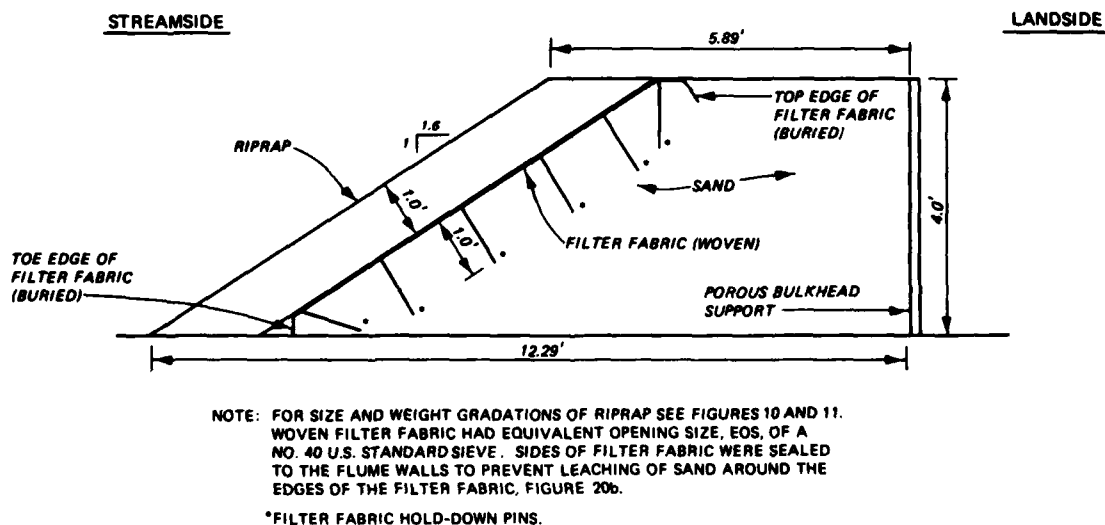


Figure 21. Plan 5B, sand streambanks with 1.0 ft of riprap and woven filter fabric protection

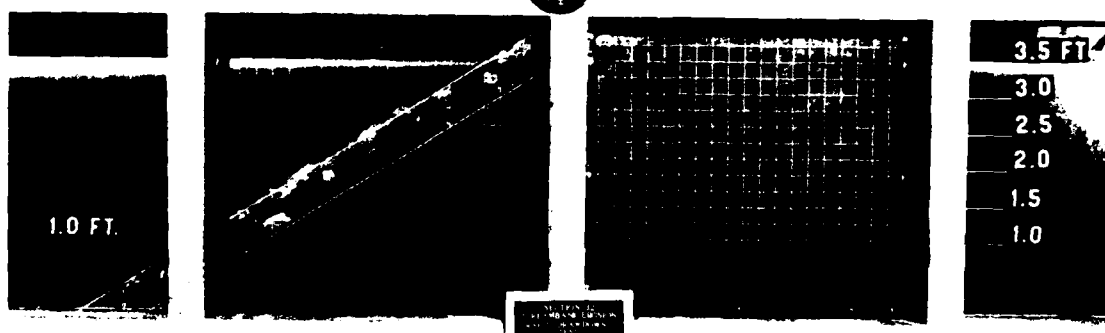


Figure 22. Plan 5

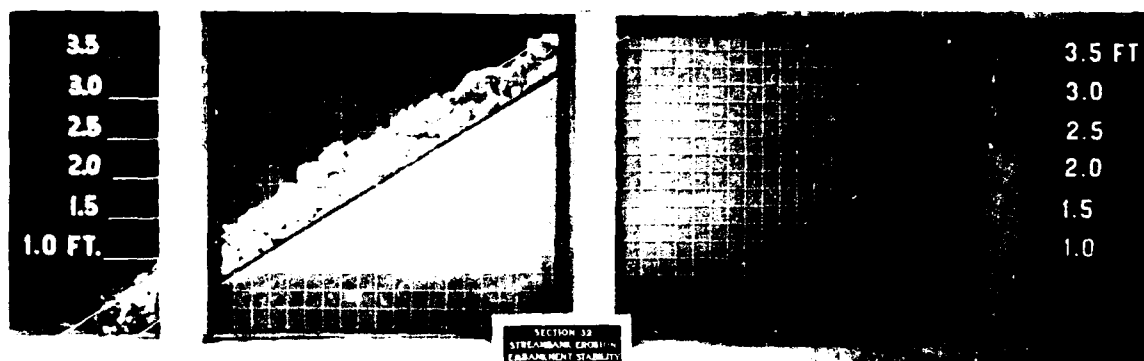


Figure 23. Plan 5A

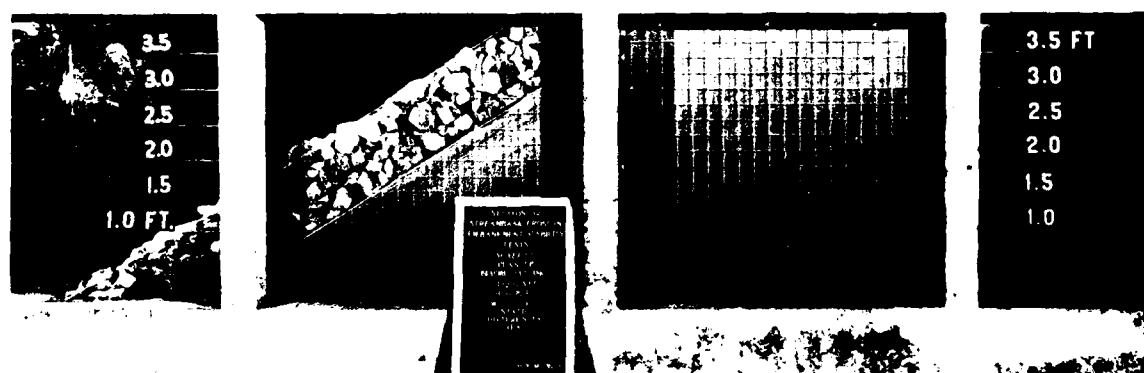


Figure 24. Plan 5B

As shown in Figures 3 and 10, the D_{85} size of the Reid-Bedford model sand was approximately 0.38 mm and a U. S. standard number 40 sieve has openings of 0.42 mm. Therefore from Equation 8:

$$\frac{D_{85} \text{ Sand}}{EOS 40} = \frac{0.38 \text{ mm}}{0.42 \text{ mm}} = 0.90$$

This fell slightly short of the design criteria and added conservatism to the test results for the plans that utilized the woven filter fabric. As shown in the test results, this slight diversion from the exact design criteria did not have a significant effect on the stability of the plans that used the woven filter fabric. The filter fabric was tested to ensure that it did not impair the flow of water either into or out of the streambank. This was checked by measuring the gradient ratio which is the ratio of the seepage gradient through the fabric and 1 in. of soil to the gradient through 2 in. of soil specimen. The gradient ratio, determined by the procedures described in CW-02215, should not exceed 3. Laboratory measurements showed a gradient ratio of 1.4 between the woven filter fabric and the sand. On the test section, the filter fabric was buried at both the toe and crest of the slope and was held in place by using 1-ft-long steel pins fitted with 1-in.-diam caps. The initial tests on Plan 5 resulted in sand leaching between the filter fabric and the flume walls; therefore, the sides of the filter fabric were sealed to the flume walls with silicone sealer for both the static differential head and drawdown tests (Figure 20a). For the wave-stability tests, wooden strips were installed along the sides of the streambank and the filter fabric was stapled to the strips as well as being sealed to the walls with silicone sealer (Figure 20b). The wooden strips and staples were necessary to keep from breaking the silicone seals at the flume walls. The plan where the woven filter fabric was sealed to the flume walls was referred to as Plan 5A.

19. Plan 5B, Figures 21 and 24, was a protected sand streambank. Plan 5B was identical with Plan 5A except for the increased riprap-layer thickness of 1.0 ft used in Plan 5B.

20. Plan 6, Figures 25 and 28, was a protected sand streambank identical with Plan 5A except for the nonwoven, or random mesh, filter fabric that was used in Plan 6. The nonwoven filter fabric was installed in the same manner as described in paragraph 18 and Figures 20a and 20b. The nonwoven filter fabric had an EOS of 50. From Equation 8

$$\frac{D_{85}^{\text{Soil}}}{\text{EOS } 50} = \frac{0.38 \text{ mm}}{0.297 \text{ mm}} = 1.28 > 1.0$$

and the gradient ratio for the nonwoven filter fabric was 1.4.

21. Plan 6A, Figures 26 and 29, was a protected sand streambank. Plan 6A was identical with Plan 6 except for the increased riprap-layer thickness of 1.0 ft used in Plan 6A.

22. Plan 6B, Figures 27 and 30, was a protected sand streambank identical with Plan 6A except for the 2-in.-thick layer of sand placed between the riprap and filter fabric in Plan 6B. In the prototype, a layer of sand is often placed over the filter fabric to help prevent tearing or puncturing of the filter fabric during the riprap placement.

23. Plan 7, Figures 31 and 33, was an unprotected sand streambank. The streambank was 4 ft high, had a crown width of 3.5 ft, and had side slopes of 1V on 1.6H on both the streamside and the landside of the structure. This plan was tested prior to the installation of the porous bulkhead support used on the landside of all other plans.

24. Plan 8, Figures 32 and 34, was a protected sand streambank. The sand streambank was identical with Plan 1. The streamside face was protected by riprap-filled cells. The cells were constructed of 3/4-in. marine plywood (in the prototype, the cells could be fabricated of timbers, concrete, plastics, etc.) and consisted of twelve 1-cu-ft chambers. The cells were placed from the toe to an elevation of 3.2 ft and filled with the same size riprap as had been used on previous plans with riprap protection. The area below the toe of the cells was constructed with the same size riprap. No filter was used between the riprap-filled cells and the sand. Previous model tests of the riprap-filled cells were conducted at a 1:4 scale for a range of wave heights, wave periods,

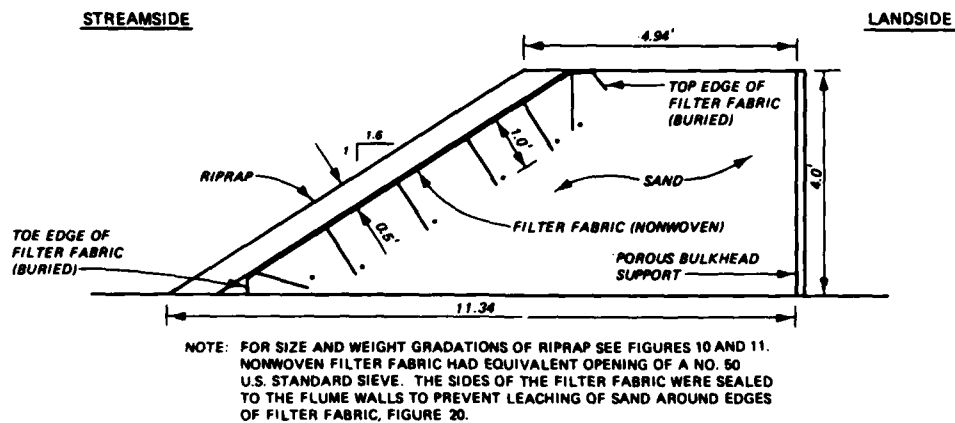


Figure 25. Plan 6, sand streambank with 0.5 ft of riprap and nonwoven filter fabric protection

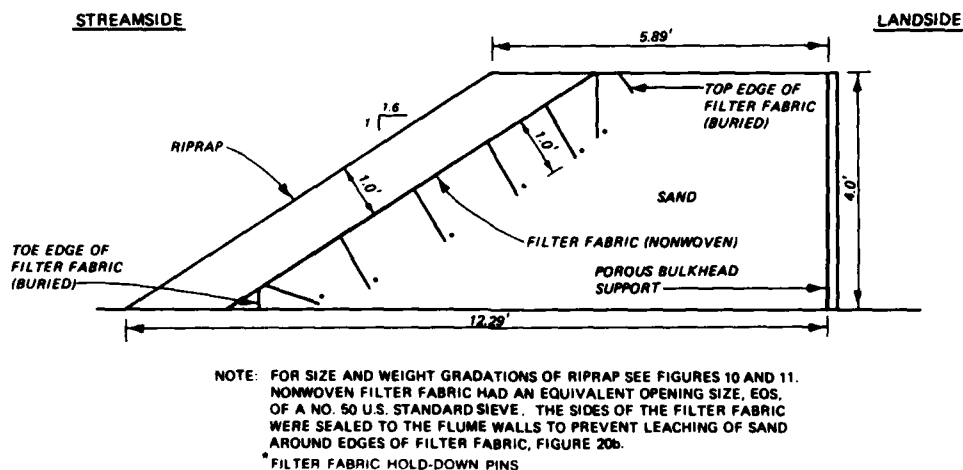


Figure 26. Plan 6A, sand streambank with 1.0 ft of riprap and nonwoven filter fabric protection

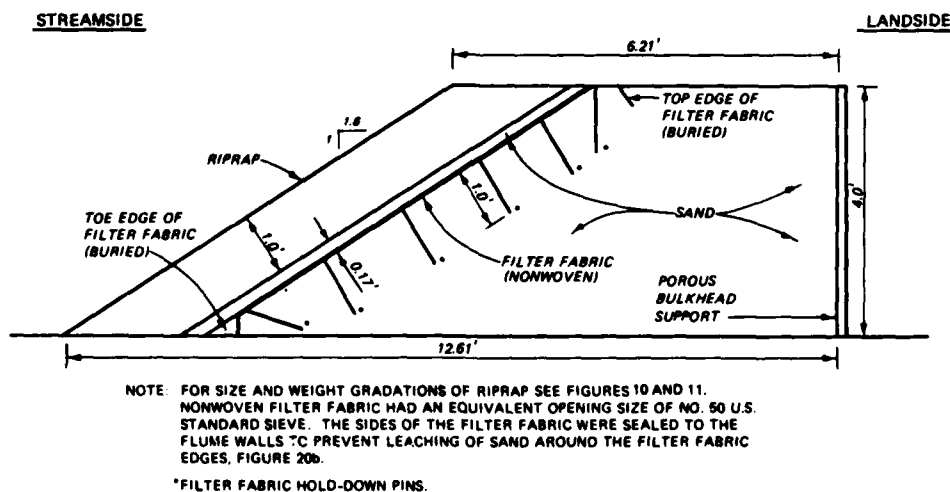


Figure 27. Plan 6B, sand streambank with 1.0 ft of riprap, 0.17 ft of sand and nonwoven filter fabric protection

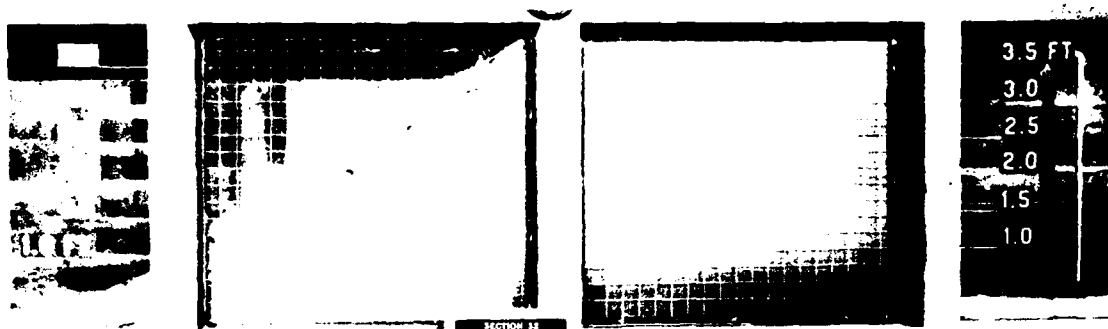


Figure 28. Plan 6

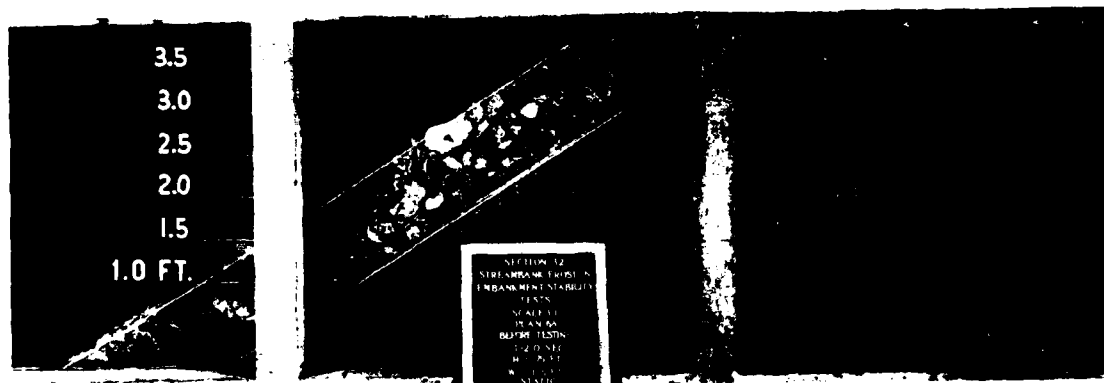


Figure 29. Plan 6A

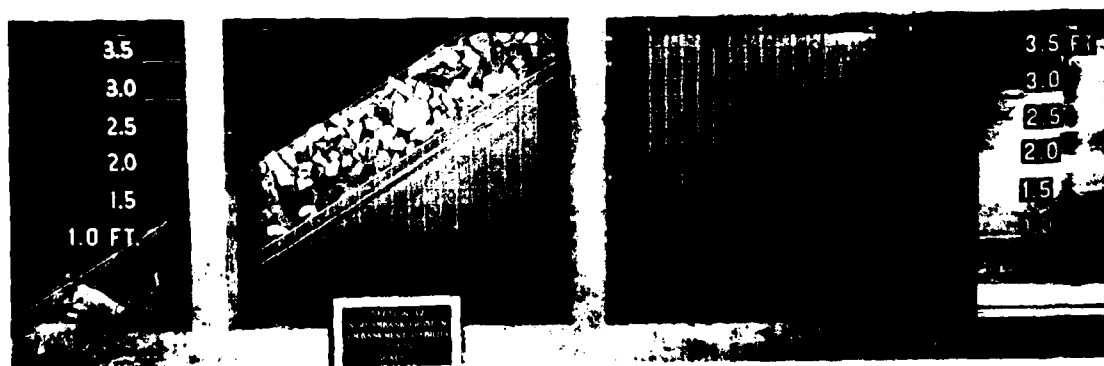


Figure 30. Plan 6B

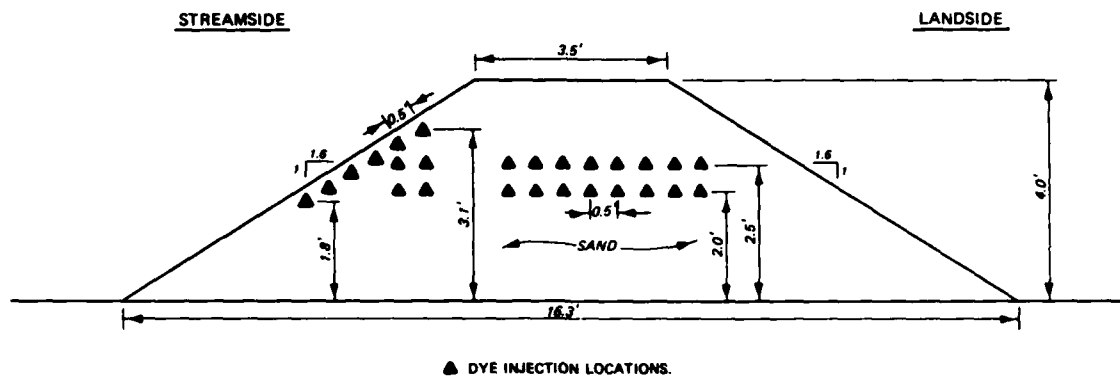


Figure 31. Plan 7, unprotected sand streambank

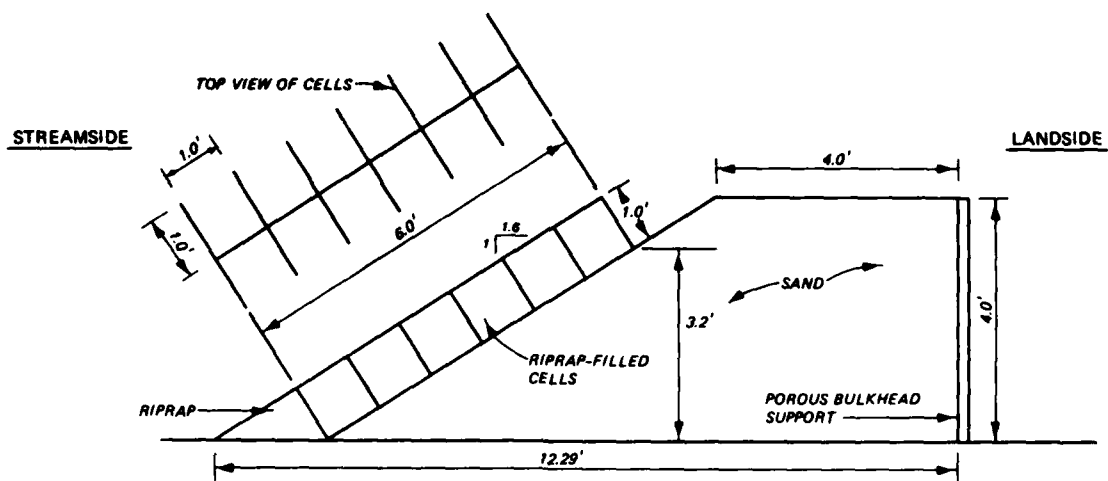


Figure 32. Plan 8, sand streambank with riprap-filled cells protection

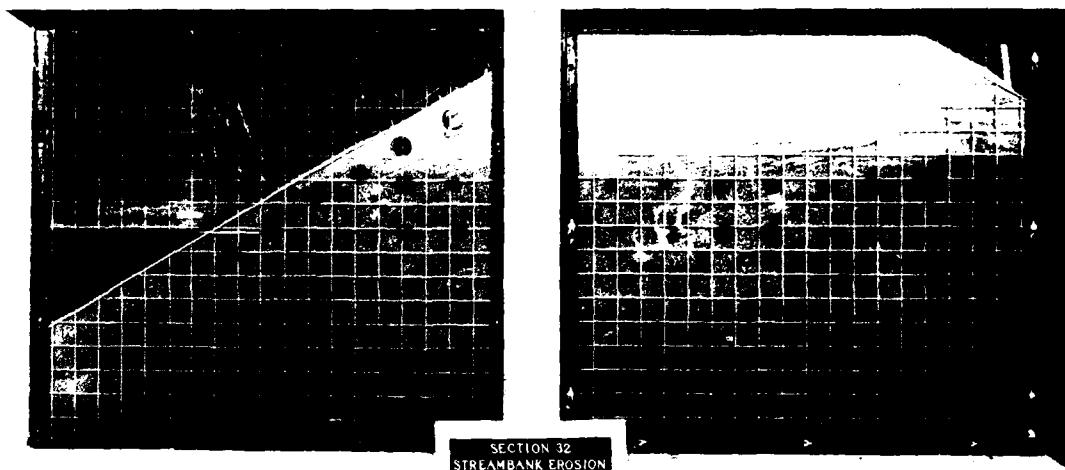


Figure 33. Plan 7

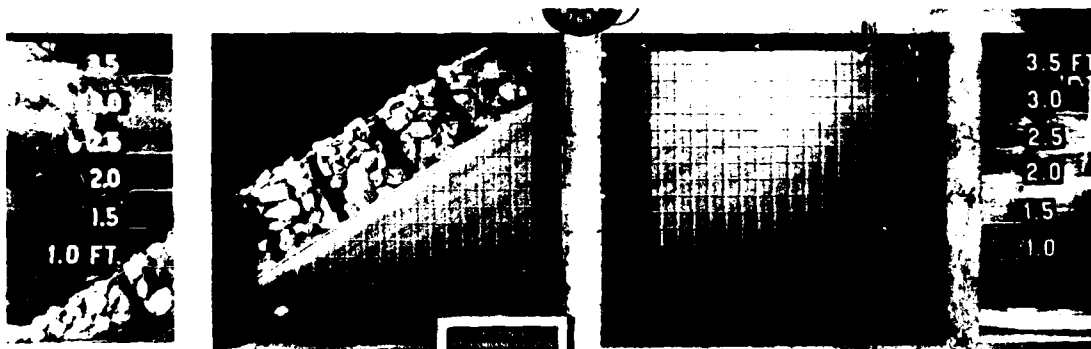


Figure 34. Plan 8

and angles of wave attack and the results are reported in Appendix B-8.

25. Plan 8A, Figures 35-37 and 40, was a protected sand streambank. Plan 8A was identical with Plan 8 except for the material used to fill the cells and the area below the toe of the cells. A gravel mix ranging in size from 1 in. to 1/2 in. (Figure 35) and in weight from 0.16 lb to 0.013 lb (Figure 36) was used in Plan 8A. Like Plan 8, no filter was placed between the cells and the sand.

26. Plan 8B, Figures 38 and 41, was a protected sand streambank. Plan 8B was identical with Plan 8A except for the 0.1-ft-thick layer of granular filter material that was placed between the gravel-filled cells and the streambank in Plan 8B. The filter size and gradation were calculated using the methods and design criteria discussed in paragraph 14. The calculations showed that a one-layer granular filter should be adequate. Filter A (Figures 10 and 12) fit well within the upper and lower limits of the size and gradation of the filter needed. This is the same filter that was used in Plans 3 and 3A. The filter layer thickness was arbitrarily set at 0.1 ft. This thickness was still well below the 9-in. minimum specified in the design criteria. It was felt that if this thickness proved adequate, then the 9-in. minimum thickness recommended for the prototype structures should be adequate.

27. Plan 8C, Figures 39 and 42, was a protected sand streambank. Plan 8C was identical with Plan 8B except for the nonwoven filter fabric that was used in place of the granular filter layer. The nonwoven filter fabric was identical with the fabric used in Plans 6, 6A, and 6B.

Static Differential Head Tests

28. The differential head tests consisted of maintaining constant, but different, water levels on the landside and the streamside of the streambank. A streamside water depth of 1.0 ft was used for all tests, and landside water depths of 1.5, 2.0, 2.95, and 3.0 ft were used to produce differential heads across the streambank of 0.5, 1.0, 1.95, and 2.0 ft, respectively.

29. Plan 1 was subjected to a differential head of 0.5 ft.

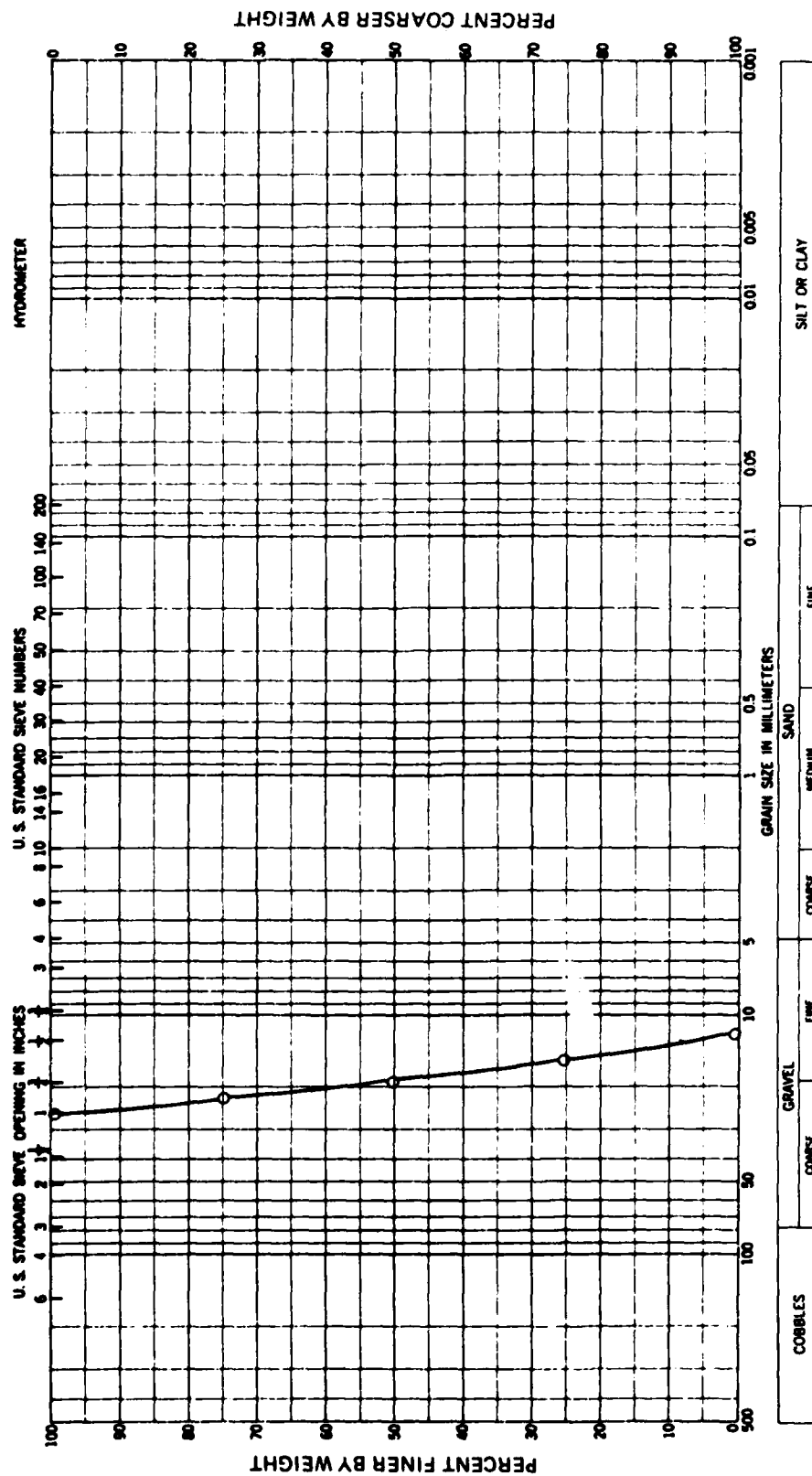


Figure 35. Size gradation curve for gravel mix

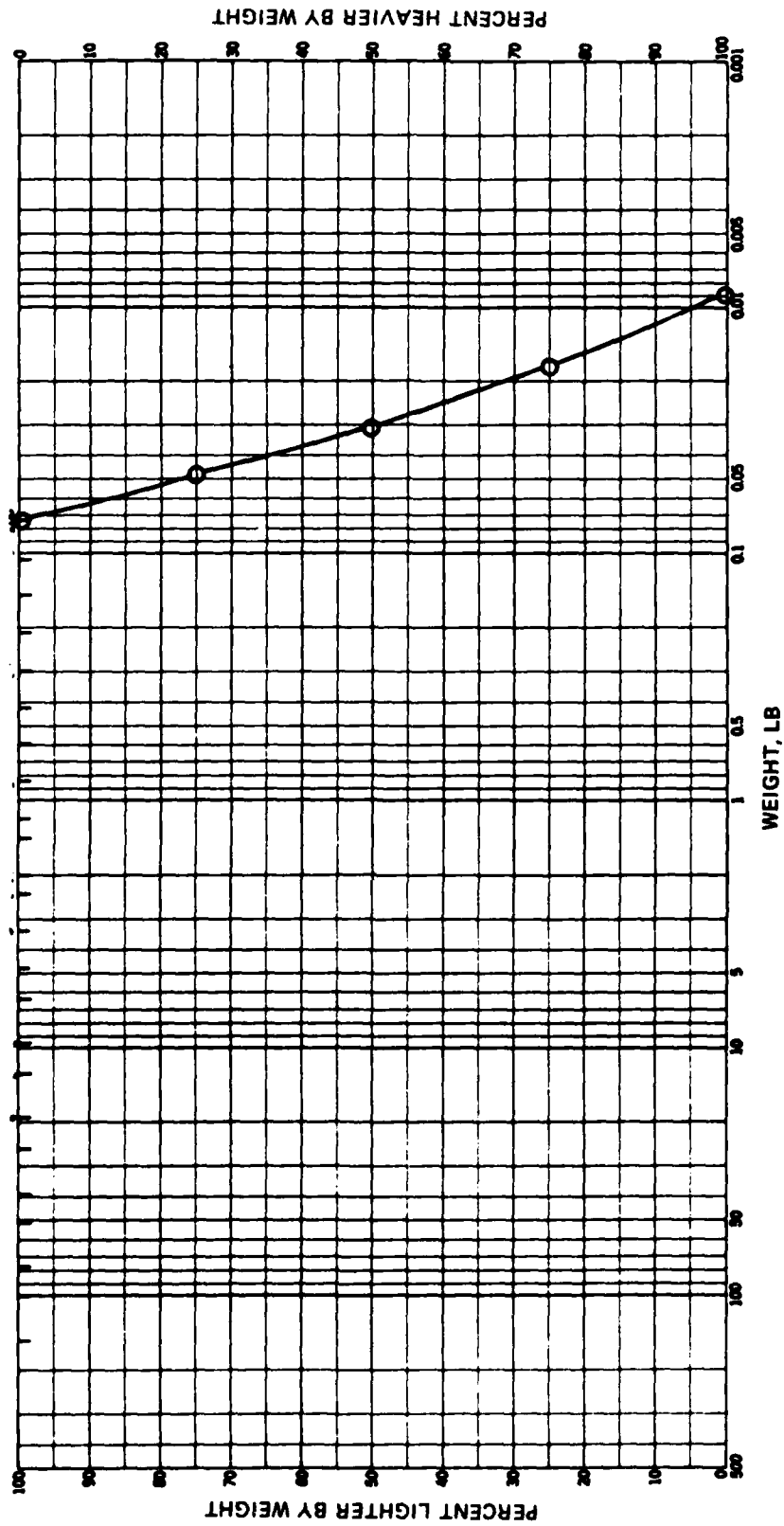


Figure 36. Weight gradation curve for gravel mix

Figure 43 shows Plan 1 at the start of the test. The streambank showed a slight instability at and slightly above the swl but the damage in this area was progressing at a very slow rate. After 48 hr of testing, the damage to the slope was progressing at such a slow rate that it was hard to distinguish any change in the slope over a period of several hours. The test was stopped at 48 hr and the damage to the slope is shown in Figure 44.

30. Plan 1 was rebuilt and Figure 45 shows the streambank at the start of the 1.0-ft-static differential head test. The damage to the slope became progressively worse as the test proceeded and had not stabilized when the test was stopped after 461 hr (about 19 days). Figure 46 shows conditions at the end of the test; Figure 47 shows the condition of the streambank slope at intervals throughout the test.

31. Plan 1 was not rebuilt after the 1.0-ft-static differential head test; the landside water depth was increased to 3.0 ft and the already damaged streambank was subjected to a 2.0-ft static differential head. The erosion of the slope occurred in the same manner but at a faster rate than had occurred with the 1.0-ft static differential head. After 252 hr (10.5 days) of erosion induced by the 2.0-ft differential head, the streambank had totally failed. Between hours 250 and 252, the landside water breached the crown of the streambank, allowing free flow of water over the streambank. Figures 48 and 49 show the condition of the streambank at 5 days and 10 days during the test.

32. Plan 2 was exposed to a 1.95-ft static differential head. The 1V-on-4H slope eroded to a slope equivalent to the hydraulic grade line during the first 85 min of the test (Figure 50). This occurred by progressive head cutting and erosion of the slope that proceeded from the toe to the crown of the structure. Once the head cutting reached the crown of the streambank, the landside water breached the crown and within 6 min the streambank had eroded to the condition shown in Figure 51.

33. Plan 3 was exposed to a static differential head of 2.0 ft. Figure 52 shows the streambank at the start of the test. The riprap protection, granular filter layers, and sand streambank were

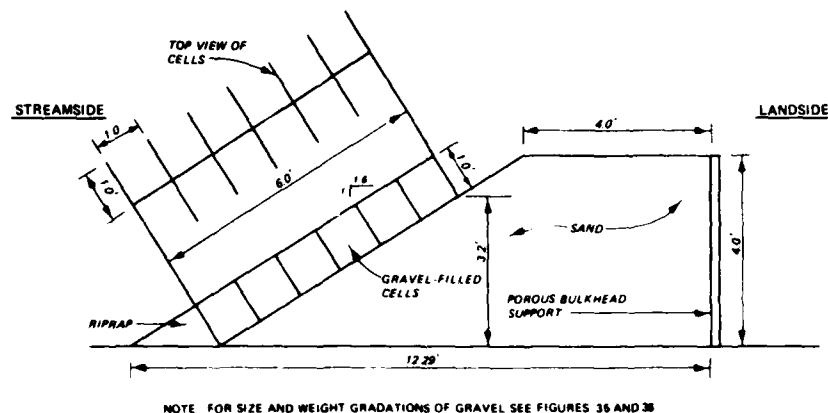


Figure 37. Plan 8A, sand streambank with gravel-filled cells protection

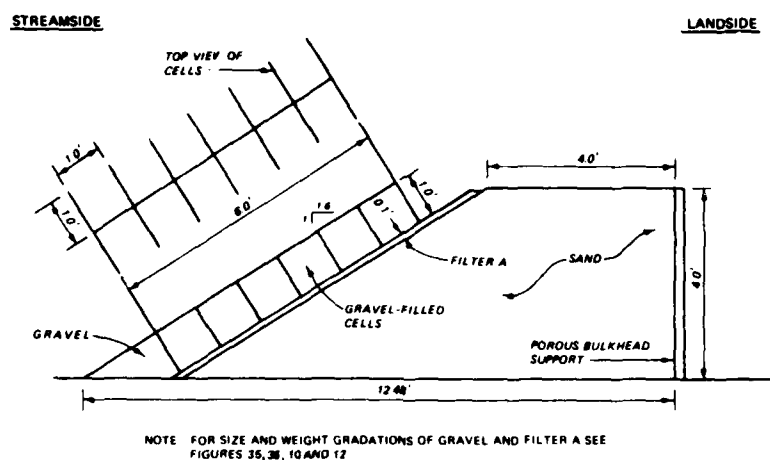


Figure 38. Plan 8B, sand streambank with gravel-filled cells and filter (one well-graded rock layer) protection

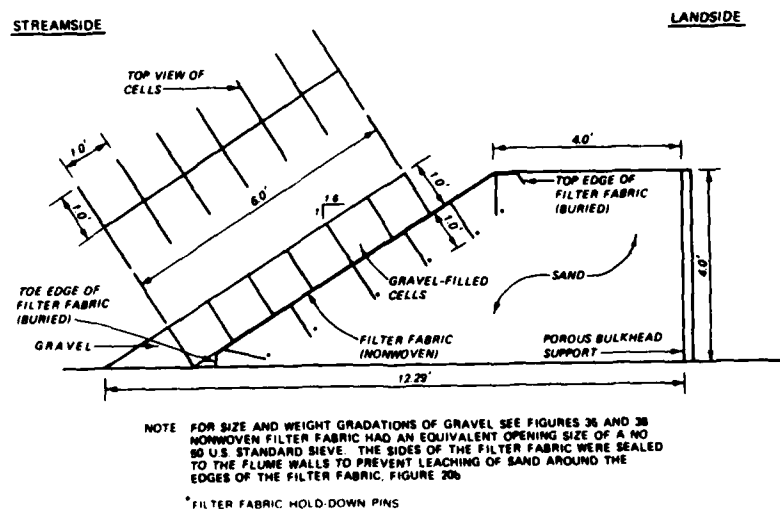


Figure 39. Plan 8C, sand streambank with gravel-filled cells and nonwoven filter fabric protection



Figure 40. Plan 8A

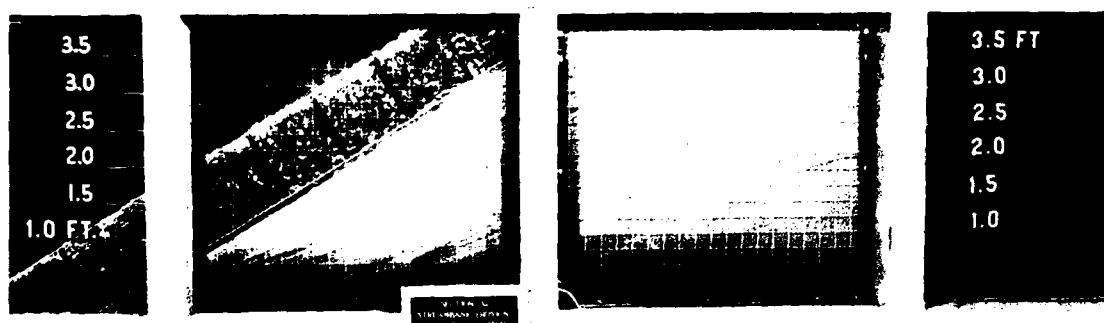


Figure 41. Plan 8B



Figure 42. Plan 8C

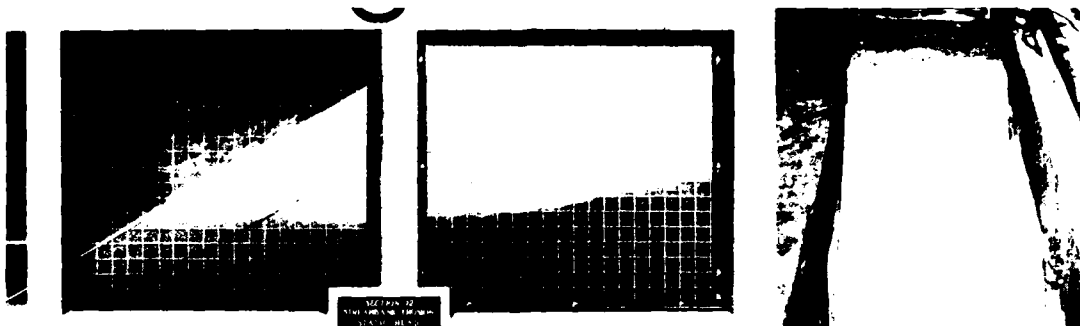


Figure 43. Plan 1, at start of the 0.5-ft static differential head test



Figure 44. Plan 1, after the 0.5-ft static differential head test





Figure 45. Plan 1, at start of the 1.0-ft static differential head test



Figure 46. Plan 1, after the 1.0-ft static differential head test



d. 11 days

e. 14 days

f. 17 days

Figure 47. Plan 1, at various times throughout the
1.0-ft static differential head test



Figure 48. Plan 1, after 5 days of the 2.0-ft static differential head test

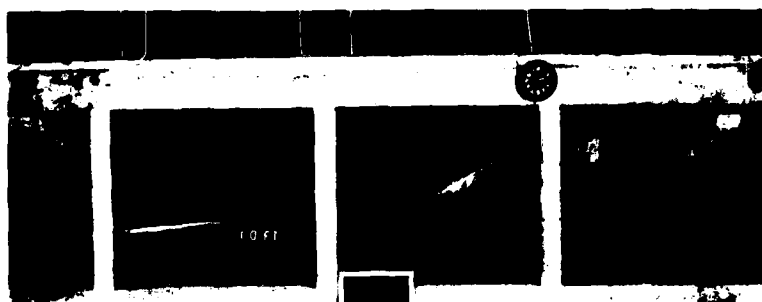


Figure 49. Plan 1, after 10 days of the 2.0-ft static differential head test



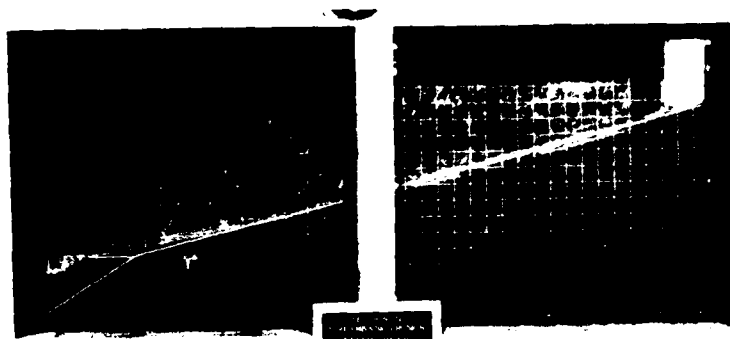


Figure 50. Plan 2, after 85 min of the 1.95-ft static differential head test

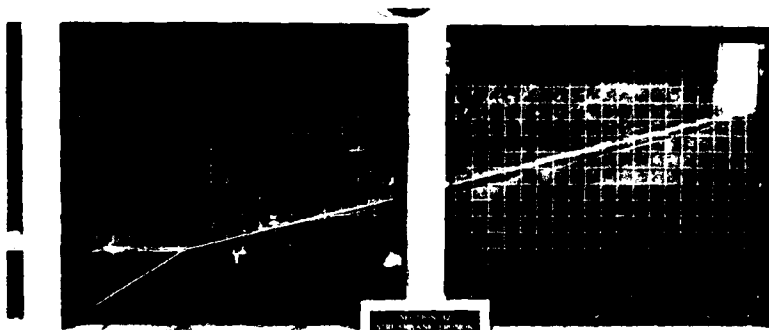


Figure 51. Plan 2, after 91 min of the 1.95-ft static differential head test, end of test

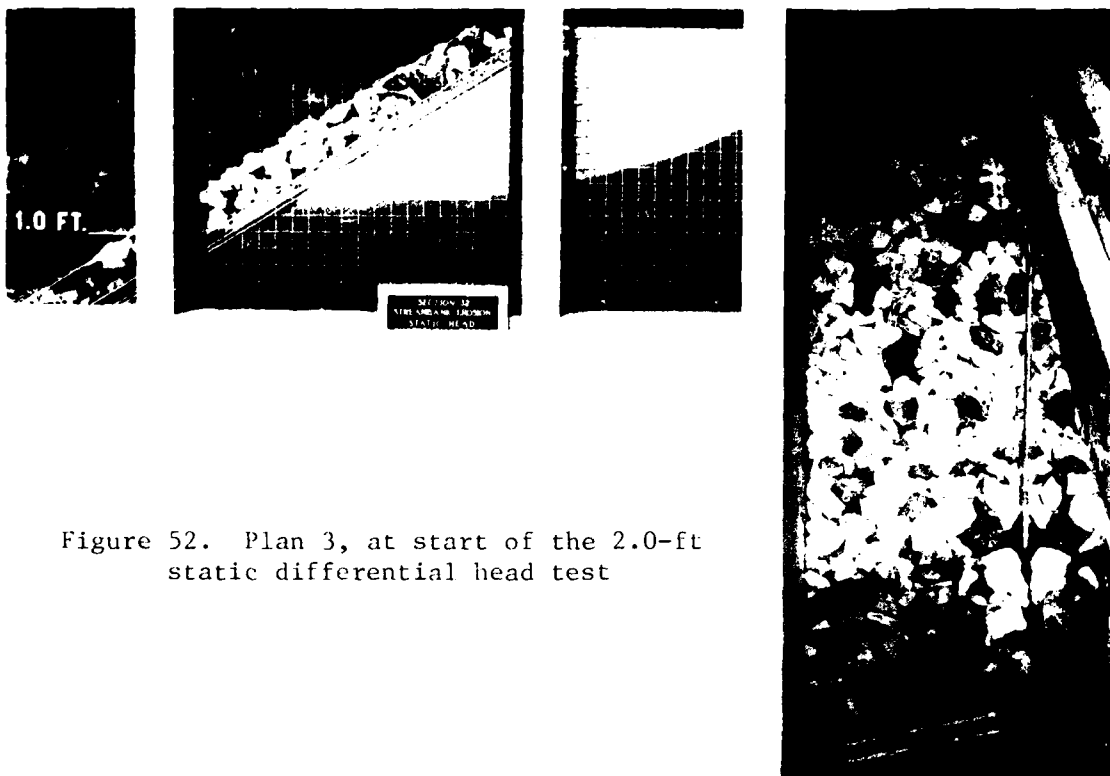


Figure 52. Plan 3, at start of the 2.0-ft static differential head test

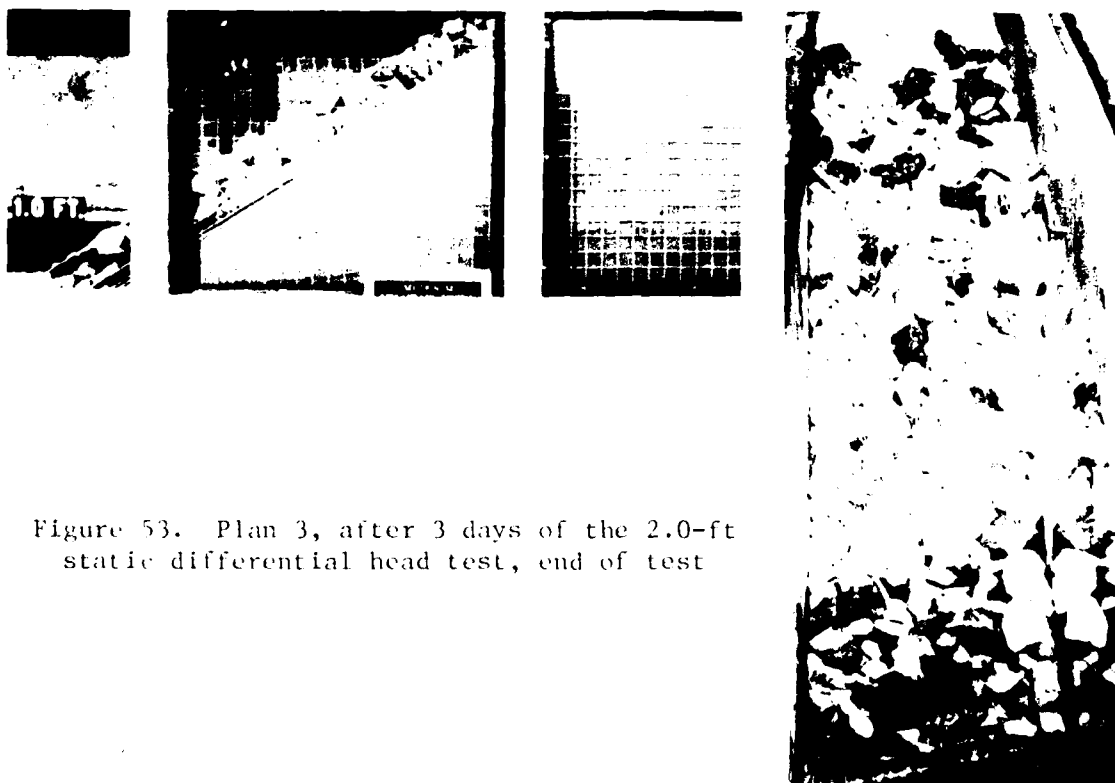


Figure 53. Plan 3, after 3 days of the 2.0-ft static differential head test, end of test

unquestionably stable under the seepage flow produced by the 2.0-ft static differential head and the test was stopped after 3 days. Figure 53 shows Plan 3 at the end of the test.

Tests of Drawdown Followed by Static Differential Head

34. Drawdowns followed by static differential head tests were conducted by starting with landside and streamside water depths of 3.5 ft. The streamside water depth was dropped to 0.5 ft at a rate of either 2.0, 4.0, or 30.0 ft/hr while the landside water depth was maintained at 3.5 ft. These ending landside and streamside water depths were maintained for a sufficient amount of time to see if the 3.0-ft static differential head would continue to cause or would initiate failure of the plan being tested.

35. Plan 1 was exposed to drawdown rates of 2.0, 4.0, and 30.0 ft/hr followed by 20 min of 3.0-ft static differential head. The sand streambank was rebuilt between each testing. The unprotected sand streambank failed at all of the drawdown rates, and continued to fail throughout the static differential head portion of each of the tests. Figures 54, 55, and 56 show Plan 1 before, at various times throughout, and at the end of the 2.0, 4.0, and 30.0 ft/hr drawdown tests, respectively. As shown in the photographs, the streambank failure rate varied with the drawdown rate; but at the end of all the drawdown and static differential head tests, the streambank profiles were almost identical. The eroded portion of the bank, above the streamside water elevation, had degraded to a slope that was very close to the slope of the hydraulic grade line through the streambanks.

36. Plan 3 was exposed to drawdown rates of 2.0, 4.0, and 30.0 ft/hr followed by 1.0 hr of 3.0-ft static differential head. Figure 57 shows Plan 3 before testing the drawdown rate of 2.0 ft/hr. As shown in Figure 58 the riprap, filter layers, and sand streambank showed no instability at the end of either the 2.0 ft/hr drawdown or the 3.0-ft static differential head, respectively. The test section was not rebuilt and the streamside water level was raised to the initial 3.5-ft

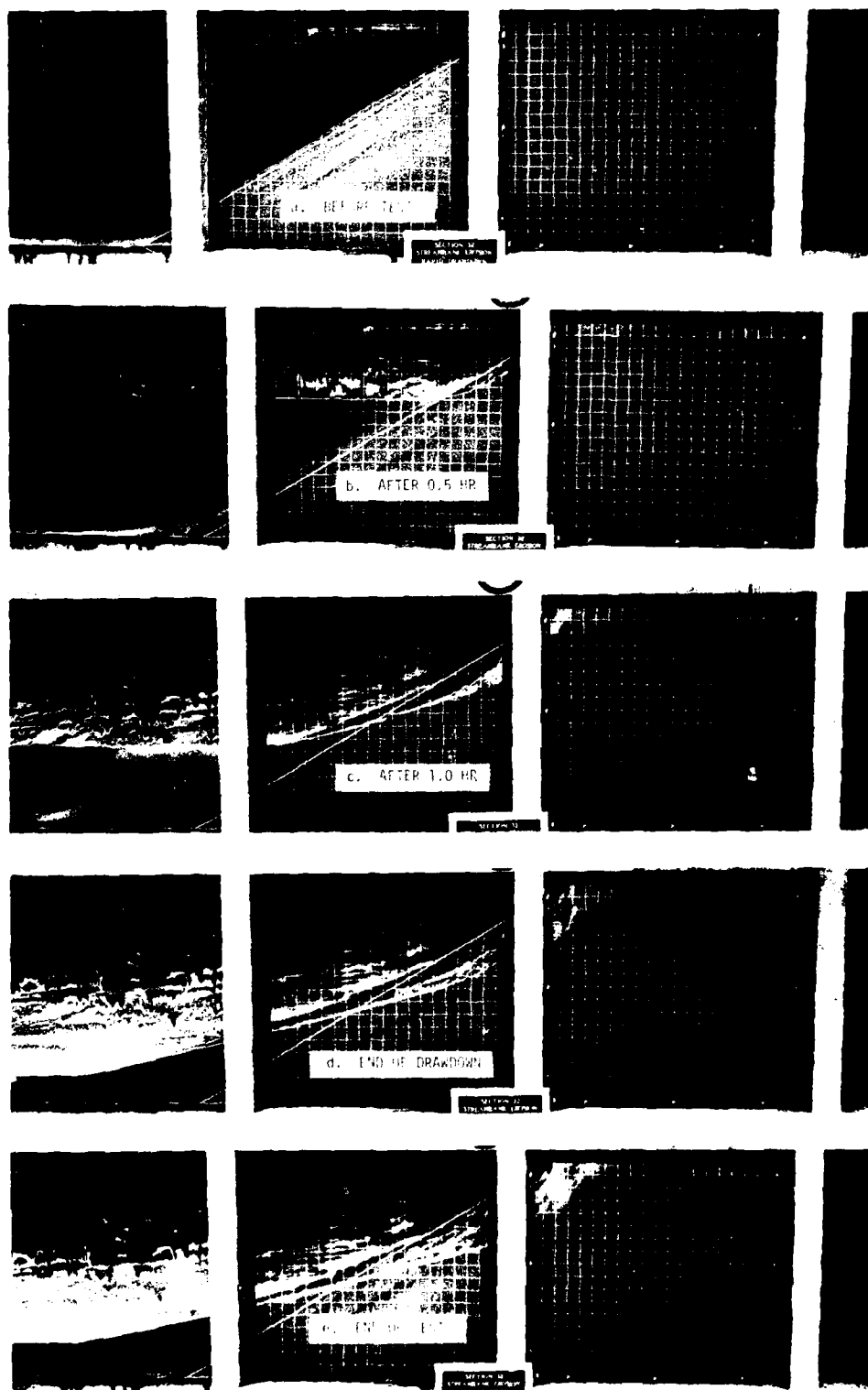


Figure 54. Plan 1, before, at various times during, and at end of the 2.0-ft/hr drawdown test

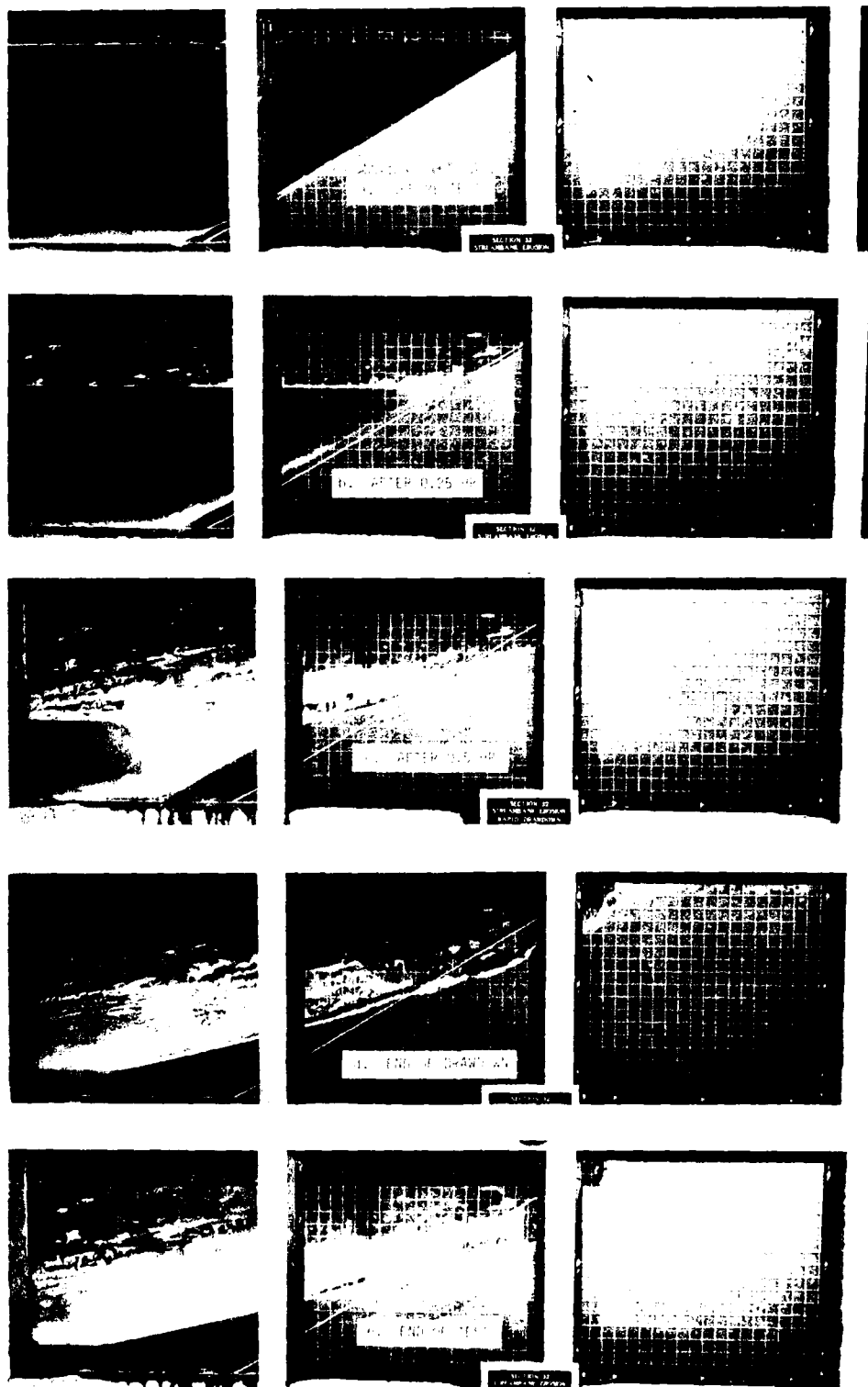


Figure 55. Plan 1, before, at various times during, and at end of the 4.0-ft/hr drawdown test

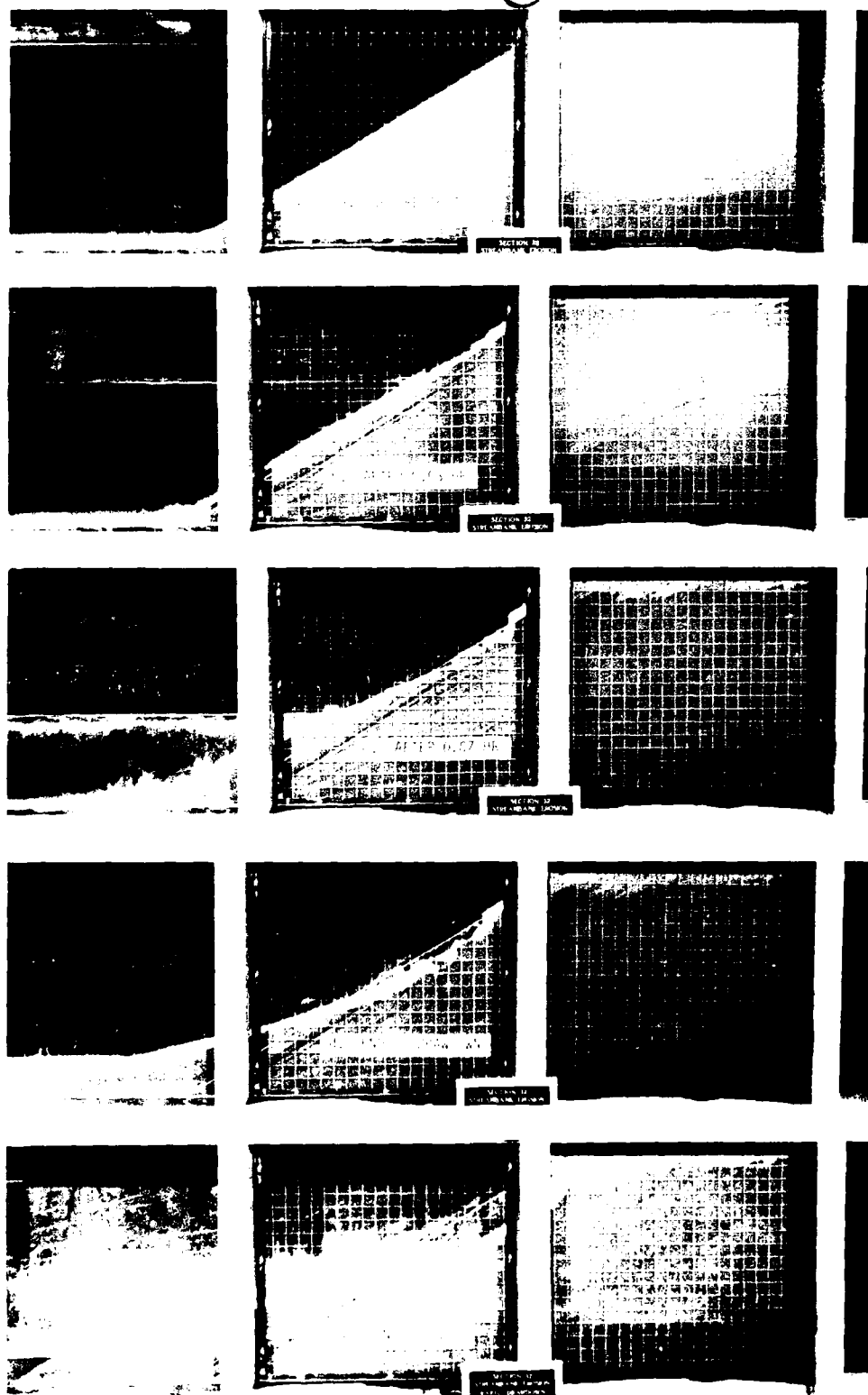


Figure 56. Plan 1, before, at various times during, and at end of the 30.0-ft/hr drawdown test

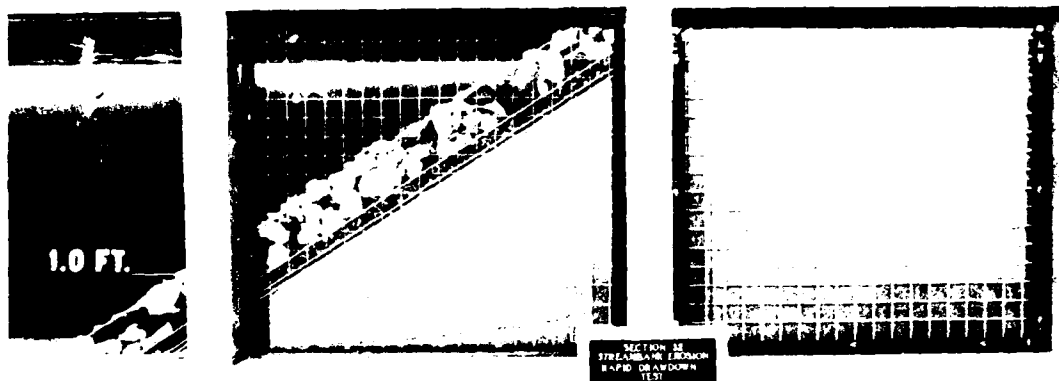


Figure 57. Plan 3, before the 2.0-ft/hr drawdown test

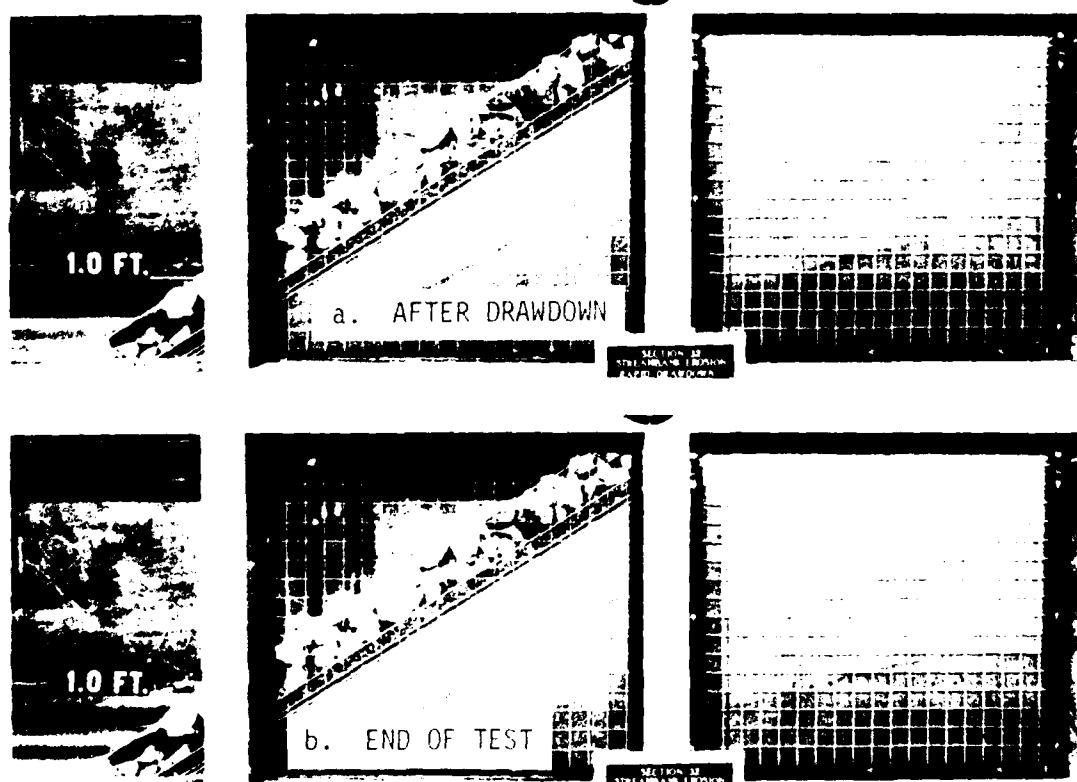


Figure 58. Plan 3, after drawdown and at end of the 2.0-ft/hr drawdown test

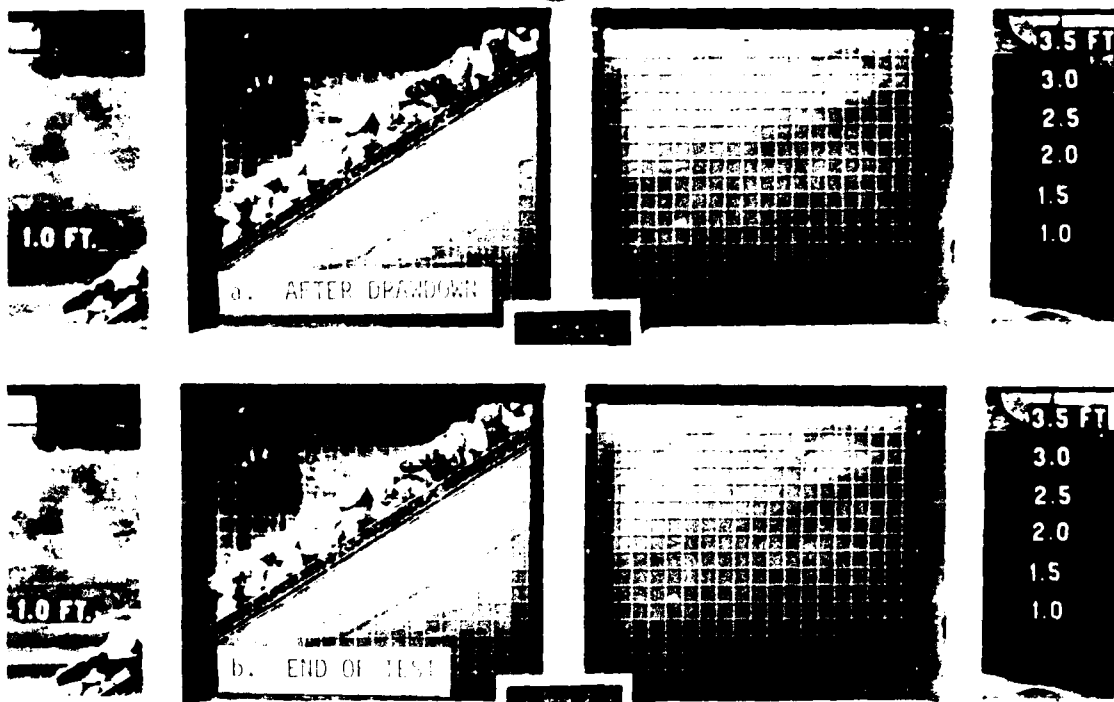


Figure 59. Plan 3, after drawdown and at end of the 4.0-ft/hr drawdown test

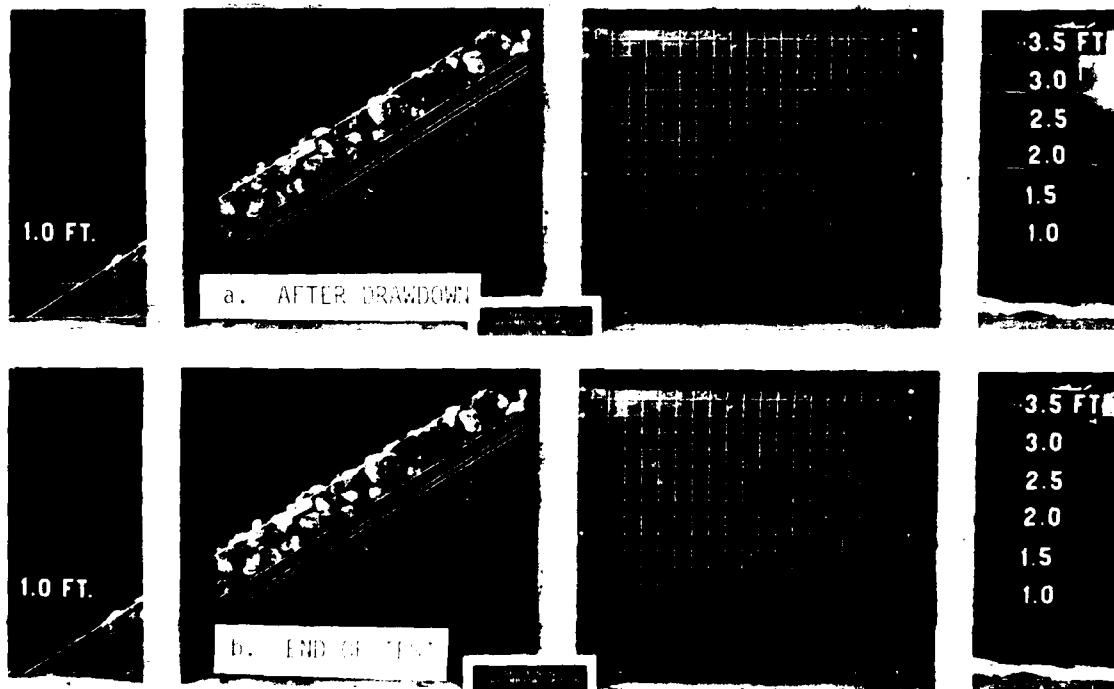


Figure 60. Plan 3, after drawdown and at end of the 30.0-ft/hr drawdown test

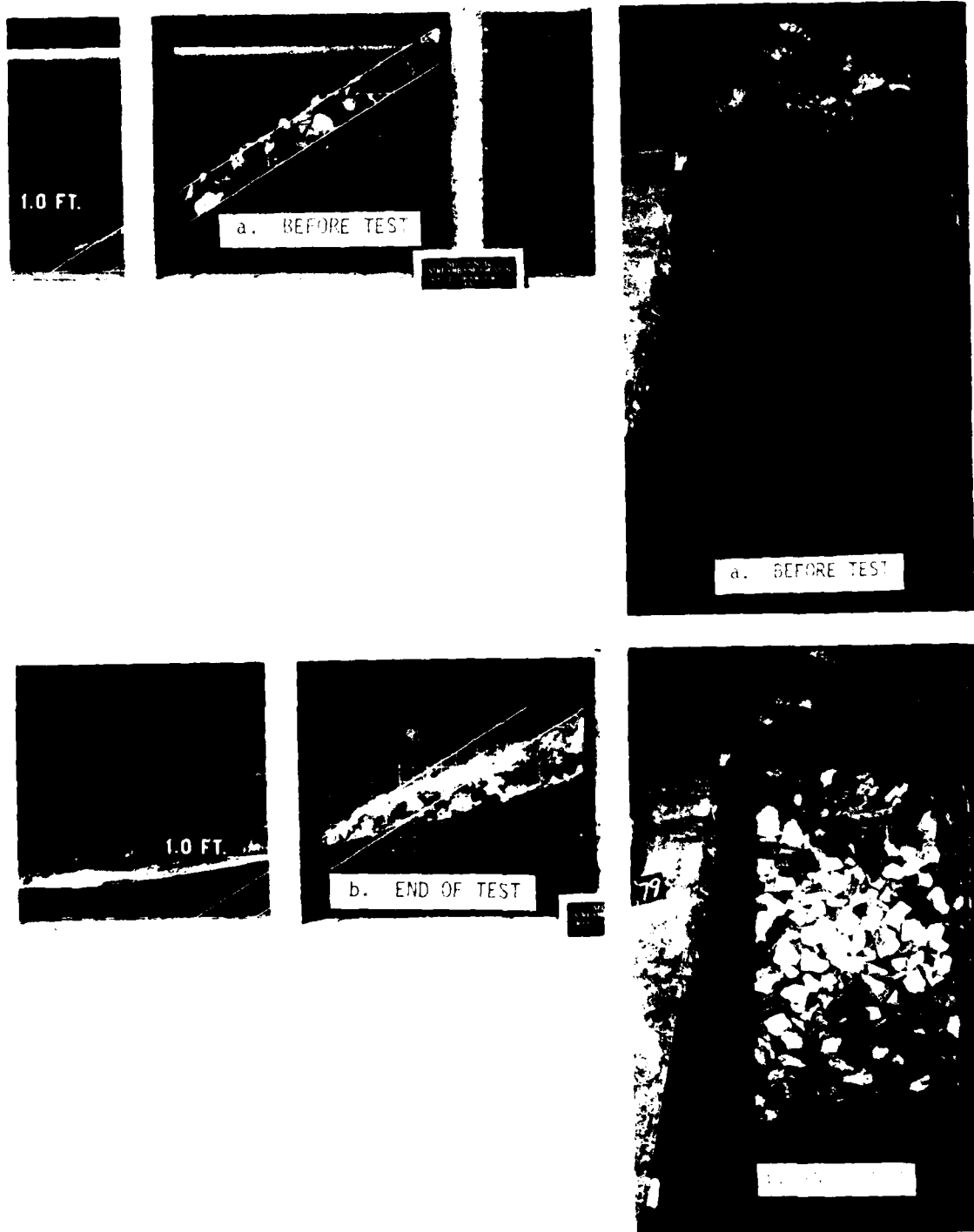


Figure 61. Plan 4, before and at end of the 2.0-ft/hr drawdown test

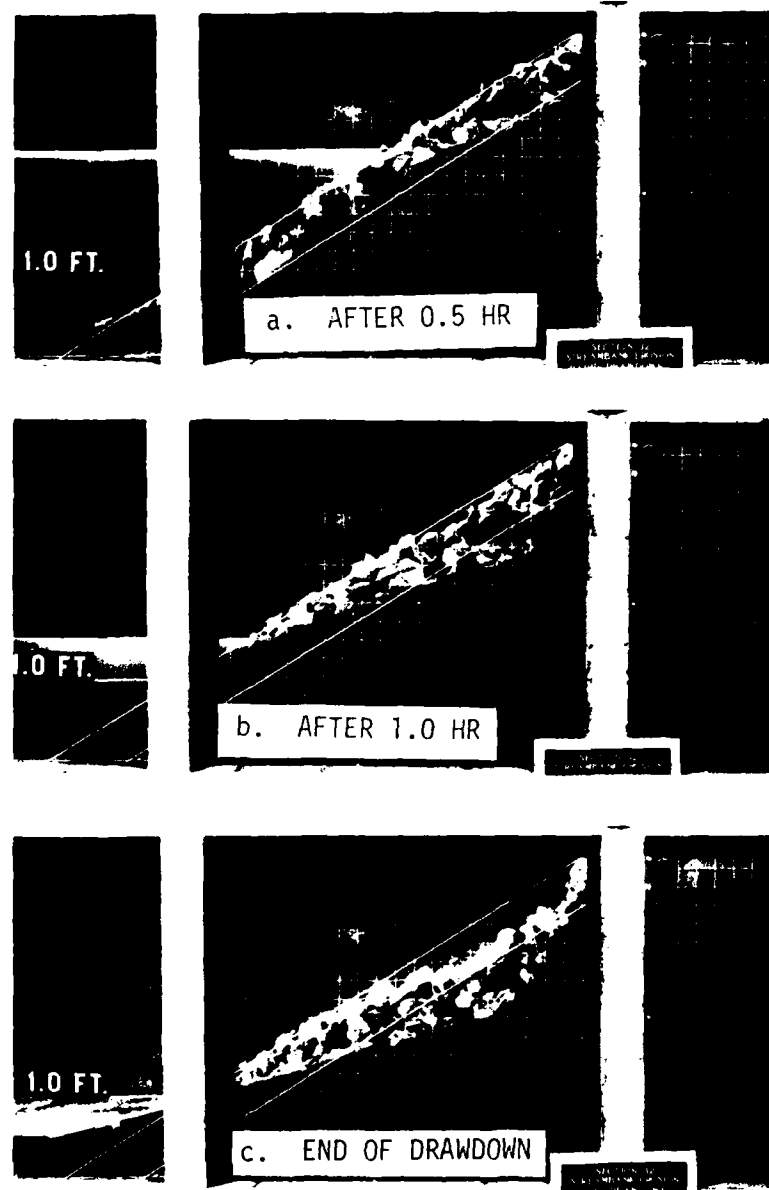


Figure 62. Plan 4, at various times during the 2.0-ft/hr drawdown test

depth and the plan was exposed to a 4.0-ft/hr drawdown rate followed by 1.0 hr of 3.0-ft static differential head. Plan 3 showed no instability at the end of either the drawdown or static differential head tests, as evident in Figure 59. The streamside water level was raised to the 3.5-ft depth and Plan 3 was exposed to a 30.0-ft/hr drawdown rate followed by 1.0 hr of 3.0-ft static differential head. Figure 60 shows that Plan 3 had accrued no damage at the end of the 30.0-ft/hr drawdown and 3.0-ft static differential head tests.

37. Plan 4 was tested for a drawdown rate of 2.0-ft/hr followed by 1.0 hr of 3.0-ft static differential head. Figure 61a shows Plan 4 before testing. With no filter between the riprap and the sand, the sand leached through the riprap protection during both the drawdown and 3.0-ft static differential head portions of the test. The final condition of Plan 4 (Figure 61b), was very similar to Plan 1 (Figure 54) after the same test conditions. Figure 62 shows the condition of Plan 4 at various times throughout the test. The slopes of both Plans 1 and 4 showed continuing damage throughout the tests and had not stabilized when the tests were stopped. The final slopes on both plans were very close to the slope of the hydraulic grade lines through the structures.

38. Plan 5 was exposed to a 2.0-ft/hr drawdown followed by 1.0 hr of 3.0-ft static differential head. Figure 63a shows Plan 5 before testing. After approximately 1.0 ft of drawdown (0.5 hr of the 2.0-ft/hr drawdown rate), the streambank began to fail due to sand leaching around edges of the woven filter fabric adjacent to the flume wall and viewing window. This failure continued for the remainder of the drawdown test and throughout the 1.0 hr of 3.0-ft static differential head. The rate of failure was much slower than that observed in Plans 1 and 4 when exposed to the same test conditions, but like Plans 1 and 4, the sand streambank of Plan 5 would have completely failed if the 3.0-ft static differential head had been maintained for a sufficient period of time. After-test photographs, Figure 63b, show that a significant amount of sand had leached around the woven filter fabric and had been deposited at the streambank toe.

39. Plan 5A was tested for drawdown rates of 2.0, 4.0, and

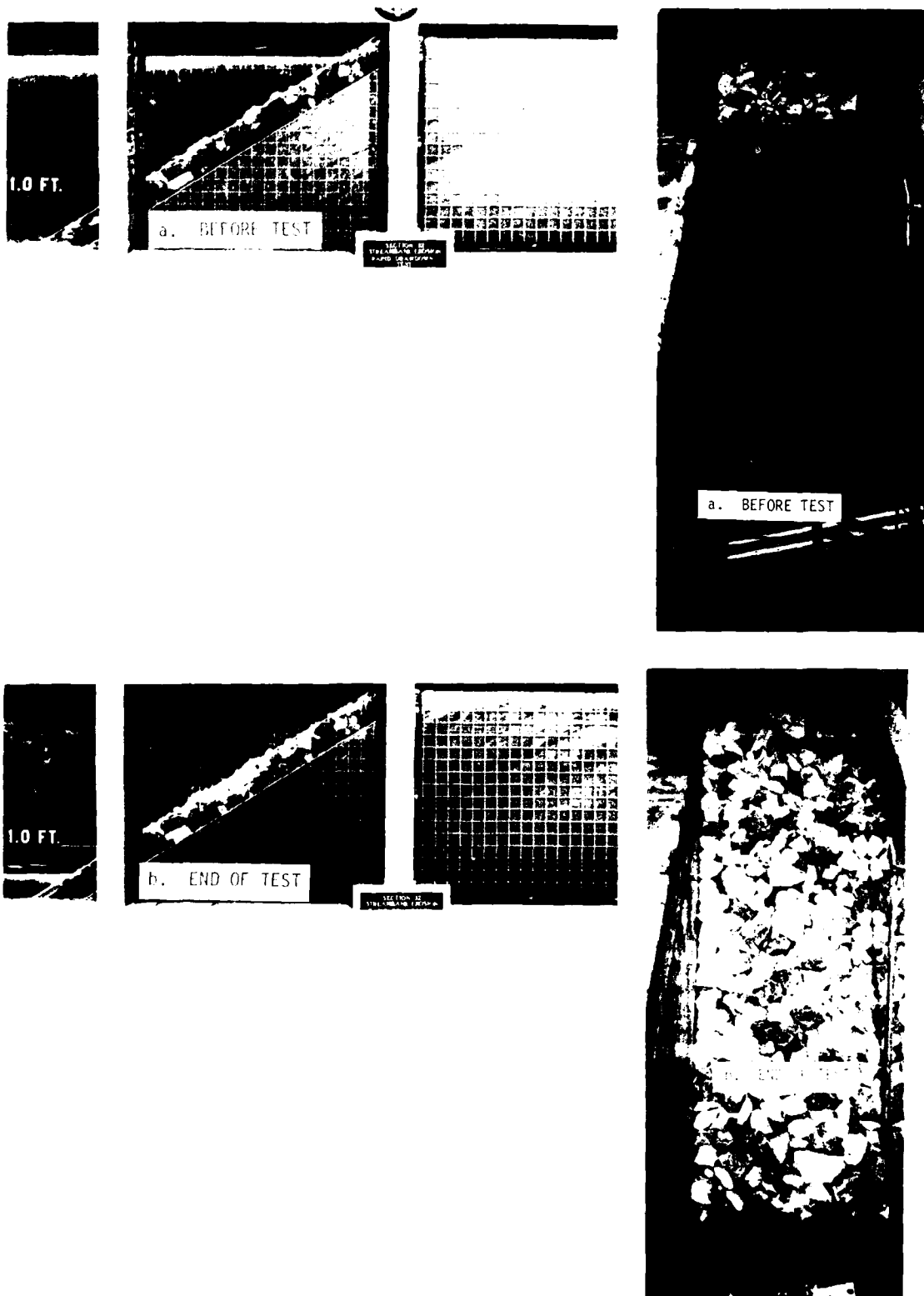


Figure 63. Plan 5, before and at end of the 2.0-ft/hr drawdown test

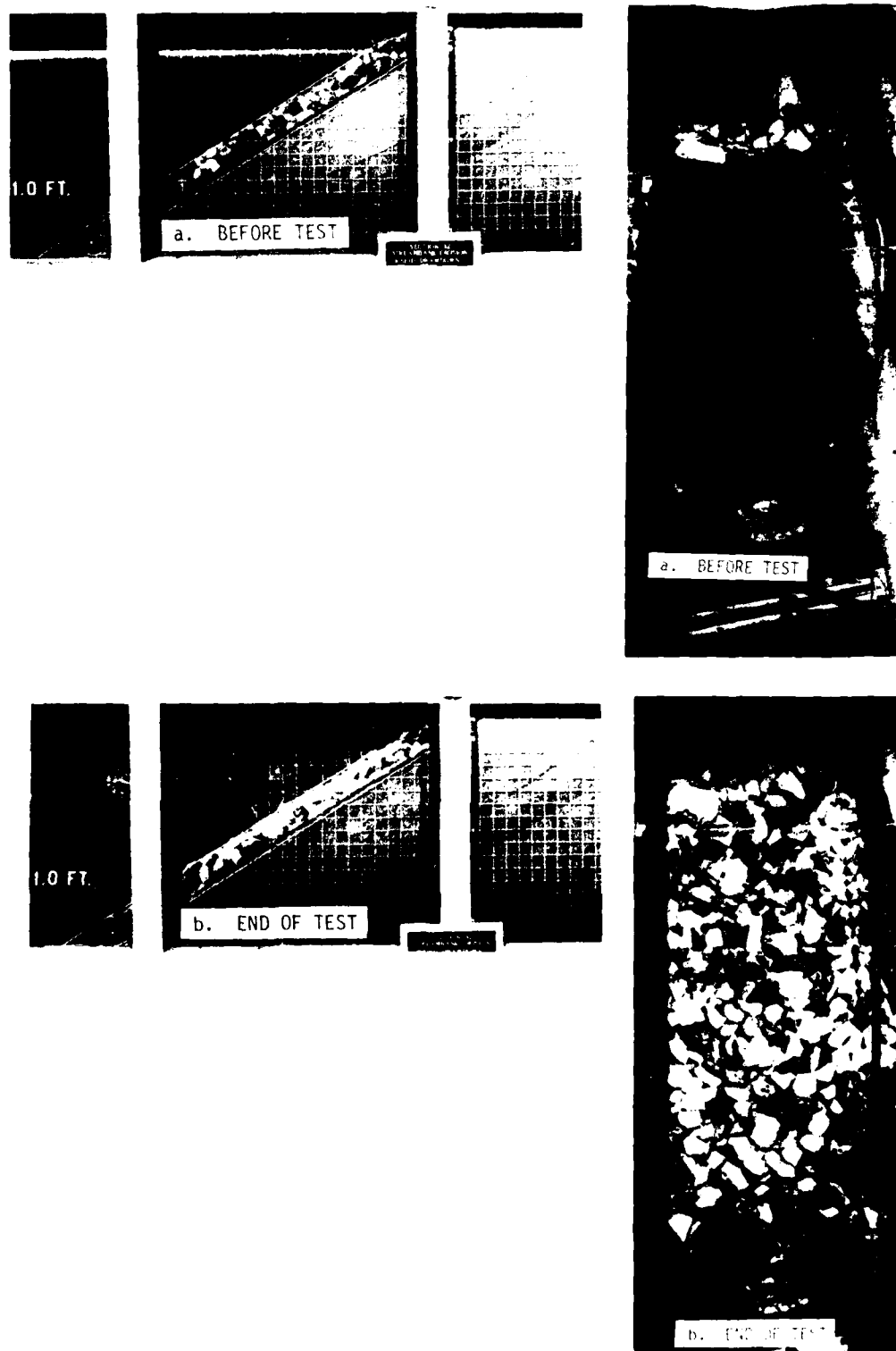


Figure 64. Plan 5A, before and at end of the 2.0-ft/hr drawdown test

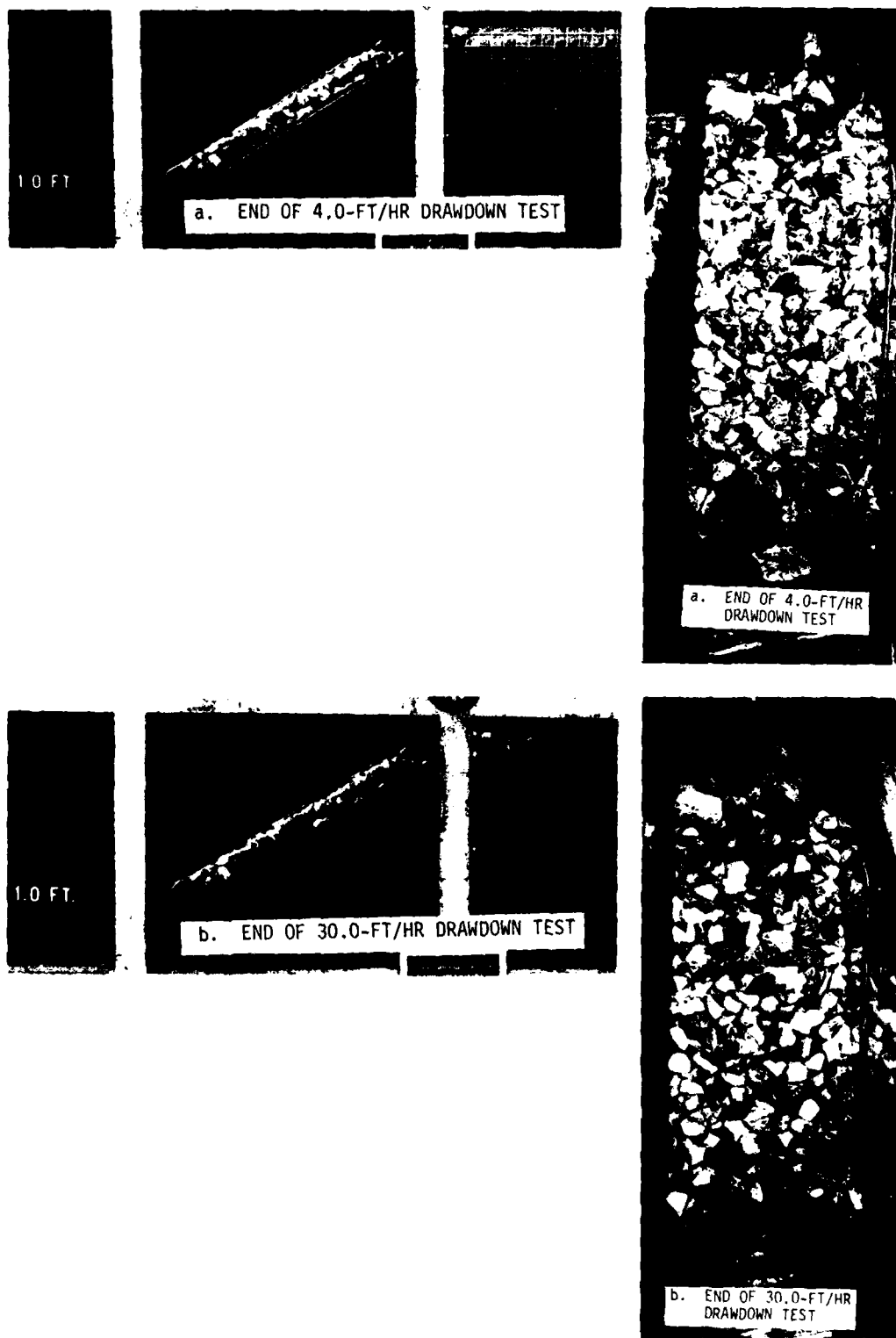


Figure 65. Plan 5A, at end of the 4.0-ft/hr drawdown test and at end of the 30.0-ft/hr drawdown test

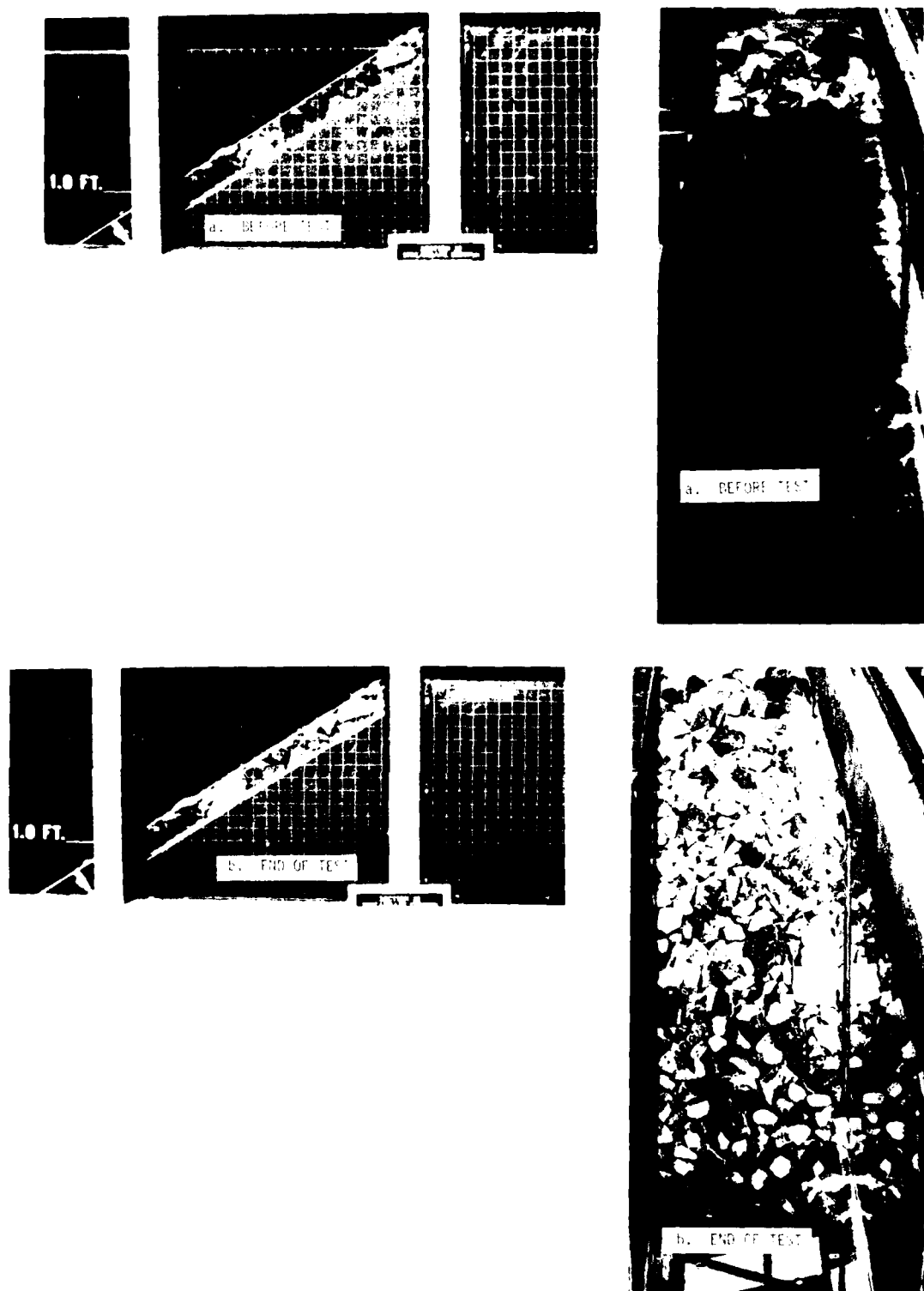


Figure 66. Plan 6, before and at end of the 2.0-ft/hr drawdown test

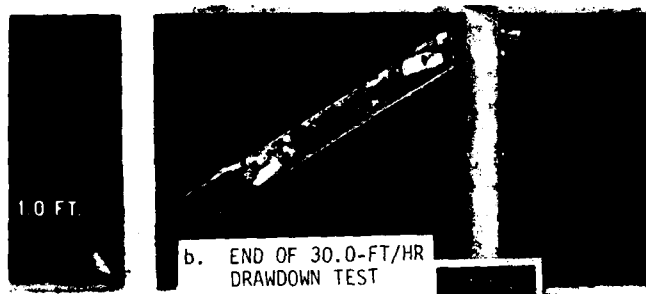
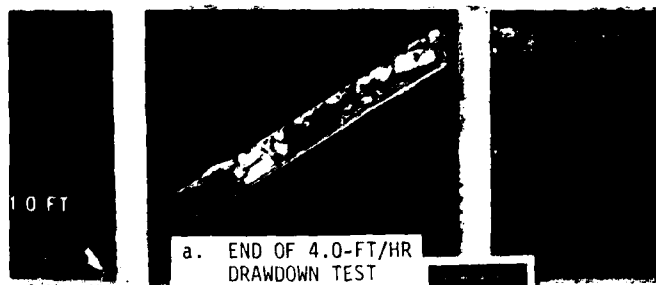


Figure 67. Plan 6, at end of the 4.0-ft/hr drawdown test and
at end of the 30.0-ft/hr drawdown test

30.0 ft/hr, and each drawdown test was followed by 1.0 hr of 3.0-ft static differential head. With the edges of the woven filter fabric sealed to the flume wall and viewing window, as shown in Figure 20a, Plan 5A proved to be totally stable for all the combined drawdown and static differential head tests. The test section was not rebuilt between subsequent tests. Figure 64a shows Plan 5A before testing the 2.0-ft/hr drawdown rate. Figures 64b, 65a, and 65b show Plan 5A after testing each of the combined drawdown and static differential head test conditions.

40. Plan 6 was exposed to drawdown rates of 2.0, 4.0, and 30.0 ft/hr, each of which was followed by 1.0 hr of 3.0-ft static differential head. The nonwoven filter fabric was sealed in the same manner as the woven filter fabric in Plan 5A. No riprap, filter, or stream-bank instability was observed for any of the combined drawdown and static differential head test conditions. The test section was not rebuilt between tests, and Figure 66a shows Plan 6 before the 2.0-ft/hr drawdown test. Figures 66b, 67a, and 67b show Plan 6 after testing each of the combined drawdown and static differential head conditions.

Wave Penetration Tests

41. Plan 7 was exposed to 0.2- to 1.0-ft nonbreaking waves with wave periods ranging from 2.0 to 6.0 sec. Both the landside and stream-side water depths were maintained at 2.0 ft. By injecting dye into the sand streambank, at the points indicated in Figure 31, and then exposing the structure to wave attack, it was possible to get an indication of whether or not these short-period fluctuations in the streamside water-surface elevation could create sufficient differential heads across the streambank and maintain them for a long enough period of time to induce seepage flow in the sand; and also if seepage was induced, does it occur very deep in the streambank.

42. A control test was conducted to see if the dye would show any net movement in any one direction when no wave action was occurring. The landside and streamside water depths were brought up to 2.0 ft and

maintained at that static level. The structure was allowed to stand for 1.0 hr (sufficient time for the water to reach a static capillary rise elevation in the streambank). Dye was injected and the outer perimeters of the dye injection patterns were outlined. After 3.0 hr, though some diffusion of the dye occurred, no net migration of the dye in a given direction had occurred. Thus, it can be concluded that if any net transport of the dye occurs during wave action, this motion can be attributed to seepage flow induced by the short-period fluctuations in the landside water-surface elevation.

43. Four wave penetration tests were conducted (Plan 7 being rebuilt each time) with headwater and tailwater depths of 2.0 ft as shown below:

<u>Test No.</u>	<u>Wave Period sec</u>	<u>Nonbreaking Wave Height ft</u>	<u>Test Time min</u>	<u>Figures</u>
1	6.0	0.25 and 0.50	1.0 and 1.5	68
2	4.0	0.25 and 0.50	1.0 and 1.5	69
3	2.0	0.50 and 1.00	1.0 and 1.5	70
4	2.0	0.20 and 0.40	1.5 and 1.0	71

For each test, the flume was flooded to a 2.0-ft depth and the dye injected in the same manner as described in the control test. After each of these rebuildings and dye injections, the structure was exposed to the nonbreaking wave conditions given above. Before, during, and after test photographs (Figures 68-71) were taken during this test series. These photographs show the high degree of instability inherent in the unprotected sand streambank when exposed to short-period waves. Though it is not obvious in some of the photographs, observations during the test showed that seepage flow is induced by these short-period, nonbreaking waves and that flow occurs up to 4 to 5 ft back into the streambank.

Wave Stability Without a Static Differential Head Across the Streambank

44. Plans 1, 3, 4A, 5A, and 6 were exposed to 2.0- and 4.0-sec, 0.70-ft and/or 2.0-sec, 0.75-ft nonbreaking waves without a static

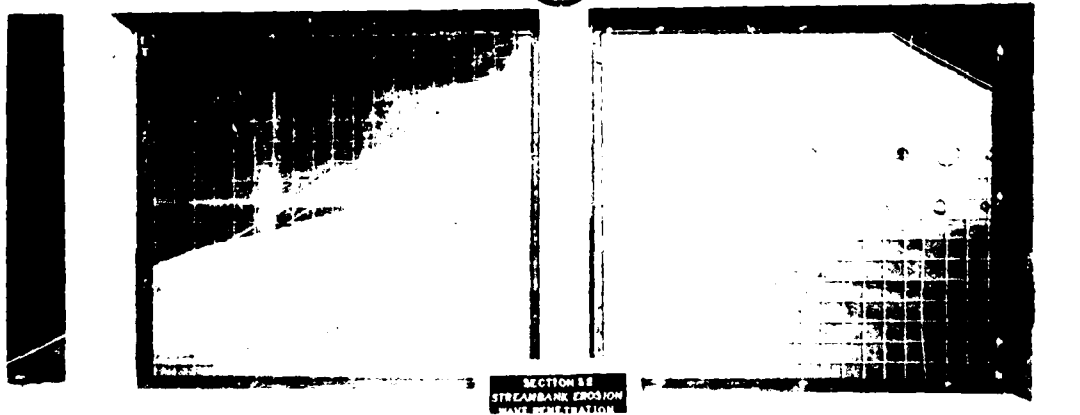
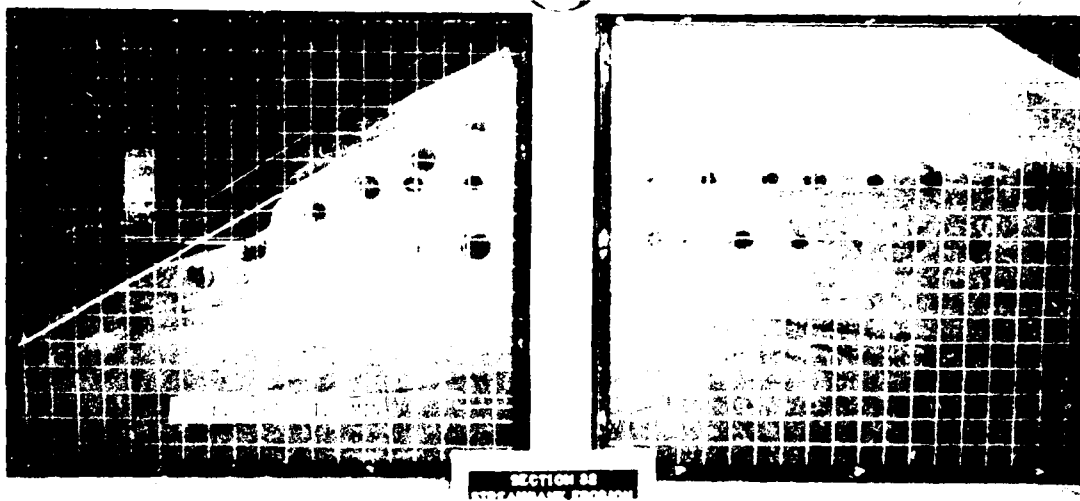
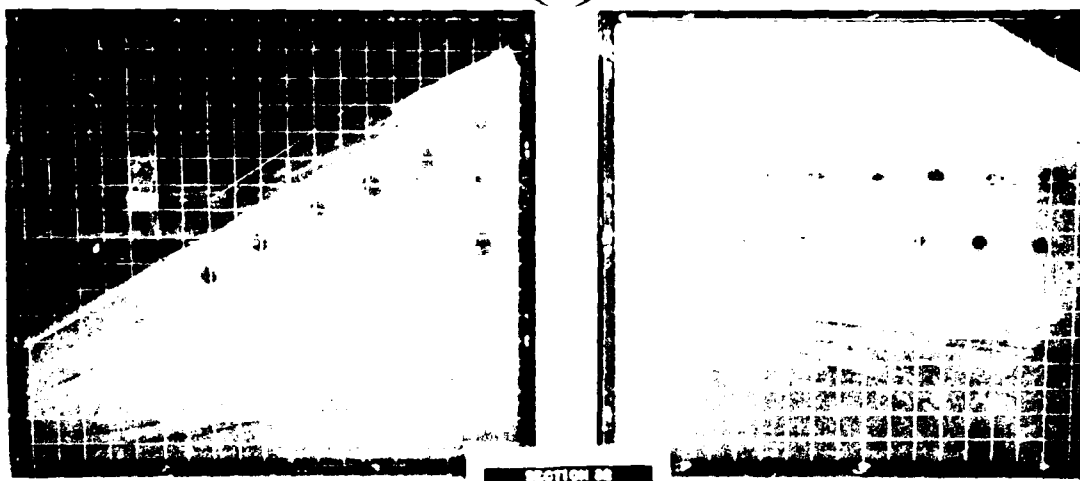


Figure 68. Plan 7, before testing, after 1.0 min, and at end of Test 1

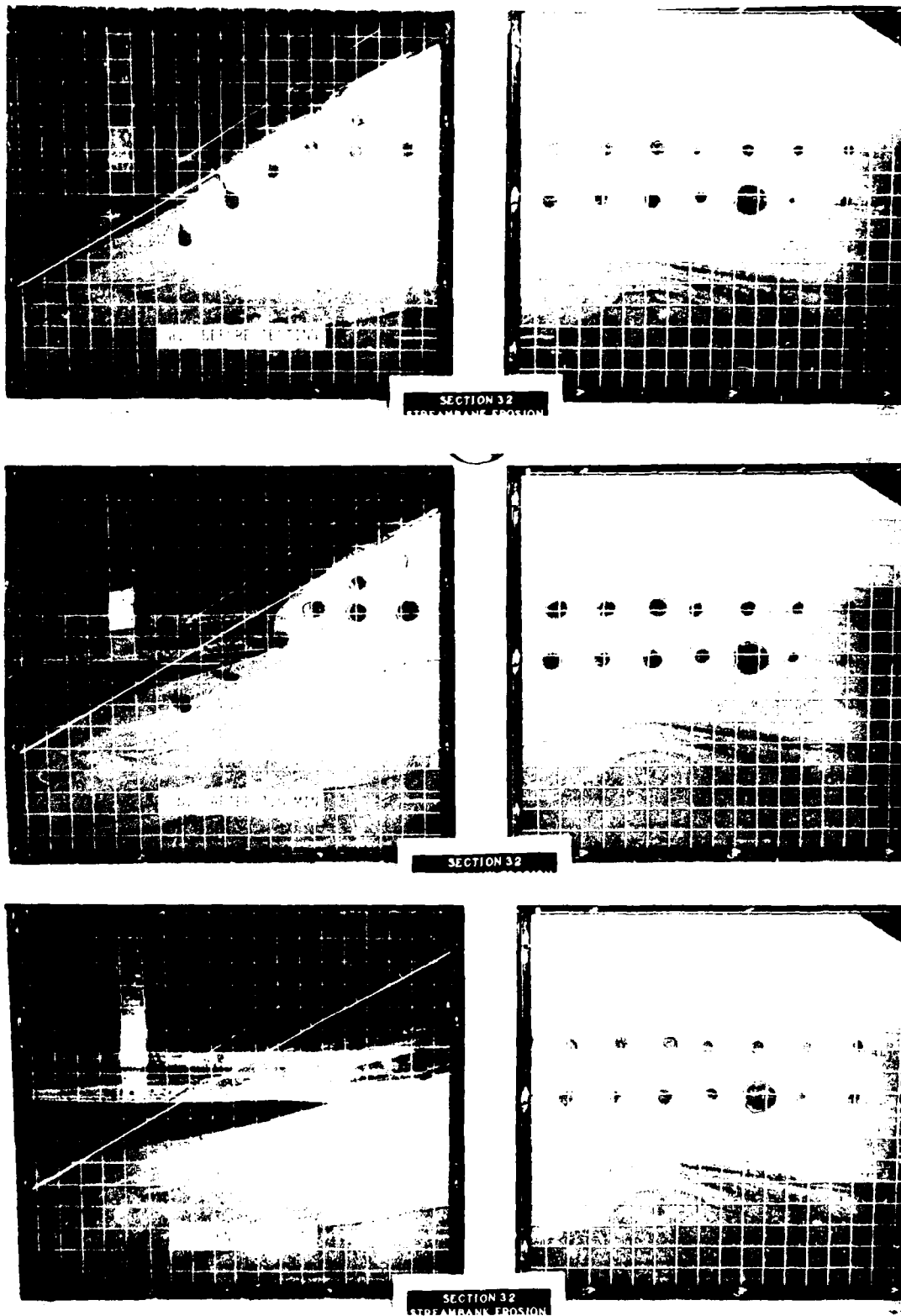


Figure 69. Plan 7, before testing, after 1.0 min, and at end of Test 2

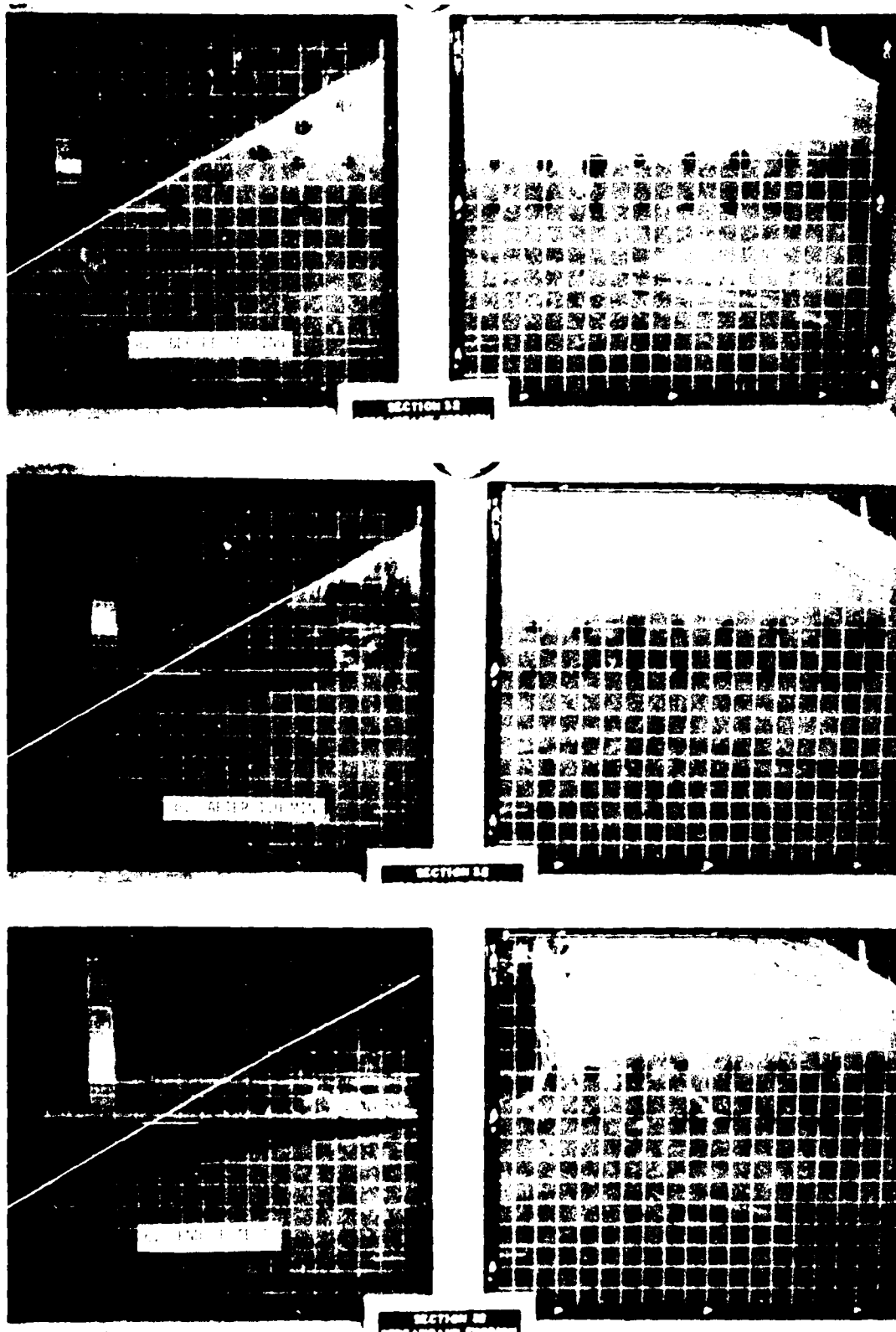


Figure 70. Plan 7, before testing, after 1.0 min, and at end of Test 3

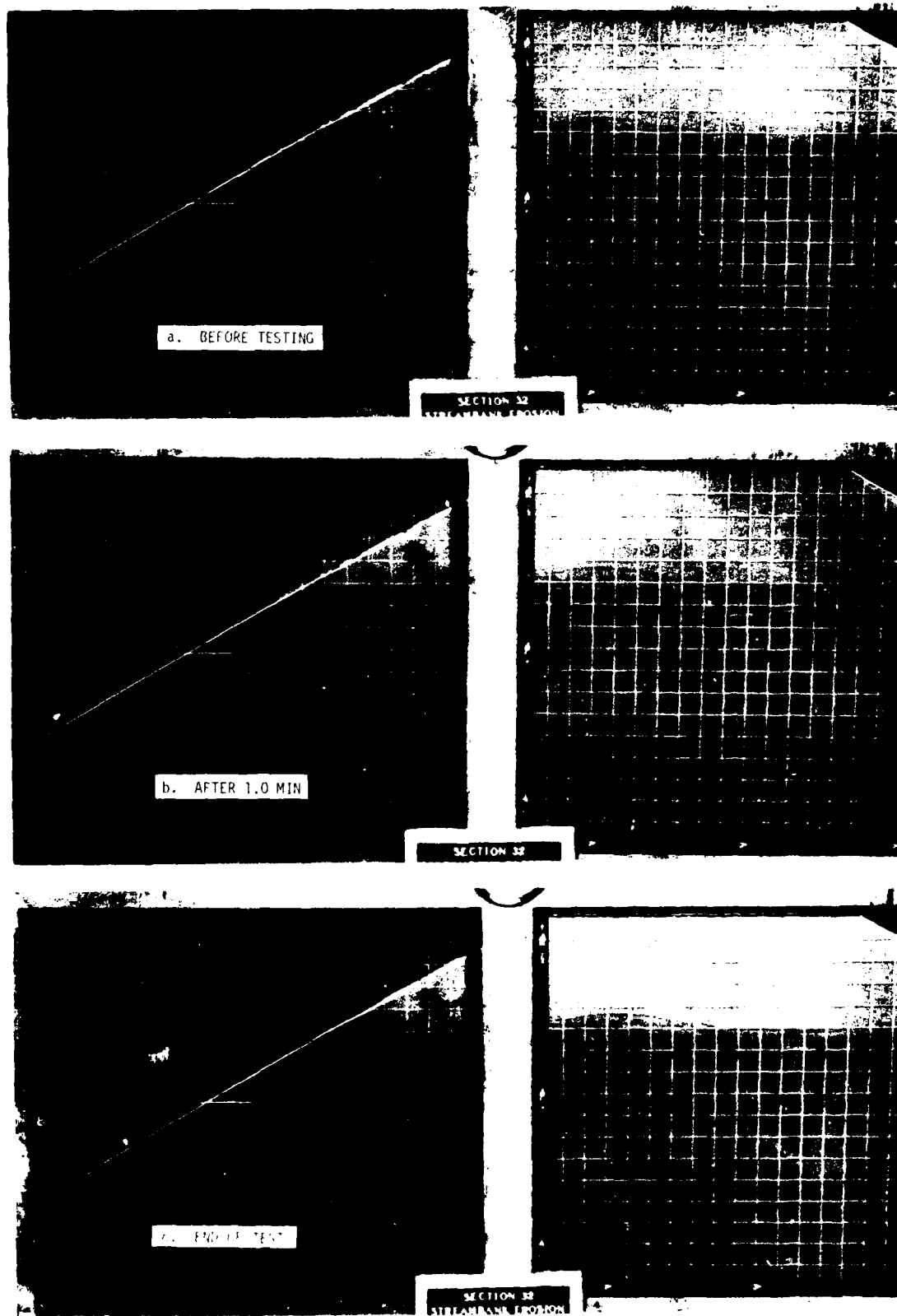


Figure 71. Plan 7, before testing, at 1.0 min, and at end of Test 4

differential head across the streambank (both landside and streamside water depths were maintained at 2.0 ft). These tests were conducted to demonstrate and compare the effect of wave attack on protected and unprotected sand streambanks without the influence of seepage flow induced by differential heads across the streambanks. (The combined effect of wave attack and seepage flow will be addressed in the next section.) All test plans were built and tested at least twice using the same test conditions. This was done to help ensure that stability, or instability, was not due to any added strength, or weakness, inadvertently built into each structure. If the results of the initial and repeat tests were not similar a third test, and on some occasions a fourth test, was conducted. For reporting purposes, the most representative test results are given of what occurred on each plan for at least two of the tests using the identical test conditions. Each plan was exposed to intermittent wave attack until such a time that damage to the structure had stopped or the structure was considered failed. In most instances, where the structure was considered failed, further damage would have occurred had the wave attack been continued. A structure was considered failed if the sand showed any degree of sustained erosion. This means that a slowly progressing, continuous erosion of the sand was considered to be as critical as erosion that progressed at a fast rate. An example of this would be erosion occurring due to a hole in the protective filter fabric (slow progressing) as compared with the erosion occurring on a unprotected streambank (fast progressing). In many instances the protective cover layers sustained minor to moderate damage but the streambank remained stable. These structures were not considered failed as long as the resulting damage to the cover layer, or layers, had stabilized well before the end of the test and the sand showed either no damage or very minor damage that had stabilized before the test was concluded.

45. Plans 3, 5A, and 6 were exposed to 2.0- and 4.0-sec, 0.70-ft nonbreaking waves. All three plans accrued minor to moderate damage to the riprap protection; but in all cases, displacement of the protective riprap layer stabilized well before the end of the tests. At no time were any of the filters exposed to direct wave attack due to holes

occurring in the riprap layer. The granular filter and both of the fabric filters performed adequately. With both the woven and nonwoven filter fabrics, a small amount of sand migrated downslope between the filter fabric and the streambank. In most all tests, the downslope sand movement beneath the filter fabric stopped once the void areas on the lower slope had filled; but in a few cases, a small amount of sand leached out from beneath the filter fabric toe. This leaching could occur as the toe of the filter fabric was trenched into the streambank but was not sealed to the flume floor in the same manner as it had been sealed to the walls (Figure 20b). The void areas referred to above were those areas where the filter fabric was not held tightly to the slope by the overburden of riprap; thus, these areas could bulge out until they were stretched tight by the sand migrating downslope. It should be noted that the sand migration was a surface movement and was not due to a subsidence, or slipping, of the entire streambank. This sand migration did not occur when the two-layer, granular filter system was used between the riprap and sand (Plan 3). Figures 72-77 are before and after test views of Plans 3, 5A, and 6 for one testing of each test condition. It should be noted that in the after-testing, streamside views of Plan 5A and 6, all of the sand at the toe of the structures did not leach from beneath the filter fabric. The major portion of this sand resulted from sand being placed on the top of the filter fabric when the toe of the fabric was being entrenched into the streambank (Figures 19 and 25).

46. Plans 1, 3, 4A, and 6 were exposed to 2.0-sec, 0.75-ft non-breaking waves. Plans 1 and 4A failed and would have continued to deteriorate had the tests been continued. Plans 3 and 6 showed similar results to that which occurred when they were exposed to the 2.0- and 4.0-sec, 0.70-ft nonbreaking waves. Some increased riprap displacement was noted with this higher wave height, but all damage had stopped before the end of each test and in no instance did either of Plans 3 or 6 fail to protect the sand streambank. Some downslope movement of sand occurred beneath the filter fabric in Plan 6. This movement was the same, both in type and amount, as had occurred in Plans 5A and 6 when

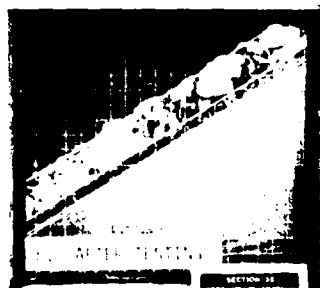
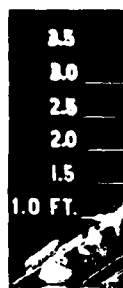
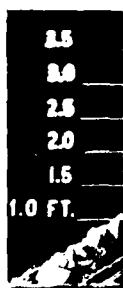


Figure 72. Plan 3, before and after testing 2.0-sec,
0.70-ft nonbreaking waves

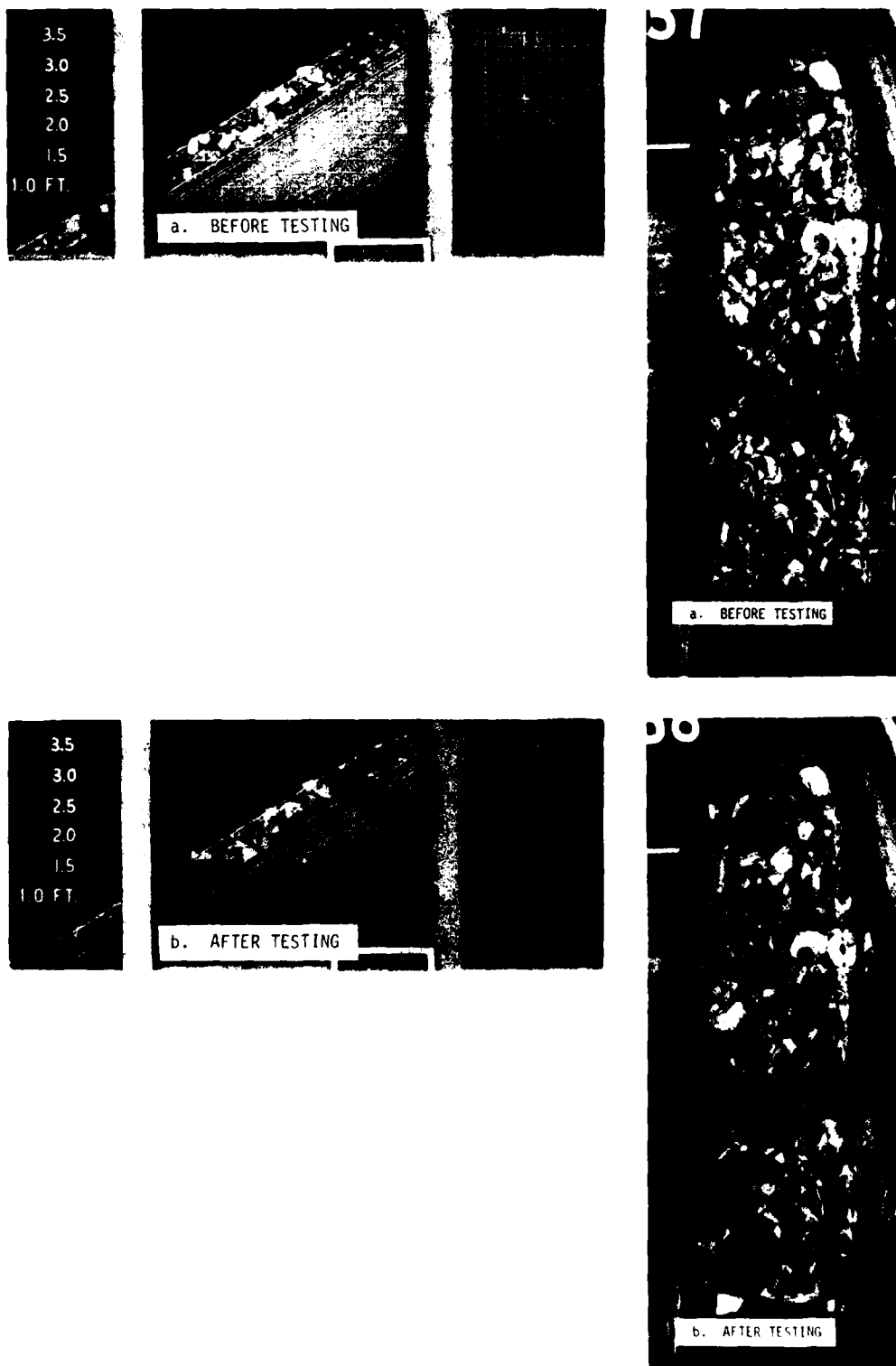


Figure 73. Plan 3, before and after testing 4.0-sec,
0.70-ft nonbreaking waves

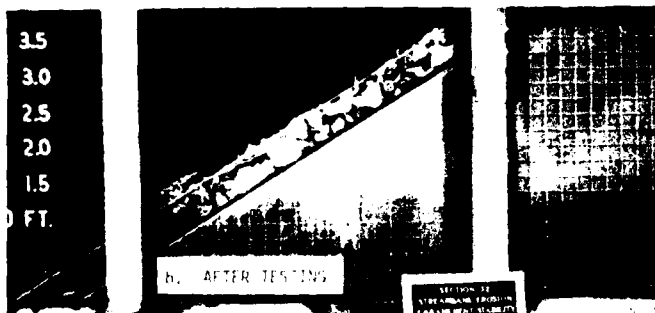
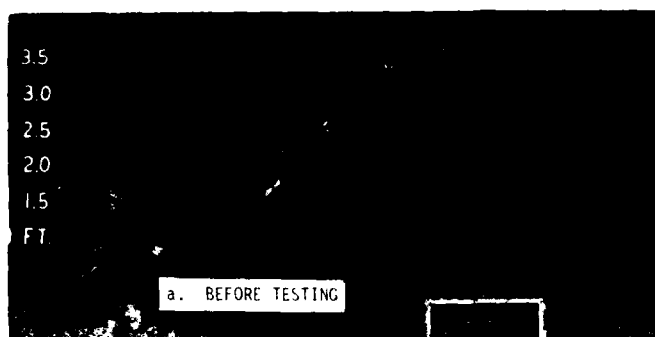


Figure 74. Plan 5A, before and after testing 2.0-sec,
0.70-ft nonbreaking waves

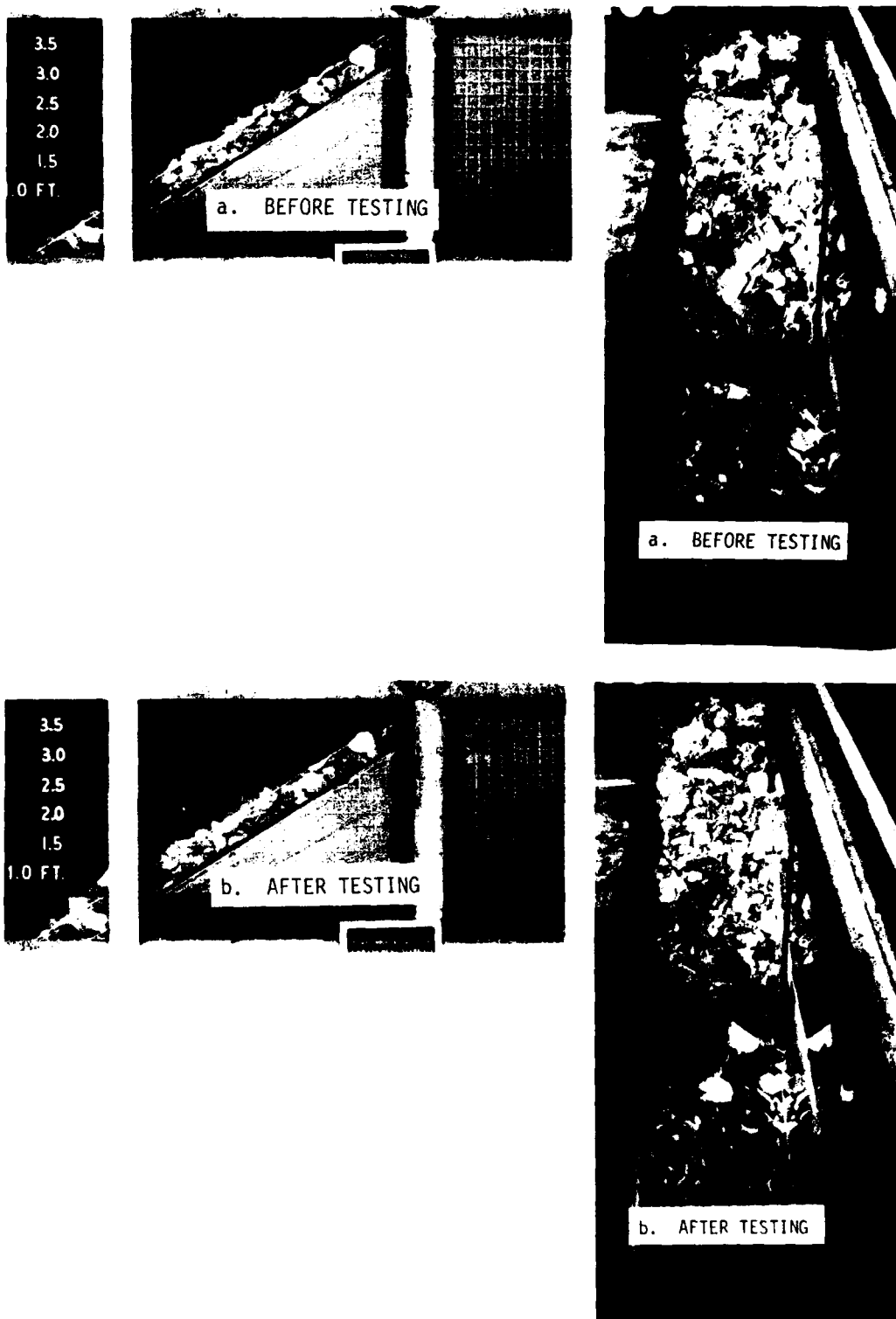


Figure 75. Plan 5A, before and after testing 4.0-sec, 0.70-ft nonbreaking waves

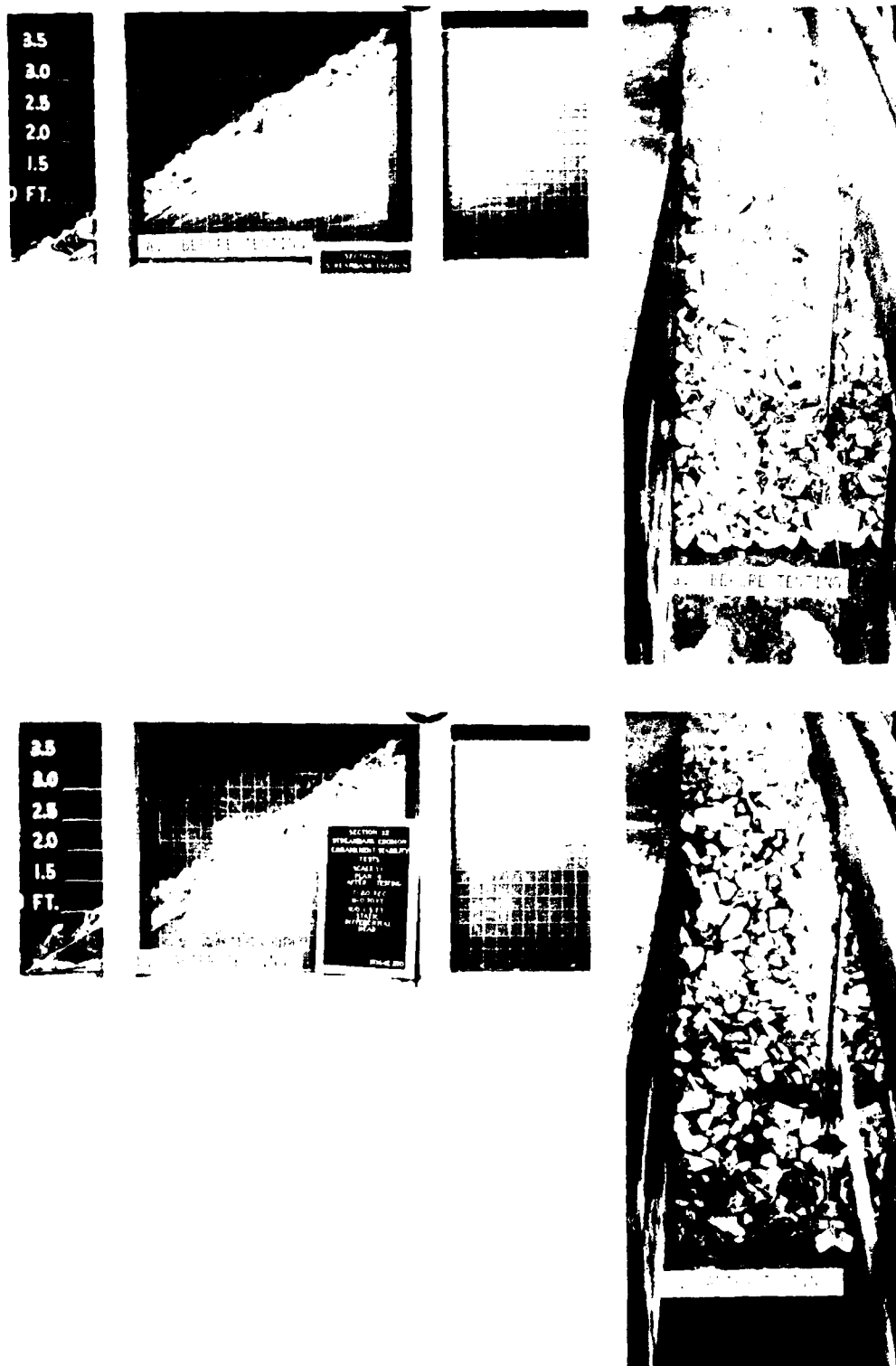


Figure 76. Plan 6, before and after testing 2.0 sec,
0.70-ft nonbreaking waves

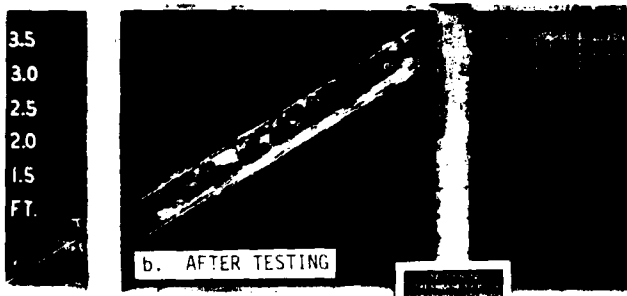


Figure 77. Plan 6, before and after testing 4.0-sec,
0.70-ft nonbreaking waves

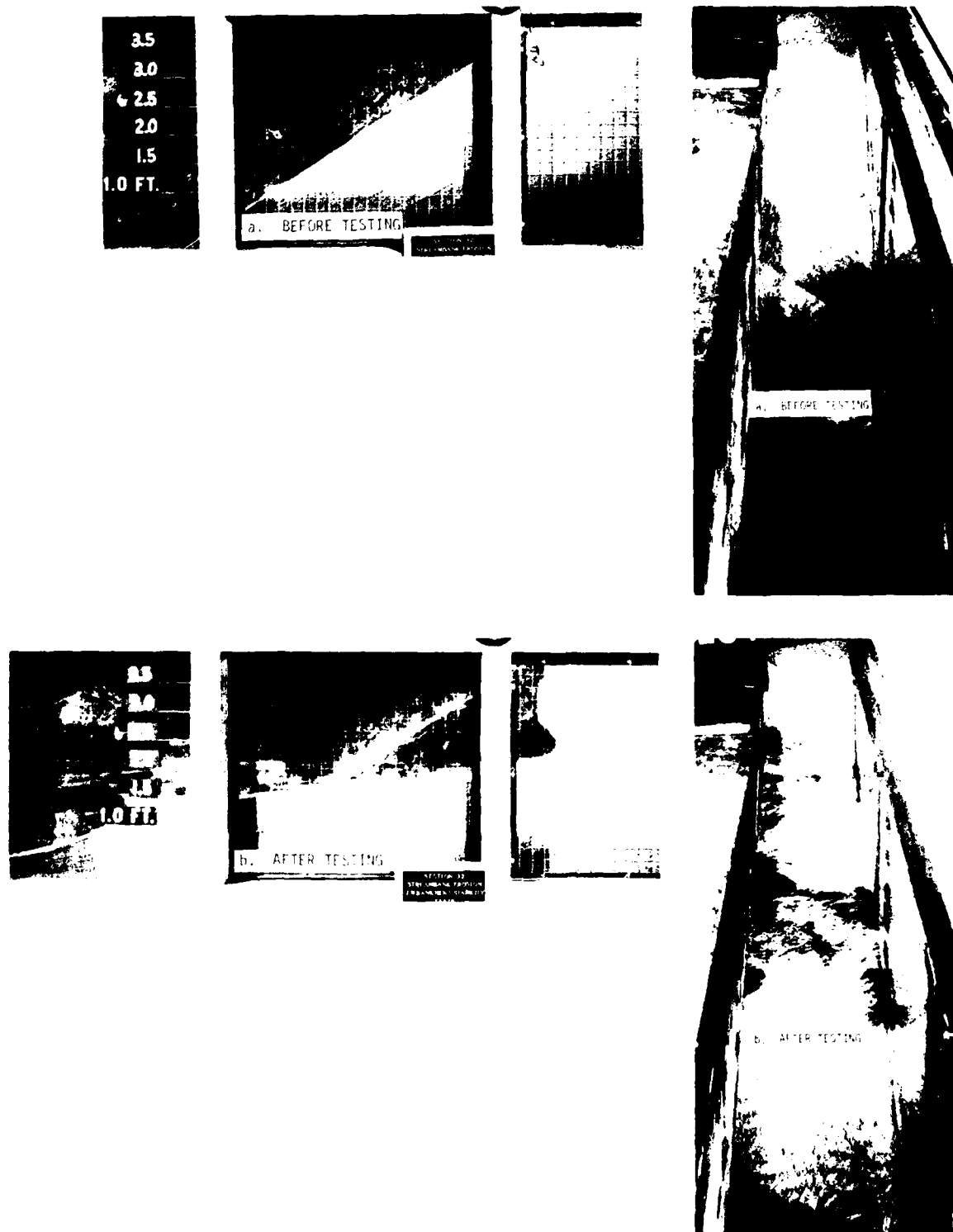


Figure 78. Plan 1, before and after testing 2.0-sec,
0.75-ft nonbreaking waves

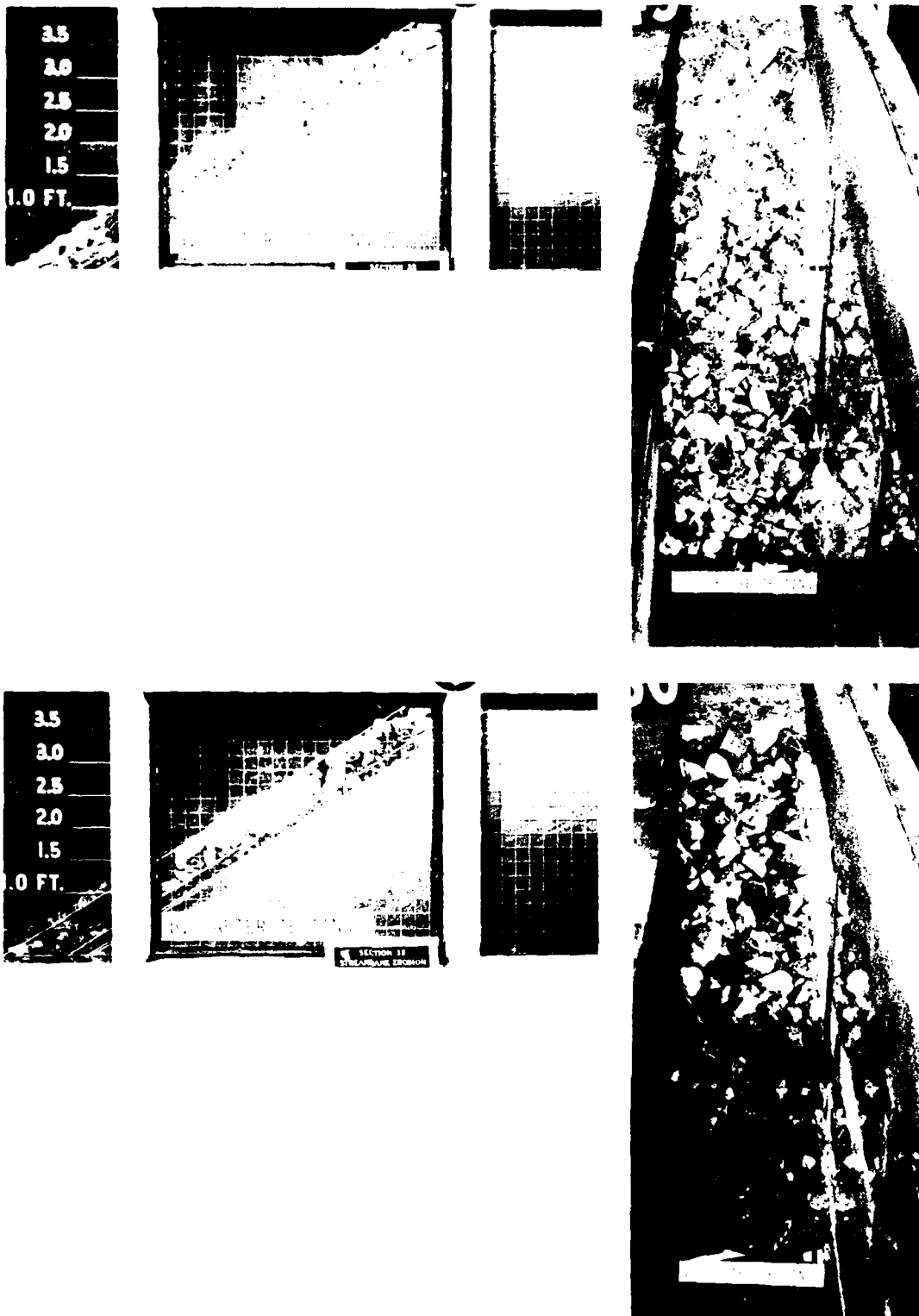


Figure 79. Plan 3, before and after testing 2.0-sec,
0.75-ft nonbreaking waves

AO-A121 132

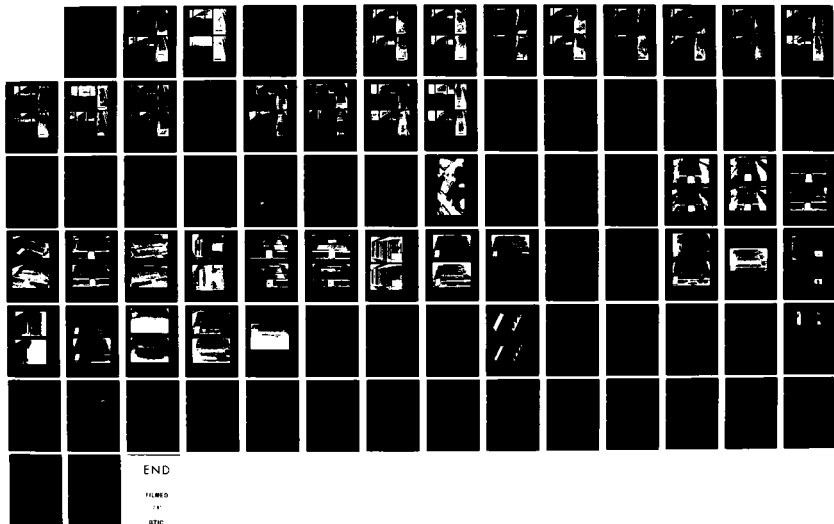
THE STREAMBANK EROSION CONTROL EVALUATION AND
DEMONSTRATION ACT OF 1974 S. (U) ARMY ENGINEER
WATERWAYS EXPERIMENT STATION VICKSBURG MS HYDRA.

474

UNCLASSIFIED

M P KEOWN ET AL. DEC 81 WES/TR/H-77-9-APP-B F/G 13/2

NL

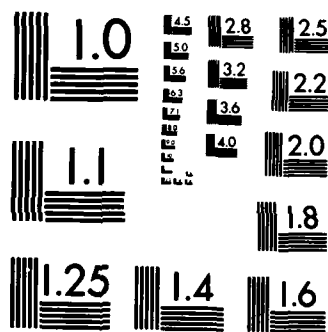


END

FILMED

14

DTIC



MICROCOPY RESOLUTION TEST CHART
NATIONAL BUREAU OF STANDARDS-1963-A

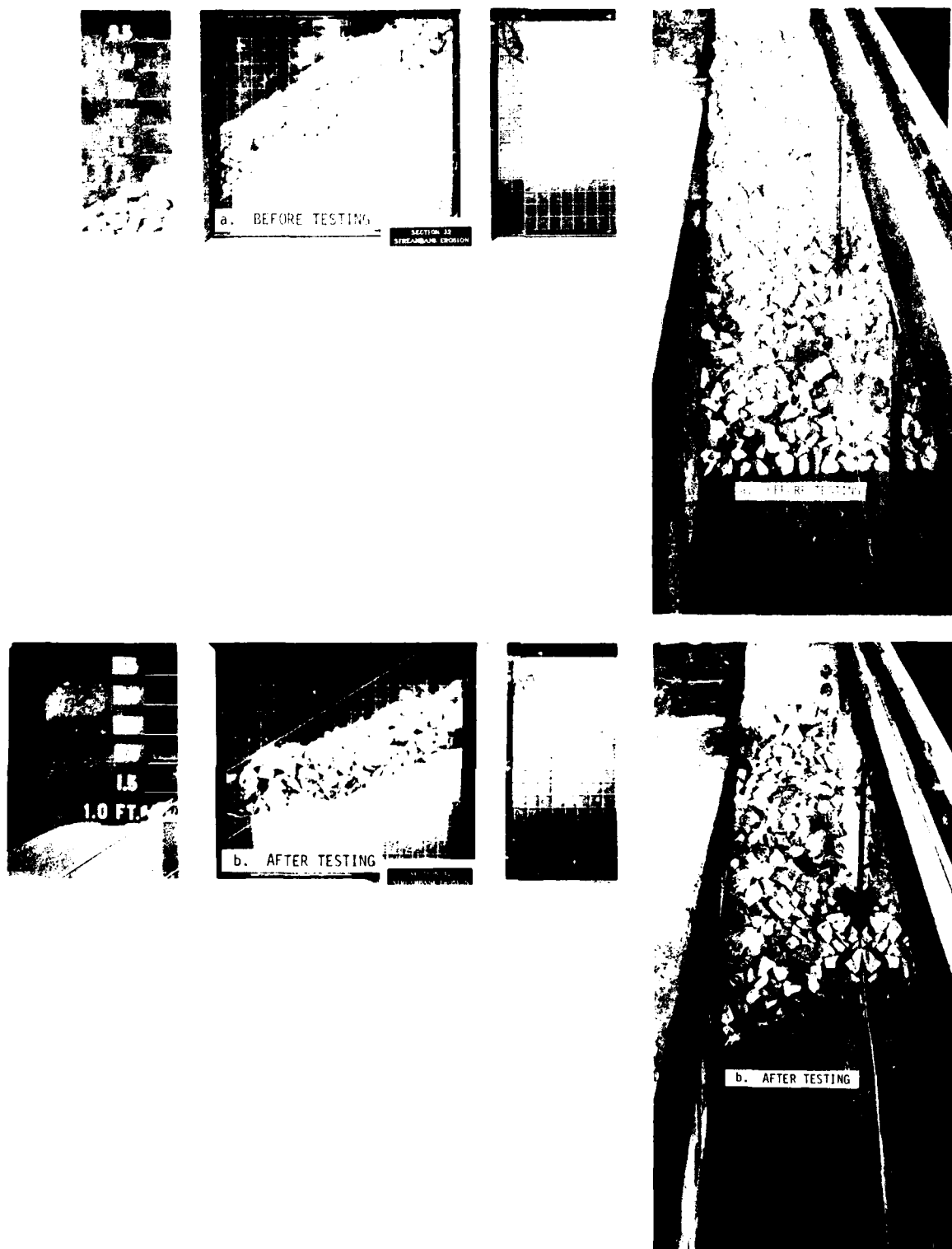


Figure 80. Plan 4A, before and after testing 2.0-sec,
0.75-ft nonbreaking waves

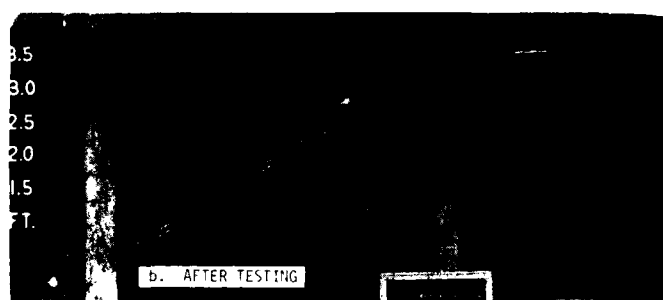
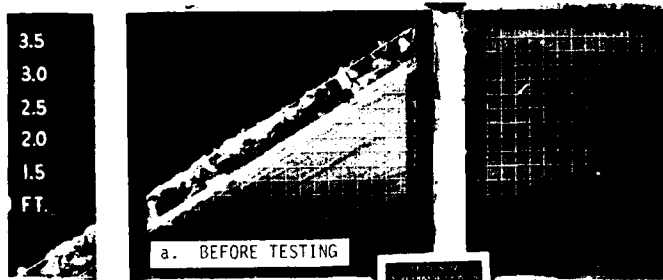


Figure 81. Plan 6, before and after testing 2.0-sec,
0.75-ft nonbreaking waves

exposed to the 0.70-ft nonbreaking waves discussed in paragraph 45. Figures 78-81 show the condition of Plans 1, 3, 4A, and 6 both before and after exposure to the 2.0-sec, 0.75-ft nonbreaking waves.

Wave Stability with a Static Differential
Head Across the Streambank

47. Plans 3, 3A, 5A, 5B, 6, 6A, 6B, 8, 8A, 8B, and 8C were exposed to 2.0- and 4.0-sec, 0.70-ft and/or 2.0-sec, 0.75-ft nonbreaking waves with a 1.5-ft static differential head across the streambank (the landside and streamside water depths were maintained at 3.5 and 2.0 ft, respectively). These tests were conducted to demonstrate and compare the combined effect of wave attack and seepage flow, induced by a continuous differential head, on various streambank protection methods. Each plan was exposed to intermittent wave attack, until such time that damage to the structure had stopped or the structure was considered failed. A constant 1.5-ft static differential head was maintained throughout the test. All tests were run twice using the same test conditions and almost all tests showed good repeatability. Where there was a difference in test results, the test showing the greatest damage was reported. Structure failure was based on the same criteria discussed in paragraph 44.

48. Plans 3, 5A, and 6 were exposed to 2.0- and 4.0-sec, 0.70-ft nonbreaking waves. All plans showed comparable damage to the riprap as had occurred with the same wave conditions without the static differential head. None of the test sections failed in that the sand streambank never accrued any significant degree of erosion. In the cases where minor erosion occurred, this damage subsided well before the end of the test. Some disruption and minor leaching of the granular filters into the riprap occurred in Plan 3 during the 2.0-sec wave period tests. Also Plans 5A and 6 showed the same downslope movement of sand beneath the filter fabrics as had occurred during the tests where the static differential head was not used. The amount of movement was very similar to these earlier tests, and movement appeared to subside during the test. Figures 82-87 show the condition of the plans both before and after each test.

49. Plan 3 (Figure 88a) was tested with 2.0-sec, 0.75-ft nonbreaking waves and the 1.5-ft static differential head to see if the increased wave height would cause a larger amount of disruption and leaching of granular filters than what had occurred with the 0.70-ft waves. The riprap sustained moderate damage and the granular filter was exposed and started to leach through the riprap. This did not result in any significant damage to the sand streambank. All damage had subsided at the end of the test and the granular filter that leached through the riprap can hardly be detected in the after-test photographs (Figures 88b).

50. The riprap thickness was increased to 1 ft in Plans 3A, 5B, and 6A (Figures 89a, 90a, and 91a, respectively), to see if this would add some reserve stability to the riprap and reduce the amount of wave energy reaching the filters and sand. These plans were exposed to 2.0-sec, 0.75-ft nonbreaking waves combined with the 1.5-ft static differential head. Only a minor amount of riprap displacement occurred in Plan 3A while a moderate amount of displacement occurred in Plans 5B and 6A. The amount of damage accrued by Plan 3A was significantly less than what had occurred in Plan 3 when exposed to the identical test conditions. The damage in Plans 5B and 6A was similar to what had occurred in Plans 5A and 6 when exposed to the 2.0- and 4.0-sec, 0.70-ft waves combined with the 1.5-ft static differential head. The granular filters on Plans 3A showed no instability or leaching into the riprap. With the increase from 0.5- to 1.0-ft thickness of riprap, there was an obvious decrease in the amount of wave energy reaching the granular filters. Movement of sand beneath the filter fabrics, as noted during earlier tests with the fabric filters, continued to occur in Plans 5B and 6A. The movement of sand in Plan 5B was significant enough to create a hole in the sand streambank (Figure 90b). As with the riprap displacement that occurred on all three plans, the movement of sand under the filter fabric of Plan 5B had stopped well before the end of the test. The after-test conditions of all three plans are shown in Figures 89b, 90b, and 91b.

51. To help prevent the tearing or puncturing of the filter fabric, some contractors place a layer of sand over the filter fabric

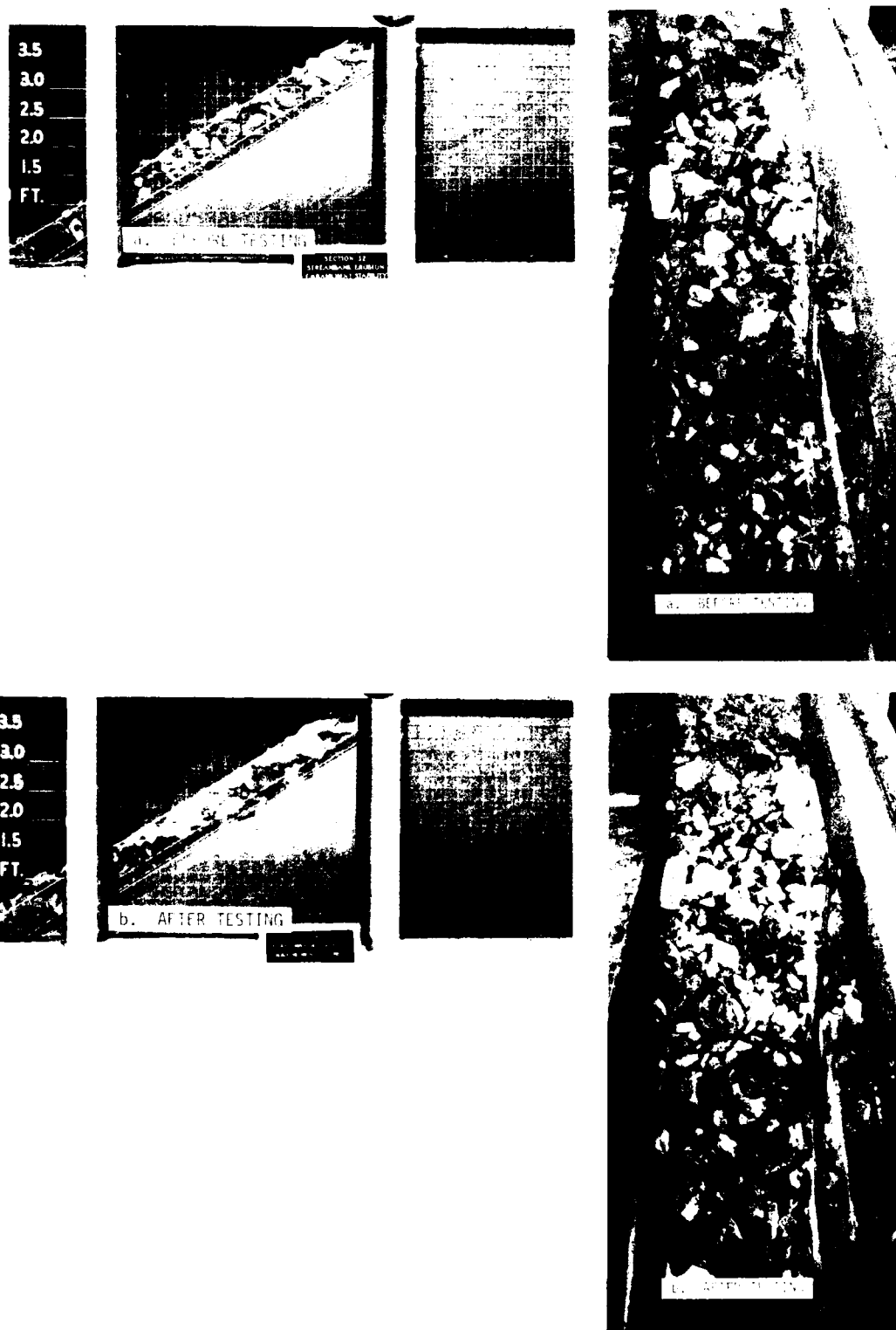


Figure 82. Plan 3, before and after testing 2.0-sec, 0.70-ft non-breaking wave combined with 1.5-ft static differential head

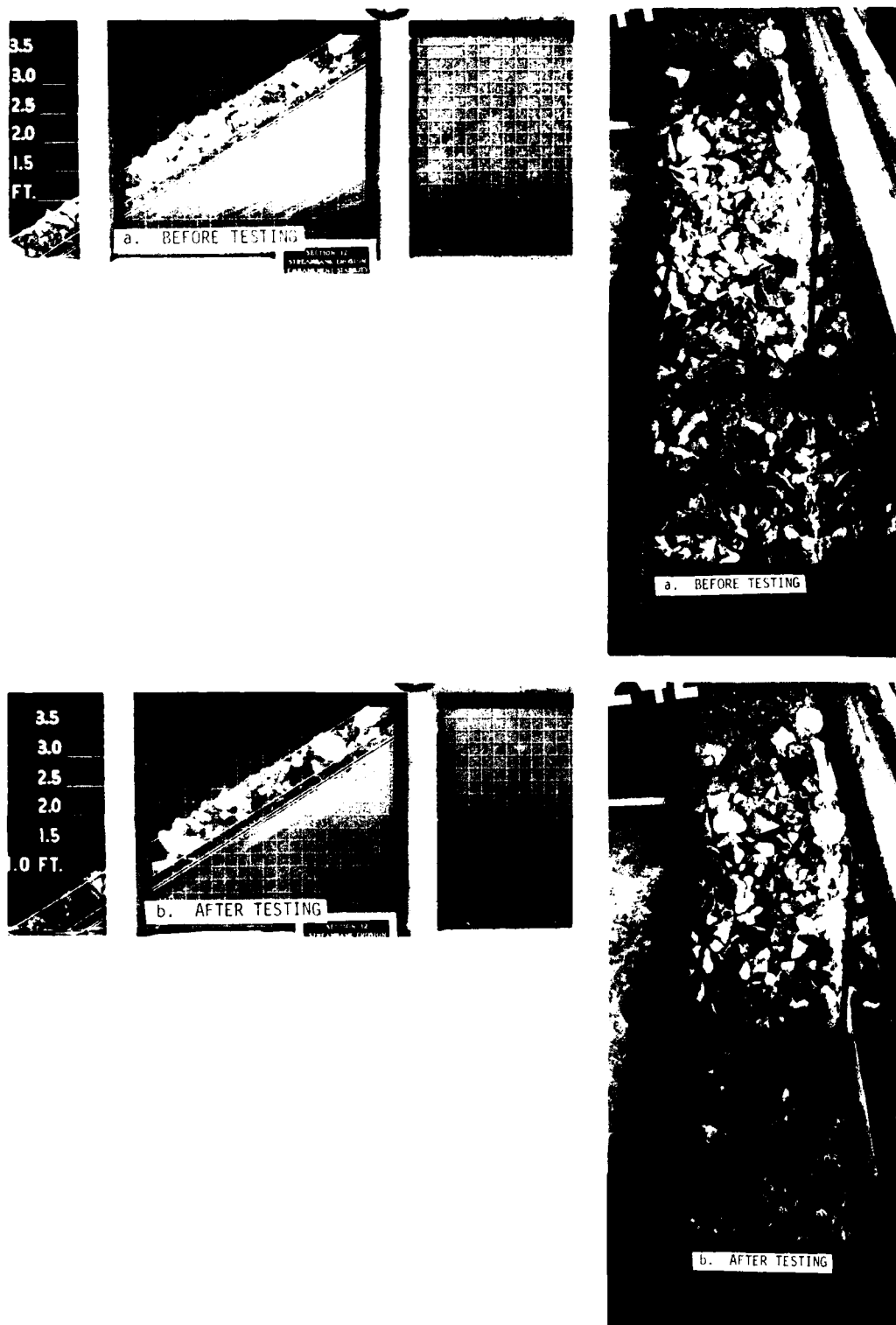


Figure 83. Plan 3, before and after testing 4.0-sec, 0.70-ft non-breaking wave combined with 1.5-ft static differential head

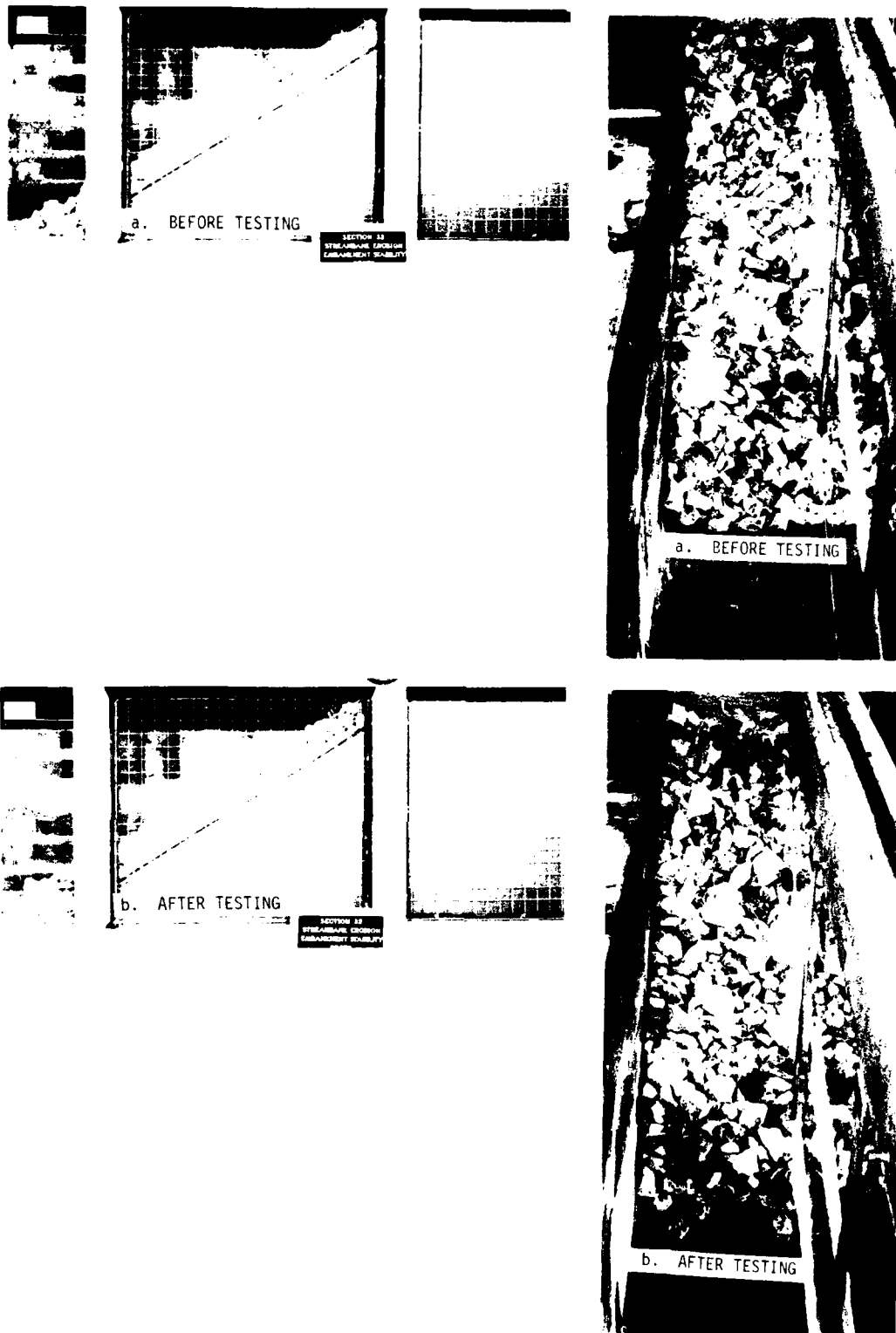


Figure 84. Plan 5A, before and after testing 2.0-sec, 0.70-ft non-breaking wave combined with 1.5-ft static differential head

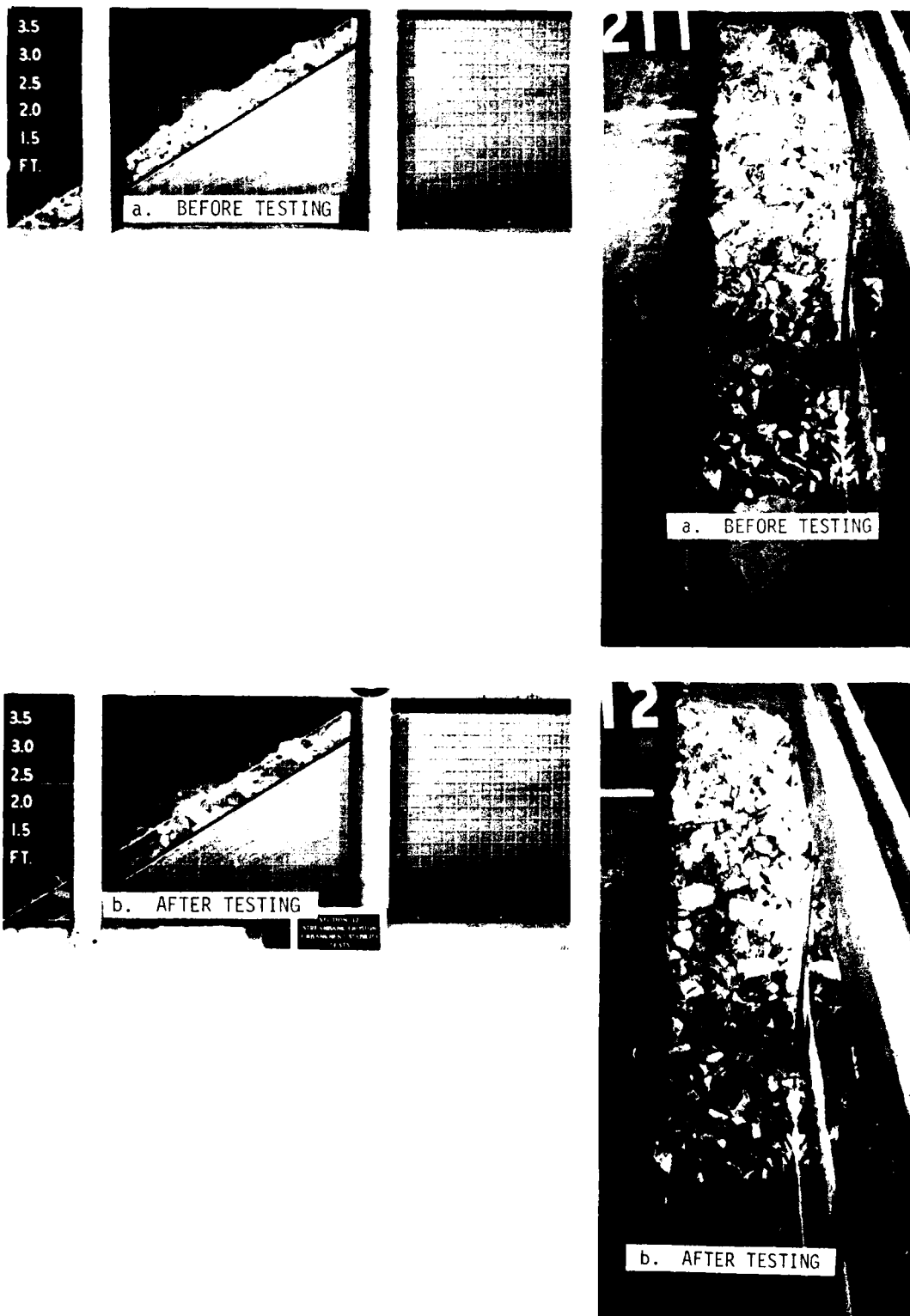


Figure 85. Plan 5A, before and after testing 4.0-sec, 0.70-ft non-breaking wave combined with 1.5-ft static differential head

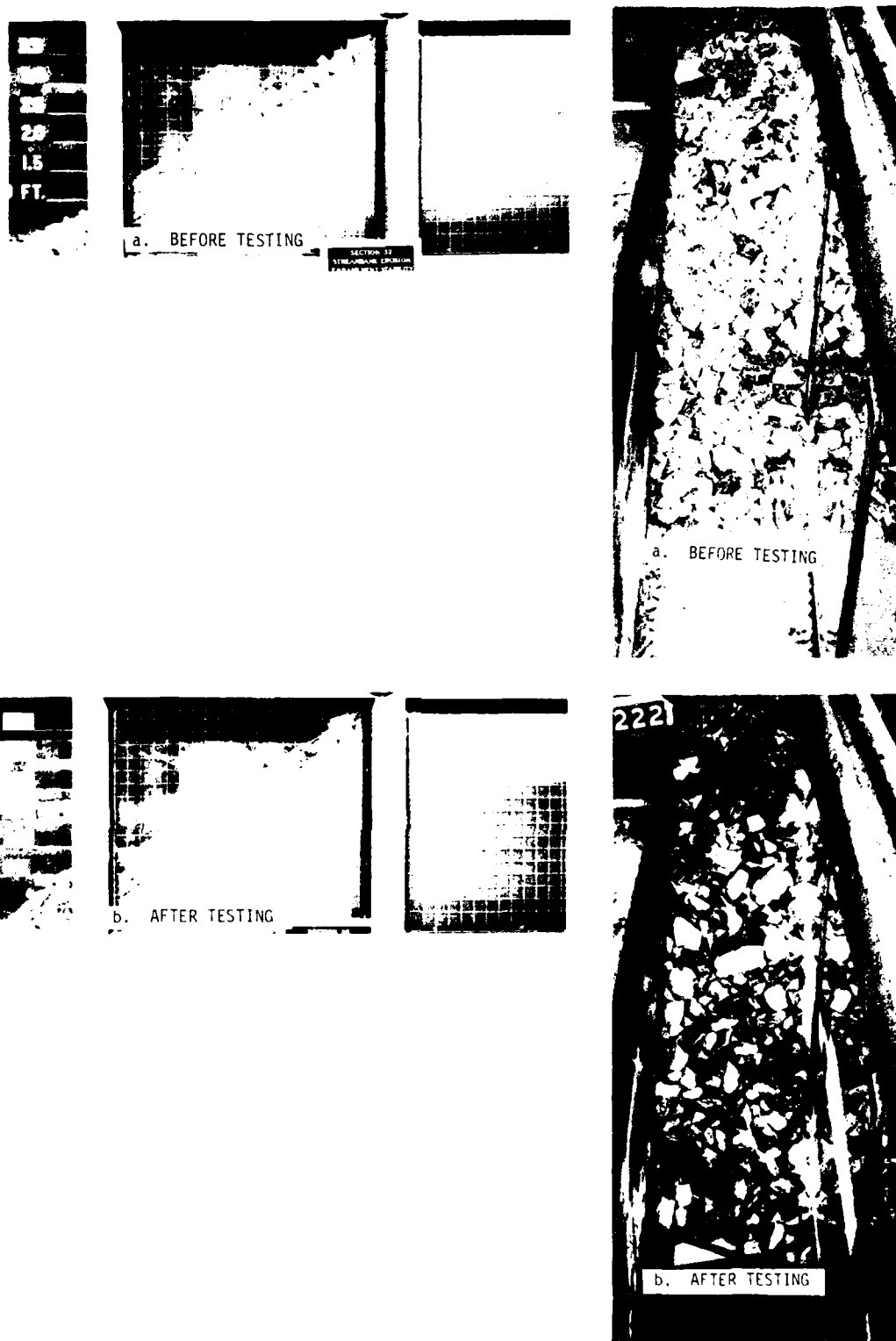


Figure 86. Plan 6, before and after testing 2.0-sec, 0.70-ft non-breaking wave combined with 1.5-ft static differential head

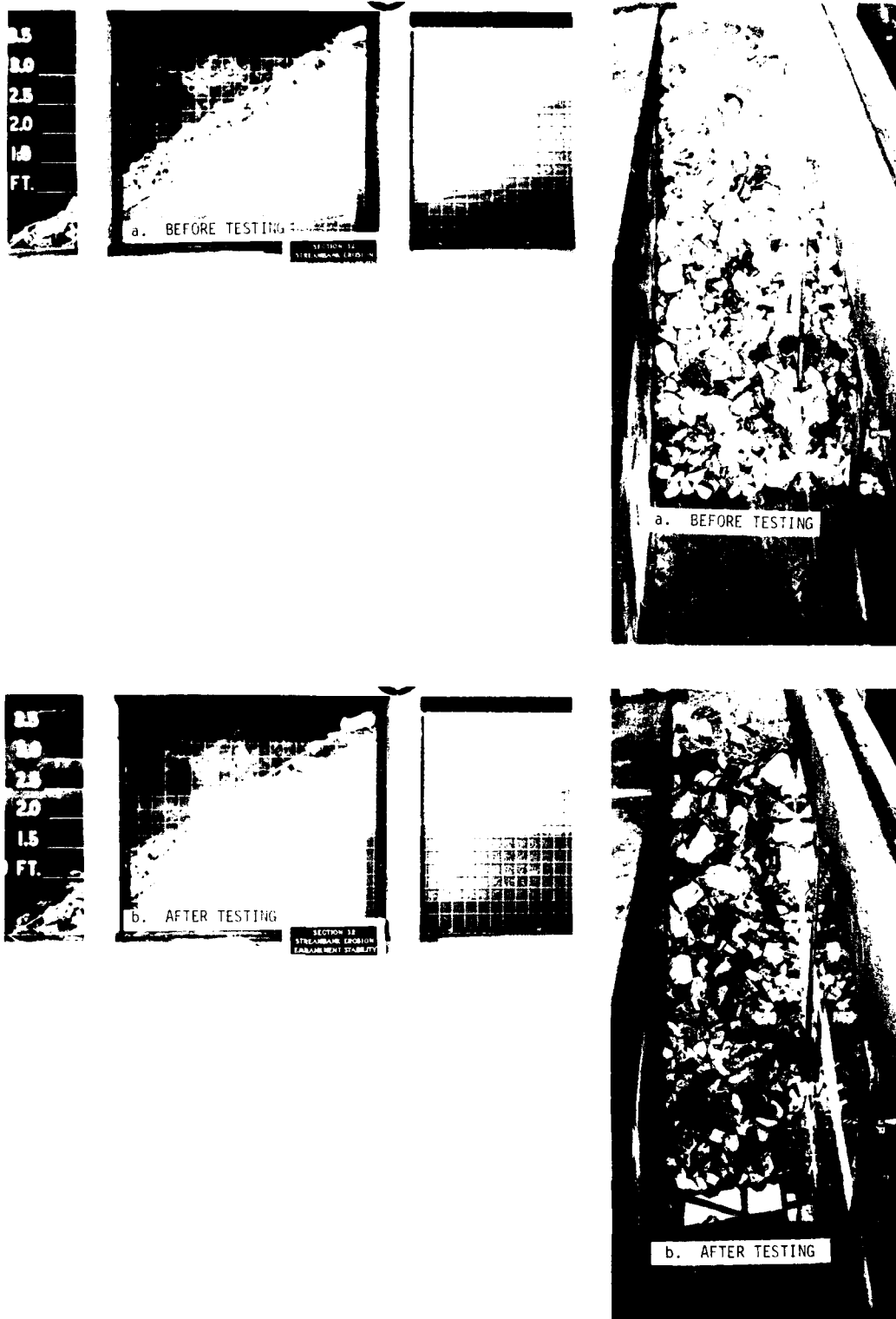


Figure 87. Plan 6, before and after testing 4.0-sec, 0.70-ft non-breaking wave combined with 1.5-ft static differential head



Figure 88. Plan 3, before and after testing 2.0-sec, 0.75-ft non-breaking wave combined with 1.5-ft static differential head

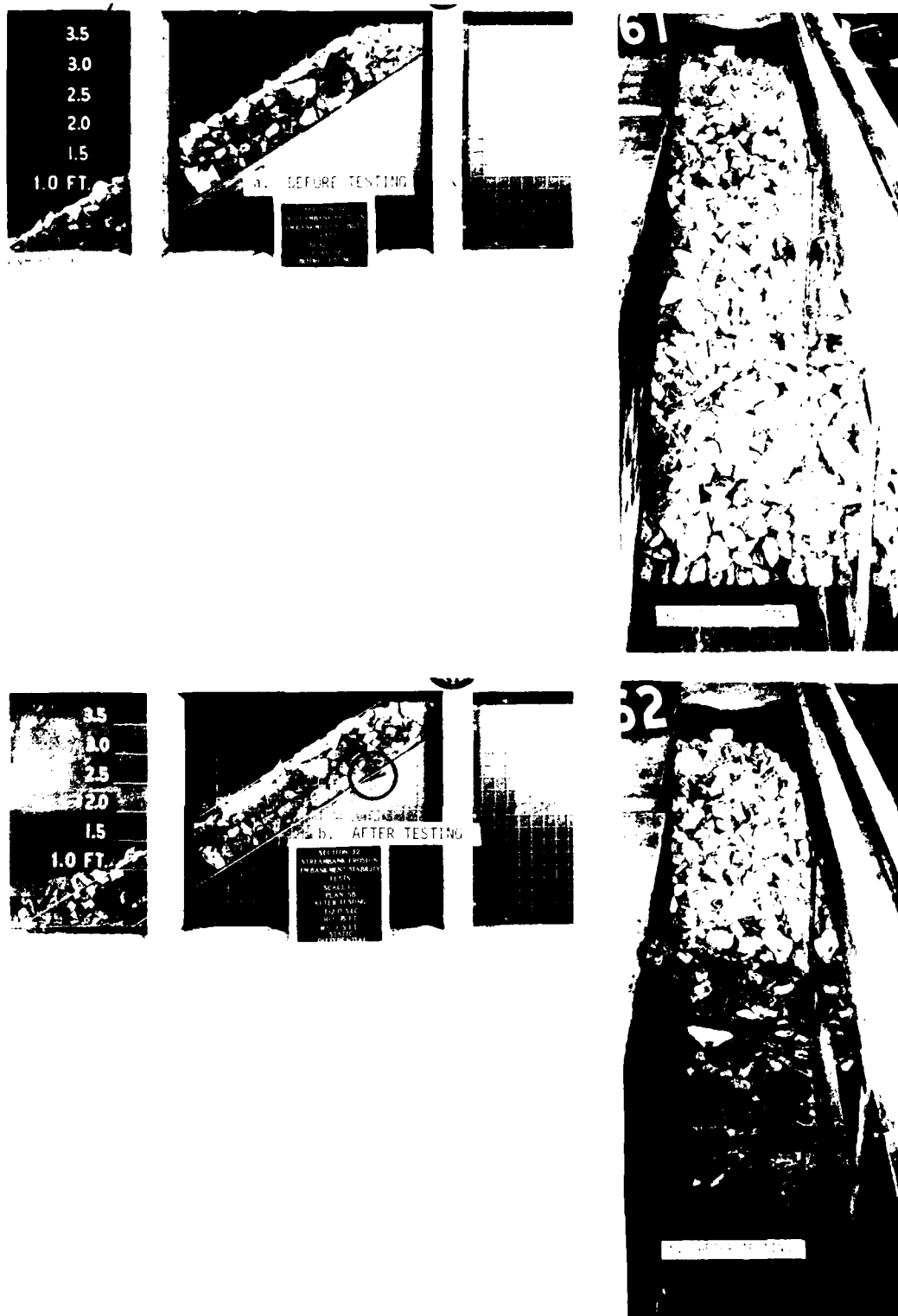


Figure 90. Plan 5B, before and after testing 2.0-sec, 0.75-ft non-breaking wave combined with 1.5-ft static differential head

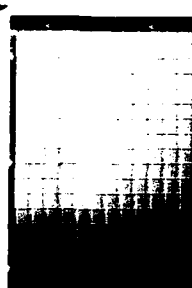
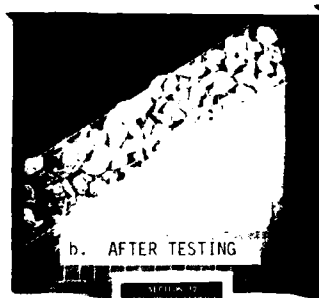
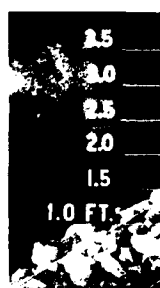
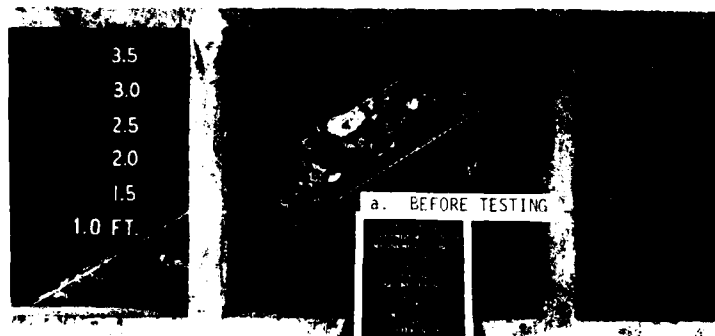


Figure 91. Plan 6A, before and after testing 2.0-sec, 0.75-ft non-breaking wave combined with 1.5-ft static differential head

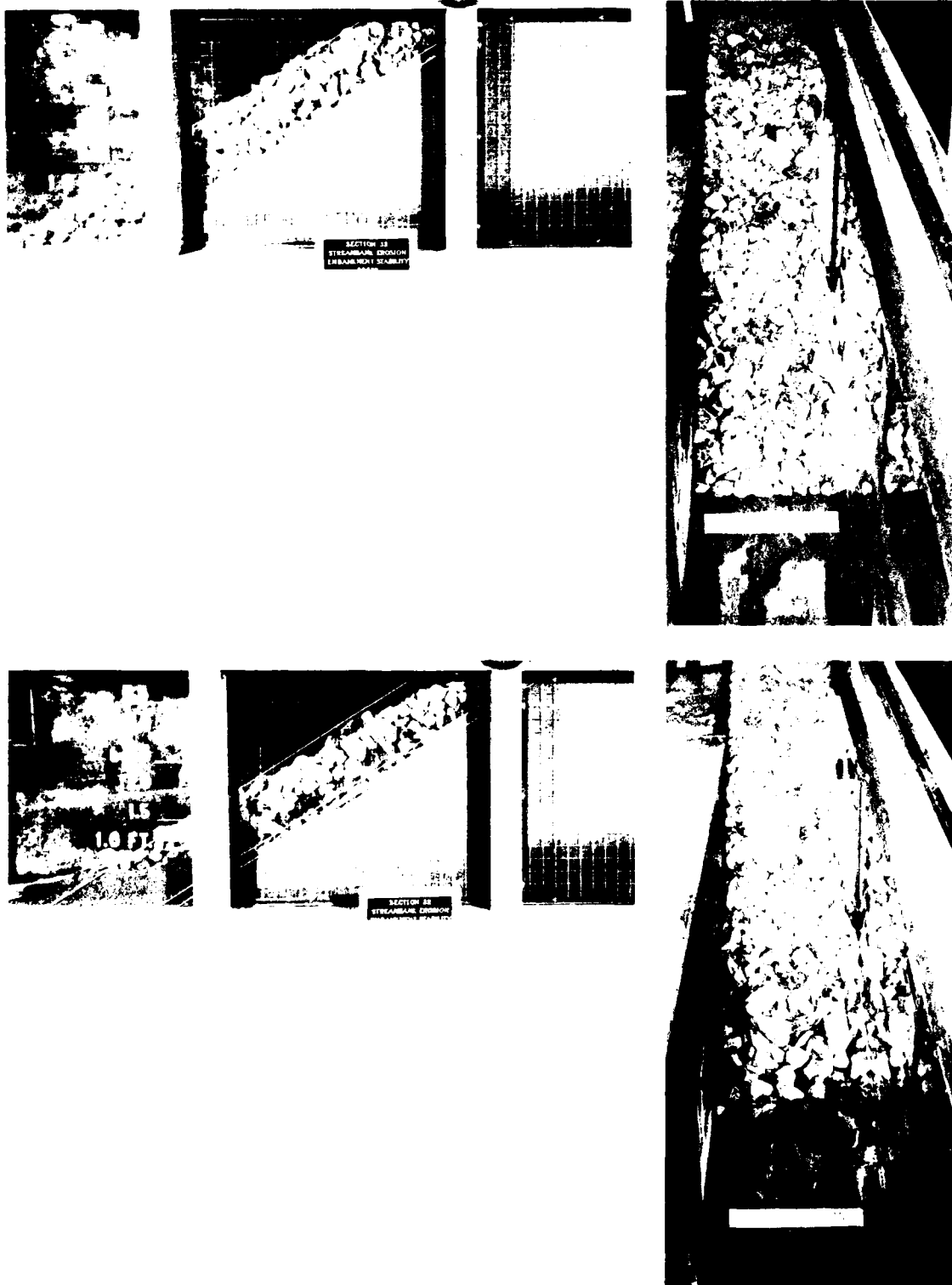


Figure 92. Plan 6B, before and after testing 2.0-sec, 0.75-ft non-breaking wave combined with 1.5-ft static differential head

prior to the riprap placement. Some question arose as to what effect the sand layer might have on the riprap stability. Tests were conducted on Plan 6B, Figure 92a, to give some insight into what effect a 2-in. layer of sand might have. After exposure to the 2.0-sec, 0.75-ft non-breaking waves combined with a 1.5-ft static differential head, all of the 2-in. sand layer in the wave action zone had been displaced downslope. As the sand displaced, the riprap covering subsided into this area. As the riprap subsided, it also moved downslope somewhat; but as shown in after-test photographs (Figure 92b) the overall riprap stability was the same as had been observed in Plan 6A when exposed to the same test conditions.

52. Plan 8, Figure 93a, was tested to see if the riprap-filled cells would increase the stability of the streambank when a riprap protective layer was used and no filter was placed between the riprap and the sand. The cells were not needed for stability of the riprap, as the riprap had already been shown to be stable in Plan 6A when exposed to 2.0-sec, 0.75-ft nonbreaking waves combined with a 1.5-ft static differential head. No riprap was displaced by wave action during the test; but the riprap did subside in each cell as the sand eroded from beneath it. The wave action produced rapid streambank erosion during the first part of the test. As the test progressed, a sand berm formed at the toe of the slope and the wave-induced erosion diminished. The streambank erosion produced by the seepage flow, induced by the static differential head, continued throughout the test and had not subsided when the test was stopped. The streambank was considered failed and had the test been continued, the crown of the structure would have eventually been breached. Figure 93b shows the condition of Plan 8 when the test was stopped.

53. Plan 8A, Figure 94a, was tested to see if gravel-filled cells would be stable for the 2.0-sec, 0.75-ft nonbreaking wave action and also would act as a filter to prevent the sand from leaching out through the protective covering. During the first part of the test, the gravel was displaced from the cells in the wave action zone but this displacement stopped well before the end of the test. The combined wave action

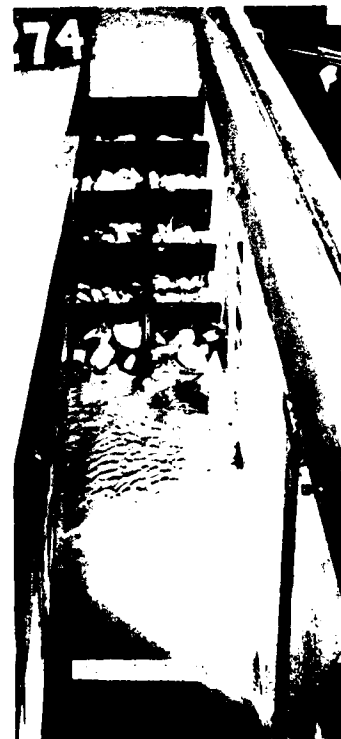
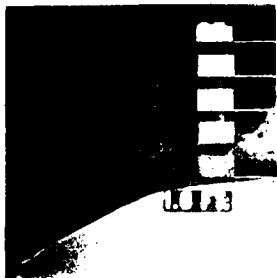
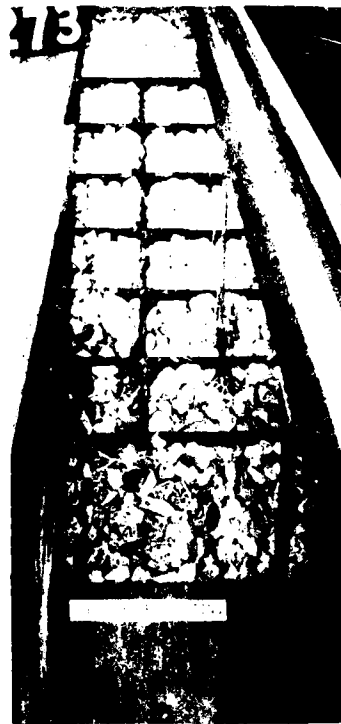
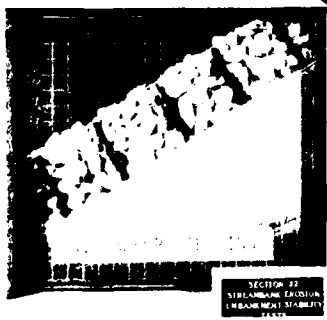


Figure 93. Plan 8, before and after testing 2.0-sec, 0.75-ft non-breaking wave combined with 1.5-ft static differential head

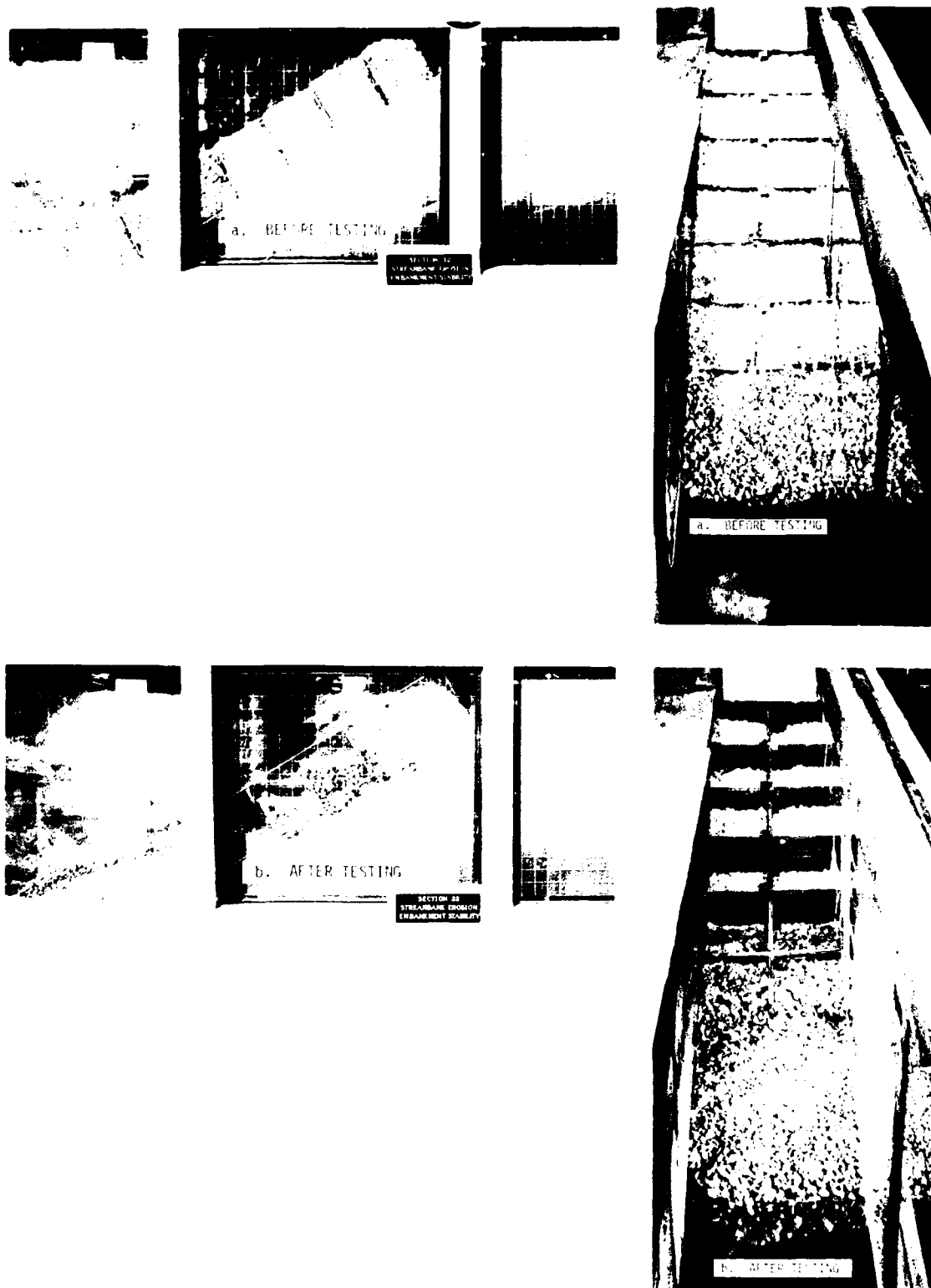


Figure 94. Plan 8A, before and after testing 2.0-sec, 0.75-ft non-breaking wave combined with 1.5-ft static differential head

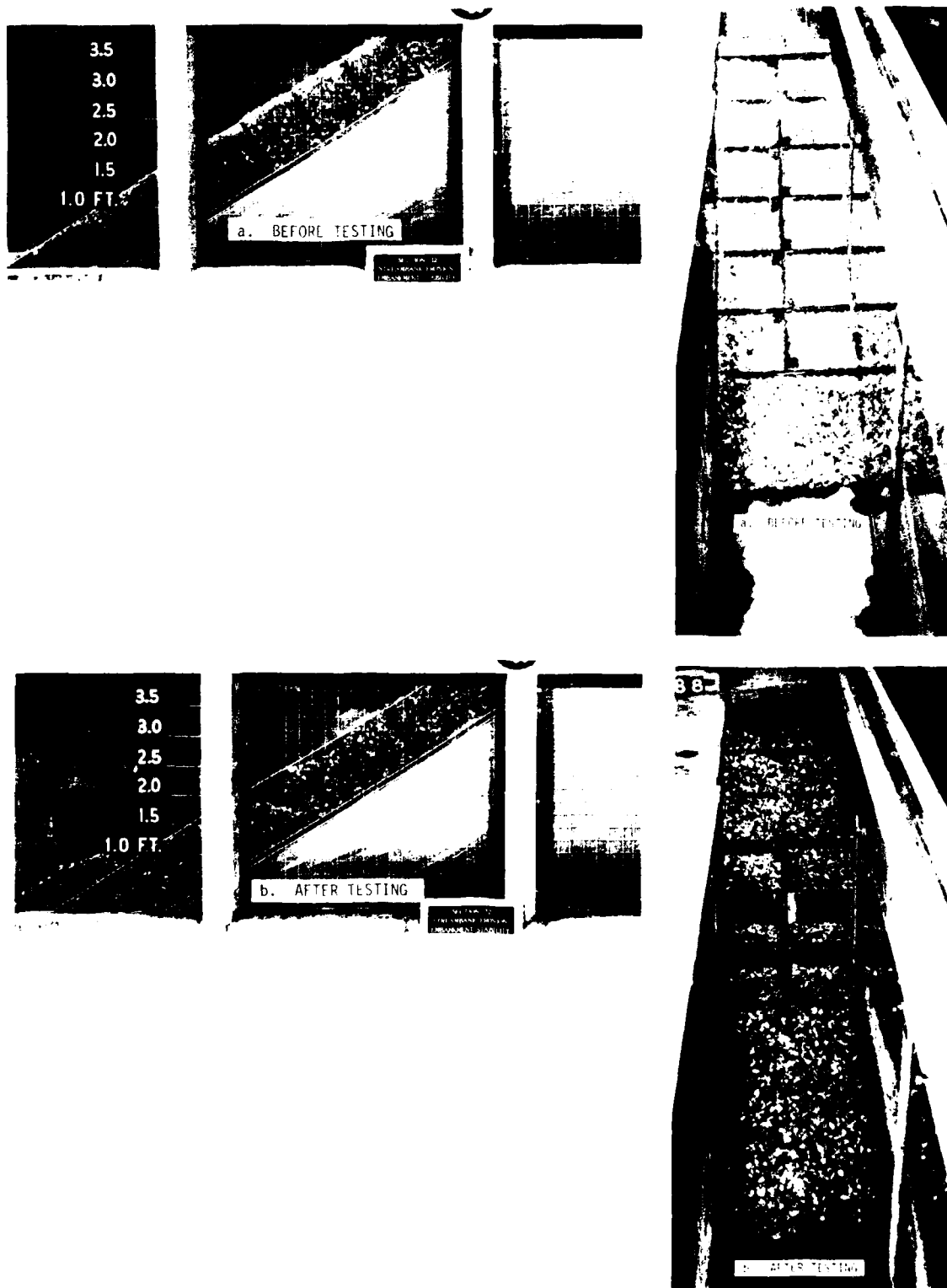


Figure 95. Plan 8B, before and after testing 2.0-sec, 0.75-ft non-breaking wave combined with 1.5-ft static differential head

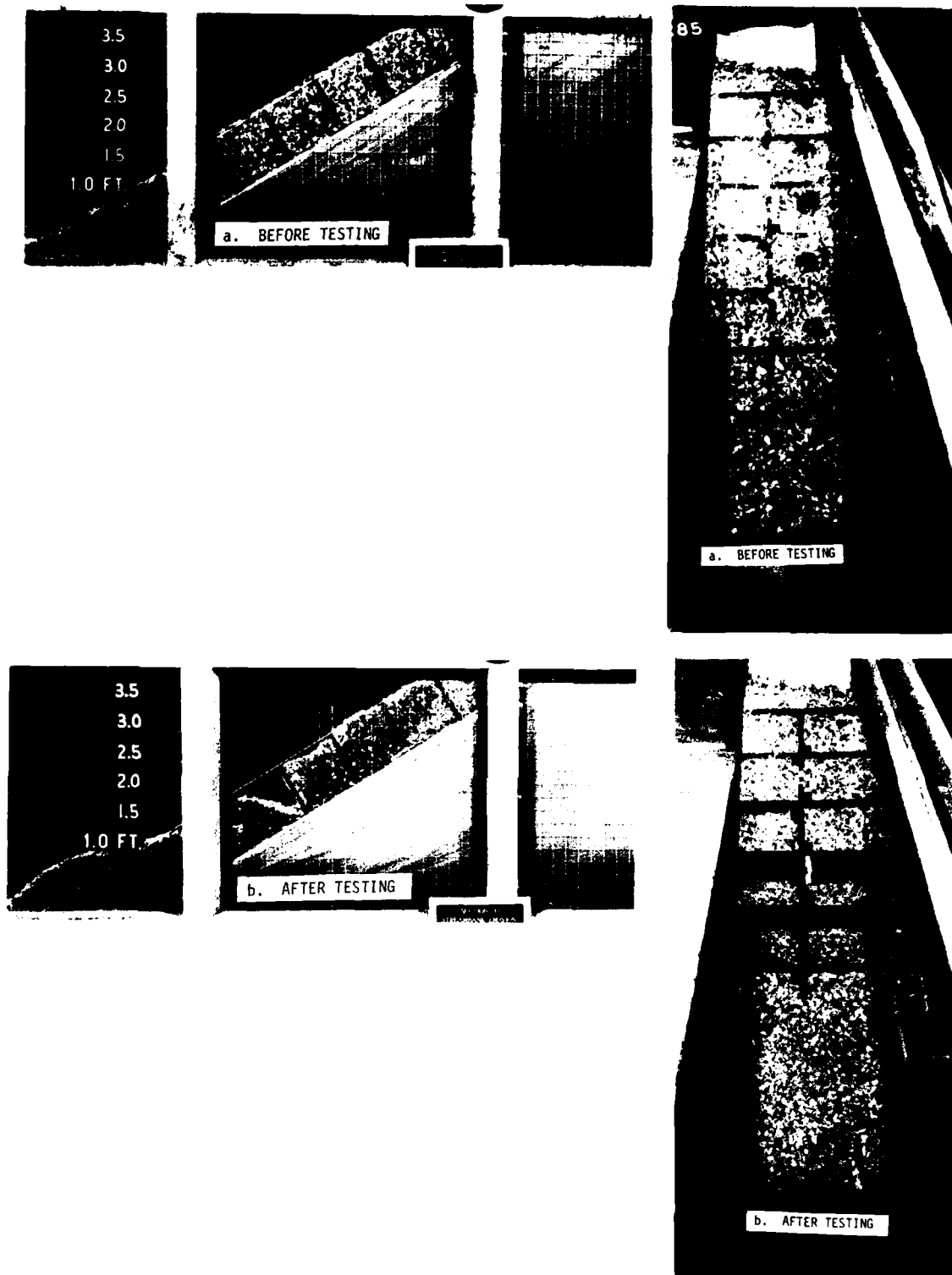


Figure 96. Plan 8C, before and after testing 2.0-sec, 0.75-ft non-breaking wave combined with 1.5-ft static differential head

and seepage flow caused the sand streambank to leach through the protective covering but this erosion proceeded at a much slower rate than had occurred in Plan 8. When the test was stopped the streambank was considered failed. The sand was still leaching and the rate of erosion was not decreasing with time. This indicated that the crown of Plan 8A would have eventually been breached had the wave action and static differential head test conditions been continued for a long enough period of time. Figure 94b shows Plan 8A when the test was stopped.

54. Plan 8B, Figure 95a, was tested to see if a 0.1-ft-thick layer of granular filter between the cells and the streambank would prevent the sand from leaching through the gravel-filled cells. The structure was exposed to 2.0-sec, 0.75-ft nonbreaking waves combined with a 1.5-ft static differential head across the structure. The cells at and below the swl were partially emptied, but the granular filter and streambank were not exposed to direct wave action. At the end of the test, the displacement of the gravel had stopped; and as shown in after-test photographs, Figure 96b, the granular filter and streambank showed no sign of damage.

55. Plan 8C, Figure 96a, was exposed to the same test conditions as Plan 8B to see if the nonwoven filter fabric would be as effective as the granular filter in stabilizing the sand streambank. At the end of the test, Plan 8C looked identical with the test results in Plan 8B except for a minor hole in the sand beneath the filter fabric. This hole was located above the swl. It appeared that the hole occurred due to both downslope movement of the sand beneath the filter fabric and a small break in the seal where the fabric was attached to the viewing windows. The hole appeared early in the test and did not worsen as the test proceeded. At the conclusion of the test, all damage to the structure had stopped. Figure 96b shows the condition of Plan 8C after testing.

PART IV: SUMMARY AND OBSERVATIONS

56. The test results reported herein demonstrate two causes of instability of noncohesive streambank material: nonbreaking wave attack and seepage flow. Waves can be either boat- or wind-generated and seepage flow is induced by a hydraulic gradient in the streambank. The hydraulic gradient occurs due to a difference in the water-surface elevations between the groundwater table and the stream, river, or reservoir. The hydraulic gradient produces flow into the streambank when the groundwater table is low relative to the stream or reservoir level and produces flow out of the streambank when these conditions are reversed. The latter case is usually the most damaging and was the only condition considered in this test series. Table 1 is an outline of the tests conducted and a tabulation of the figures that relate to each of the tests.

57. During the conduct of the demonstrations and based on the test conditions and results reported herein, the following observations were made:

- a. Plans 1 and 2 (unprotected streambanks) and Plans 4 and 5 (protected streambanks) showed high degrees of instability when exposed to seepage flow out of the streambanks while Plans 3, 5A, and 6 (protected streambanks) showed no instability.
- b. Plans 1 and 7 (unprotected streambanks) and Plan 4A (protected streambanks) were unstable when exposed to wave attack. Plans 3, 5A, and 6 (protected streambanks) showed little or no instability when exposed to the same wave conditions.
- c. Plans 8 and 8A (protected streambanks) were very unstable when exposed to the combined wave and seepage flow conditions, while Plans 3, 3A, 5A, 5B, 6, 6A, 8B, and 8C (protected streambanks) showed little or no instability when exposed to the same test conditions.
- d. When filter fabric is being used in lieu of granular filters, care must be taken to ensure that the fabric is not punctured and that the sides and toe of the filter fabric are sealed, or trenched, so that leaching of the streambank sand does not occur in these areas. Methods of attaching adjacent sections of filter fabric together was not addressed in this test series, but it is obvious that care needs to be taken to ensure that good sewn, overlapped, or welded seams are used to prevent leaching of

the streambank sand through the seams. The tests did indicate that noncohesive streambank material tends to migrate downslope beneath the filter fabric when the streambank is exposed to wave attack and/or seepage flow out of the streambank. This downslope movement of sand did not occur beneath the granular filters when the test sections were exposed to the same wave and/or seepage flow conditions.

- e. The 1.0-ft-thick layer of riprap showed more reserve stability than the 0.5-ft-thick layer. This was due to more material being available to move into damaged areas that occurred on the structure. This larger thickness also provided better streambank protection from wave attack in that more wave energy was dissipated before it reached the filter and streambank.
- f. For the limited amount of tests conducted in Plan 6B, it appears that a 2-in.-layer of sand placed over a filter fabric, to help protect the filter during riprap placement, does not have an adverse effect on the riprap or streambank stability; but it does result in movement of the riprap that otherwise would not have occurred. Therefore, if this movement is not wanted, the sand layer should not be used.
- g. All of the protective cover layers that proved successful in stabilizing the sand streambank, during wave attack and/or seepage flow out of the streambank, failed when the filters were removed from the designs. Both the riprap (a graded design for wave attack) and the gravel-filled cells withstood the design level wave attack combined with seepage flow induced by a hydraulic gradient of 0.21. These designs failed under the same test conditions when adequate filters, granular or fabric, were not provided. The same riprap gradation, placed over granular or fabric filters, was tested for drawdown rates up to 30 ft/hr and proved successful in stabilizing the sand streambank. This same gradation of riprap without a filter failed when exposed to 2-ft/hr drawdown. These tests have shown that protective cover layers that are adequately designed to be stable in a highly turbulent wave environment will not provide the needed streambank protection if adequate filters are not provided to reduce the wave energy reaching the sand streambank and prevent leaching of the sand when seepage flow out of the streambank is occurring due to a hydraulic gradient produced by either a drawdown or a static differential head condition.

REFERENCES

Office, Chief of Engineers, U. S. Army. 1971. "Earth and Rock-Filled Dams, General Design and Construction Consideration," EM 1110-2-2300, Washington, D. C.

_____. 1977. "Plastic Filter Fabric," CW-02215, Washington, D. C.

_____. 1978. "Design and Construction of Levees," EM 1110-2-1913, Washington, D. C.

_____. 1978. "Slope Protection Design for Embankments in Reservoirs," ETL 1110-2-222, Washington, D. C.

Poplin, J. K. 1965 (Sep). "Dynamic Bearing Capacity of Soils; Dynamically Loaded Small-Scale Footing Tests on Dry, Dense Sand," Technical Report No. 3-599, Report 2, U. S. Army Engineer Waterways Experiment Station, CE, Vicksburg, Miss.

Table 1
Outline Summary of Tests Conducted

-
- I. Static Differential Head Tests
 - A. Differential head = 0.5 ft; Plan 1, Figures 43 and 44
 - B. Differential head = 1.0 ft; Plan 1, Figures 45-47
 - C. Differential head = 1.95 ft; Plan 2, Figures 5, 50, and 51
 - D. Differential head = 2.0 ft
 - 1. Plan 1, Figures 48 and 49
 - 2. Plan 3, Figures 52 and 53
 - II. Rapid Drawdown Followed by 3.0-ft Static Differential Head Tests
 - A. Drawdown rate = 2.0 ft/hr
 - 1. Plan 1, Figure 54
 - 2. Plan 3, Figures 57 and 58
 - 3. Plan 4, Figures 61 and 62
 - 4. Plan 5, Figure 63
 - 5. Plan 5A, Figure 64
 - 6. Plan 6, Figure 66
 - B. Drawdown rate = 4.0 ft/hr
 - 1. Plan 1, Figure 55
 - 2. Plan 3, Figure 59
 - 3. Plan 5A, Figure 65a
 - 4. Plan 6, Figure 67a
 - C. Drawdown rate = 30.0 ft/hr
 - 1. Plan 1, Figure 56
 - 2. Plan 3, Figure 60
 - 3. Plan 5A, Figure 65b
 - 4. Plan 6, Figure 67b
 - III. Wave Penetration Tests, 2.0-, 4.0-, and 6.0-sec, 0.25- and 1.0-ft nonbreaking waves; Plan 7, Figures 68-71 and tabulation on page B-7-55.

(Continued)

Table 1 (Concluded)

IV. Wave Attack Without a Static-Differential Head Across the Streambank

A. Wave Periods = 2.0 and 4.0 sec; Nonbreaking Wave Height = 0.70 ft

1. Plan 3, Figures 72 and 73
2. Plan 5A, Figures 74 and 75
3. Plan 6, Figures 76 and 77

B. Wave Period = 2.0 sec; Nonbreaking Wave Height = 0.75 ft

1. Plan 1, Figure 78
2. Plan 3, Figure 79
3. Plan 4A, Figure 80
4. Plan 6, Figure 81

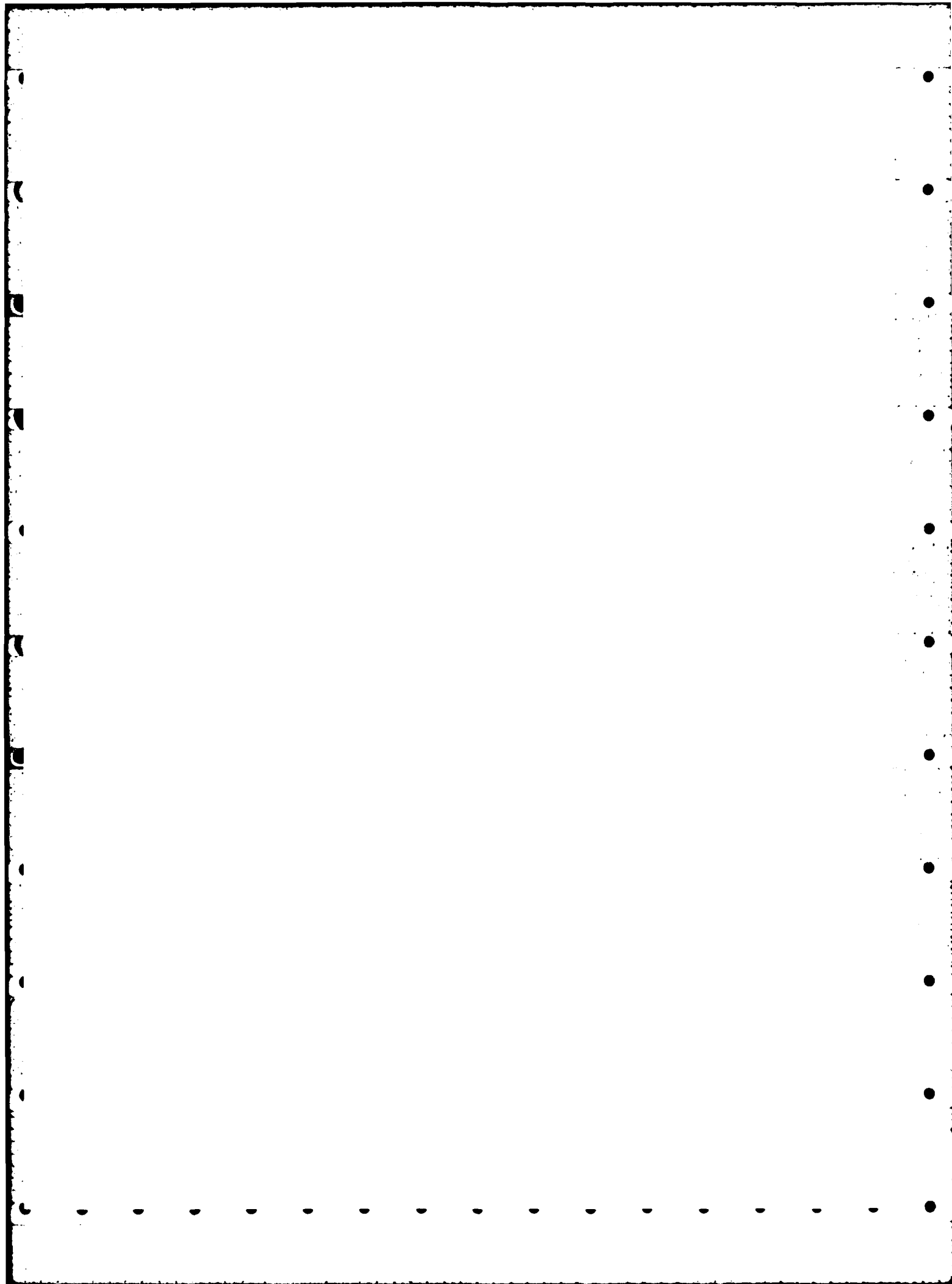
V. Wave Attack Combined with a 1.5-ft Static Differential Head Across the Streambank

A. Wave Periods = 2.0 and 4.0 sec; Nonbreaking Wave Height = 0.70 ft

1. Plan 3, Figures 82 and 83
2. Plan 5A, Figures 84 and 85
3. Plan 6, Figures 86 and 87

B. Wave Periods = 2.0 sec; Nonbreaking Wave Height = 0.75 ft

1. Plan 3, Figure 88
2. Plan 3A, Figure 89
3. Plan 5B, Figure 90
4. Plan 6A, Figure 91
5. Plan 6B, Figure 92
6. Plan 8, Figure 93
7. Plan 8A, Figure 94
8. Plan 8B, Figure 95
9. Plan 8C, Figure 96



WAVE STABILITY STUDY OF RIPRAP-FILLED CELLS

SECTION 32 PROGRAM
STREAMBANK EROSION CONTROL EVALUATION AND DEMONSTRATION
WAVE STABILITY STUDY OF RIPRAP-FILLED CELLS

Hydraulic Model Investigation

PART I: INTRODUCTION

The Prototype

1. Availability and ease of construction have made riprap the predominant method used for protecting streambanks from erosive forces. In many instances, the size of riprap needed for stability is not available locally and must be transported to the construction area. Depending on distance, the transporting costs may exceed the benefits derived from the riprap protection. When such a problem arises, alternative methods of bank protection using locally available material must be considered.

Purpose of Model Study

2. Both two-dimensional (2-D) and three-dimensional (3-D) hydraulic model investigations were conducted to test a new streambank protection concept. The concept, referred to as "Riprap-Filled Cells," consists of containerizing the riprap; and the various plans tested will be described in detail in later sections of this report. The idea behind the concept is the ability to use smaller riprap to protect streambank from wave attack that would normally require much larger riprap for stability.

PART II: THE MODEL

Design of Model

3. An undistorted linear scale of 1:4, model to prototype, was selected for both the 2-D and 3-D wave stability models. Scale selection was determined by size of model materials, capabilities of the wave generator, and water depth at the toe of the test sections. Based on Froude's model law* and the linear scale of 1:4, the following model-to-prototype relations were derived. Dimensions are in terms of length (L) and time (T).

<u>Characteristics</u>	<u>Dimensions</u>	<u>Model-Prototype Scale Relations</u>
Length	L	$L_r = 1:4$
Area	L^2	$A_r = L_r^2 = 1:16$
Volume	L^3	$V_r = L_r^3 = 1:64$
Time	T	$T_r = L_r^{1/2} = 1:2$

4. The relationship between the weight of model and prototype riprap was based on the following transference equation:**

$$\frac{(W_r)_m}{(W_r)_p} = \frac{(\gamma_r)_m}{(\gamma_r)_p} \left(\frac{L_m}{L_p} \right)^3 \left[\frac{(S_r)_p - 1}{(S_r)_m - 1} \right]^3 \quad (1)$$

where

subscripts m, p = model and prototype quantities, respectively

W_r = weight of individual stone, lb

* J. C. Stevens et al. 1942. "Hydraulic Models," Manual on Engineering Practice No. 25, American Society of Civil Engineers, New York, N. Y.

** R. Y. Hudson. 1974 (Jan). "Concrete Armor Units for Protection Against Wave Attack," Miscellaneous Paper H-74-2, U. S. Army Engineer Waterways Experiment Station, CE, Vicksburg, Miss.

γ_r = specific weight of individual stone, pcf
 L_m/L_p = linear scale of model
 S_r = specific gravity of an individual stone relative to the water in which it is placed, i.e.,
 $S_r = \gamma_r/\gamma_w$
 γ_w = specific weight of water, pcf

Specific weights of the stone and water were assumed to be the same in the model as they are in the prototype, 165 pcf and 62.4 pcf, respectively. Therefore Equation 1 reduces to:

$$\frac{(W_r)_m}{(W_r)_p} = \left(\frac{L_m}{L_p}\right)^3 \quad (2)$$

Representation of Streambank Slopes

5. The streambank slopes were represented by wooden frameworks which were filled with sand and the sand was overlaid with a sand-cement crust (Figure 1). With the state of the art as it is today, the

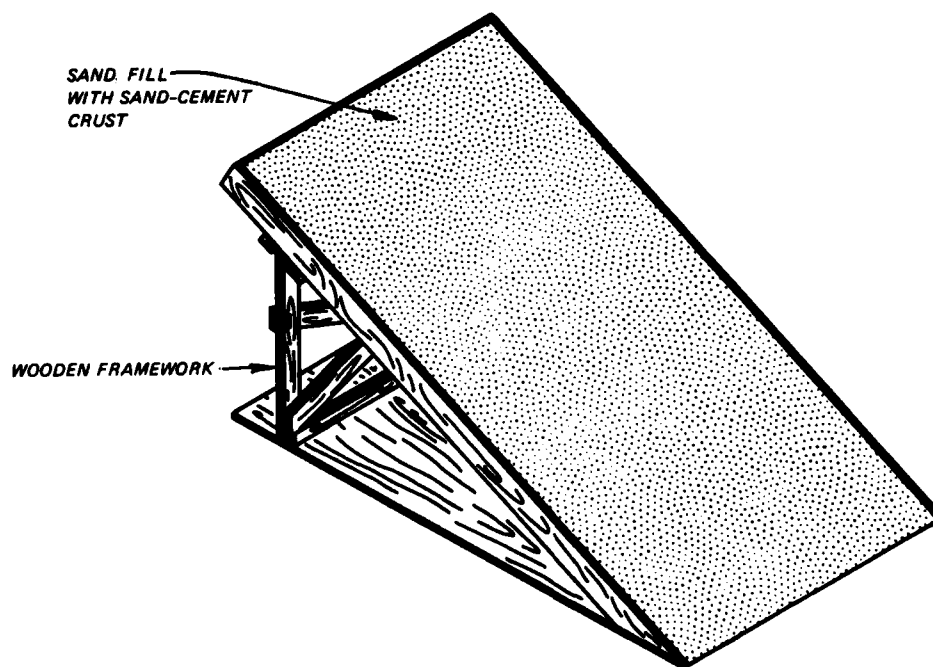


Figure 1. Wooden framework with sand fill and sand-cement crust

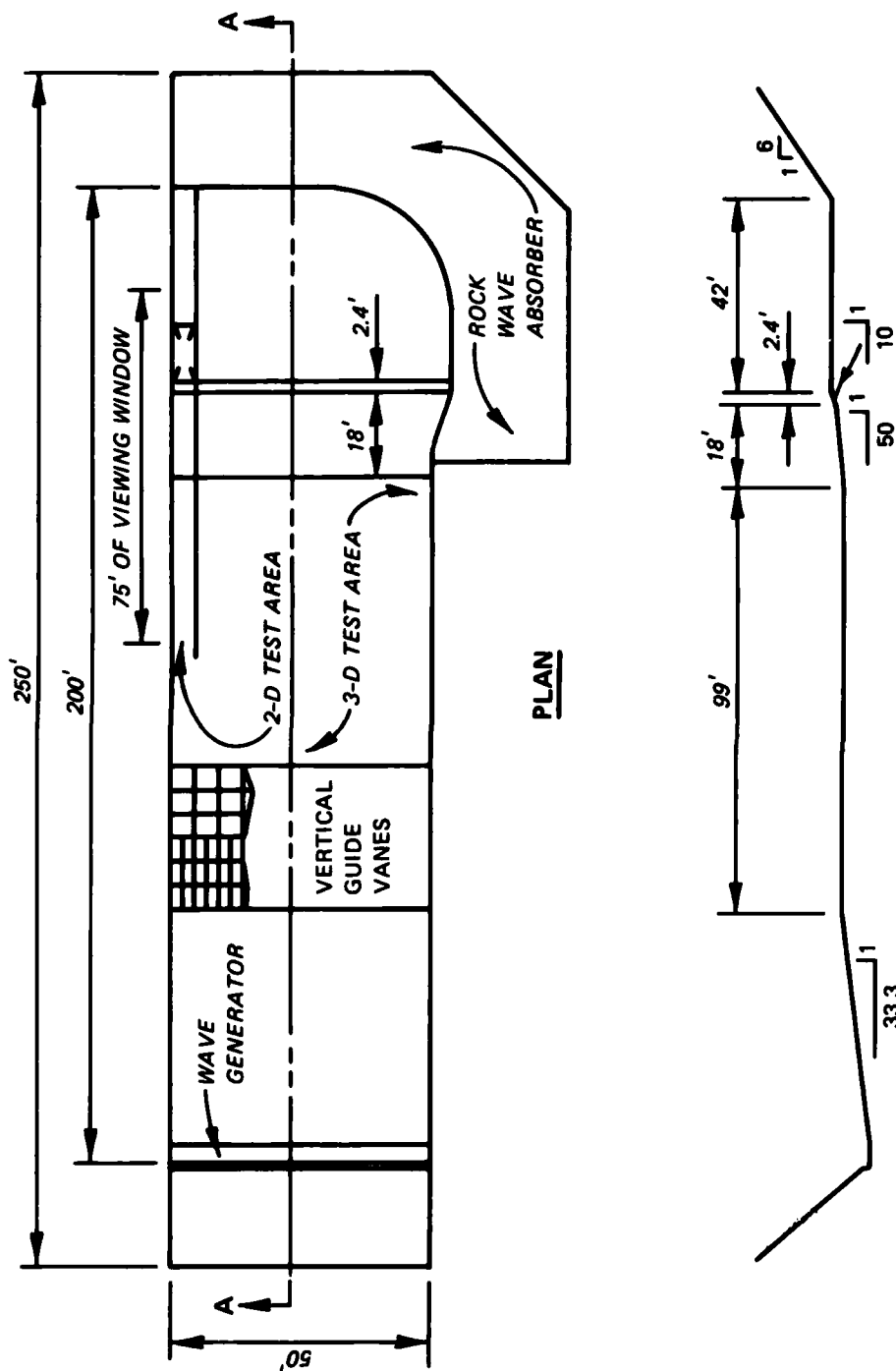
interaction of waves and streambank soils can only be simulated at a 1:1 scale. Therefore, for these 1:4-scale model tests the streambank stability was not tested and the soil was assumed to be impermeable and stable once the protection was placed on the slope. Only the stability against wave attack of the bank protection concept was tested.

Test Facilities and Equipment

6. All tests were conducted in an L-shaped concrete flume 250 ft long, 50 and 80 ft wide at the top and bottom of the L, respectively, and 4.5 ft deep (Figure 2). The 2-D tests, 90-deg wave attack, and 3-D tests, 60- and 30-deg wave attack, were tested in the flat bottom portion of the flume as indicated in Figures 2 and 3. The photograph was taken from an elevated angle, looking from the wave generator toward the test sections. The flume was equipped with a paddle-type wave generator capable of producing monochromatic waves of various periods and heights. Changes in water-surface elevations, as a function of time (wave heights), were measured by parallel, resistance, electrical wave-height gages and recorded on chart paper by an electrically operated oscillograph. The electrical output of each gage was directly proportional to its submergence depth.

Selection of Test Conditions

7. All tests were conducted for a streambank slope of 1V on 2H. Prototype wave heights ranging from 1.0 to 3.0 ft for wave periods of 2.0, 4.0, and 6.0 sec were chosen as representative of wind- and boat-generated waves. A prototype water depth of 8 ft was modeled for all tests; this water depth ensured that all waves were free of depth limitations and were mostly nonbreaking waves as are found on rivers and streams. All plans were tested for angles of wave attack of 90 deg (2-D model, wave direction 1), 60 deg (3-D model, wave direction 2), and 30 deg (3-D model, wave direction 3).



SECTION A-A

Figure 2. Flume geometry and wave stability testing area

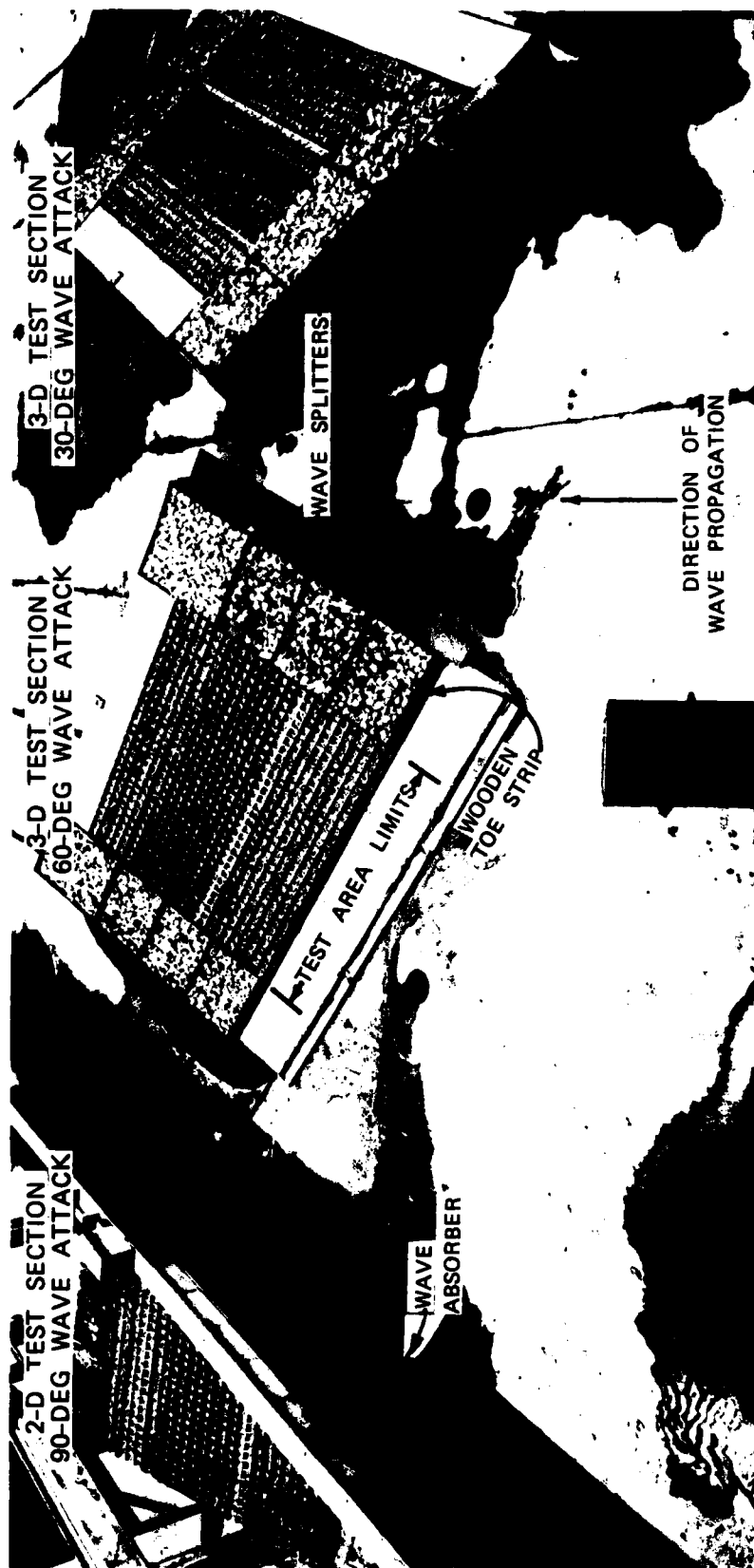


Figure 3. Orientation of test sections in test facility

PART III: TESTS AND RESULTS

Development of Plans

8. Four plans were tested. Plans 1 and 2 (Plates 1 and 2) consisted of 1-ft-cube cells. In Plan 1 the cells were filled with 0.58- to 4.6-lb riprap (Figure 4), whereas in Plan 2 the cells were only half-full of the same size riprap. Plans 3 and 4 (Plates 3 and 4) consisted of 2-ft-high by 4-ft-wide by 1.5-ft-deep rectangular cells. The same size riprap as used in Plans 1 and 2 was used to half-fill and completely fill the cells in Plans 3 and 4, respectively. The riprap-filled cells extended 4.5 ft vertically below the still-water level (swl) on all four plans and extended 6.75 and 7.2 ft vertically above the swl in Plans 1 and 2, and Plans 3 and 4, respectively. Wooden toe strips were used on all four plans, on both the 2-D and 3-D test sections, to hold the cells at the proper elevation on the streambank slopes. Galvanized sheet metal was used to construct the model cells. In the prototype, the cells could be manufactured out of wood, concrete, plastics, etc., depending on available materials and manpower capabilities. The cells could be manufactured in place on the streambank or they could be pre-fabricated units which could be transported to and set into place on the streambank slopes. The banks would have to be graded to a uniform slope and some means of anchoring the cells would have to be used. Two methods of anchoring, though not model-tested, could be: (a) partial or complete burying of the cells into the bank, or (b) construction of a longitudinal stone dike of large riprap along the toe of the slope and buttressing the base of the cells against it. Any anchoring method used needs to be substantial as the weight of the riprap-filled cells could be quite large and the downslope component of this weight will increase with increasing streambank steepness.

Discussion of Results

9. Plan 1 (Figures 5, 9, and 13) was exposed to 2.0-sec,

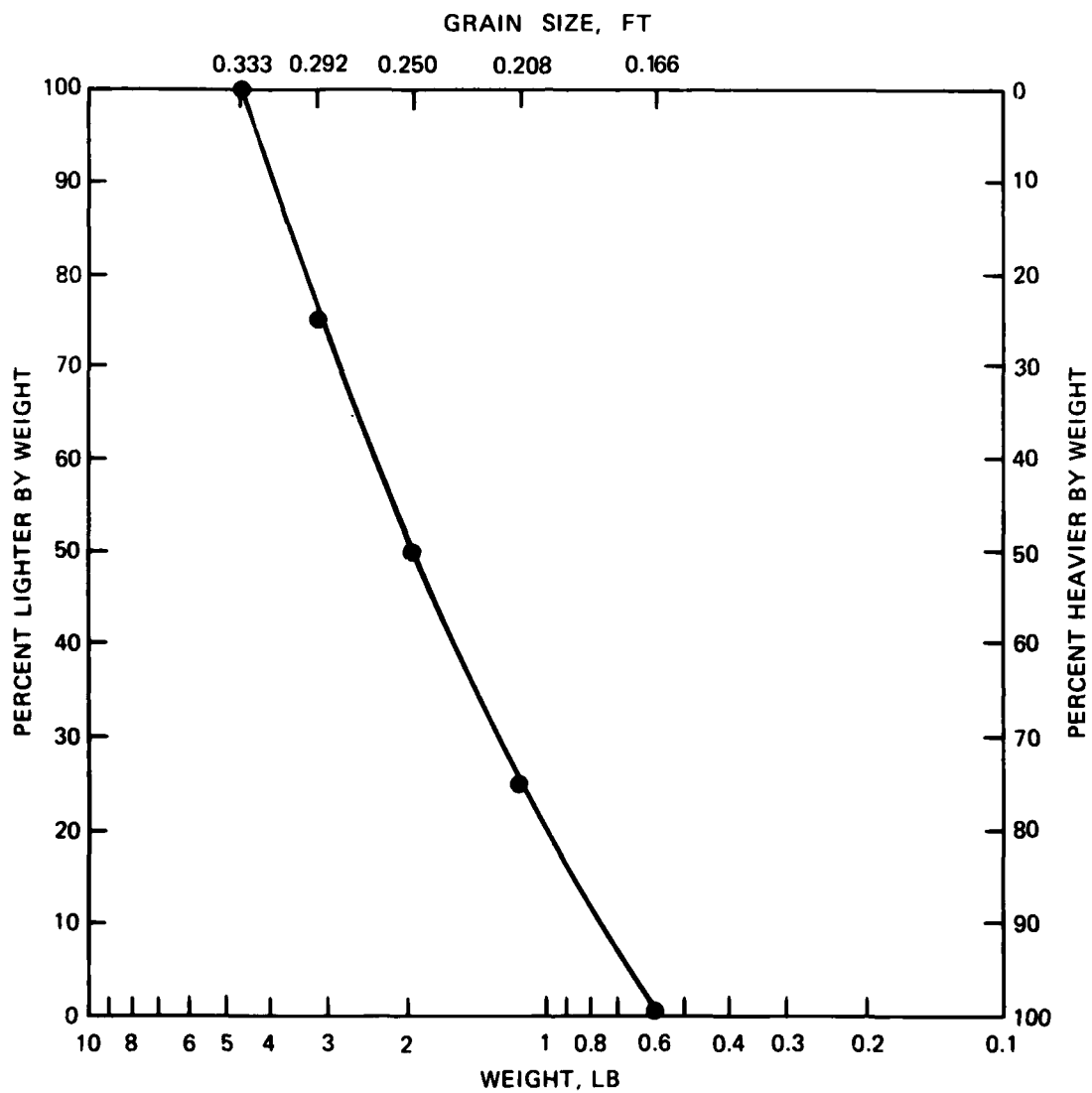


Figure 4. Riprap weight and size gradation, prototype

1.0- to 1.75-ft, 4.0-sec, 1.0- to 3.0-ft, and 6.0-sec, 1.0- to 2.5-ft nonbreaking waves for incident wave angles of 90, 60, and 30 deg. Some partial emptying of the cells occurred in the wave action zone, but none of the cells were emptied enough to cause bank exposure. The volume of riprap removed from the cells varied from one-fourth to two-thirds of the cell volume with the maximum emptying occurring at the swl. The 90- to 60-deg angles of wave attack caused similar damage, whereas the 30-deg angle of wave attack appeared to cause less riprap displacement. The area of cells showing emptying increased with increasing wave height and wave period. The structures were rebuilt after testing each wave period. Figures 6-8, 10-12, and 14-16 show the stabilized conditions of Plan 1 after testing the range of wave heights at each wave period for the three angles of wave attack.

10. Plan 2 (Figures 17, 19, and 21) was exposed to the three angles of wave attack with 2.0-sec, 1.75-ft, 4.0-sec, 3.0-ft, and 6.0-sec, 2.5-ft nonbreaking waves. Some downslope shifting of the riprap in the individual cells occurred, but no emptying of the cells occurred. Reorientation of the riprap in the cells did not result in any bank exposure, but the riprap thickness became very thin toward the upslope side of the cells in the wave action zone. The structures were not rebuilt between testing of subsequent wave conditions and Figures 18, 20, and 22 show the conditions of Plan 2 at the end of testing. Most likely Plan 2 could have withstood higher wave heights, but these were the maximum heights that could be produced for the water depth and wave periods using the available wave generator.

11. Plan 3 (Figures 23, 25, and 28) was exposed to 2.0-sec, 1.0- to 2.0-ft, and 6.0-sec, 1.0- to 3.0-ft nonbreaking waves. Photographs were taken and the structures were rebuilt after testing the range of wave heights at each wave period. For the two wave periods and three angles of wave attack, Plan 3 was stable for wave heights up to and including 1.5 ft. Some reorientation of the riprap occurred in the individual cells but no bank exposure occurred. Wave heights above 1.5 ft caused spot exposure of the streambank. No riprap was displaced out of the cells, but it shifted downslope and forward in the cells causing

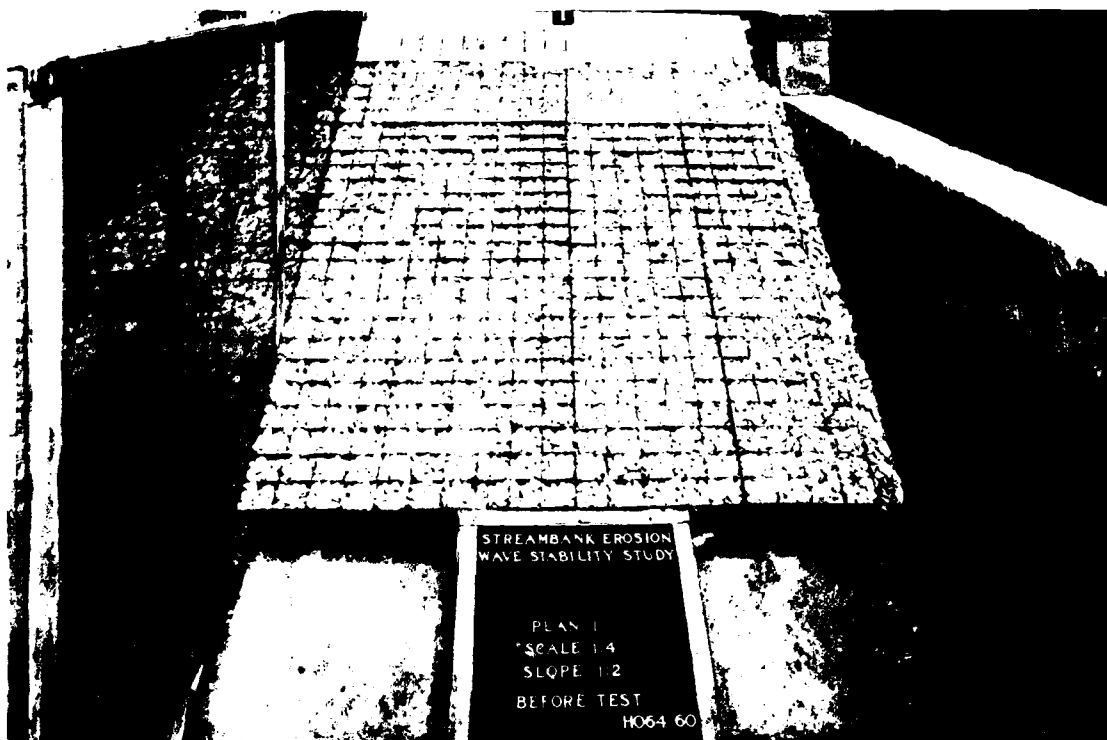


Figure 5. Plan 1, before 90-deg wave attack; wave direction 1



Figure 6. Plan 1, after exposure to 2.0-sec, 1.0- to 1.75-ft nonbreaking waves; wave direction 1

B-8-10



Figure 7. Plan 1, after exposure to 4.0-sec, 1.0- to 3.0-ft nonbreaking waves; wave direction 1



Figure 8. Plan 1, after exposure to 6.0-sec, 1.0- to 2.5-ft nonbreaking waves; wave direction 1

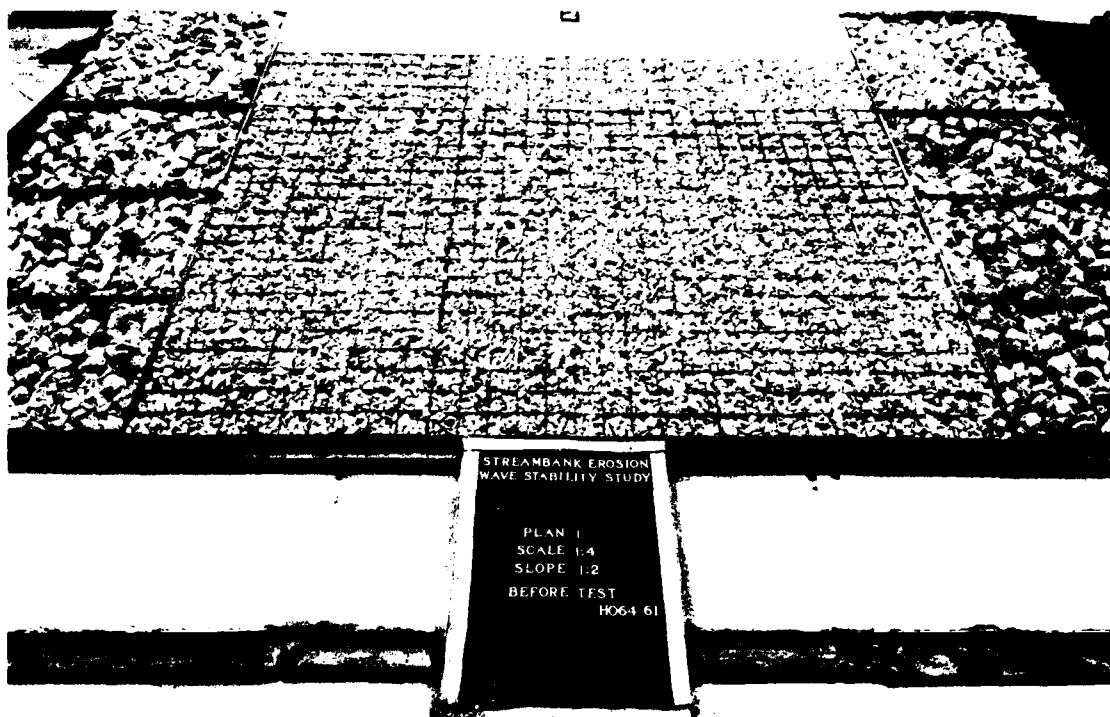


Figure 9. Plan 1, before 60-deg wave attack; wave direction 2

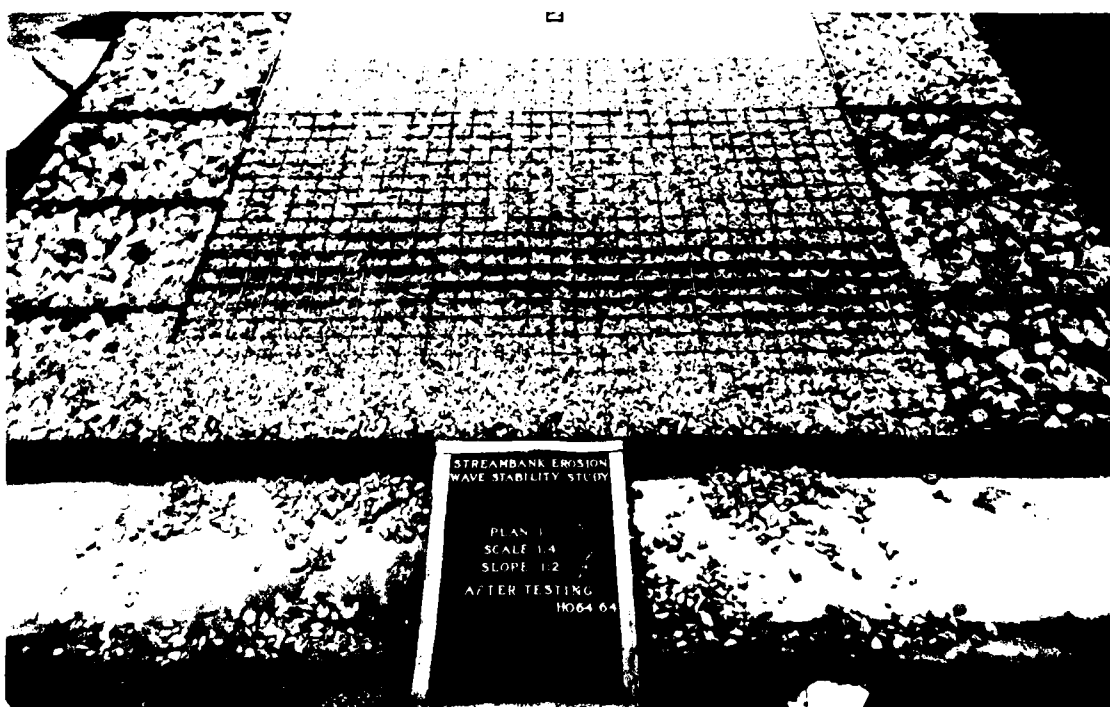


Figure 10. Plan 1, after exposure to 2.0-sec, 1.0- to 1.75-ft nonbreaking waves; wave direction 2

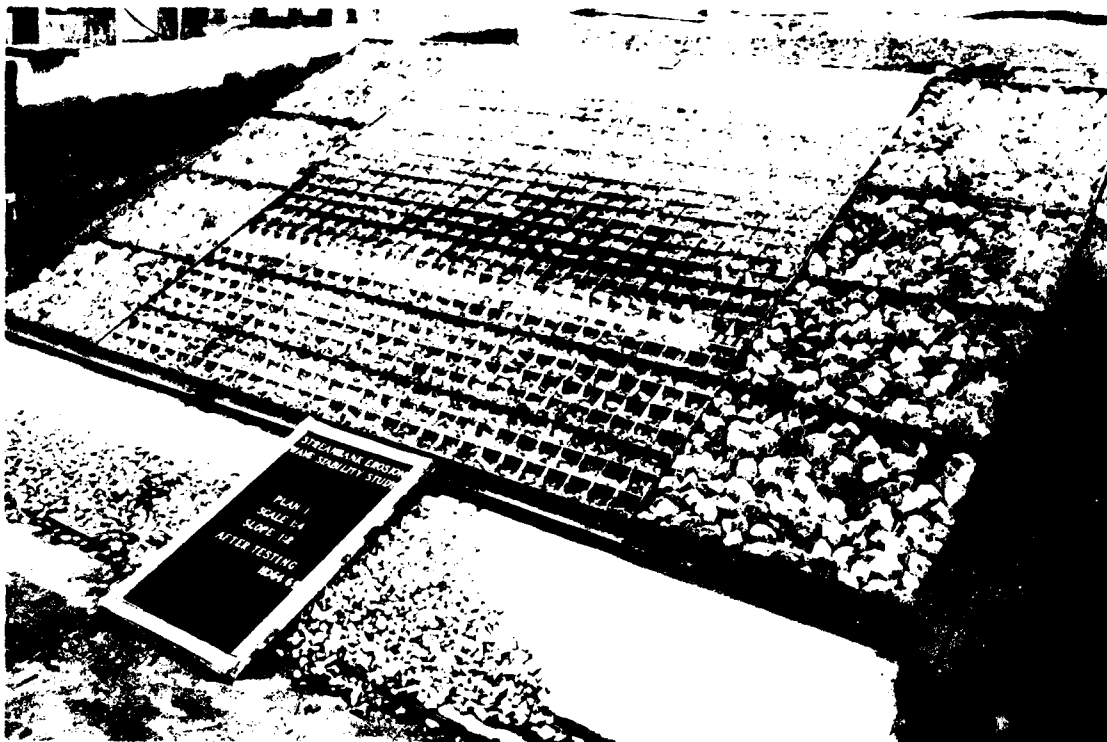


Figure 11. Plan 1, after exposure to 4.0-sec, 1.0- to 3.0-ft nonbreaking waves; wave direction 2



Figure 12. Plan 1, after exposure to 6.0-sec, 1.0- to 2.5-ft nonbreaking waves; wave direction 2



Figure 13. Plan 1, before 30-deg wave attack; wave direction 3



Figure 14. Plan 1, after exposure to 2.0-sec, 1.0- to 1.75-ft nonbreaking waves; wave direction 3

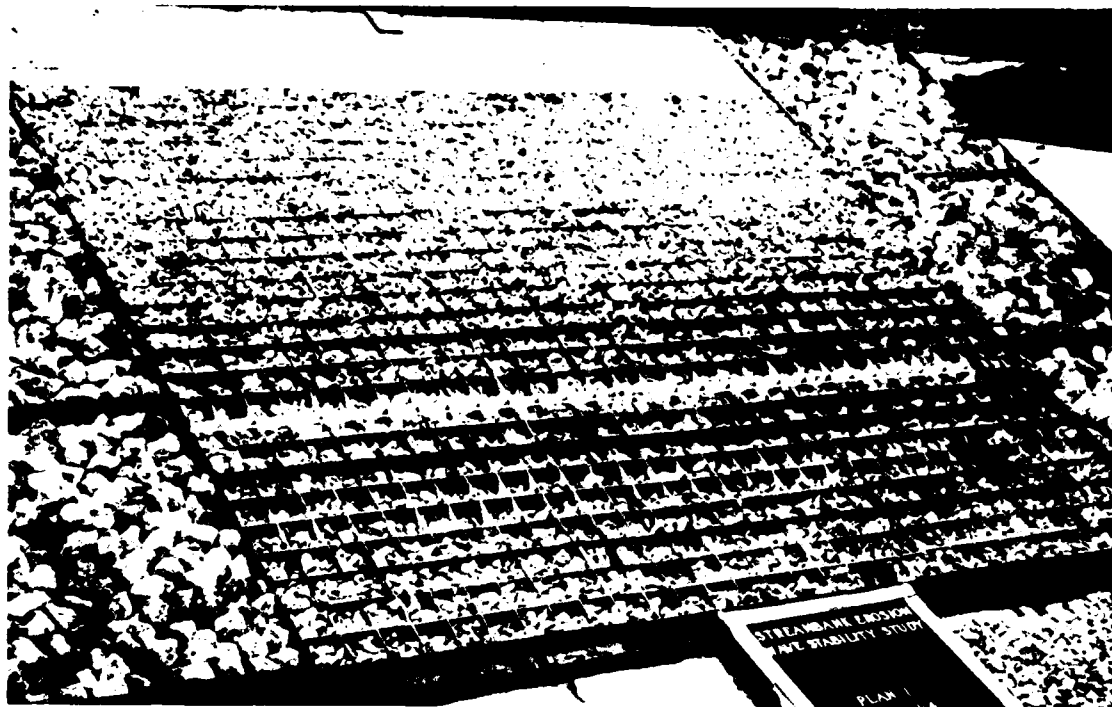


Figure 15. Plan 1, after exposure to 4.0-sec, 1.0- to 3.0-ft nonbreaking waves; wave direction 3



Figure 16. Plan 1, after exposure to 6.0-sec, 1.0- to 2.5-ft nonbreaking waves; wave direction 3

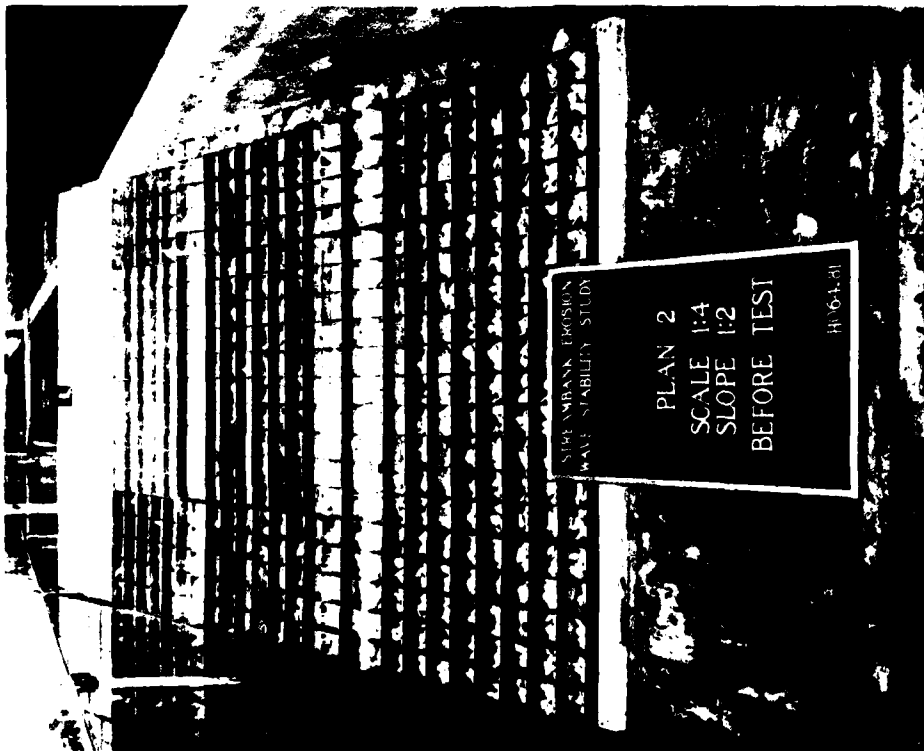


Figure 17. Plan 2, before wave attack
from wave direction 1

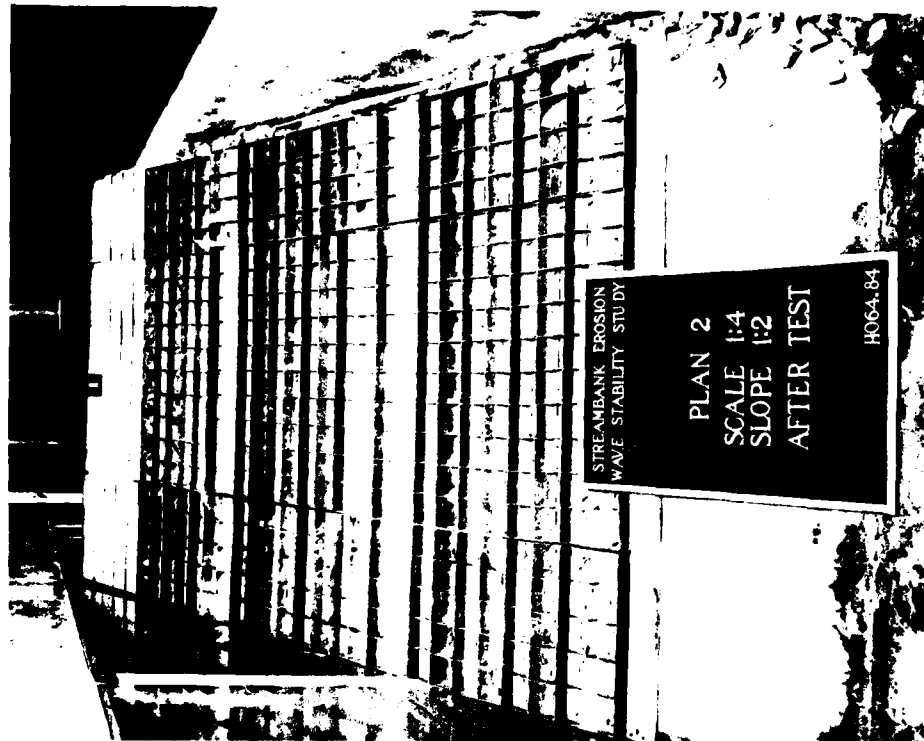


Figure 18. Plan 2, after exposure to 2.0-sec,
1.75-ft, 4.0-sec, 3.0-ft, and 6.0-sec, 2.5-ft
nonbreaking waves; wave direction 1

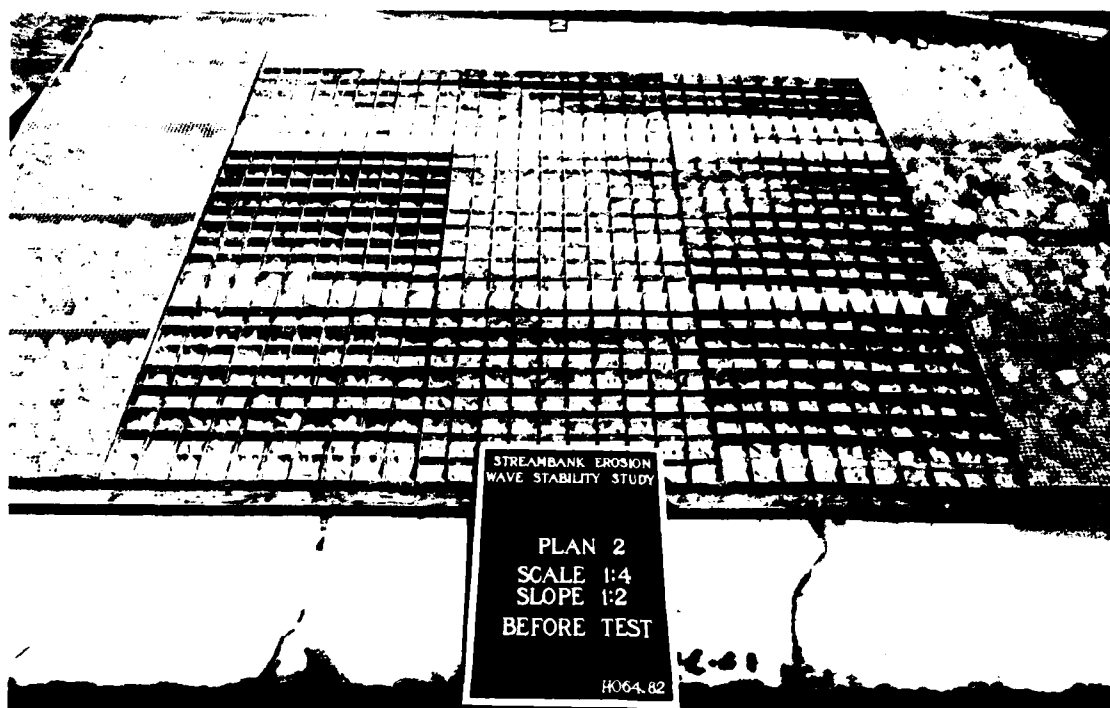


Figure 19. Plan 2, before wave attack from wave direction 2

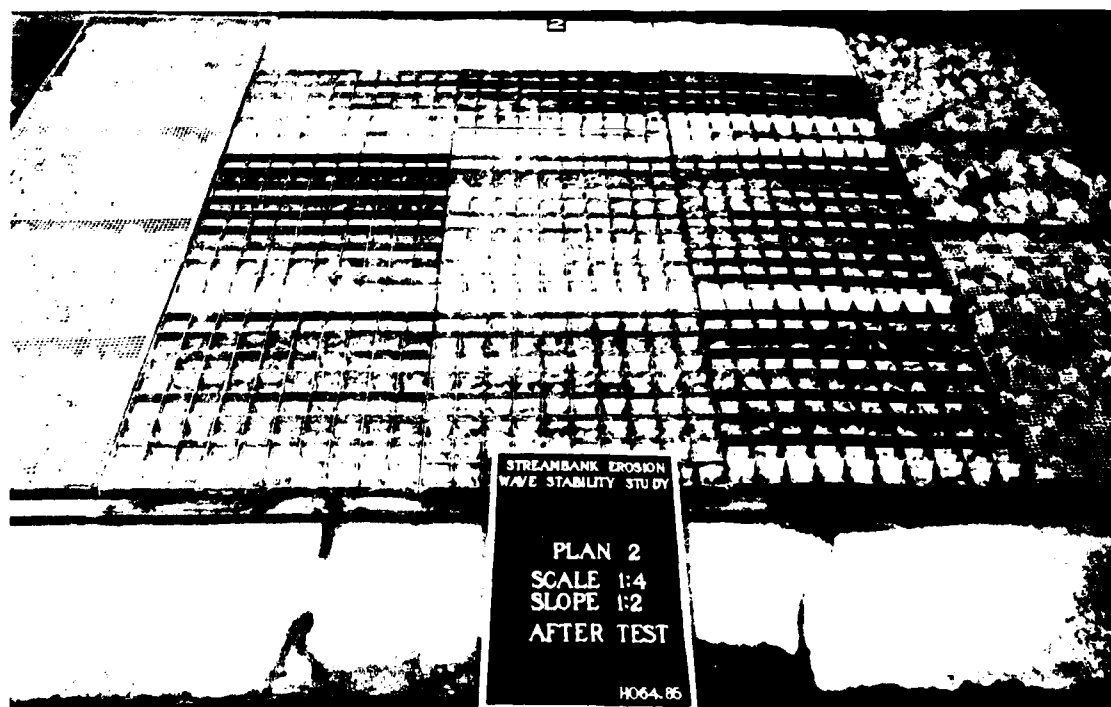


Figure 20. Plan 2, after exposure to 2.0-sec, 1.75-ft, 4.0-sec, 3.0-ft, and 6.0-sec, 2.5-ft nonbreaking waves; wave direction 2



Figure 21. Plan 2, before wave attack from wave direction 3



Figure 22. Plan 2, after exposure to 2.0-sec, 1.75-ft, 4.0-sec, 3.0-ft, and 6.0-sec, 2.5-ft nonbreaking waves; wave direction 3



Figure 23. Plan 3, before wave attack from wave direction 1

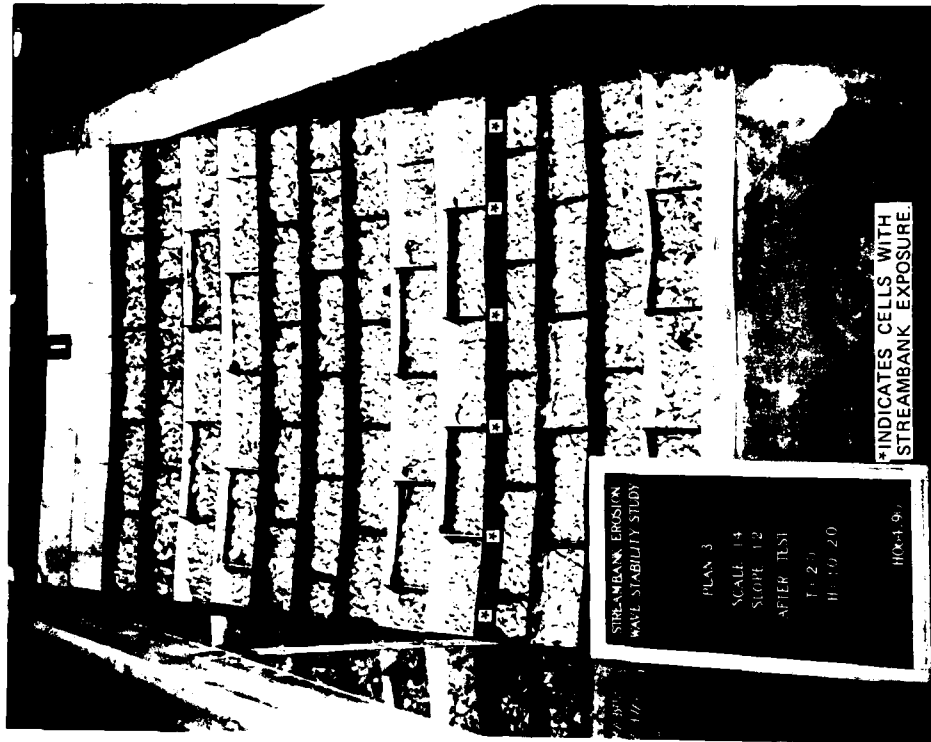


Figure 24. Plan 3, after exposure to 2.0-sec, 1.0- to 2.0-ft nonbreaking waves; wave direction 1

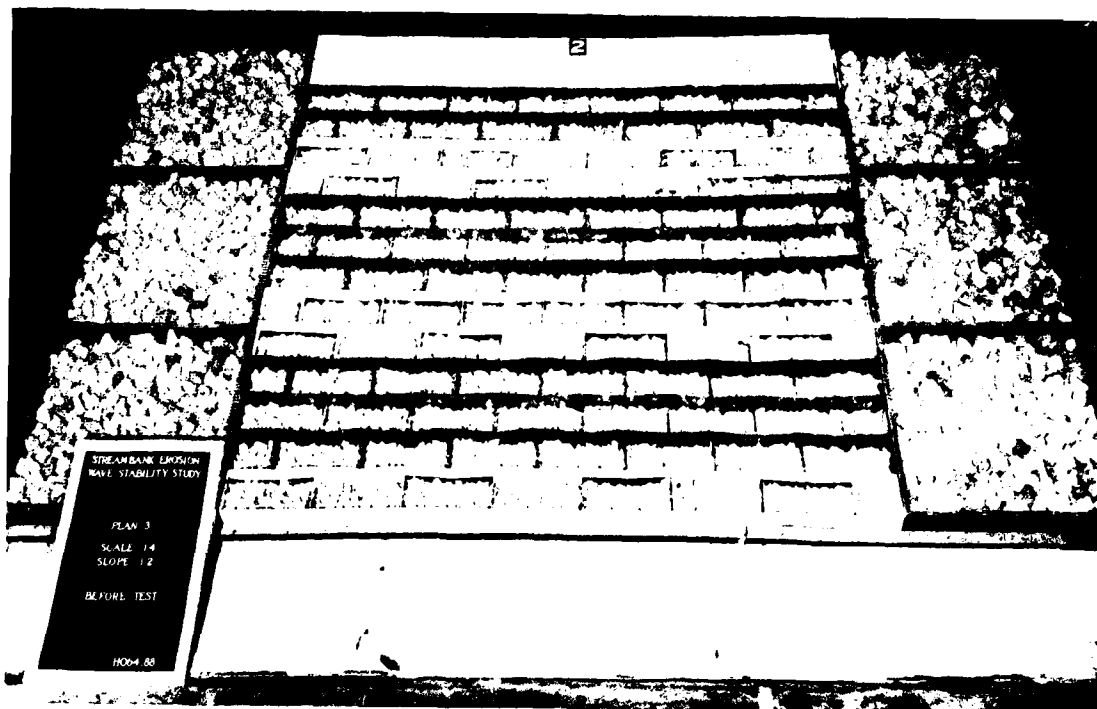


Figure 25. Plan 3, before wave attack from wave direction 2



Figure 26. Plan 3, after exposure to 2.0-sec, 1.0- to 2.0-ft nonbreaking waves; wave direction 2

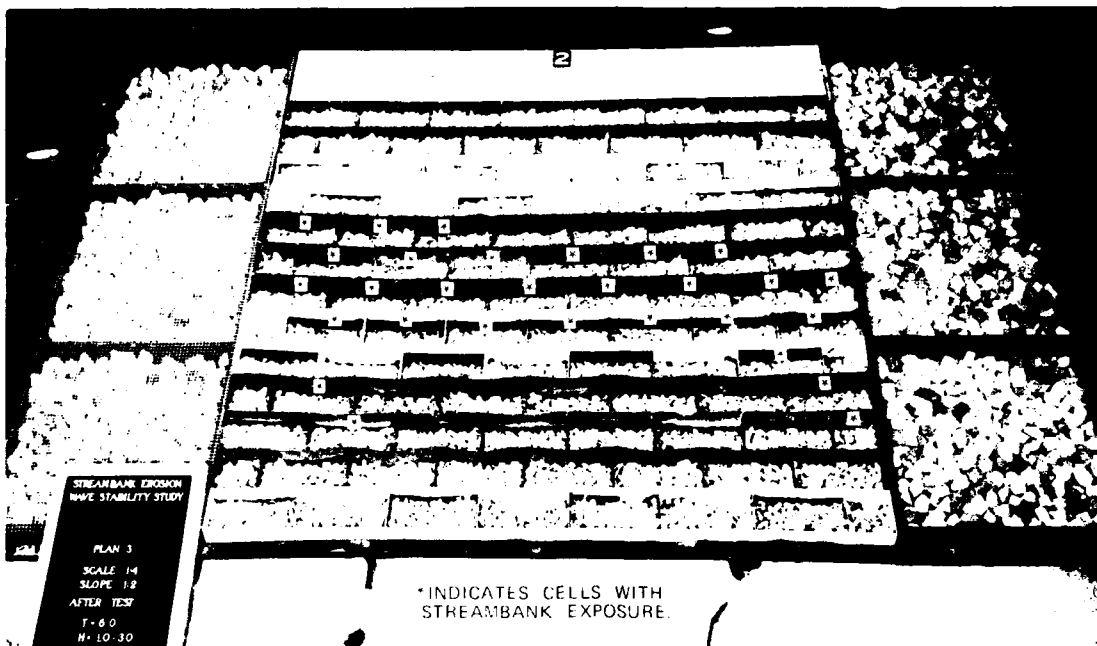


Figure 27. Plan 3, after exposure to 6.0-sec, 1.0- to 3.0-ft nonbreaking waves; wave direction 2

exposure of the streambank in the upper side of some cells. The bank exposure is indicated in after-test photographs, Figures 24, 26, 27, 29, and 30. For the 2.0-sec wave period, the 90- and 60-deg incident wave angles produced more riprap movement than the 30-deg incident wave angle. For the 6.0-sec wave period, riprap movement in the cells was similar for all three incident wave angles.

12. The 6.0-sec wave period produced the most severe wave attack and riprap movement during testing of Plan 3. For this reason, Plan 4 (Figures 31, 35, and 39) was only tested for the 6.0-sec wave period. Nonbreaking wave heights from 1.0 to 3.0 ft were tested for incident wave angles of 90, 60, and 30 deg. Plan 4 sustained its most severe damage from the 60-deg wave attack with the 30-deg wave attack causing somewhat less damage and the 90-deg wave attack causing the least damage. For all three angles of wave attack, no streambank exposure occurred for wave heights up to and including 2.0 ft. The 3.0-ft wave heights caused bank exposure for the 60- and 30-deg wave attack angles but only a maximum of two-thirds emptying of some cells for the 90-deg angle of wave

attack. As with all plans previously reported, riprap movement had stopped at the end of the tests and Figures 32, 36, and 40 show the conditions of Plan 4 after testing.

13. During the testing of Plan 4, photographs were taken to show the wave action produced by the three angles of wave attack. The wave runup and rundown are shown in Figures 33, 34, 37, and 38 for the 90- and 60-deg wave attack angles. Figure 41 shows the waves moving across the cells being exposed to an incident angle of 30 deg.

14. Runup (R_u) and rundown (R_d) were observed and recorded for all the wave conditions tested on Plans 1-4. Runup is the distance a wave progresses upslope, measured vertically above the swl, and the rundown is the distance a wave progresses downslope, measured vertically below the swl. These data are presented in Table 1. Relative runup (R_u/H) as a function of wave steepness (H/L) and relative depth (d/L) are presented in Plates 5-8 and 9-11, respectively, where d = water depth, H = wave height, and L = wavelength. Plates 12-15 and 16-18 present relative rundown (R_d/H) as a function of H/L and d/L , respectively. Due to the very limited data for Plan 4, plots of R_u and R_d versus d/L are not presented.

15. These data show both R_u and R_d for Plans 1-4 subjected to nonbreaking waves to be functions of H/L , d/L , and angle of wave attack. In general, the 60-deg angle of wave attack produced the largest R_u and R_d with the 90-deg angle of wave attack showing the next highest values. The 30-deg angle of wave attack produced the smallest values of R_u and R_d . There were sufficient data on Plans 1 and 3 to see a general trend for both R_u and R_d to decrease with increasing values of H/L and d/L . Due to the limited amount of data on Plans 2 and 4, trends of R_u and R_d as functions of H/L and d/L are not well defined.

16. No major differences in R_u and R_d were observed for the two cell sizes tested. When the cells of Plans 1 and 4 were full of riprap the R_u and R_d were larger than what occurred for the same wave conditions in Plans 2 and 3, respectively. As riprap was displaced

and the cells of Plans 1 and 4 became partially emptied, the R_u and R_d decreased and were similar to what occurred in Plans 2 and 3, respectively.



Figure 28. Plan 3, before wave attack from wave direction 3

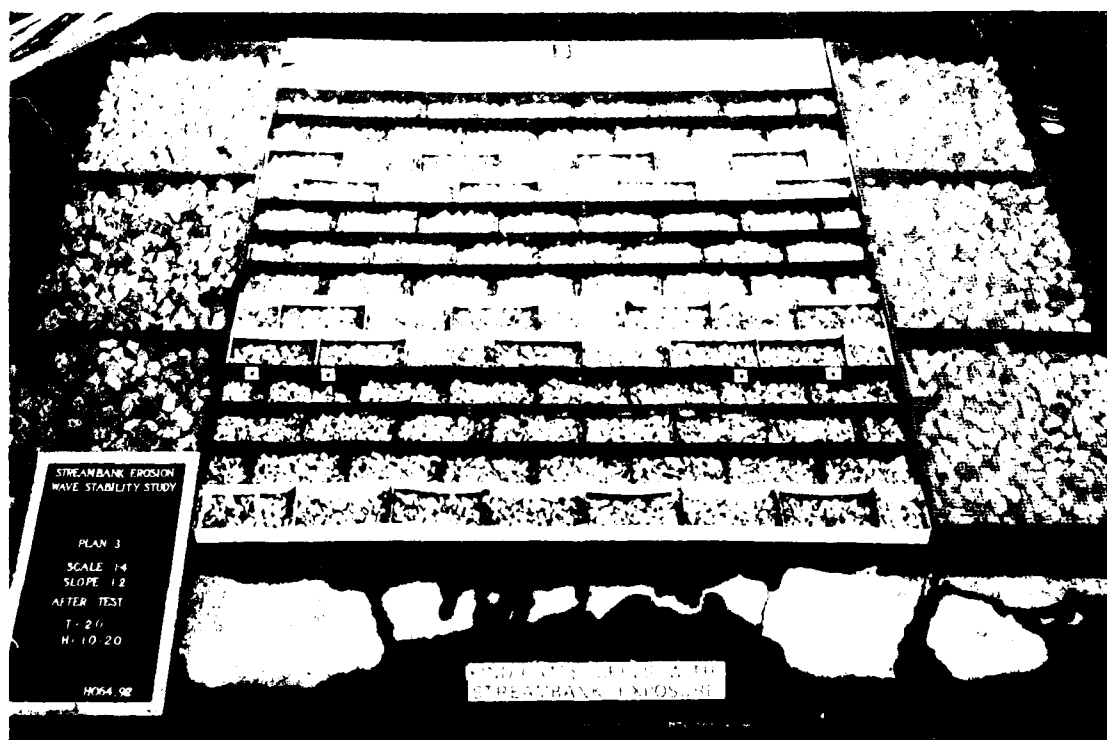


Figure 29. Plan 3, after exposure to 2.0-sec, 1.0- to 2.0-ft nonbreaking waves; wave direction 3

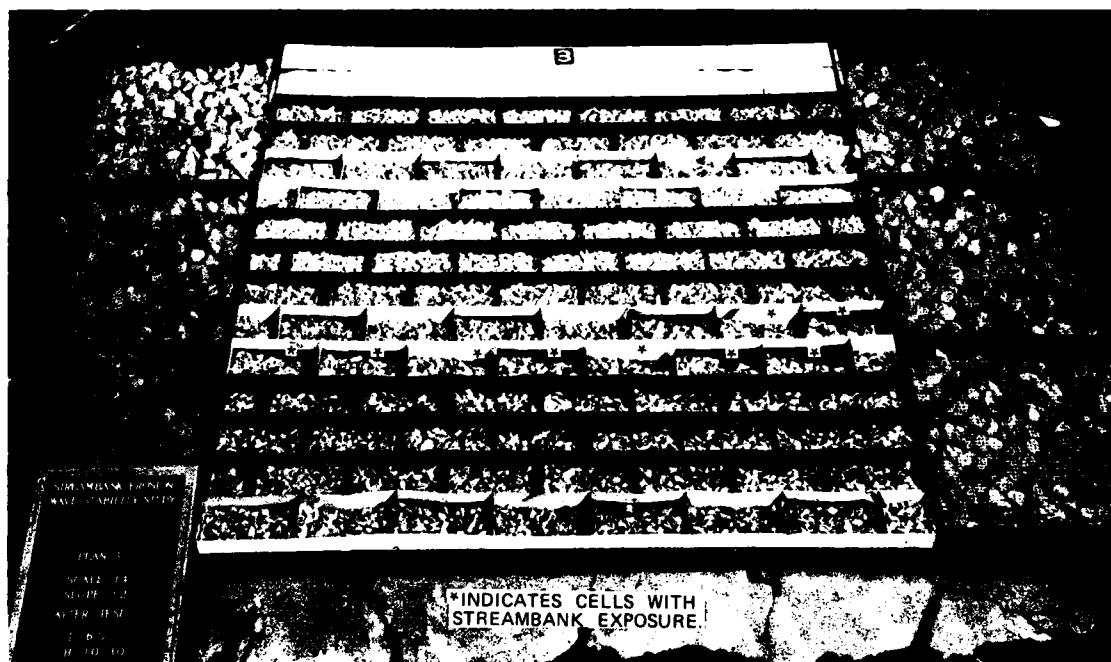


Figure 30. Plan 3, after exposure to 6.0-sec, 1.0- to 3.0-ft nonbreaking waves; wave direction 3

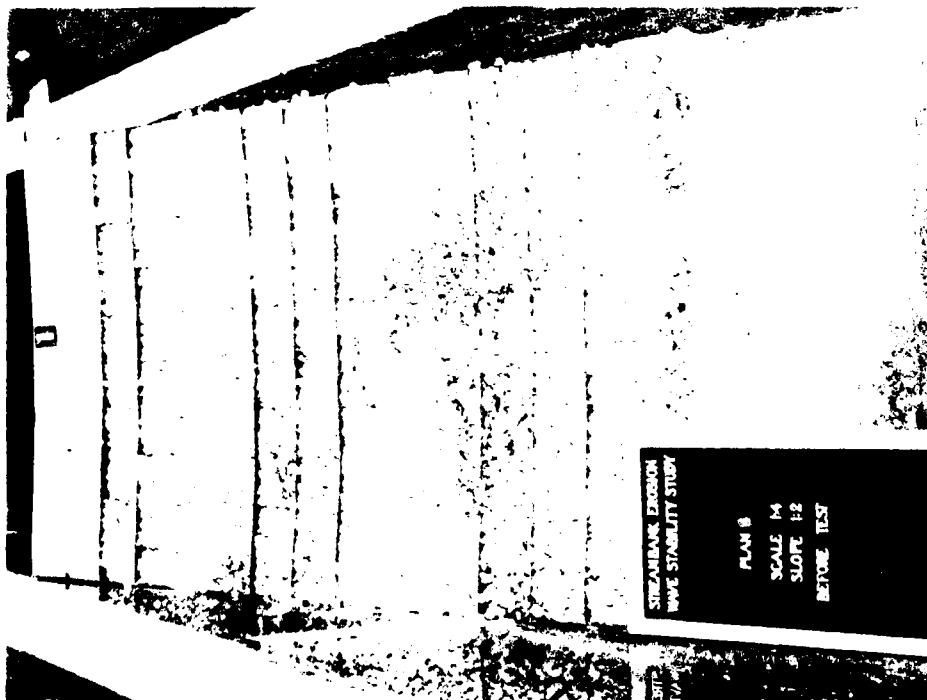


Figure 31. Plan 4, before wave attack from wave direction 1

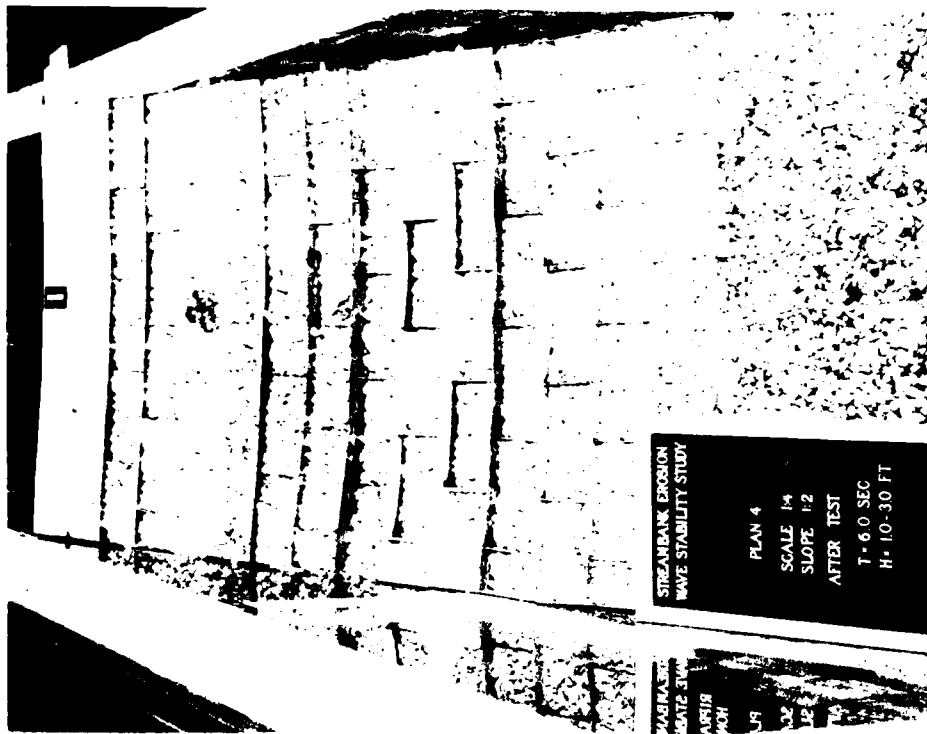


Figure 32. Plan 4, after exposure to 6.0-sec, 1.0- to 3.0-ft nonbreaking waves; wave direction 1



Figure 33. Wave runup on Plan 4 for 6.0-sec,
3.0-ft nonbreaking waves; wave direction 1

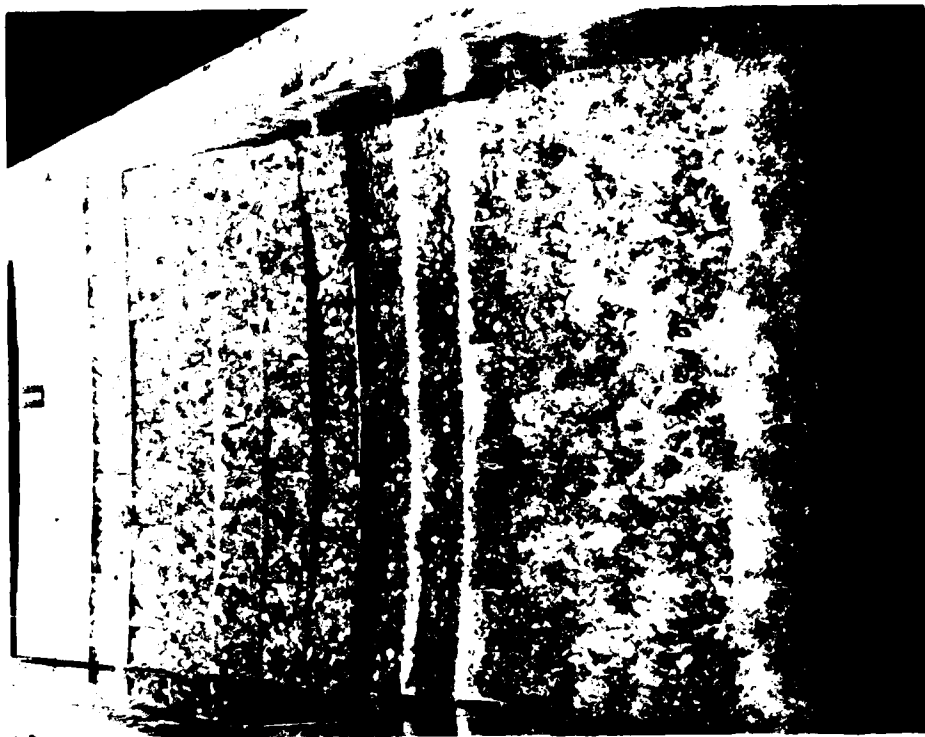


Figure 34. Wave rundown on Plan 4 for 6.0-sec,
3.0-ft nonbreaking waves; wave direction 1

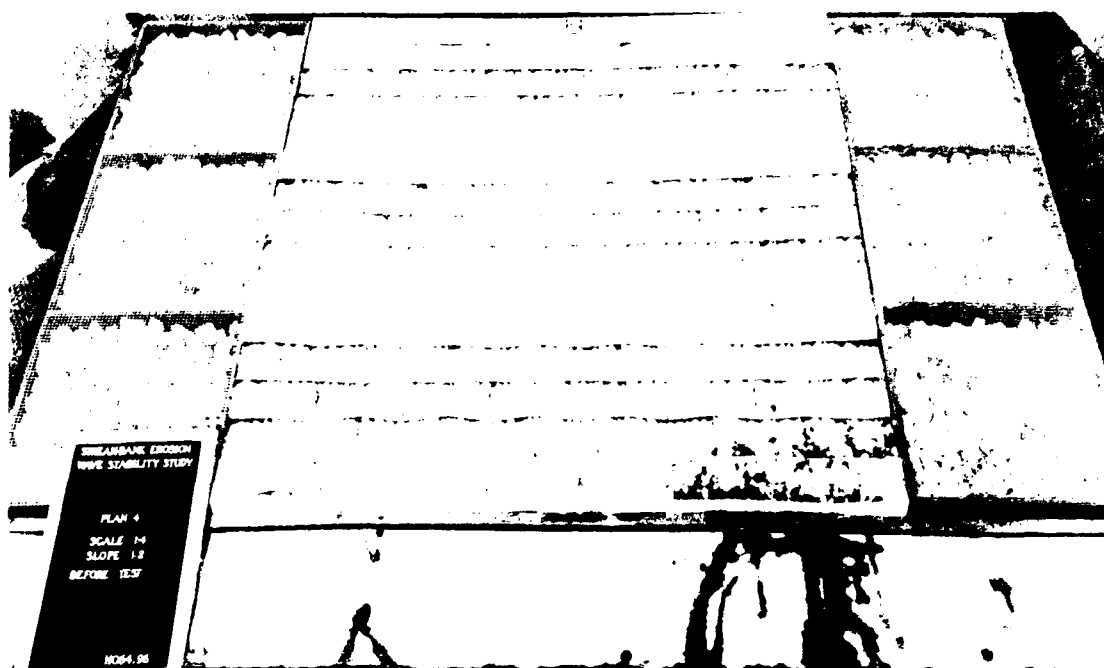


Figure 35. Plan 4, before wave attack from wave direction 2

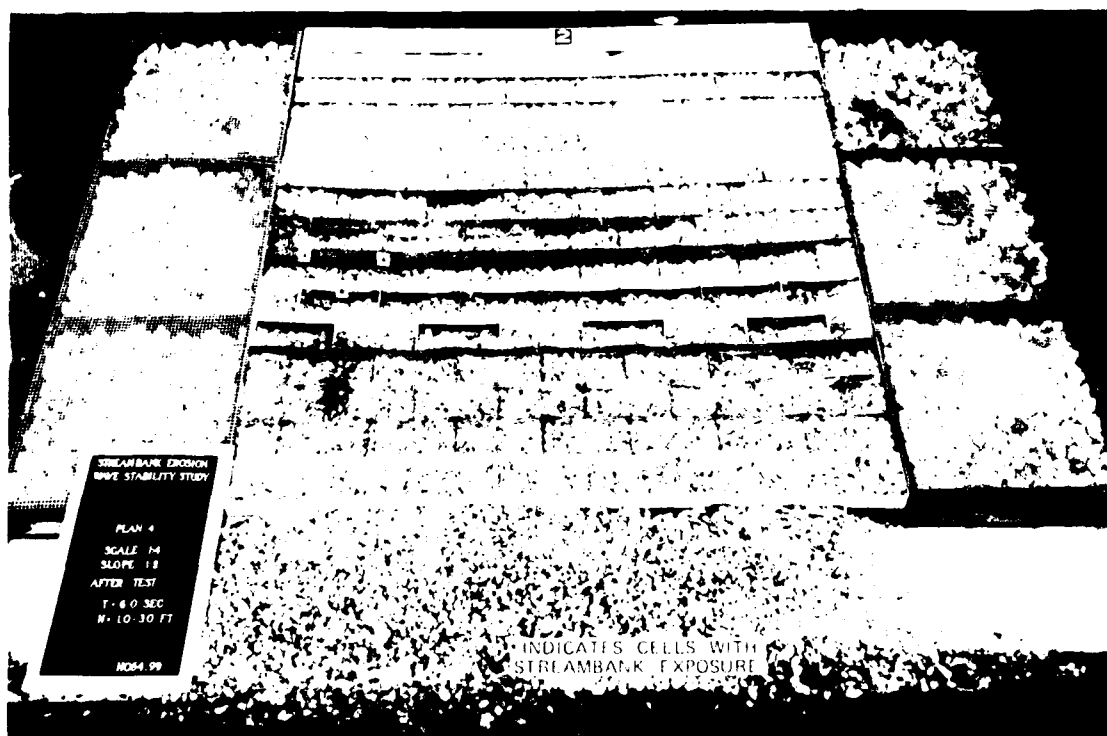


Figure 36. Plan 4, after exposure to 6.0-sec, 1.0- to 3.0-ft nonbreaking waves; wave direction 2

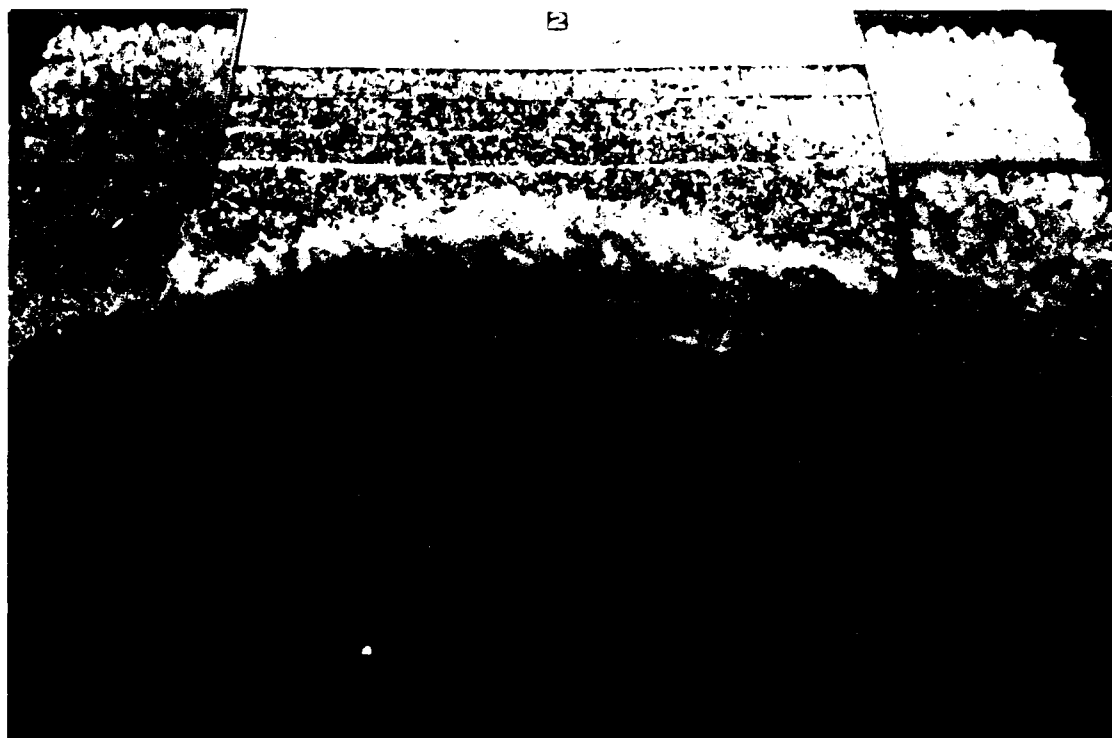


Figure 37. Wave runup on Plan 4 for 6.0-sec, 3.0-ft nonbreaking waves; wave direction 2

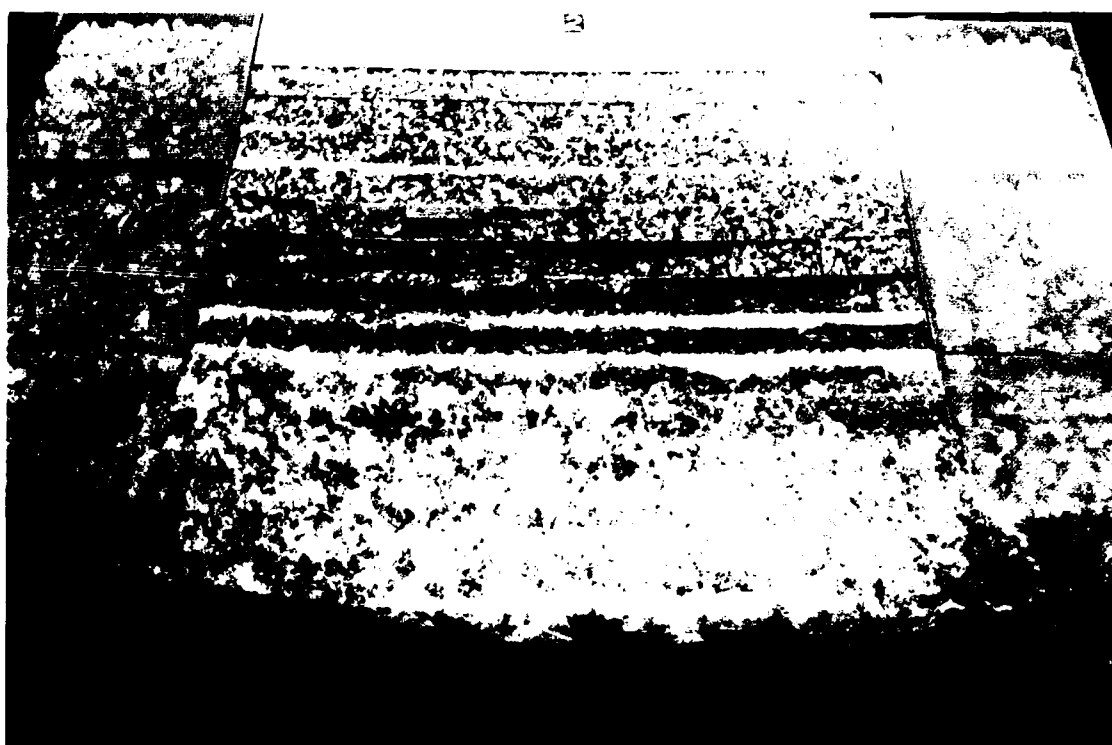


Figure 38. Wave rundown on Plan 4 for 6.0-sec, 3.0-ft nonbreaking waves; wave direction 2

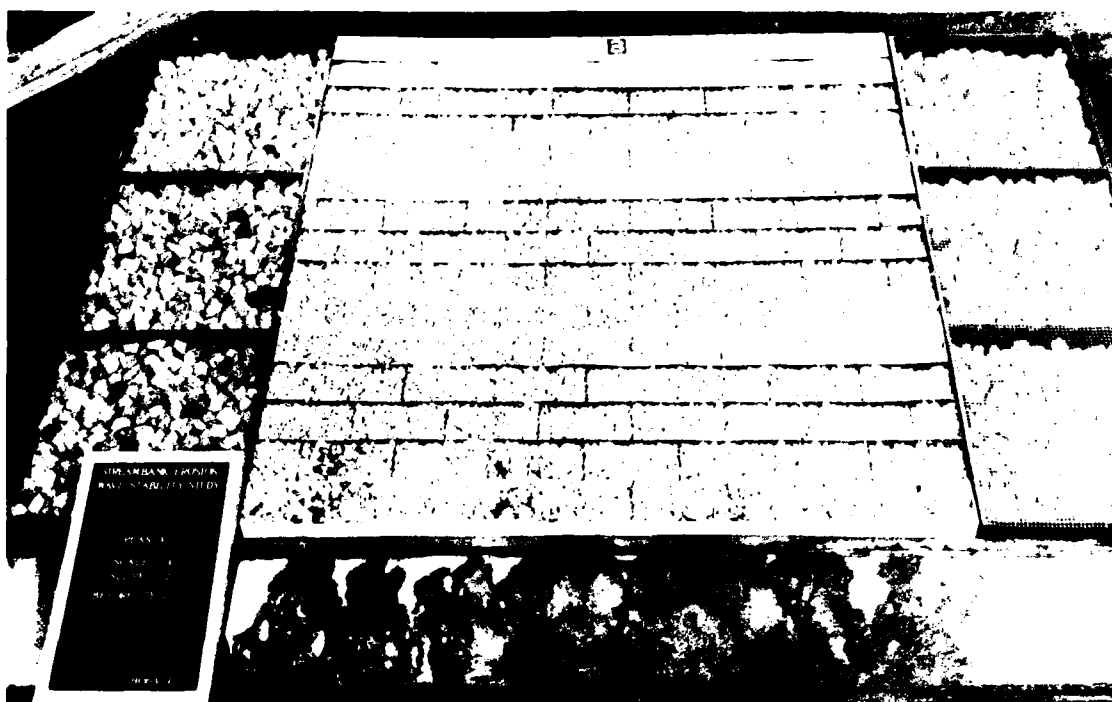


Figure 39. Plan 4, before wave attack from wave direction 3

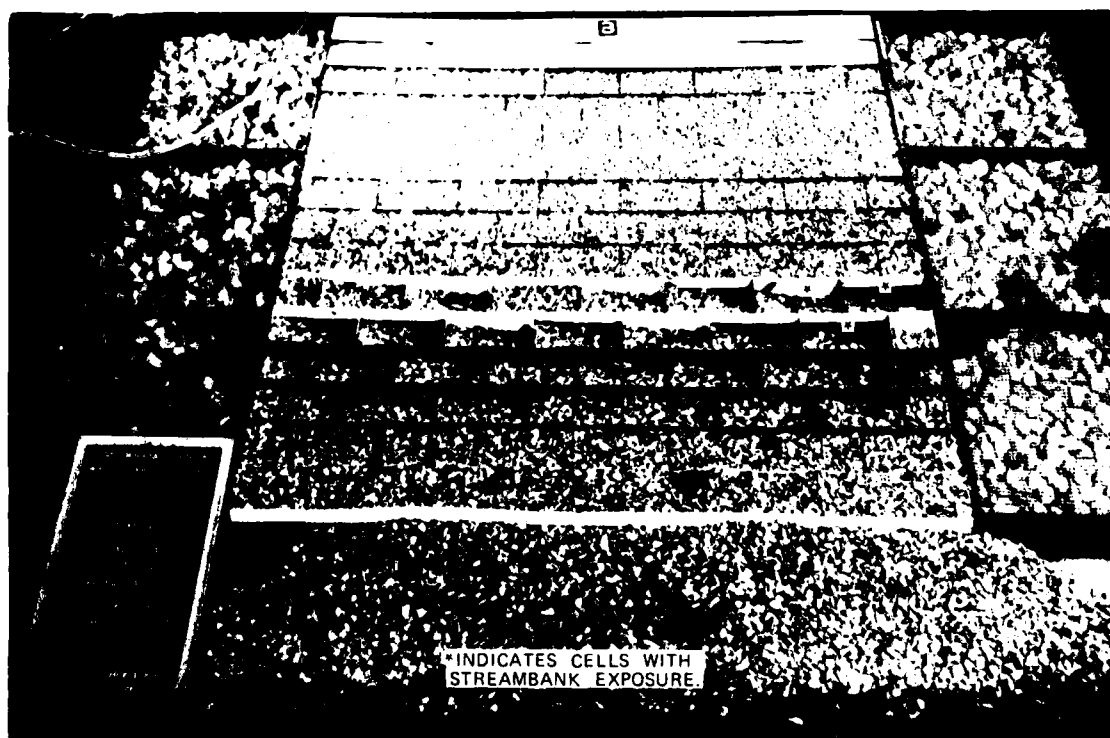


Figure 40. Plan 4, after exposure to 6.0-sec, 1.0- to 3.0-ft nonbreaking waves; wave direction 3

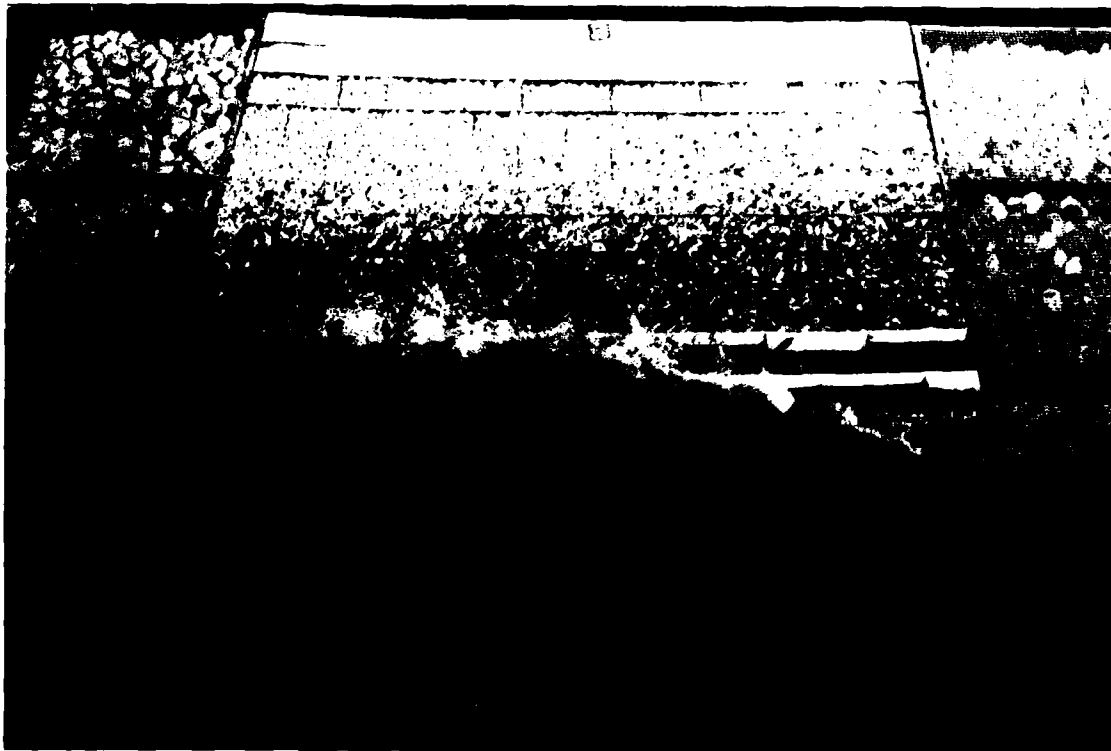


Figure 41. Wave runup on Plan 4 for 6.0-sec, 3.0-ft
nonbreaking waves, wave direction 3

PART IV: CONCLUSIONS FROM 1:4-SCALE MODEL TESTS

17. Based on the 1:4-scale model tests and results reported herein for the "riprap-filled cells" bank protection placed on 1V-on-2H streambank slopes that are assumed to be stable and impermeable and for angles of wave attack of 90, 60, and 30 deg, it is concluded that:

- a. Plans 1 and 2 (1-ft-cube cells, full and half-full) are stable (no streambank exposure) for 2.0-sec, 1.0- to 1.75-ft, 4.0-sec, 1.0- to 3.0-ft, and 6.0-sec, 1.0- to 2.5-ft nonbreaking waves.
- b. Plan 3 (rectangular cells, half-full) was stable for non-breaking wave heights up to and including 1.5 ft for wave periods of 2.0 and 6.0 sec. Wave heights exceeding this produced spot exposures of the streambank.
- c. Plan 4 (rectangular cells, full) was stable for 6.0-sec, nonbreaking wave heights up to and including 2.0 ft. Wave heights exceeding 2.0 ft produced spot exposures of the streambank.
- d. Both runup (R_u) and rundown (R_d) for Plans 1-4 subjected to nonbreaking waves appear to be functions of wave steepness (H/L), relative depth (d/L), and angle of wave attack. The angles of wave attack, listed in descending magnitudes of R_u and R_d produced, are 60, 90, and 30 deg. Plans 1^u and 3 show trends of decreasing R_u and R_d for increasing values of H/L and d/L . Insufficient data are available for these trends to be well defined for Plans 2 and 4.

PART V: DISCUSSION AND RECOMMENDATIONS

18. Limited 2-D tests at a 1:1 scale have been conducted on the 1-ft-cube cells with both gravel and riprap fill. These tests indicate that as with other bank protection concepts, care must be taken to provide an adequate filter between the cells and the streambank composed of noncohesive soils. More detailed results of these tests are included in Appendix B-7.

19. The cell depth needed for stability of riprap fill increases with increasing steepness of the streambank slope and increasing height of the individual cells (Figure 42). If the cell is full of riprap and begins to empty under wave attack, the riprap surface usually approaches

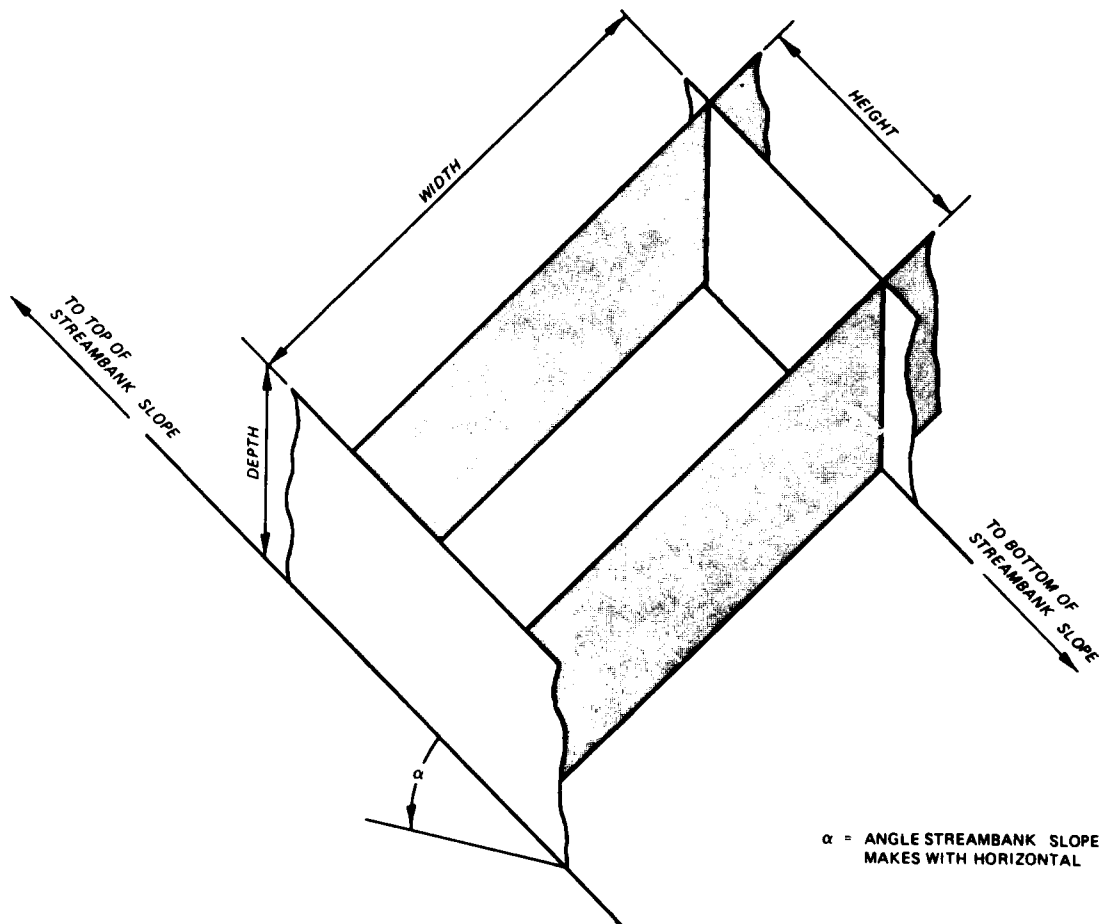


Figure 42. Nomenclature for cell sizing

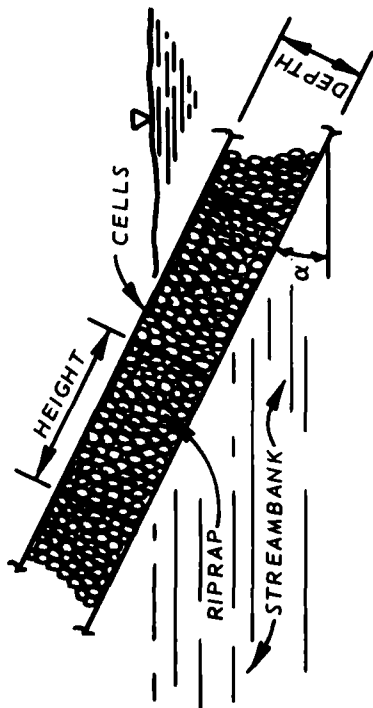
approximately a horizontal profile. If the cell is not deep enough to contain the riprap for the cell height and streambank slope, bank exposure will occur in the upper portion of the cells (Figures 43a and 43b, and Figures 24, 26, 27, and 30). Partial emptying of the cells will most likely not cause streambank exposure if a sufficient cell depth is used for a given streambank slope and cell height (Figures 43c and 43d). The following equation could be used as a starting point for selecting the cell depth.

$$\text{Depth} \geq 1.33 \times \tan \alpha \times \text{Height} \quad (3)$$

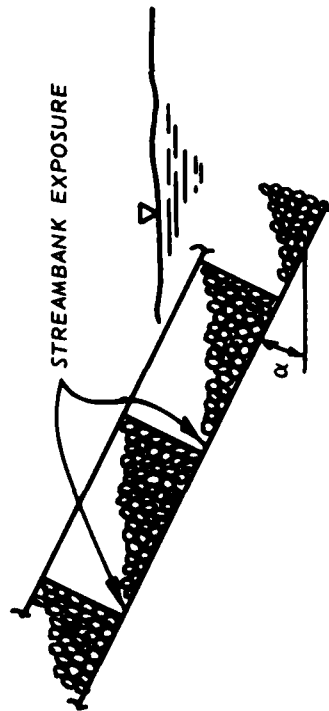
To allow for an adequate thickness of riprap a cell height of less than 10 to 12 in. would not be recommended. Even so, this cell height will not assure that streambank exposure will not occur. If the riprap is too light relative to the incident wave energy, the cell could be emptied more than what is depicted in Figure 43d.

20. As stated earlier, model cells were constructed of galvanized sheet metal due to ease of construction. Methods and material for prototype construction have not been investigated. It is recommended that close scrutiny be given to the economics of building and placing the cells. Once the cost of prototype construction is better understood, an economic analysis could be done to determine the most economical bank protection method. In some cases, transporting larger riprap to an area lacking a local source may be less costly than the construction and placing of the riprap-filled cells.

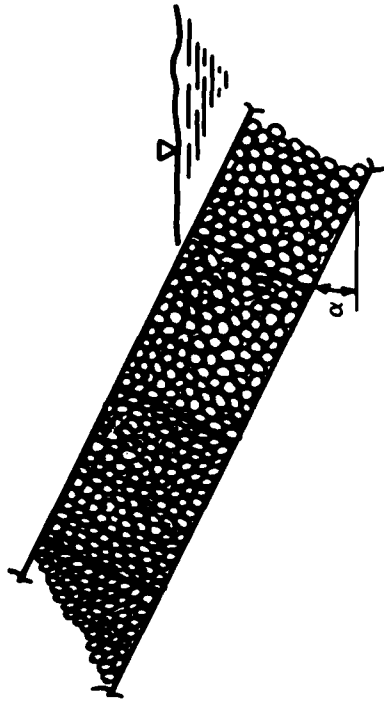
21. Further testing is needed to gain more insight into the riprap-filled cells concept. Additional testing should pursue the optimizing of cell size and geometry and riprap weight relative to incident wave periods, wave heights, angles of wave attack, current velocity, and streambank slopes.



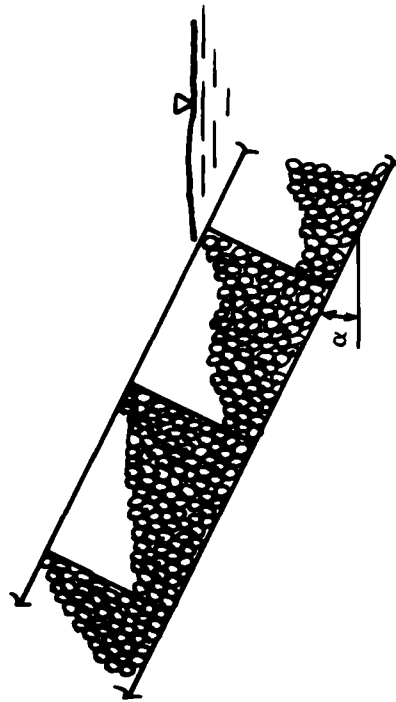
a. Cells filled before wave attack;
 α = angle streambank slope makes
 with horizontal



b. Cells partially emptied by wave attack



c. Cells filled before wave attack.



d. Cells partially emptied by wave attack.

Figure 43. Cross-sectional views of riprap-filled cells

Table 1
Values of R_u/H and R_d/H for Riprap-Filled Cells

d/L	T , sec	H , ft	H/L	R_u , ft	R_u/H	R_d , ft	R_d/H
<u>Plan 1, 90-deg Wave Attack</u>							
0.09	6.0	1.0	0.011	1.56	1.56	1.56	1.56
0.09	6.0	1.5	0.016	2.45	1.63	1.56	1.04
0.09	6.0	2.0	0.022	2.92	1.46	2.02	1.01
0.09	6.0	2.5	0.027	3.81	1.52	2.45	0.98
0.14	4.0	1.0	0.017	1.56	1.56	1.56	1.56
0.14	4.0	1.5	0.026	2.24	1.49	1.56	1.04
0.14	4.0	2.0	0.035	3.35	1.68	1.34	0.67
0.14	4.0	2.5	0.043	3.94	1.58	2.45	0.98
0.14	4.0	3.0	0.052	4.75	1.58	2.02	0.67
0.40	2.0	1.0	0.050	1.13	1.13	0.89	0.89
0.40	2.0	1.5	0.074	1.79	1.19	0.89	0.59
0.40	2.0	1.75	0.087	1.56	0.89	0.68	0.39
<u>Plan 1, 60-deg Wave Attack</u>							
0.09	6.0	1.0	0.011	2.02	2.02	1.56	1.56
0.09	6.0	1.5	0.016	3.35	2.23	2.02	1.35
0.09	6.0	2.0	0.022	4.24	2.12	2.45	1.23
0.09	6.0	2.5	0.027	5.60	2.24	2.45	0.98
0.14	4.0	1.0	0.017	1.79	1.79	1.79	1.79
0.14	4.0	1.5	0.026	3.13	2.09	1.56	1.04
0.14	4.0	2.0	0.035	3.81	1.91	1.56	0.78
0.14	4.0	2.5	0.043	4.70	1.88	2.45	0.98
0.14	4.0	3.0	0.052	5.60	1.89	1.79	0.60
0.40	2.0	1.0	0.050	0.89	0.89	0.45	0.45
0.40	2.0	1.5	0.074	1.79	1.19	0.89	0.59
0.40	2.0	1.75	0.087	1.56	0.89	1.13	0.65
<u>Plan 1, 30-deg Wave Attack</u>							
0.09	6.0	1.0	0.011	1.56	1.56	1.13	1.13
0.09	6.0	1.5	0.016	2.02	1.35	1.56	1.04
0.09	6.0	2.0	0.022	--	--	2.45	1.23
0.09	6.0	2.5	0.027	2.45	0.98	1.79	0.72
0.14	4.0	1.0	0.017	1.13	1.13	1.34	1.34
0.14	4.0	1.5	0.026	1.79	1.19	1.56	1.04
0.14	4.0	2.0	0.035	2.45	1.23	2.02	1.01
0.14	4.0	2.5	0.043	2.24	0.90	2.45	0.98
0.14	4.0	3.0	0.052	2.92	0.97	2.45	0.82

(Continued)

(Sheet 1 of 3)

Table 1 (Continued)

d/L	$T, \text{ sec}$	$H, \text{ ft}$	H/L	$R_u, \text{ ft}$	R_u/H	$R_d, \text{ ft}$	R_d/H
<u>Plan 1, 30-deg Wave Attack (Continued)</u>							
0.40	2.0	1.0	0.050	1.34	1.34	0.45	0.45
0.40	2.0	1.5	0.074	1.34	0.89	1.13	0.75
0.40	2.0	1.75	0.087	0.68	0.39	1.13	0.65
<u>Plan 2, 90-deg Wave Attack</u>							
0.09	6.0	2.5	0.027	4.24	1.70	4.5	1.80
0.14	4.0	3.0	0.052	5.60	1.87	4.5	1.50
0.40	2.0	1.75	0.087	2.45	1.37	0.89	0.51
<u>Plan 2, 60-deg Wave Attack</u>							
0.09	6.0	2.5	0.027	4.70	1.88	2.29	0.92
0.14	4.0	3.0	0.052	6.03	2.01	3.35	1.12
0.40	2.0	1.75	0.087	2.24	1.28	0.89	0.51
<u>Plan 2, 30-deg Wave Attack</u>							
0.09	6.0	2.5	0.027	2.45	0.98	2.68	1.07
0.14	4.0	3.0	0.052	2.24	0.75	2.02	0.67
0.40	2.0	1.75	0.087	1.56	0.89	0.89	0.51
<u>Plan 3, 90-deg Wave Attack</u>							
0.09	6.0	1.0	0.011	1.07	1.07	1.97	1.97
0.09	6.0	2.0	0.022	2.50	1.25	1.97	0.99
0.09	6.0	3.0	0.033	3.76	1.25	2.68	0.89
0.40	2.0	1.0	0.050	0.72	0.72	1.07	1.07
0.40	2.0	1.5	0.074	1.16	0.77	1.07	0.71
0.40	2.0	1.75	0.087	1.61	0.92	1.43	0.82
0.40	2.0	2.0	0.099	1.61	0.81	1.61	0.81
<u>Plan 3, 60-deg Wave Attack</u>							
0.09	6.0	1.0	0.011	1.61	1.61	2.33	2.33
0.09	6.0	2.0	0.022	3.22	1.61	2.15	1.08
0.09	6.0	3.0	0.033	5.72	1.91	3.04	1.01
0.40	2.0	1.0	0.050	0.72	0.72	1.07	1.07
0.40	2.0	1.5	0.074	1.25	0.83	1.07	0.71
0.40	2.0	1.75	0.087	1.79	1.02	1.79	1.02
0.40	2.0	2.0	0.099	1.79	0.90	1.61	0.81

(Continued)

(Sheet 2 of 3)

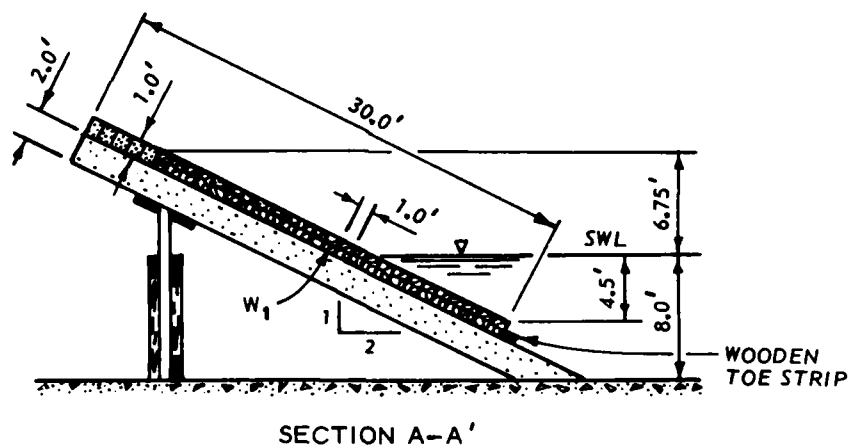
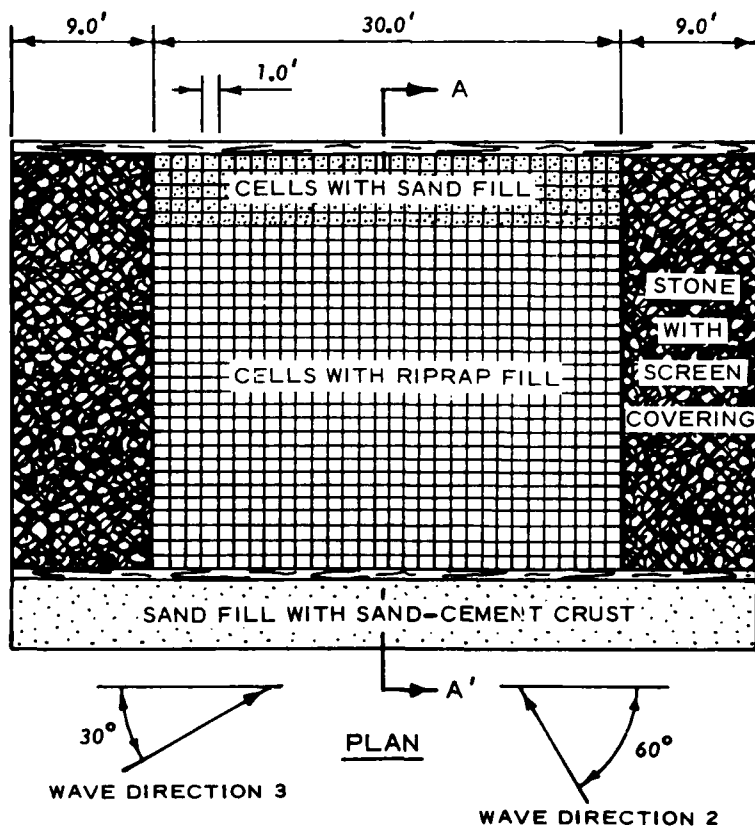
Table 1 (Concluded)

<u>d/L</u>	<u>T , sec</u>	<u>H , ft</u>	<u>H/L</u>	<u>R_u , ft</u>	<u>R_u/H</u>	<u>R_d , ft</u>	<u>R_d/H</u>
<u>Plan 3, 30-deg Wave Attack</u>							
0.09	6.0	1.0	0.011	0.72	0.72	1.07	1.07
0.09	6.0	2.0	0.022	2.15	1.08	2.15	1.08
0.09	6.0	3.0	0.033	2.68	0.89	2.15	0.72
0.40	2.0	1.0	0.050	0.54	0.54	0.89	0.89
0.40	2.0	1.5	0.074	1.07	0.71	0.89	0.59
0.40	2.0	1.75	0.087	0.89	0.51	1.25	0.71
0.40	2.0	2.0	0.099	0.89	0.45	1.07	0.54
<u>Plan 4, 90-deg Wave Attack</u>							
0.09	6.0	1.0	0.011	1.43	1.43	1.25	1.25
0.09	6.0	2.0	0.022	2.68	1.34	2.33	1.17
0.09	6.0	3.0	0.033	4.47	2.68	1.16	0.89
<u>Plan 4, 60-deg Wave Attack</u>							
0.09	6.0	1.0	0.011	1.79	1.79	2.15	2.15
0.09	6.0	2.0	0.022	3.58	1.79	2.86	1.43
0.09	6.0	3.0	0.033	6.44	2.15	4.50	1.50
<u>Plan 4, 30-deg Wave Attack</u>							
0.09	6.0	1.0	0.011	0.89	0.89	1.25	1.25
0.09	6.0	2.0	0.022	2.15	1.08	1.97	0.99
0.09	6.0	3.0	0.033	3.22	1.07	2.86	0.95

(Sheet 3 of 3)



B-8-39



MATERIAL CHARACTERISTICS

MODEL: $W_1 = 0.072 - 0.009$ -LB STONE @ 165 PCF

PROTOTYPE**: $W_1 = 4.61 - 0.58$ -LB STONE @ 165 PCF

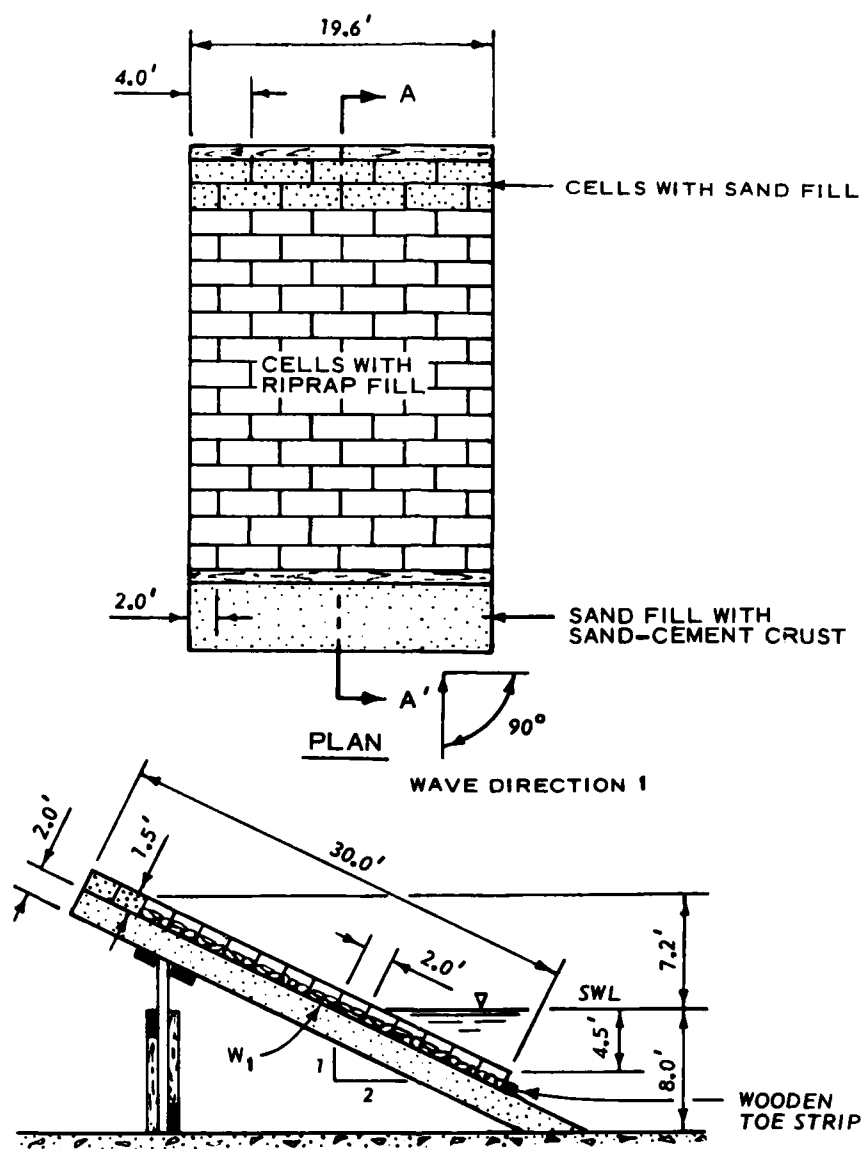
NOTE: ALL DIMENSIONS ARE PROTOTYPE MEASUREMENTS

- * PLAN 1, CELLS FULL OF RIPRAP
- PLAN 2, CELLS HALF-FULL OF RIPRAP

** SEE FIGURE 4 FOR RIPRAP GRADATION

RIPRAP-FILLED CELLS 3-DIMENSIONAL MODEL

PLANS 1 AND 2*
MODEL SCALE 1:4



SECTION A-A'

MATERIAL CHARACTERISTICS

MODEL: $W_1 = 0.072 - 0.009\text{-LB STONE @ 165 PCF}$

PROTOTYPE**: $W_1 = 4.61 - 0.58\text{-LB STONE @ 165 PCF}$

NOTE: ALL DIMENSIONS ARE
PROTOTYPE MEASUREMENTS

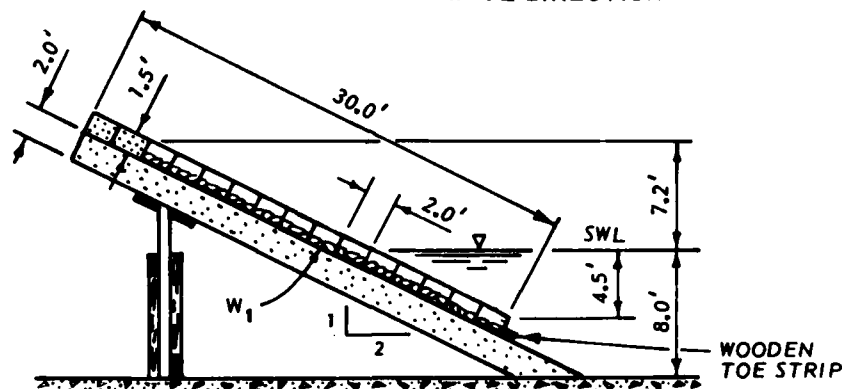
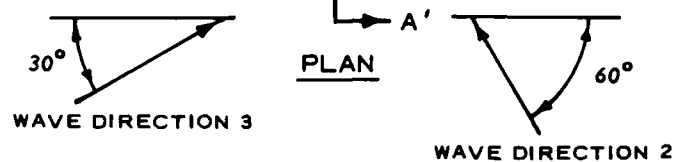
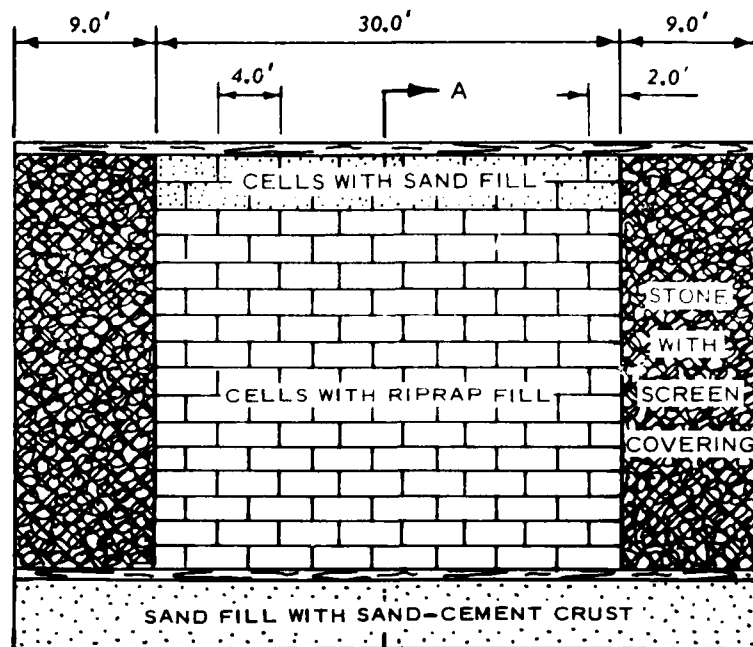
- * PLAN 3, CELLS HALF-FULL
OF RIPRAP
- PLAN 4, CELLS FULL OF RIPRAP

** SEE FIGURE 4 FOR
RIPRAP GRADATION

**RIPRAP-FILLED CELLS
2-DIMENSIONAL MODEL**

PLANS 3 AND 4*
MODEL SCALE 1:4

PLATE 3



SECTION A-A'

MATERIAL CHARACTERISTICS

MODEL: $W_1 = 0.072 - 0.009$ -LB STONE @ 165 PCF

PROTOTYPE**: $W_1 = 4.61 - 0.58$ -LB STONE @ 165 PCF

NOTE: ALL DIMENSIONS ARE
PROTOTYPE MEASUREMENTS

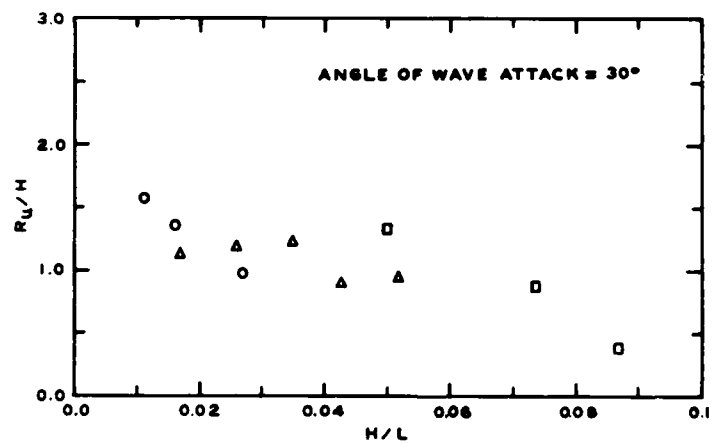
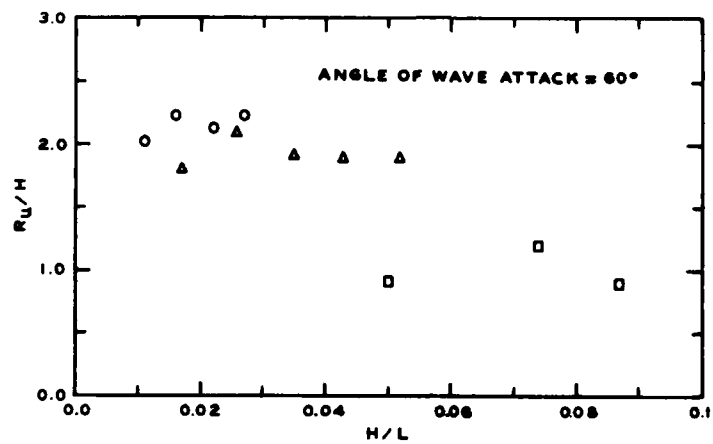
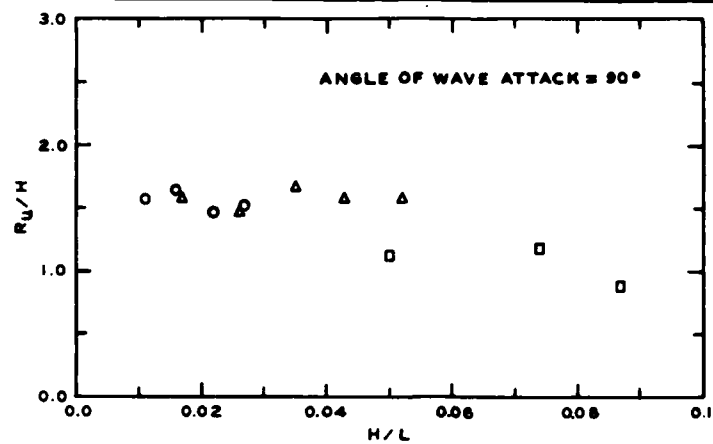
- * PLAN 3, CELLS HALF-FULL
OF RIPRAP
- PLAN 4, CELLS FULL OF RIPRAP

- ** SEE FIGURE 4 FOR
RIPRAP GRADATION

**RIPRAP-FILLED CELLS
3-DIMENSIONAL MODEL**

PLANS 3 AND 4*

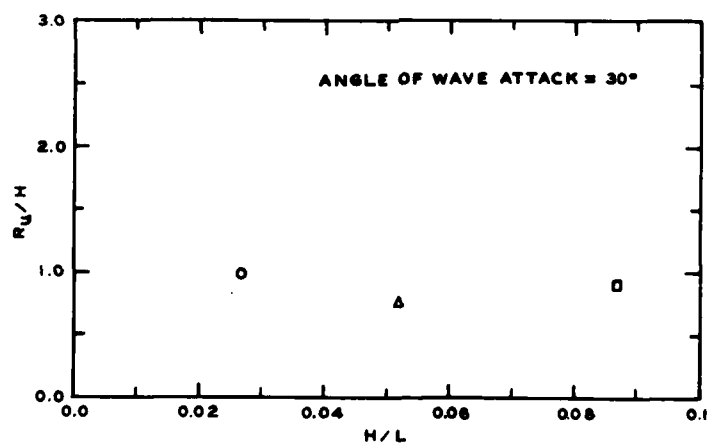
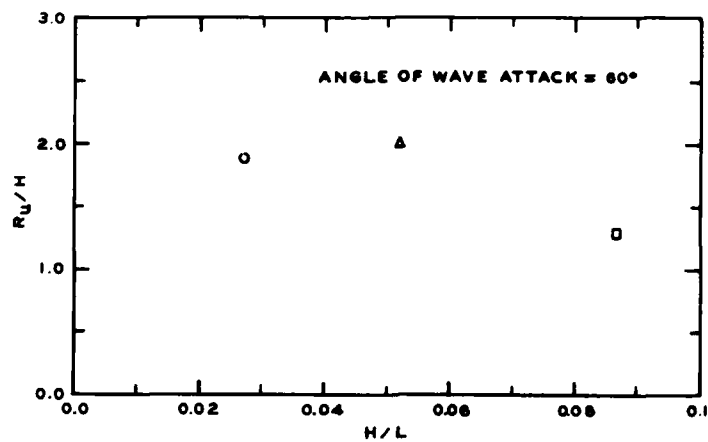
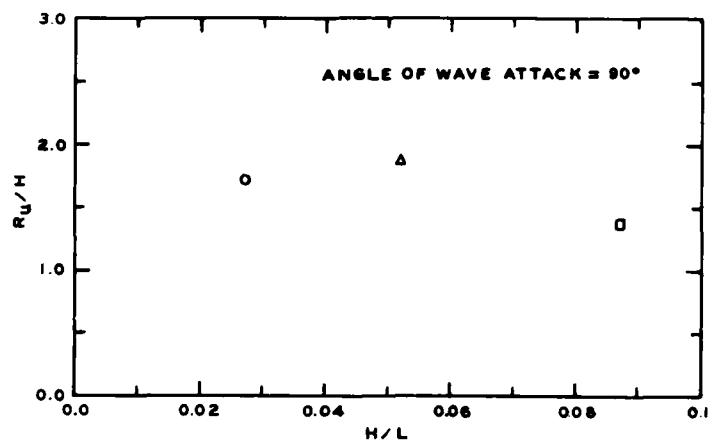
MODEL SCALE 1:4



LEGEND

SYMBOL	d/L	T, SEC
○	0.09	6.0
△	0.14	4.0
□	0.40	2.0

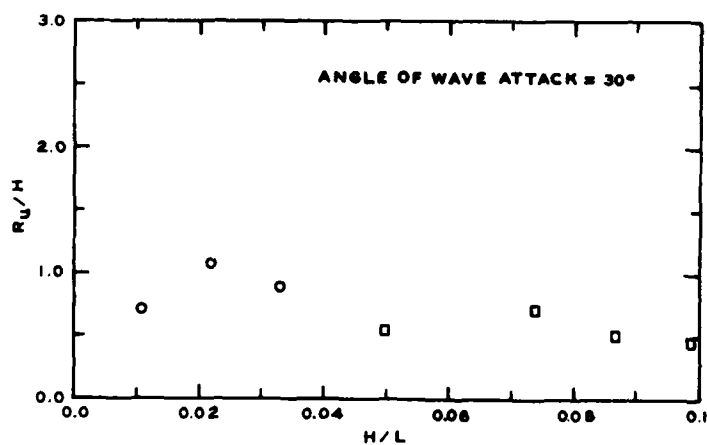
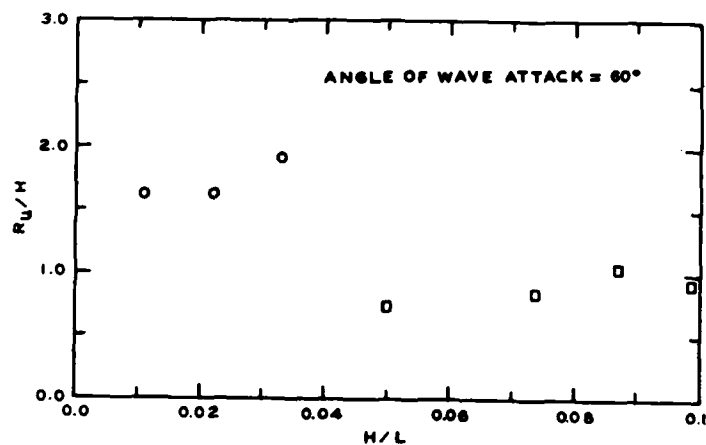
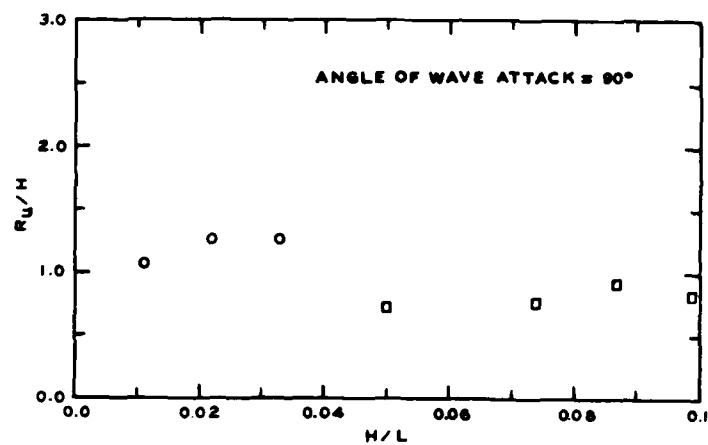
RELATIVE RUNUP (R_u/H)
VS
WAVE STEEPNESS (H/L)
PLAN I



LEGEND

SYMBOL	d/L	T, SEC
○	0.09	6.0
△	0.14	4.0
□	0.40	2.0

RELATIVE RUNUP (R_u/H)
VS
WAVE STEEPNESS (H/L)
PLAN 2

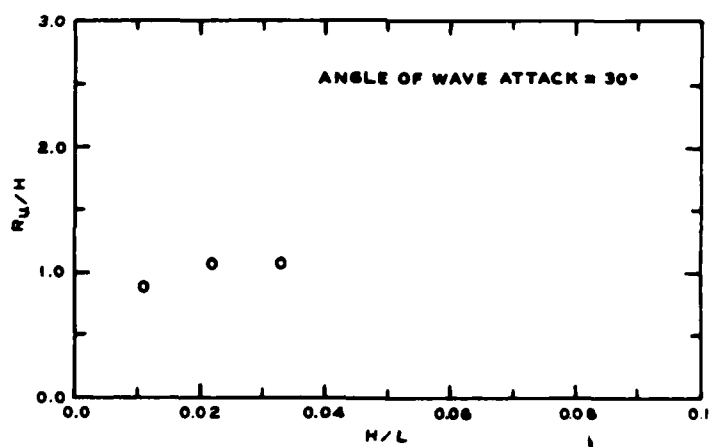
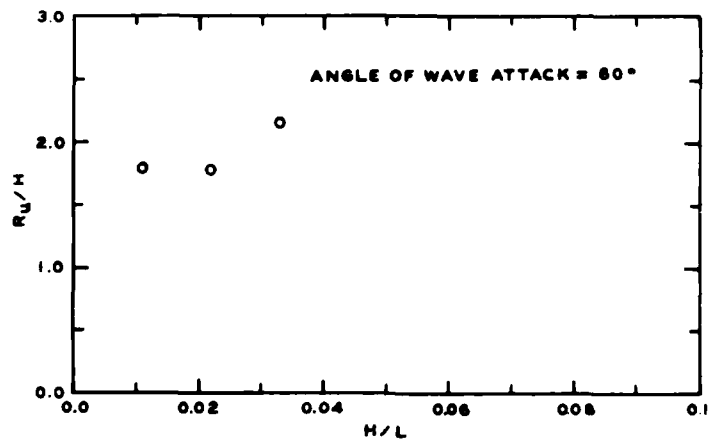
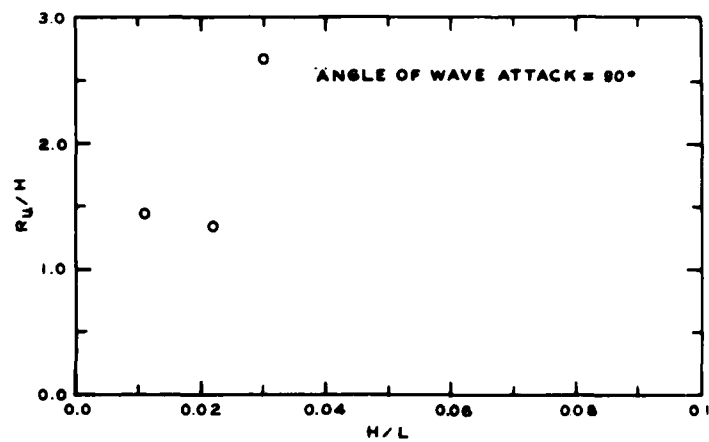


LEGEND

SYMBOL	d/L	T, SEC
○	0.08	6.0
□	0.40	2.0

RELATIVE RUNUP (R_u/H)
VS
WAVE STEEPNESS (H/L)
PLAN 3

PLATE 7



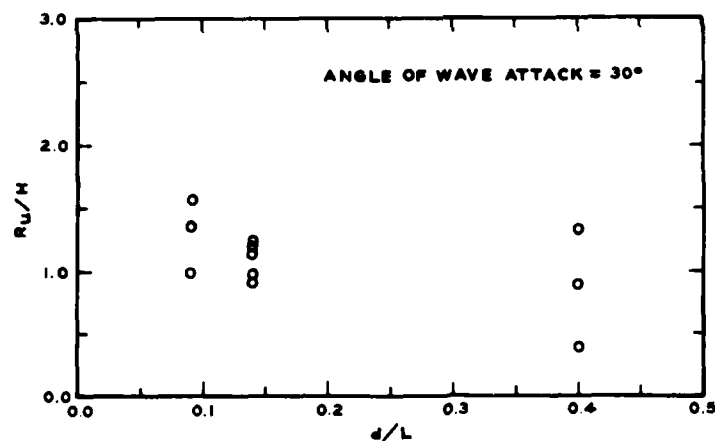
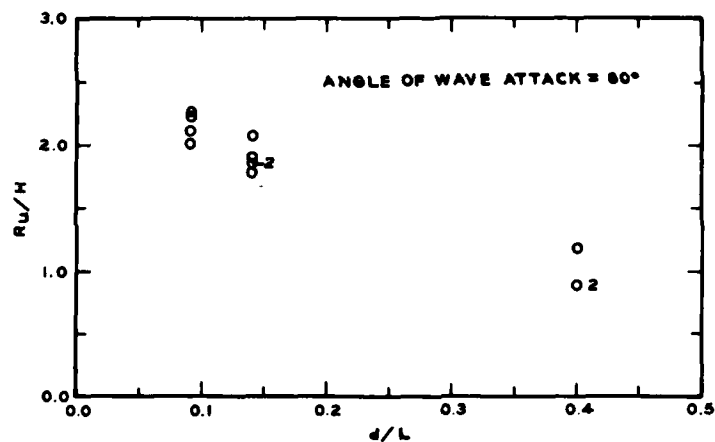
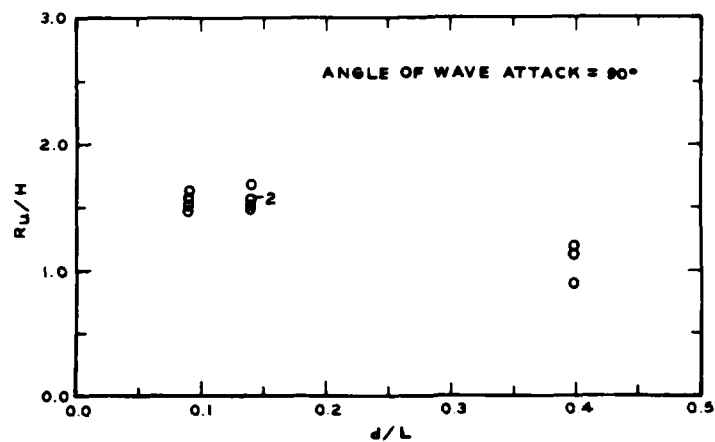
LEGEND

<u>SYMBOL</u>	<u>H/L</u>	<u>T, SEC</u>
O	0.09	6.0

RELATIVE RUNUP (R_u/H)
VS
WAVE STEEPNESS (H/L)
PLAN 4

PLATE 8

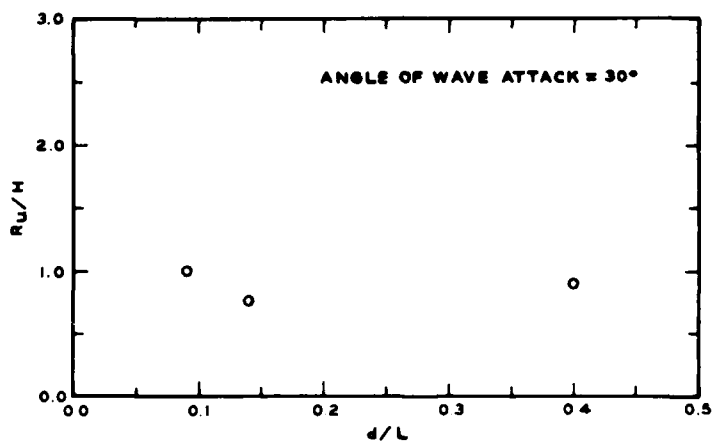
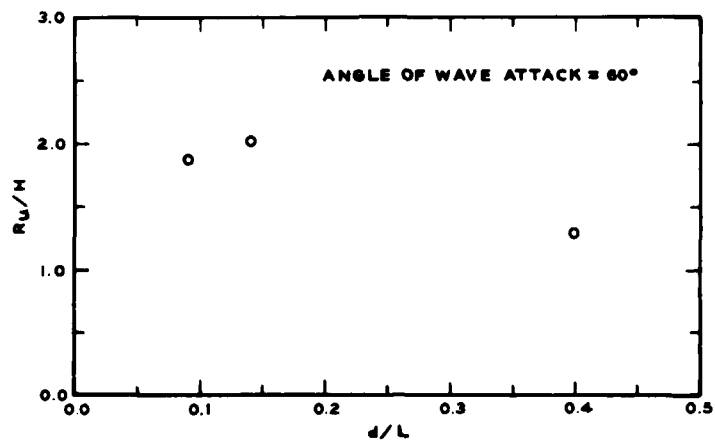
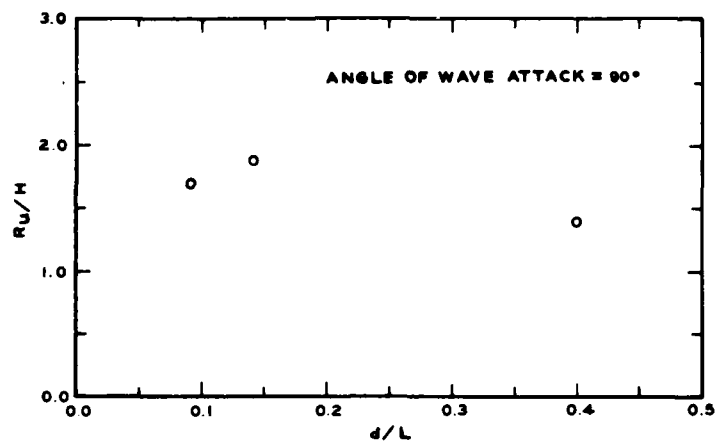
B-8-46



NOTE NUMBERS BESIDE DATA POINTS
INDICATE THAT THE NUMBER
OF DATA POINTS EXCEED ONE.

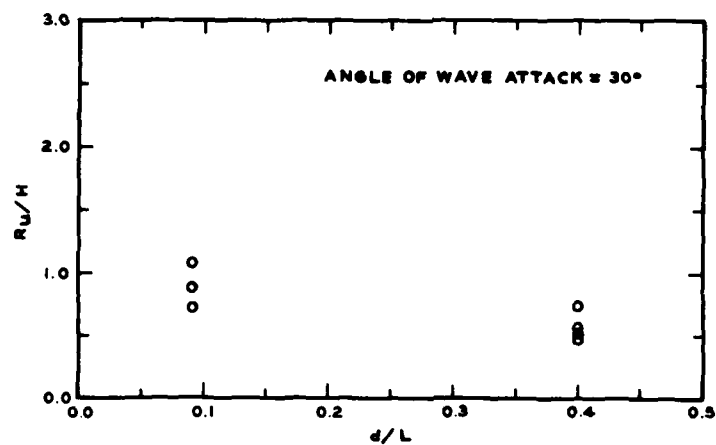
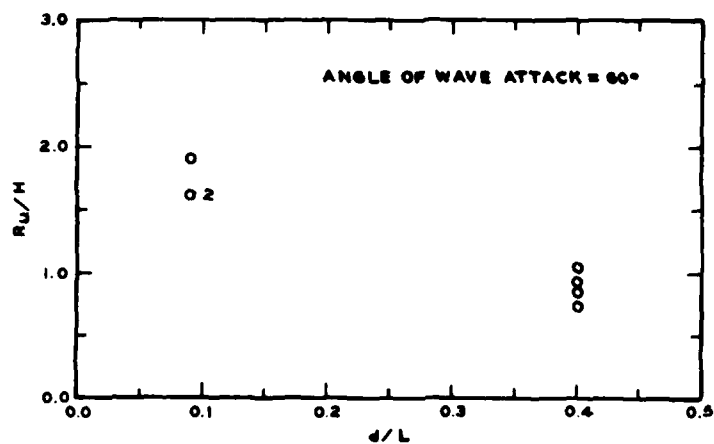
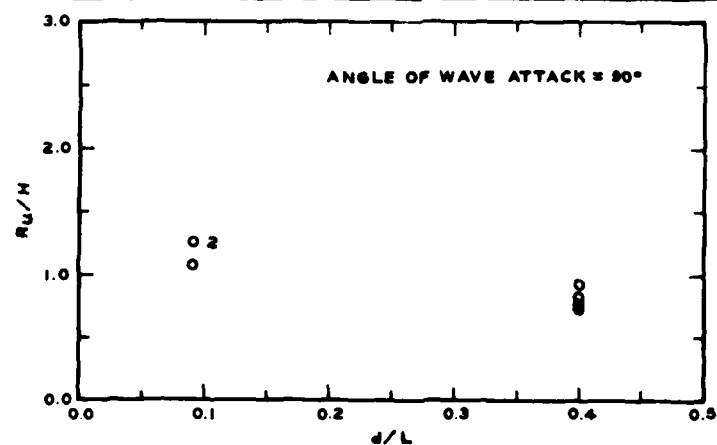
RELATIVE RUNUP (R_u/H)
VS
RELATIVE DEPTH (d/L)
PLAN 1

PLATE 9



RELATIVE RUNUP (R_u/H)
VS
RELATIVE DEPTH (d/L)
PLAN 2

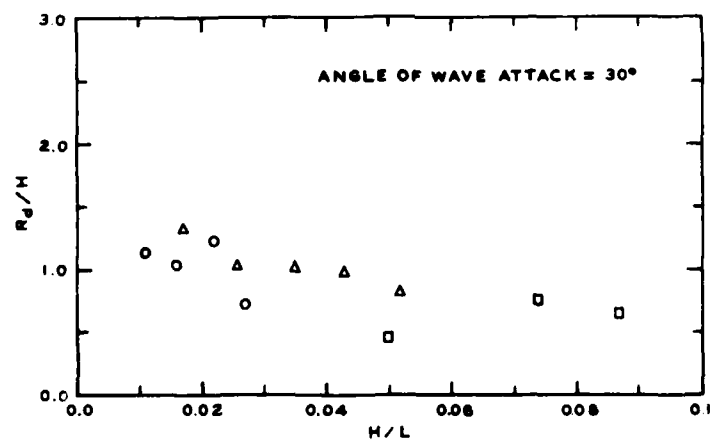
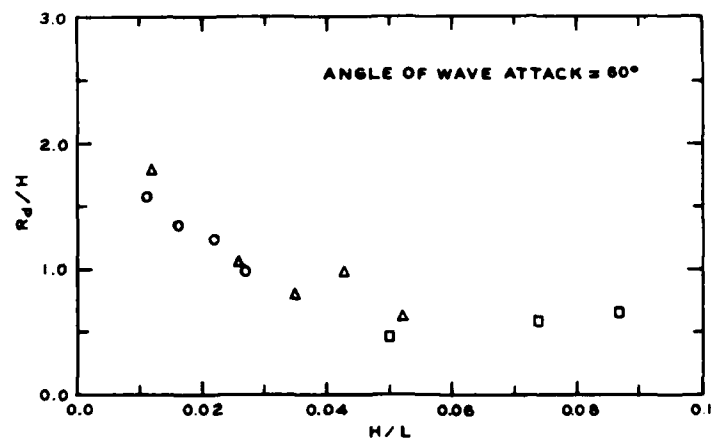
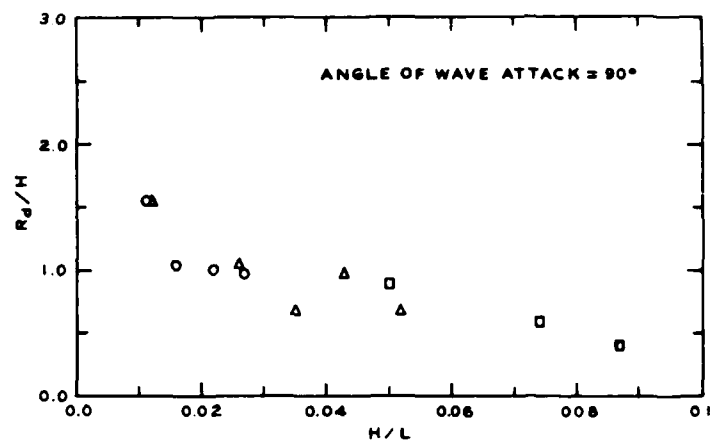
PLATE 10



NOTE: NUMBERS BESIDE DATA POINTS
INDICATE THAT THE NUMBER
OF DATA POINTS EXCEED ONE

RELATIVE RUNUP (R_u/H)
VS
RELATIVE DEPTH (d/L)
PLAN 3

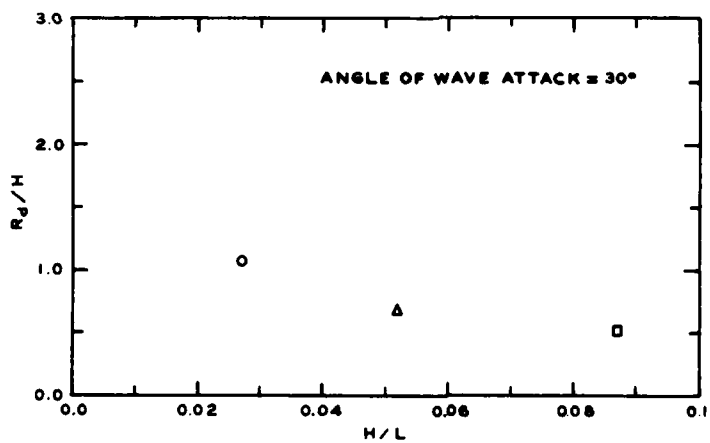
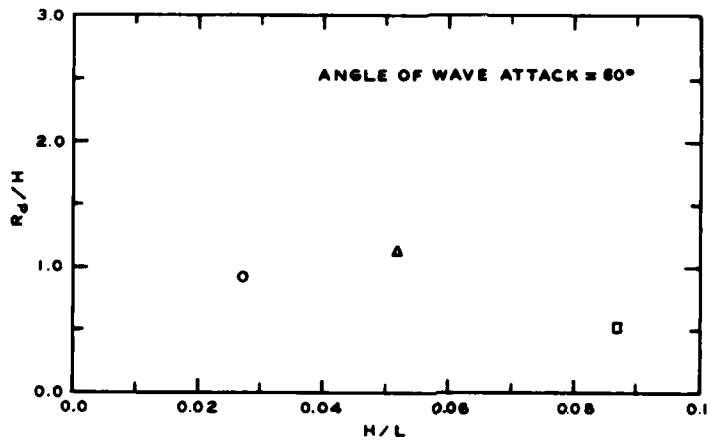
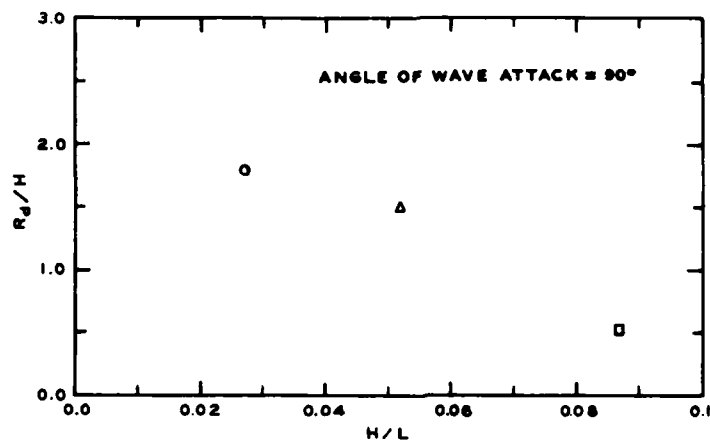
PLATE 11



LEGEND

SYMBOL	H/L	T, SEC
○	0.09	6.0
△	0.14	4.0
□	0.40	2.0

RELATIVE RUNDOWN (R_d/H)
VS
WAVE STEEPNESS (H/L)
PLAN I

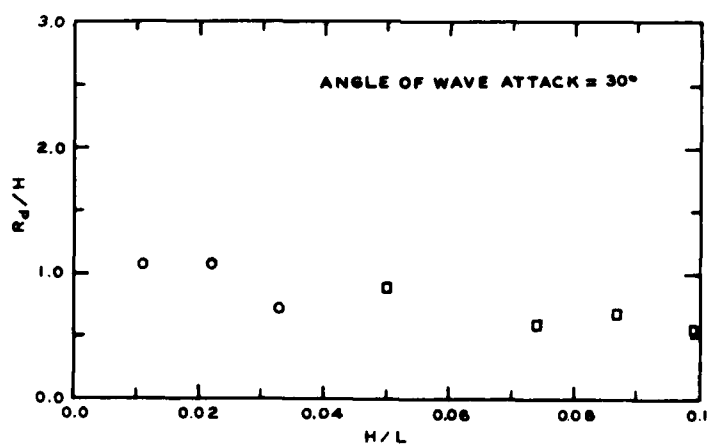
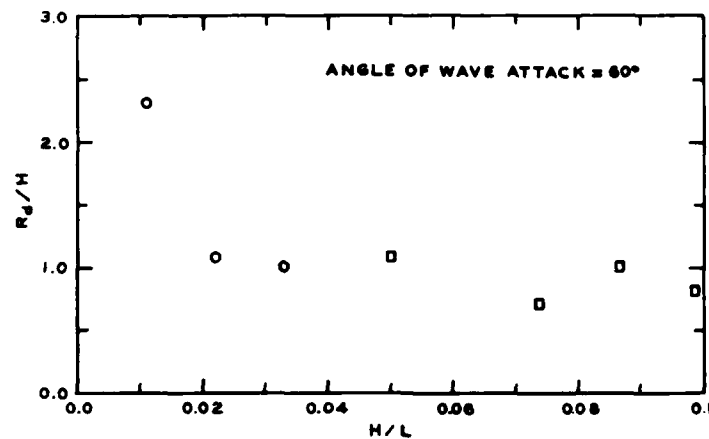
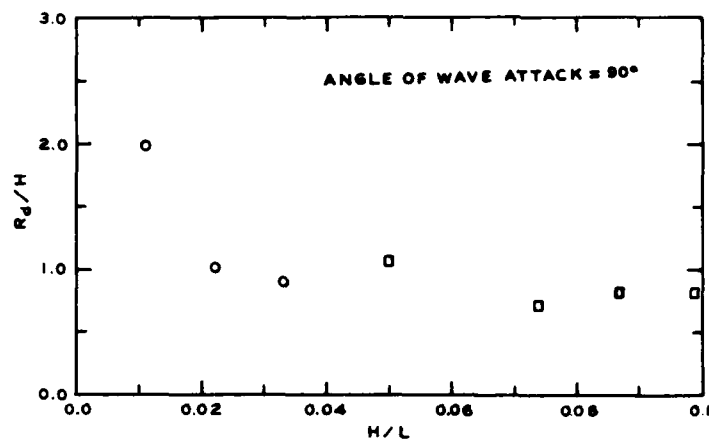


LEGEND

SYMBOL	d/L	T, SEC
○	0.09	6.0
△	0.14	4.0
□	0.40	2.0

RELATIVE RUNDOWN (R_d/H)
VS
WAVE STEEPNESS (H/L)
PLAN 2

PLATE 13

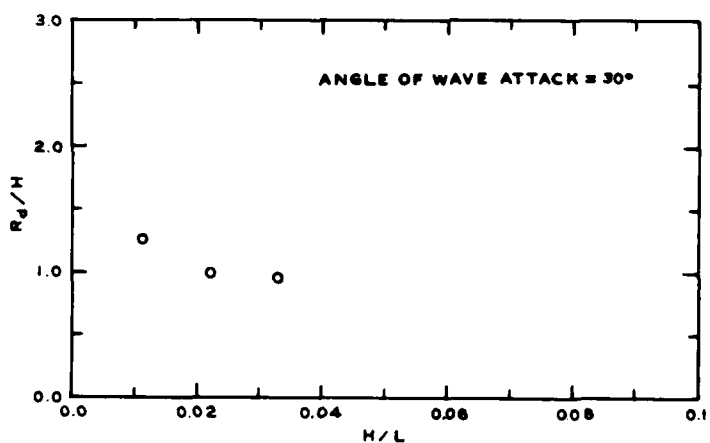
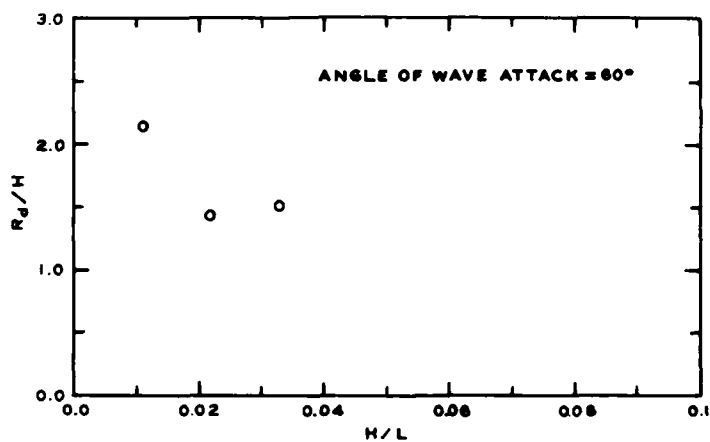
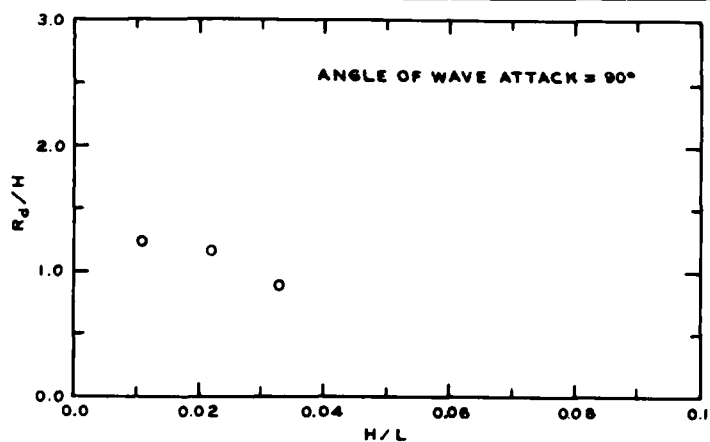


LEGEND

SYMBOL	d/L	T, SEC
○	0.09	6.0
□	0.40	2.0

RELATIVE RUNDOWN (R_d/H)
VS
WAVE STEEPNESS (H/L)
PLAN 3

PLATE 14

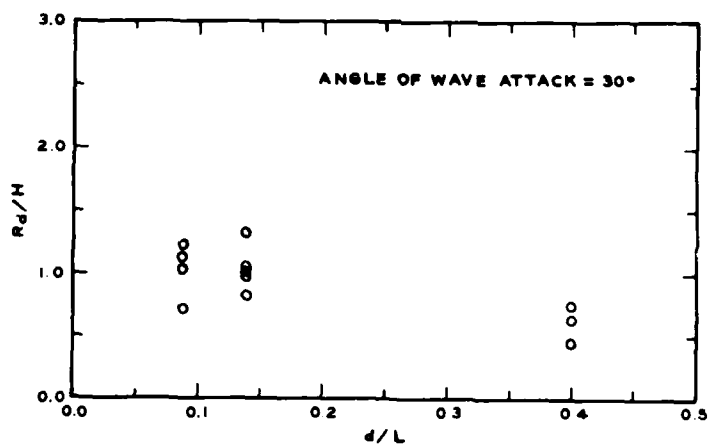
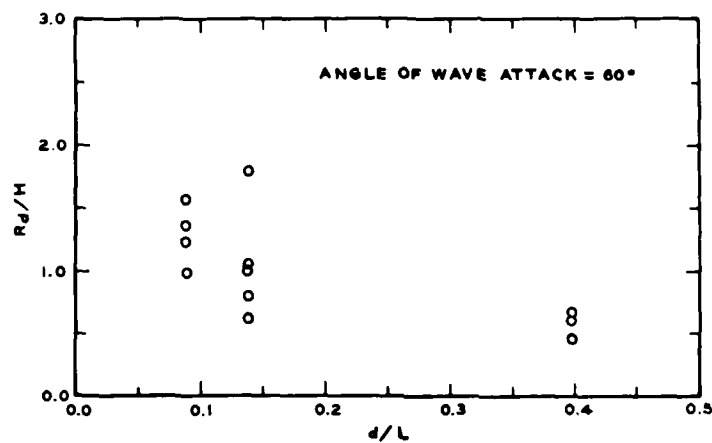
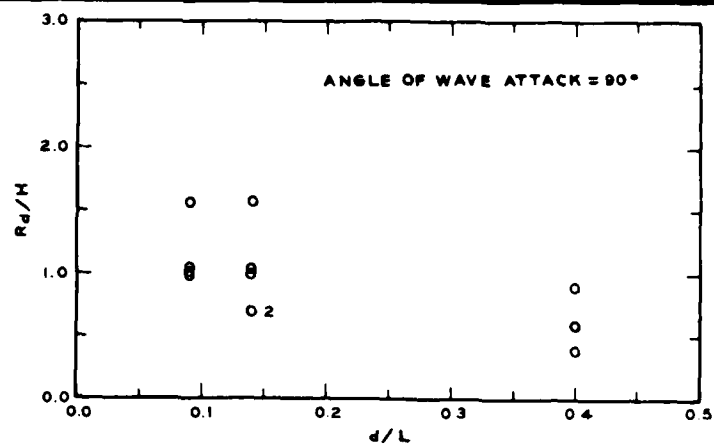


LEGEND

SYMBOL	d/L	T, SEC
O	0.09	6.0

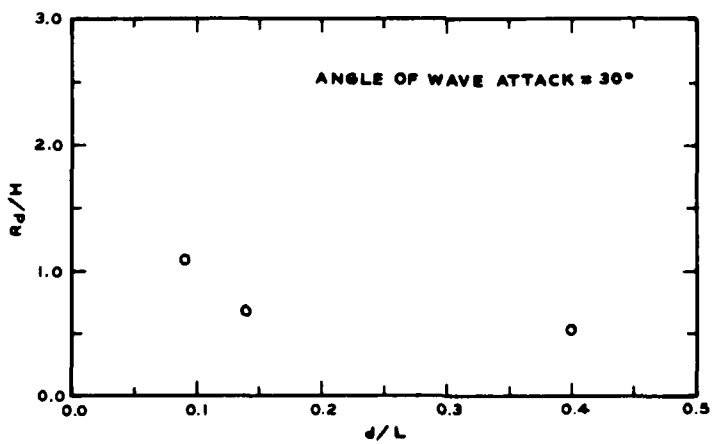
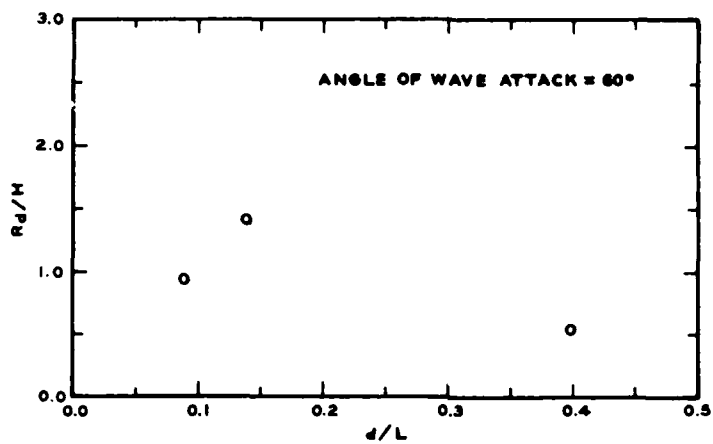
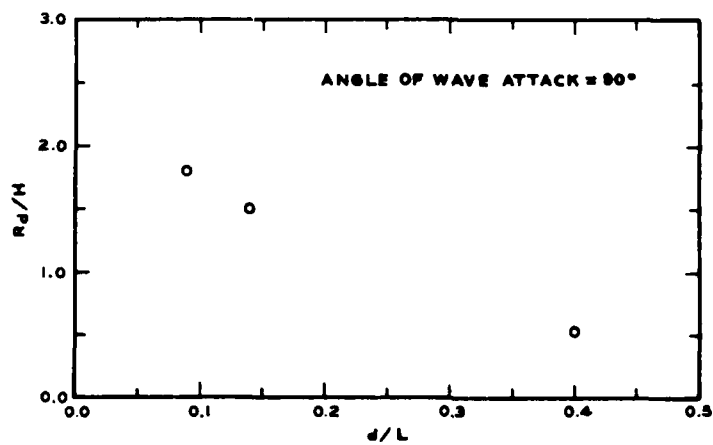
RELATIVE RUNDOWN (R_d/H)
VS
WAVE STEEPNESS (H/L)
PLAN 4

PLATE 15



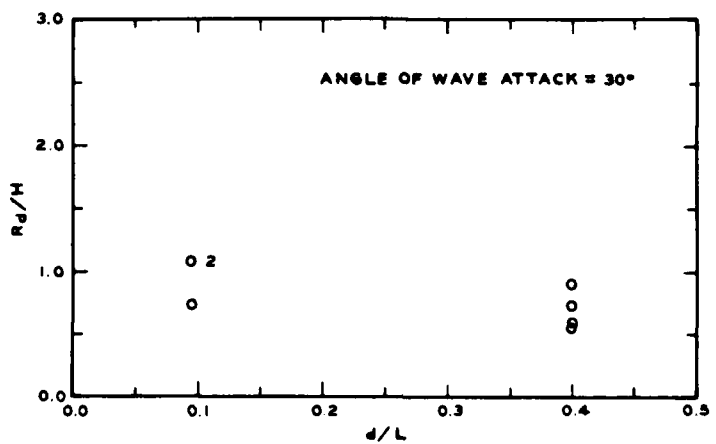
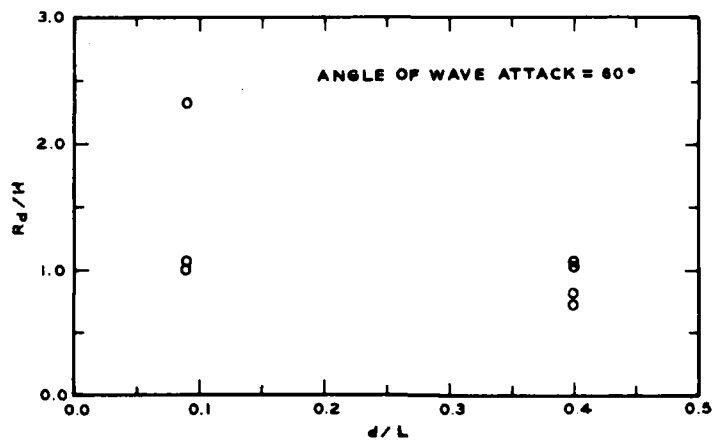
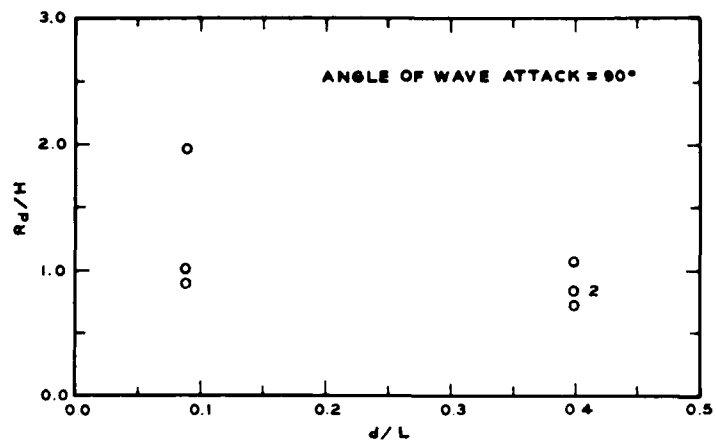
NOTE: NUMBERS BESIDE DATA POINTS
INDICATE THAT THE NUMBER
OF DATA POINTS EXCEED ONE

RELATIVE RUNDOWN (R_d/H)
VS
RELATIVE DEPTH (d/L)
PLAN I



RELATIVE RUNDOWN (R_d/H)
VS
RELATIVE DEPTH (d/L)
PLAN 2

PLATE 17



NOTE: NUMBERS BESIDE DATA POINTS
INDICATE THAT THE NUMBER
OF DATA POINTS EXCEED ONE.

RELATIVE RUNDOWN (R_d/H)
VS
RELATIVE DEPTH (d/L)
PLAN 3